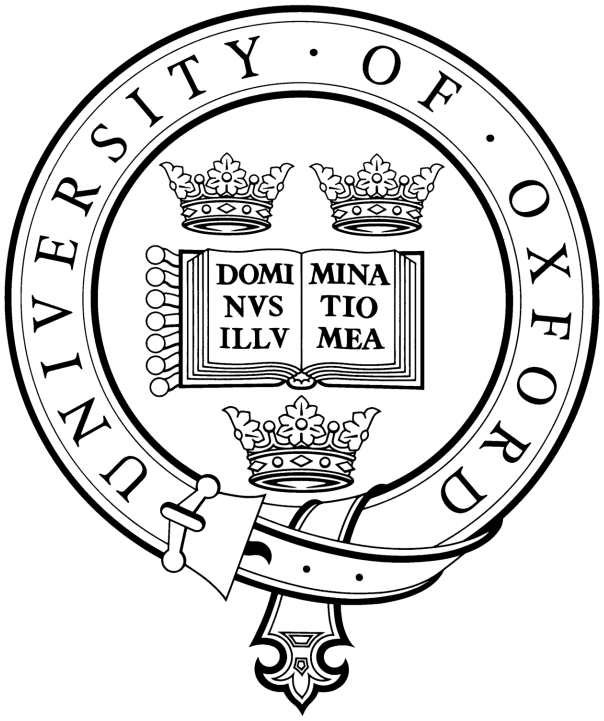

Investigating the lymphatic system in intestinal inflammation

Rahul Prashanth Ravindran

Wadham College
University of Oxford

A thesis submitted in partial fulfilment of the requirements for the degree of Doctor of Philosophy

Michaelmas Term 2023

Abstract

We set out to understand the colonic lymphatic vasculature in the context of outflow from the colon, with the ambition of using this knowledge to develop methods to promote exit of inflammatory cells from the tissue as an alternative way to treat patients with inflammatory bowel disease. Our studies converged on the identification of tissue folds as central anatomical units that orchestrate interstitial fluid outflow from the colon. We observed that the luminal surface of the mammalian colon is characterised by undulations of the mucosa and submucosa forming tissue folds. In humans these included haustral folds and intrahaustral folds of lesser prominence between muscular bands of taenia coli. Mice lacked taenia coli and haustra but nonetheless possessed folds, especially in the proximal colon. The functional significance of these colonic tissue undulations, beyond increasing surface area for absorption, had not previously been determined. Here, through murine in vivo and 3D imaging studies, we show that tissue folds orchestrated the collection and outflow of interstitial fluid from the colon. We demonstrate that lymphatics line the base of colonic crypts and specifically branched toward the epithelium within folds. Colonic folds functioned as reservoirs feeding lymphatic and venous outflow, and phagocytic scavenging by fold-associated mononuclear phagocytes augmented this reservoir property. Colonic lymphoid follicles were enriched within these tissue folds, surrounded by lymphatics and postcapillary venules. Human colonic lymphoid follicles were likewise positioned within the elevation of tissue folds. Our findings suggest that colonic folds are distinct anatomical units conserved across species that organise uptake, immunosurveillance, and outflow of interstitial cargo, while restraining the spread of inflammation. Indeed, the loss of tissue folds during ulcerative colitis may facilitate distal-to-proximal spread of pathology.

Acknowledgements

The completion of this thesis stands as a testament to the support and guidance provided by numerous individuals and groups, as well generous financial assistance from the Medical Research Council, without which this work would not have been possible. While space limitations prevent an exhaustive list, the contributions of key individuals have been highlighted here.

My deepest appreciation goes to my brilliant supervisory team at the Kennedy Institute in Oxford, whose influence has been profound throughout this journey. Professor Chris Buckley's enthusiasm, mentorship and support from the project's inception have significantly shaped my academic trajectory. Professor Fiona Powrie's clarity of thought and desire to crystalise a testable hypothesis have been invaluable skills for me to learn. Dr Matthias Friedrich's scientific rigour and guidance in experimental methodology from the start of my time in the lab have been hugely valued. Finally, my Director of Graduate studies, Professor Mark Coles' willingness to discuss all things science and sketch lymphatic diagrams on his whiteboard together have been most enjoyable and fruitful. The collaborative and curious nature of the Buckley-Coles, Powrie, and Friedrich groups has been a privilege to be a part of and the collective team spirit has propelled this research forward.

A special acknowledgment is reserved for Professor Gwen Randolph, whose scientific inquisitiveness and interdisciplinary approach has been inspiring to learn from. My research visits to her laboratory at Washington University in Saint Louis were very exciting phases of this project. I am specifically most grateful to Dr Rafael Czepielewski, who was immediately welcoming and supportive on my arrival to the lab. We worked together on many experiments and spurred one another on in advancing our understanding of the colonic lymphatic vasculature. To me, this was the quintessential example of

team science, which I will never forget. I am also indebted to Dr Daniel Lee and Dr Bernd Zinselmeyer for their vital assistance and helpful discussions in several phases of the research, including progressing our abilities in tissue clearing and imaging to new levels. I am also grateful to the entire Randolph lab for welcoming me, helping with experiments, and sharing their knowledge. My gratitude extends to Jonathan Webber for his help with cell sorting, Dr Cathy Ma, who helped with the human histopathology and Professor Young-Kwon Hong for providing the Prox1-GFP mice which were essential for our imaging studies. Professor Simon Travis has been a mentor to me since starting my research journey within the field of Gastroenterology and I am very thankful for his advice, support, and continuous encouragement to pursue a career in clinical academia. I am also thankful to Professor David Jackson for sharing his vast insight on the lymphatic system and brainstorming several helpful ideas and lines of thinking together.

My family, including my parents, sister and parents-in-law have provided constant love and encouragement and have been great motivators throughout this journey. I am also deeply grateful to my church family for their friendship, prayers, support, and encouragement throughout my research.

A special mention goes out to my golfing buddy, Hunter, whose lessons on the importance of staying optimistic and playing the next shot to the best of one's ability, regardless of the current situation, have been a guiding philosophy in navigating challenges during the DPhil, as well as in life.

Lastly, my heartfelt gratitude goes to my wife, Iona. Her unwavering love, support, and understanding amid the highs and lows of this research journey are not possible to describe here. Our shared experiences during the DPhil, including our marriage, the arrival of our wonderful daughter, Bella, and living together in the American Midwest as a family, have made this chapter of my life a truly unforgettable one.

Declaration of authorship

I hereby declare that the data presented in this thesis is my own work and to the best of my knowledge contains no materials previously published or written by another person, or which have been accepted for the award of any degree or diploma at the University of Oxford, or any other educational institution. Any contributions made to the research by others is explicitly acknowledged within the text of this thesis.

List of abbreviations

ACKR: Atypical Chemokine Receptor
AHR: Aryl hydrocarbon receptor
BEC: Blood endothelial cell
CCL: Chemokine (C-C motif) ligand
CD: Crohn's disease
cDNA: Complementery deoxyribonucleic acid
CHAPS: 3-((3-cholamidopropyl) dimethylammonio)-1-propanesulfonate
CLV: Collecting lymphatic vessel
CSF1: Colony stimulating factor 1
CSF1R: Colony stimulating factor 1 receptor
CXCL: Chemokine (C-X-C motif) ligand
DAB: 3,3'-Diaminobenzidine
DAPI: 4',6-diamidino-2-phenylindole
DNA: Deoxyribonucleic acid
DSS: Dextran sulfate sodium
EDTA: Ethylenediaminetetraacetic acid
EpCAM: Epithelial cellular adhesion molecule
FACS: Fluorescence-activated cell sorting
FCS: Foetal calf serum
Fib: Fibroblast
FITC: Fluorescein isothiocyanate
FMO: Fluorescence minus one
GFP: Green fluorescent protein
HEPES: 2-[4-(2-hydroxyethyl)piperazin-1-yl]ethanesulfonic acid
Hh: Helicobacter hepaticus
IFNg: Interferon gamma
Il10r: Interleukin 10 receptor
IL1b: Interleukin 1 beta
IL6: Interleukin 6
LEC: Lymphatic endothelial cell
LED: Light emiting diode
LPS: Lipopolysaccharide
Lyve1: Lymphatic vessel endothelial hyaluronan receptor 1
MHC: Major histocompatibility complex
MLN: Mesenteric lymph node
MNP: Mononuclear phagocyte
NMDEA: N-Methyldiethanolamine
PBS: Phosphate buffered saline
Pdpn: Podoplanin
PFA: Paraformaldehyde
PLP: Periodate-lysine-paraformaldehyde
RNA: Ribonucleic acid
S1P: Sphingosine-1-phosphate
TLO: Tertiary lymphoid organ
TLS: Tertiary lymphoid structure
TNFα: Tumour necrosis factor alpha
UC: Ulcerative colitis
VEGFA: Vascular endothelial growth factor A
VEGFB: Vascular endothelial growth factor B
VEGFC: Vascular endothelial growth factor C
VEGFD: Vascular endothelial growth factor D
VEGFR1: Vascular endothelial growth factor receptor 1
VEGFR2 (Kdr): Vascular endothelial growth factor receptor 2
VEGFR3 (Flt4): Vascular endothelial growth factor receptor 3

Table of Contents

1 Introduction

1.1 Overview

Despite significant research on the topic and numerous advances made over the past couple of decades, inflammatory bowel disease (IBD) remains a disease with a significant therapeutic gap with patients having primary non-response or secondary loss of response to all available therapies. The overarching aim of this thesis centres around better understanding of the pathogenesis of IBD, with the longer-term ambition of using this knowledge to facilitate the development of novel therapeutic agents. We begin by considering the numerous aetiological factors implicated in the pathogenesis of IBD. Following this, we turn to assess the classes of therapy in the context of how they affect leukocyte accumulation in the tissue, which is a key feature of the disease.

We then consider where the gaps are and particularly focus in on the exit of immune cells from the intestinal tissue. This highlights the dearth of knowledge that exists on intestinal outflow, particularly in the colon, which forms the focus of this thesis. Our key underlying reason for studying outflow from the colon was to understand whether stimulating exit of immune cells from the colonic tissue could aid in the resolution of intestinal inflammation. Prior to addressing this, we had to understand the steady state. Exit of cells and interstitial fluid from tissue is mediated by lymphatic vessels, and therefore this introduction moves to focus in on the current knowledge of the intestinal lymphatic vasculature, first in homeostasis, then in inflammation. We conclude with the hypothesis and thesis aims.

1.2 Inflammatory Bowel Disease

Inflammatory bowel disease (IBD), comprising of Crohn's Disease (CD) and Ulcerative Colitis (UC), is a chronic immune-mediated inflammatory disease with a prevalence exceeding 0.3% and an increasing incidence in the developing world (1). IBD is a multi-system disorder with an incompletely understood aetiology. Numerous factors have been implicated in contributing to IBD including genetic (2, 3), microbial (4), dietary (5), and environmental (6), which are all independent areas of research. One of the central aspects of the disease is an inappropriate intestinal immune response, where, in homeostasis, a fine balance must be maintained between tolerance and activation of the immune system. Much work has sought to understand what initiates and propitiates intestinal inflammation that leads to significant complications such as ulceration, strictures, fistulation, and perforation of the intestine, if left untreated. Multiple immune pathways have been implicated in the pathogenesis of IBD (7); however, blockade with various agents still leaves a significant therapeutic gap. This suggests that the pathogenesis is not fully explained by modulating the immune system in isolation. Therefore, consideration of other factors that interact with the immune system is essential.

1.3 Principles of leukocyte accumulation in tissue with a focus on the intestine

The general principles of leukocyte accumulation in the tissue are made up of a balance between the factors outlined in the following diagram:

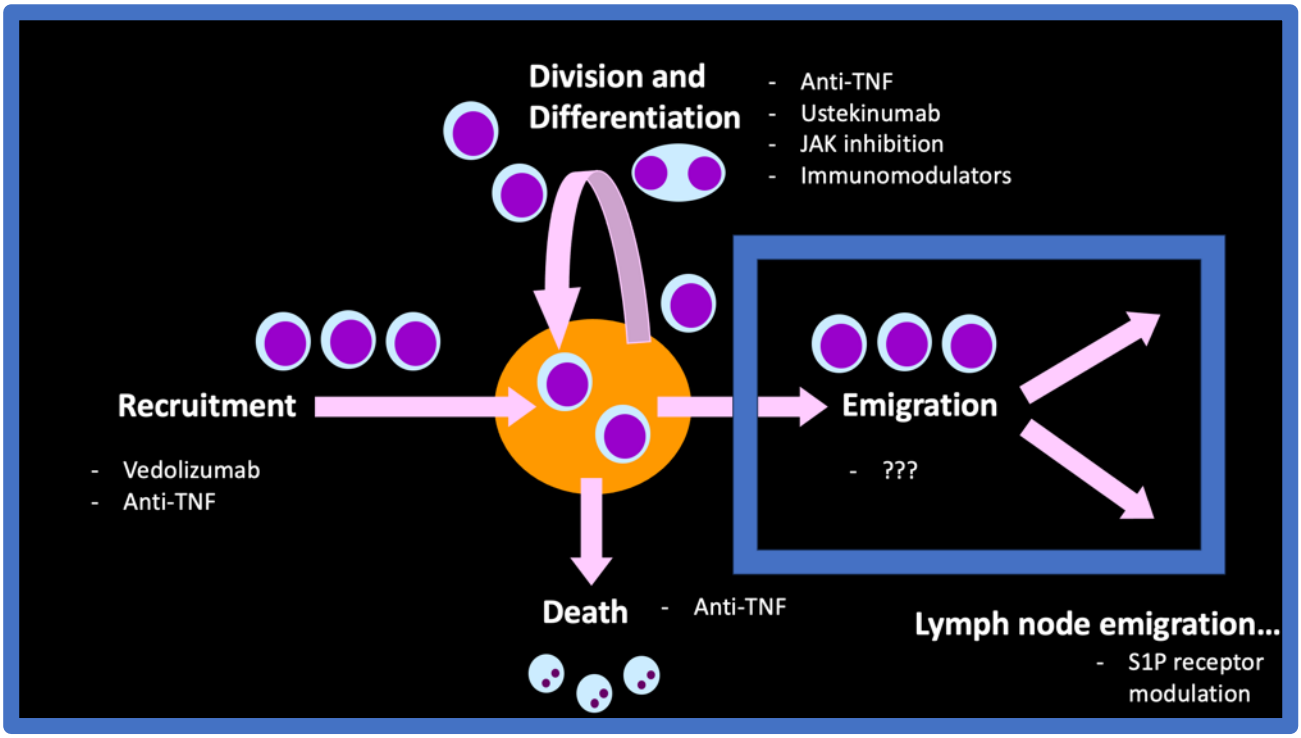

This diagram is specifically populated with examples of therapeutic agents used to treat IBD that affect each component of leukocyte accumulation. We will consider these aspects in turn in relation to currently utilised therapeutics. The initial therapeutic strategies for IBD revolved around the use of corticosteroids, with the seminal trial being published in 1955 by Truelove and Witts (8). To this day, the precise mechanism by which steroids induce remission of intestinal inflammation is not fully understood. It is known that they function via binding to intracellular glucocorticoid receptors – these receptors are widely expressed and binding results in numerous changes in gene expression and multiple off-target effects. Modern therapies have a far greater specificity based on biological understanding of the targets driving inflammation. We will focus on the various aspects that are involved in leukocyte accumulation in turn, and specifically consider existing therapies that target

these pathways in the context of IBD. We will conclude by highlighting the aspects that have been relatively neglected, and therefore form the focus of this thesis.

Recruitment of leukocytes to the tissue forms a key aspect of leukocyte accumulation in IBD. Leukocyte recruitment is a multi-step process initiated by leukocyte rolling and crawling on the vessel wall, followed by leukocyte arrest on the endothelium then finally transmigration across the endothelial cells of the vessel into the tissue (9–11). Inflammation induces changes in the endothelium that increases its permeability to circulating leukocytes, involving factors such as tumour-necrosis factor alpha (TNFα) (12). TNFα can also induce upregulation of integrins and selectins on the luminal endothelial surface which aids in leukocyte recruitment (13). Antibody targeting of TNFα was the first successful biologic treatment to be used to treat IBD (14), and is also effective across other tissues, with efficacy first being demonstrated in rheumatoid arthritis (14). This shows how understanding these principles are relevant in designing therapies to work across tissues.

More recently, the focus on inhibiting intestinal recruitment of leukocytes was targeted by creating an antibody that binds to and blocks the integrin α4 called natalizumab. This is expressed on leukocytes that are destined to migrate to the brain (α4β1) and the intestine (α4β7) (15, 16). Natalizumab was initially licensed to treat multiple sclerosis (17) as well as Crohn's disease (16); however, it came with an increased risk of developing a progressive multifocal leukoencephalopathy caused by the JC virus, causing death in one patient with Crohn's disease in an open-label extension study (16), presumably by blocking leukocyte entry to the brain, and led to an unacceptable safety profile in the context of Crohn's disease. This highlighted the importance of being able to target the process of leukocyte trafficking to the intestine more specifically. This idea came to fruition with the development of the α4β7 inhibitor, vedolizumab, which specifically prevents leukocyte trafficking to the intestine (18). This has been a hugely transformative medication in the treatment of both Crohn's

disease and ulcerative colitis, without the associated risk in CNS infection with the JC virus (19) presumably because this is unaffected with blockade of α4β7 rather than α4β1.

Other approaches include targeting chemokine receptors specific for intestinal homing such as CCR9, which predominantly mediates trafficking to the small bowel; however, the small molecule inhibitor 'vercirnon' was unsuccessful in clinical trials (20, 21). This may have been because simply inhibiting the interaction between the chemokine CCL25 and its receptor CCR9 may have been insufficient without actually depleting the cells that express CCR9. Nonetheless, the idea of targeting molecules that imprint tissue-specific homing to the intestine forms a promising approach to identify new targets that may be targeted therapeutically. Furthermore, as these therapies are relatively safe by being gut-specific, it may be possible to combine these with other existing therapies (22). Leukocyte trafficking to the colon utilised alternative mechanisms such as GPR15 and CCR10 (23).

The location of leukocyte recruitment in tissues is thought to be in specialised regions of the vasculature known as high-endothelial venules (HEVs) or post-capillary venules (PCVs) (13). These vessels have the specific machinery required to enable the process of leukocyte extravasation, and in the gut this specifically includes Madcam1, which is the ligand for α4β7 (24, 25). An antibody targeting Madcam1, however, did not have the same efficacy as vedolizumab. In summary, recruitment to the intestine and considering the inflow of leukocytes is a strategy that has proven effective in the development of gut-specific therapeutics for IBD (26).

We next turn our attention to what happens once the cells enter the intestinal tissue, as well as what occurs to the tissue-resident cells that are already in the intestine. The success of anti-proliferative medications such as azathioprine in the maintenance of remission in IBD provides evidence that interfering with cell division is a viable strategy to reduce leukocyte accumulation in the tissue (27),

again also sharing efficacy across other disease indications. With regards to cell differentiation, cytokines in the tissue play a large role in the differentiation of immune cells in IBD (7, 28, 29). This is an expansive area of study and is only briefly mentioned here for completeness. Impairment of immune cell death is also implicated in IBD (30) and anti-TNFα therapy has shown to be effective in part due to inducing apoptosis in T cells and monocytes (31).

Cellular emigration is a concept is relatively understudied compared to the others mentioned. Emigration of cells from the tissue to the draining lymph node is mediated via the lymphatic vasculature, which also plays a crucial role in orchestrating the adaptive immune response (32). However, the stimulation of exit of immune cells from the tissue has no specific therapy that targets it that is in clinical use for inflammatory disorders.

Cellular emigration as a concept is increasingly being recognised from the perspective lymphocyte recirculation from the lymph node to the tissue. In particular, the modulation of sphingosine-1-phosphate (S1P) has recently emerged as an effective therapy in IBD (33). This signalling sphingolipid molecule is required to allow leukocytes to exit lymph nodes and return to the circulation. This depends on a gradient of S1P in the efferent lymph and S1P receptors to be expressed on leukocytes. S1P agonists have emerged that induce downregulation of the S1P receptor on the leukocyte surface therefore making leukocytes insensitive to the S1P that normally permits exit (34). This prevents leukocytes recirculating from the lymph nodes to the intestine. However, the effect of S1P modulation on emigration from the tissue to the lymph node has not received as much attention in the literature. However, a recent study conclusively showed that S1P modulation using the functional antagonist FTY720 before photoconverting the descending colon completely stopped the turnover of immune cells 24 hours later (35), highlighting that S1P also prevents cellular exit from the tissue.

One strategy to promote cellular emigration is stimulating the lymphatic vasculature to expand (lymphangiogenesis). This can be done by administering the relevant lymphangiogenic growth factors for these vessels. The most well-described is VEGF-C, which stimulates lymphangiogenesis (36). A clinical adenoviral gene therapy delivery system for VEGF-C was trialled in combination with lymph node transfer treatment for patients who had lymphoedema following breast cancer reconstruction and was well-tolerated (37), and studies are ongoing in this patient cohort (38). However, this has not yet been trialled in the context of inflammation.

As emigration from the tissue is mediated by the lymphatic vasculature, we will turn to describe this system in more detail. First this will be in the context of homeostasis, and then the role of the lymphatic system in intestinal inflammation will be discussed. Finally, we will focus in on the remaining unknowns in the field, which form the objectives of this thesis.

1.4 Overview of intestinal lymphatic anatomy and physiology

1.4.1 Macroanatomy

The lymphatic system is a vascular network distributed throughout the body that initiates from blind-ended lymphatic capillaries in tissue beds which converge to larger collecting vessels that travel to their draining lymph node. Following the lymph node, efferent collecting vessels ultimately converge with the thoracic duct. The thoracic duct delivers lymph across the lymphovenous valve to return lymph fluid and cargo to the venous circulation. In intestinal homeostasis, these lymphatic capillaries are initially found in the lacteals of the small intestine (39) and travel through the mesentery to reach their draining lymph nodes. The lymphatic capillaries of the colon are less well-described (40). The murine small intestine has a relatively straightforward drainage pattern to the mesenteric lymph nodes; however, the colon is more complex with the ascending and transverse colon draining to the pancreatic-duodenal lymph node and the descending and distal colon draining to the caudal and iliac lymph nodes (41). In mice, most mesenteric lymph nodes are found in a chain whereas in humans they are distributed more variably within the mesentery. One conceptually important point is that distinct lymph nodes drain different regions of the intestine (42), which may then impact upon immune effector function (41). A more recent discovery is that there are specialised lymphatic capillaries in the mesentery that bypass the mesenteric lymph node and transport antigens from the peritoneum directly to the mediastinal lymph nodes (43). There are excellent in-depth anatomical descriptions of the intestinal lymphatic vasculature elsewhere (39, 44), but again the focus is on the small intestine, with little description of the corresponding arrangement in the colon.

1.4.2 Microanatomy

The lymphatic system initially starts with lymphatic capillaries comprised of endothelial cells, with most evidence pointing towards a venous endothelial cell origin (45), but with some key differences. The cells themselves can loosely overlap with each other in 'button' junctions, which allows cells and fluid to intravasate into the lumen, whilst in inflammation this can change to a zipper conformation and reduce permeability (46). This stands in contrast with the blood endothelium, which supports cellular extravasation (47). Once lymph has entered these capillaries they come together to form larger collecting lymphatic vessels (CLVs) that contain valves, analogous to veins, to aid unidirectional flow towards the systemic circulation via draining lymph nodes (48) and the units between valves are called 'lymphangions' (49). The CLVs have smooth muscle cells encasing their walls to promote pumping of lymph towards the periphery. CLVs have a less permeable conformation with 'zipper' junctions that prevent extravasation of high molecular weight lymphatic contents. Furthermore, it is important to note the presence of several distinct lymphoid tissues in the intestine regulating mucosal immunity. These are reviewed elsewhere (50), yet the lymphatic drainage from these structures in the small intestine and colon remain to be clearly mapped. However, older studies support the notion of a lymphatic network further from the colon lumen, compared to that in the small intestine.

1.4.3 Physiology

The intestinal lymphatic system has wide-ranging roles in physiology. It maintains extracellular fluid homeostasis and removes substances via the lymph, and specifically in the small intestine it is also responsible for lipid absorption via lacteals (51, 52). However, the specific products absorbed in colonic lymph is unclear. Furthermore, recent studies showed that intestinal lymphatic endothelial cells themselves can produce factors to support the intestinal stem cell niche in association with

intestinal fibroblasts (53–55), highlighting a role beyond simply functioning as a conduit. Finally, the lymph contains migratory cells of the immune system responsible for priming adaptive immune responses in the mesenteric lymph nodes (32).

1.4.4 Leukocyte emigration via the lymphatic vasculature

The understanding that lymphocytes recirculate around the body via the lymph to the blood was highlighted by seminal work by Gowans in 1957 (56). He created a method to collect lymph from the thoracic duct of rats and then return this to the femoral vein. He found that returning cell-free lymph or dead cells to the venous circulation resulted in fewer cells collected from the thoracic duct over a period of four days. In comparison, when he returned live cells from the lymph back to the venous circulation, the cellular output from thoracic duct remained constant over the same four-day period. Further experiments were designed that traced the fate of the cells moving from the lymph to the systemic circulation (57). This was done using tritiated adenosine to label the RNA of cells isolated from the thoracic duct and reinfusing these cells into the venous circulation. This study highlighted that most labelled cells that were reinfused were able to home to the lymph nodes and then recirculate via the lymph, with only the minority of infused cells homing to tissues in the steady state (57). It was hypothesised that there was a special affinity of the labelled lymphocytes to the endothelium of the post-capillary venules of the lymph node, but the mechanisms were not clear at the time. Since then, the process of leukocytes crossing the blood vascular endothelium has been characterised in detail, involving steps such as attaching to the endothelium, rolling, arrest, and migration itself (58, 59).

In contrast, the mechanisms of leukocyte extravasation from the tissue to lymphatic vessels has received less attention but is increasingly understood in a parallel way (47, 60–62). Steps include

movement of the cells within the interstitial space of the tissue, followed by entry into and crawling within the lymphatic vessels. This movement is slow within the lymphatic capillaries but once the cells reach the larger collecting vessels the flow is passive and much faster. The main signal that attract cells to lymphatic vessels is the chemokine CCL21, which is constitutively expressed by lymphatic endothelial cells (63). CCL21 binds to CCR7, which expressed by various cells including dendritic cells (64, 65). CCL21 is maintained as a gradient within the perilymphatic interstitium, and this is highlighted by dendritic cells demonstrating directional migration towards lymphatic endothelial cells from up to 90 microns away (66).

To understand the cellular trafficking via the lymph, it is possible to collect the fluid and then profile the cells that are in it. However, once dendritic cells enter lymph nodes they die after a few days (65). Therefore, if one wants to profile lymph draining from the intestine, the lymphatic vessels proximal to the lymph node should be cannulated, which is only possible in larger animals. To overcome this, a method was developed to remove the mesenteric lymph nodes in rats and allow the animals to heal (67). After six weeks the animals recover and new vessels form that result in drainage of the lymph directly to the thoracic duct, and so populations of cells that leave the intestine can be profiled in this way. More recently, this technique was developed to be used in mice, where multiple populations of migratory intestinal dendritic cells have been observed (68). Finally, it is important to remember that the composition of afferent lymph and efferent lymph differ by around 10-fold magnitude in cell concentration, and the majority of cells in efferent lymph are naïve lymphocytes, that would have initially arrived to lymph node via the high endothelial venule (69).

1.5 Lymphatics in intestinal inflammation

As outlined previously, several drug classes exist to treat IBD; however, primary non-response and secondary loss of response to all current and experimental therapies remains a major clinical challenge. The variable response to treatment suggests heterogeneity in the underlying disease processes and highlights the need for a deeper understanding of the cellular basis of IBD to better treat patients who do not respond to current therapies. In particular, the lymphatics in the colon and mesentery have been neglected, despite several lines of evidence for their relevance, which we will explore.

We will consider human and animal studies in parallel and use human observations as a basis for discussion. We will broadly move from superficial to deep structures i.e., lymphatics in the intestinal wall followed by mesenteric lymphatics. Firstly, we will consider the increased lymphatic density observed in intestinal inflammation, then we will consider the concept of lymphatic 'obstruction' both in the intestine and the mesentery and how this relates to inflammation. Finally, we will consider lymphatic leakage in the mesentery and the role of creeping fat in the pathology of intestinal inflammation.

1.5.1 General principles of lymphatic changes in inflammation

We will first consider general principles of lymphatic changes in the context of inflammation before a more detailed consideration related to the intestine. Inflammation can affect vascular permeability of lymphatic vessels, as well as their pumping activity, via several cytokines (70). Of note, TNFα is able to upregulate molecules such as intercellular adhesion molecule 1 (ICAM-1), vascular cell adhesion molecule 1 (VCAM-1), and E-selectin, in lymphatic endothelial cells, which can stimulate dendritic cell

adhesion and transmigration in vitro (71). Leukocytes in tissues typically first enter the capillaries where they crawl slowly, followed by faster flow in the lymphatic collectors (62). Interestingly, in inflammation, an alternative route for dendritic cells to traffic directly into lymphatic collectors has been discovered (72), enabling cells to reach the lymph node more rapidly, but with unknown functional significance.

A further change in lymphatics in inflammation is the conformation of the junctions between neighbouring cells. Typically, lymphatic capillaries at steady state have 'button' junctions. In inflammation, lymphatics in the trachea have been observed to form zipper junctions following *Mycoplasma pulmonis* infection (73, 74). This may aggravate tissue oedema and retain dendritic cells at the site of the tissue, but the precise implications are yet to be mapped out. An example of button to zipper transition in the lacteals of the small intestine demonstrate that this results in reduced lipid absorption, and may be an avenue to design novel drugs to promote weight loss (75).

The lymph also changes in composition in the context of inflammation. When efferent lymph is sampled from the draining lymph node following subcutaneous pro-inflammatory cytokine administration, lymphocytes are initially retained within the lymph node, followed by elevated cellular output (76). This is thought to aid in the induction of immune responses by facilitating cellular interactions between immune cells. Having considered these general principles, we will now move onto the specifics of how intestinal inflammation affects the lymphatics.

1.5.2 Increased lymphatic vessel density in inflammatory bowel disease

Patients with inflammatory bowel diseases have structural changes in intestinal lymphatics. Multiple histological analyses show increased lymphatic density in the intestine (77–82) and we will highlight points of interest from these studies.

Kaiserling et al. (81) studied the histology from patients with UC who had undergone colectomy. They found increased lymphatics in the submucosa that were sometimes associated with lymphoid follicles, challenging the dogma that UC is solely a mucosal disease. Fogt et al. (78) were in agreement as they looked at the colon in UC and found again that in treated UC the lymphatic vessels were only found in the submucosa, but in inflamed tissue lymphatics were found more superficially in the lamina propria.

Pedica et al. (79) used D2-40 antibodies targeting podoplanin to look at the ileum and colon of patients with Crohn's disease compared to other intestinal diseases and healthy controls with a focus on the submucosa. They found an increased number of submucosal lymphatics in IBD, and that this was significantly more in Crohn's disease compared to UC (as well as other intestinal disorders). Rahier et al. (80) looked at ileal and colonic samples from CD and UC, as well as controls, and found that there was an increased lymphatic vessel density in both diseases. Intriguingly when divided into mucosal and submucosal changes it was found that UC had a specific increase in the mucosal lymphatics and a decrease in the submucosal lymphatics compared to colonic controls, which stands in contrast to the earlier studies suggesting increased submucosal lymphangiogenesis in UC. Therefore, the discrepancies in these findings warrant further clarification, particularly as imaging technologies have progressed since the time of these studies.

It is hard to conclude whether increased lymphatics contribute towards disease pathology or healing from these observational studies. Two studies that assess patients over time give a clue that lymphangiogenesis may be of overall benefit. The first study compared patients with Crohn's disease who relapsed after surgery to those who did not, and showed that if there was evidence of lymphangiogenesis in the intestine at the time of ileal resection, this reduced risk of recurrence (83). Similar conclusions were reached in another study that conducted histological assessments of the resection specimens of patients with Crohn's disease. They found that an increased lymphatic vessel density at the time of resection resulted in reduced chances of endoscopic recurrence at one year (84). These studies point towards a role that lymphangiogenesis plays a protective role in intestinal inflammation.

A key limitation to bear in mind whilst interpreting these data is that they all use two-dimensional imaging modalities to gain insights into a three-dimensional structure, so the conclusions reached should be interpreted cautiously. It can be envisaged that simply dilating the lymphatics can itself result in a larger perceived surface area, even when lymphatic endothelial cells are not proliferating per se. Modern advances in imaging technologies such as the use of light-sheet microscopy will enable the study of these structures and overcome these limitations (85–88).

These histological studies have demonstrated that there is an association between inflammation and lymphangiogenesis. Clearly the timing of these events is crucial and studies from patients inevitably give us only a few timepoints from which we can draw limited conclusions. This leaves it unclear as to whether lymphatics are bystanders or are playing a primary role in helping or hindering the resolution of inflammation in IBD. To shed further light on this, we will turn to studies in animal models, where dynamic datapoints can be considered in conjunction with manipulating the lymphatic system.

1.5.3 Stimulation with pro-lymphangiogenic factors improves inflammation

Stimulation of lymphangiogenesis in mouse models via systemic delivery of adenovirus expressing human vascular endothelial growth factor C (VEGF-C), the key factor identified to promote lymphangiogenesis, has been shown to both increase lymphatic vessel density and ameliorate inflammation in mouse models of colitis (82, 89). Interestingly the group found that depleting macrophages reduced the beneficial effect of VEGF-C and identified these macrophages as a resolving phenotype dependent on STAT6. This raises the question as to what aspect of VEGF-C is aiding the resolution of inflammation. It is interesting to note the broad applicability of stimulating lymphangiogenesis across different organs, as stimulation of VEGF-C also reduces inflammation in the skin (90), joint (91) and heart (92). The converse idea of inhibiting the VEGF-C receptor, VEGFR3 (FLT4), both blocks lymphatic vessel proliferation and worsens murine colitis (82, 93). Again, this is applicable across organ systems as blocking VEGF-C also worsens skin inflammation (94) and arthritis (95).

In summary, there are multiple lines of evidence that stimulating lymphangiogenesis via VEGF-C ameliorates inflammation whilst blocking VEGF-C exacerbates inflammation. However, as highlighted, it is difficult to draw strong conclusions on how much of the protective effect seen is down to lymphatic changes rather than other targets of VEGF-C. This is especially relevant with the lack of direct lymphatic outflow assessment from the colon.

1.5.4 Lymphatic obstruction in the intestine and mesentery plays a role in IBD

Lymphatic obstruction as a concept has been encountered in patients with various forms of lymphoedema (96), and a parallel question in the field of IBD is whether a similar phenomenon may be present which prevents exit of cells and fluid from the intestine and contributes towards the failure

of resolution of inflammation. A key hypothesis to consider in light of this is whether mucosal pathology is in fact a secondary event to lymphatic obstruction in Crohn's disease, which is reviewed elsewhere (97). Whilst unlikely to be a primary cause of IBD, this idea warrants consideration as a contributing factor to intestinal pathology.

Evidence for lymphatic obstruction exists in both the intestine and the mesentery in intestinal inflammation. Submucosal obstruction in ileal Crohn's disease has been noted and the cause of obstruction was initially thought to be lymphatic endothelial cells themselves, but immunohistochemical studies have shown $CD68^{+}$ macrophages that appear to be trapped in lymphatics which may be contributing towards obstruction (98). Moreover, lymphocytes are present more proximally in the lymphatic vessels in these specimens, suggesting that their exit is impaired (98). It is possible that macrophages accumulate at areas of endothelial damage, and lead to subsequent granuloma formation and lymphatic obstruction in Crohn's disease (99).

Importantly, these obstructive changes are found not only in the intestine but also the mesentery. Obstruction of the mesenteric lymphatics has been described in resection specimens from patients with Crohn's disease 40 years ago (100). A key study identified the cause of this obstruction to be lymphoid aggregates in the mesentery of patients with IBD, which may result in impingement of lymphatic drainage (101). The lymphatics in the mesentery have been studied meticulously in this work in which we see a clear association between the presence of IBD and lymphoid aggregates representing tertiary lymphoid organs (TLOs) in close proximity to the lymphatics that drain to the mesenteric lymph nodes. With this observational study it is hard to conclude whether these TLO structures are a primary pathology, or if they are forming in response to inflammation-induced lymphatic leakage of immune cells that are initially destined to reach the lymph node and prime a secondary immune response. Further work on this theme showed that a TNFα-dependent model of

murine ileal inflammation ($TNF^{\Delta ARE}$) developed analogous formation of lymphoid structures in the mesenteric lymphatics, specifically associated with sites of lymphatic valves. Tracer injections via cannulation of these vessels demonstrated impaired flow to the draining lymph node, lymphatic leakage into the mesentery and reversal of lymphatic flow (102). This study measured the direct relevance of lymphatic drainage using an intravital system in the small intestine, but this has not been done in a similar way in the colon.

1.5.5 Surgical lymphatic obstruction leads to inflammation and fibrosis

We will now turn from human lymphatic obstruction to consider surgically induced lymphatic obstruction in animal models. Studies from the 1930s in which the mesenteric lymphatics of dogs were selectively injected with sclerosant found marked intestinal wall thickening and oedema, particularly in the submucosal and muscular layers, which was enhanced with intravenous *E. coli* administration (103). Thrombosed lymphatics and lacteals that were engorged with large mononuclear cells were noted. This experimental model of intestinal lymphoedema resembled the regional enteritis described by Crohn et al. not long earlier (104).

Kalima et al. obstructed the mesenteric ileal lymphatics of 40 rats and found that this resulted in many features in common with regional enteritis (105). This study was disputed by Heatley et al. who claimed that despite obstruction by ligating mesenteric lymphatic vessels both at the bowel wall and near the root of the mesentery in rats, as well as resecting the mesenteric lymph nodes, this did not reproduce the pathological changes seen with Crohn's disease, and so questioned whether lymphatic obstruction was a key factor in the pathogenesis (100). A more recent study in non-human primates with surgical ligation of lymphatic vessels led to intestinal inflammation (106), highlighting that

lymphatic obstruction leading to inflammation may be variable in different species, but also that no clear conclusion exists on this topic.

We have considered lymphatic obstruction in the intestine and mesentery. For completion in our discussion, we are unsure whether the lymph nodes themselves are responsible for any degree of lymphatic obstruction and this is yet to be determined. Open questions remain as to what functional effect lymphatic obstruction is having and whether this skews the immune response.

1.5.6 Mesenteric changes and fat wrapping in the context of lymphatics

We have considered the role of changes in the number of lymphatic vessels and the link between physical obstruction and intestinal inflammation. Now we will turn to how functional changes in the mesenteric lymphatics may affect their ability to resolve inflammation.

As outlined earlier there are changes found in the intestinal mesentery in inflammatory bowel disease, and so an obvious question is to consider whether resecting this tissue makes any difference to patient outcome. The pioneering work of Coffey et al. utilised approaches that were developed for colorectal cancer resection (where mesenteric and lymph node resection is required in order to reduce post-operative disease recurrence) and applied this to ileal resection in Crohn's disease (107). In this setting, limited intestinal resection is the conventional surgical approach; however, this study demonstrates that there is a significantly reduced risk of recurrence if the mesentery is included in the resection (107). Furthermore, they identified a correlation between severity of inflammation in the mesentery and the intestine itself, providing evidence that Crohn's disease does not affect the intestine in isolation (107). Prospective randomised-controlled trials on this subject are ongoing.

A Japanese radiological study confirmed the significance of mesenteric inflammation by showing a strong correlation between mesenteric changes on cross-sectional CT scan with that of endoscopic changes of the intestinal mucosa in inflammation (108). Furthermore, another study has shown that persistent MRI changes are seen in patients with Crohn's disease despite having improvement in endoscopic appearances (109). This highlights that relying on clinical and endoscopic outcome measures that are used for Crohn's disease are insufficient to tell whether the pathology in question has been fully treated. A possible clinical aim is to consider more than just 'mucosal healing', but also 'mesenteric healing' (110). However, it is unknown as to whether mesenteric healing in isolation can be achieved, as the changes identified tend to suggest chronicity of inflammation.

The interaction between lymphatic vessels and adipose inflammation in the mesentery can also be considered, especially since small intestinal lymph in particular is rich in absorbed dietary lipid. It has long been thought that the collecting lymphatic vessels simply transport lymph from the tissue to the draining lymph node. However, it is increasingly recognised that lymph leakage can occur and that this can contribute towards adipose tissue inflammation (111). Furthermore, a key study highlights how long-term immune dysfunction may follow acute murine gastrointestinal infection via effects on mesenteric lymphatics (112). This study demonstrated that an acute infective or non-infective insult to the intestine can lead to chronic inflammatory changes in the mesentery and leads to leakage of cells from the mesenteric lymphatics, such as dendritic cells, into the mesentery itself. Of note, this change lasted for many months after the inflammatory insult was removed. It is tempting to speculate that this change in the mesenteric lymphatics may skew the immune response preventing normal mechanisms of immune tolerance, which may be a contributing factor to the chronic inflammation seen in IBD. Furthermore, it highlights how mucosal insults may affect deeper structures such as the mesentery via the lymphatic vessels.

Another intriguing area of IBD pathogenesis that remains incompletely understood is creeping fat. This is a curious phenomenon unique to Crohn's disease where mesenteric fat wraps around inflamed segments of intestine and this correlates with the degree of mucosal inflammation (107). Creeping fat has been a long-recognised feature of Crohn's disease but has more recently been thoroughly investigated (113). This study notes the presence of live bacteria in mesenteric adipose tissue of patients *without* IBD, and a different specific bacterial population in the creeping fat of patients with Crohn's disease. Another study has demonstrated the presence of bacteria in mesenteric adipose tissue from patients undergoing obesity surgery, and that stimulating adipocytes with bacterial DNA promoted the expression of the inflammatory cytokines TNFα and IL-6. It was also found that different organisms were found depending on whether patient's diabetic status (114). It is likely that these organisms translocate via the lymphatic vessels but this has not been shown. Furthermore, live bacteria can travel within lymphatic vessels as a conduit to bloodstream infection (115). Indeed, a study of intestinal and mesenteric resection tissue from patients with Crohn's disease imaged the mesenteric lymphatic vessels and found that they lacked tight junction proteins which may lead to leakage of mesenteric lymphatics (116). This may result in bacteria reaching these adipose tissue compartments and perhaps playing a role in the initiation of the creeping fat response seen in Crohn's disease.

1.5.7 Functional changes in lymphatics also impair resolution of inflammation

We will conclude this section by touching on other functional changes in the lymphatics that may impair the resolution of inflammation. Mice deficient in the anti-inflammatory decoy chemokine receptor D6 (also known as atypical chemokine receptor 2 or ACKR2), which is highly expressed by lymphatic endothelial cells, are more susceptible to dextran sulfate sodium (DSS)-induced colitis and have increased circulating levels of pro-inflammatory chemokines (117). Furthermore, Foxc2 mutant

mice that have impaired lymphatic drainage function due to decreased expression of Foxc2 in mesenteric collecting vessel valves develop worse intestinal inflammation in a DSS colitis model than wild-type mice (118, 119) The question of whether impaired lymphatic pumping function occurs in inflammatory bowel disease (IBD) has also been raised (120).

We have several pieces of evidence that sheds light on the relationship between the lymphatic system and intestinal inflammation. We will now conclude our discussion by considering approaches to therapeutically manipulating this system in order to aid the resolution of intestinal inflammation.

1.5.8 Resolution of intestinal inflammation and therapeutic avenues

The idea that stimulation of resolution is distinct to simply removing the inflammatory stimulus is an established idea in the field of inflammation biology (121, 122). As we have established that the presence of lymphangiogenesis in intestinal inflammation appears to be beneficial, perhaps stimulating this process is an example of such an active mechanism of resolution. However, it is especially important to dissect the differential effects of lymphangiogenesis within the intestinal tissue, at sites of lymphoid structure formation in the mesentery, and within the lymph nodes, as these are all likely to lead to different effects.

1.5.9 Regulation of intestinal lymphangiogenesis

If we would like to consider therapeutically manipulating the colonic lymphatic vessels, we must understand the regulation of intestinal lymphangiogenesis. VEGF-C is one of the most well-recognised and studied lymphangiogenic factors and VEGF-C and VEGFR3 (VEGF-C's receptor) signalling are increased in the colon of patients with IBD (82). However, several other factors that regulate

lymphangiogenesis have been described such as VEGF-A, hepatocyte growth factor, insulin-like growth factors 1 and 2, platelet-derived growth factor B (PDGF-B), and fibroblast growth factor (123).

It is important to identify which cells express these lymphangiogenic factors and the majority of studies have focused on VEGF-C, highlighting differing cellular sources. Macrophages have been implicated as a source of VEGF-C in murine models of colitis and interestingly when they are removed there is less lymphangiogenesis but also less inflammation (124). However, smooth muscle cells in the murine small intestine produce VEGF-C required for lymphatic vessel maintenance (125). Other cellular sources include ACKR1^{+} endothelial cells from human ileum in Crohn's disease (126), and myofibroblasts from the murine colon (127) have been implicated from recent single cell RNA sequencing studies, highlighting the complexity of the regulation of lymphangiogenesis in the intestine. Further study is required to particularly identify whether factors other than VEGF-C are playing a role in inflammation-induced lymphangiogenesis in the intestine, as well as the cells that produce them.

1.6 Conclusion

Consideration of the outflow of cells and fluid from the colon and its regulation is an understudied aspect in relation to IBD. This is despite lymphatic dysfunction being implicated in the pathogenesis of IBD by numerous studies. Furthermore, most work within this field has been done on the role of the lymphatics in the small intestine rather than the colon, with the role of colonic lymphatics remaining relatively obscure, beyond the general role of lymphatics across all tissues.

Furthermore, from all the studies outlined, very few have considered the 3D architecture of the lymphatics in relation to the colonic tissue. We believe that this fundamentally three-dimensional structure can only be fully appreciated with more modern forms of imaging. Furthermore, data assessing functional interstitial fluid drainage from the intestine is limited, and this is especially true in the colon. Therefore, we believe this is a ripe field for exploration, which we set out to do in this thesis as per the outlined aims in the next section.

1.7 Hypotheses and thesis aims

1.7.1 Hypotheses

1. **Lymphatic endothelial cells change in number and function in colitis**
2. **The pathway of lymphatic drainage is distinct between the small intestine and the colon**

1.7.2 Thesis aims

1. **Create a cellular atlas of lymphatic endothelial cells in the colon in health and colitis**
    - *Chapter 3*
2. **Elucidate the 3D anatomy of the colonic lymphatic vasculature and the interstitial outflow pathways from the colon**
    - *Chapter 4*
3. **Understand how the micro-anatomical arrangement of the colon promotes tissue drainage**
    - *Chapter 5*

2 Methods

2.1 Mice

2.1.1 Strains

University of Oxford

Wild-type (WT) C57BL/6 (B6) mice were bred and maintained in individually ventilated cages (IVCs) under specific pathogen-free (SPF) conditions in an accredited animal facility at the University of Oxford. They received food and water ad libitum and had 12-hour light cycles. Prox1-CreER^{T2} mice (128) were purchased from The Jackson Laboratory (#022075) and bred and maintained under the same conditions. tdTomato reporter (#007914) and diphteria toxin receptor-flox (#007900) mice were also purchase from The Jackson Laboratory.

Both females and males were used in the experiments and were at least six weeks old when used. Mice were negative for *Helicobacter spp.* and other known intestinal pathogens. All procedures at the University of Oxford were conducted in accordance with the UK Scientific Procedures Act of 1986 by a Personal Licence holder under a Project License authorised by the UK Home office (PPL: P508FFA1F).

Washington University in St Louis

Animal experiments were undertaken in accordance with Institutional Animal Care and Use Committee (IACUC) approval with IACUC approval number: 20170154. Human tissue work was authorised by the Internal Review Board (IRB), with IRB approval number: 201111038. Prox1-GFP mice used in this study were kindly donated by Professor Young-Kwon Hong.

2.1.2 Genotyping

Genotyping was conducted on Prox1-Cre-ER^{T2} mice and tdTomato reporter mice by extracting DNA from earclips, followed by PCR amplification of the regions of interest using specific primers then running on a 1.5% agarose gel. Genotyping was also done using the Transnetyx service which we ensured matched the in-house genotyping results before utilising this further.

2.1.3 In vivo colitis models

2.5% DSS (MP Biomedicals, CA, US) was administered to mice in their drinking water for six days. After this, mice were returned to normal drinking water for the remainder of the experiment. Mouse weights were monitored daily throughout the experiment to ensure weight loss did not exceed 20%. Animal experiments were not blinded due to practicalities of running the experiments.

2.1.4 Histopathological scoring

Five micron sections were prepared using a microtome and stained with haematoxylin and eosin from colonic tissue samples fixed in 4% PFA overnight. Scoring was performed according to the criteria described below. Proximal, middle, and distal colonic regions were scored separately.

EPITHELIUM HYPERPLASIA and/or GOBLET CELL DEPLETION

0	None	None
1	Mild (1.5x)	Mild (25%)
2	Moderate (2-3x)	Marked (25-50%)
3	Severe (>3x)	Substantial (>50%)

INFLAMMATION IN LAMINA PROPRIA

0	None - few leucocytes
1	Mild - some increase in leucocytes at tips of crypts OR many lymphoid follicles
2	Moderate - marked infiltrate (notable broadening of crypt)
3	Severe - dense infiltrate throughout

AREA AFFECTED (% of section)

0	None
1	up to 25%
2	25-50%
3	>50%

MARKERS OF SEVERE INFLAMMATION

0	None
1	Submucosal inflammation OR Few crypt abscesses (<5)
2	Submucosal inflammation AND Few crypt abscesses (<5)
2	Many crypt abscesses (>5) OR Extensive submucosal inflammation
3	Many crypt abscesses (>5) AND Extensive submucosal inflammation
3	Ulceration OR Extensive fibrosis

2.2 Isolation and analysis of cells

2.2.1 Isolation of colonic lymphatic endothelial cells and related cell types

Epithelial wash buffer: RPMI 1640 Medium supplemented with 1% Penicillin-Streptomycin, 10 mM HEPES, 5% fetal calf serum (FCS), and 5 mM EDTA.

Digest solution: RPMI 1640 Medium supplemented with 1% Penicillin-Streptomycin, 10 mM HEPES, Liberase TL 100 µg/ml and DNAse I 40 µg/ml.

FACS buffer: PBS supplemented with 1% BSA and 5 mM EDTA.

The colons of mice were removed following sacrifice using a CO2 chamber. The caecum was removed and discarded, and colons were cut open longitudinally using scissors taking care to remove as much mesenteric fat as possible. The remaining faeces contents were cleaned out. At this stage, small pieces from proximal, middle, and distal colon were cut with a scalpel and taken for histology (put into 4% PFA) and RNA (put into RNA later). The remaining colon (most of the tissue) was immediately placed into 50 ml Falcon tubes containing 15 ml epithelial wash buffer on ice until all the colons for the experiment had been processed. Following this, samples were incubated in epithelial wash buffer with agitation in a shaking incubator at 200 rpm and at 37°C for 30 minutes to aid in the removal of epithelial cells and associated mucous. The samples were then each vortexed for 10 seconds before replacing the epithelial wash solution and proceeding with two further washes for 15 minutes each following the same steps as previously, resulting in a total of three epithelial washes. The supernatant was noted to be clearer each wash as fewer epithelial cells were shed with each successive wash. After this step, the colon pieces were washed twice in cold digest solution without any enzyme or DNAse I to remove the EDTA, which inhibits the enzymatic activity of the digestion enzyme if present.

Next, the colon pieces were cut into very small pieces on a Petri dish to aid with the digestion, and then added to 50 ml Falcon tubes containing 10 ml of digest solution. The samples were then incubated again in a shaking incubator at 200 rpm at 37°C for 30 minutes. Following this, the cells were filtered through mesh into 10 ml of ice-cold FACS buffer and spun down at 500 x *g* for five minutes at 4°C with maximum acceleration and maximum deceleration prior to being resuspended in a further 10 ml of ice-cold FACS buffer. The remaining pieces on the mesh were collected and added to the same tube with a top up of digestion solution for two further rounds, giving a total of three rounds of digestion to ensure the whole tissue had been digested. Following the full digestion of the tissue, a fixed number of counting beads were added to the sample to be able to count the number of cells and then the pellets were transferred to a 96-well V-bottom plate where they could be more easily worked with for the remaining steps.

2.2.2 Cell staining

Cell suspensions were first treated with Fc block in FACS buffer for 20 minutes on ice in the dark in the same 96-well V-bottom plate they were transferred into. Following this they were spun down at 500 x *g* for five minutes at 4°C with maximum acceleration and maximum deceleration prior to being stained with Fixable Viability Dye e780 (eBioscience) in PBS for 20 minutes on ice in the dark. After another spin at 500 x *g* for five minutes the FACS antibodies were incubated with the cells in FACS buffer for 20 minutes on ice in the dark. Finally, the cells were spun down the same way and were then resuspended in FACS tubes in 300 µl FACS buffer containing DAPI, which were then ready to be analysed on the flow cytometer.

2.2.3 Flow cytometry

Cells were vortexed briefly prior to running on BD LSRFortessa. The acquired data was then analysed on FlowJo version 10.9 (BD).

2.2.4 Cell sorting

Cells were prepared identically to how they were prepared for flow cytometry analysis and were sorted using BD FACSAria III and BD FACSDiva 8.0.1. The gating strategy for specific sorts are in the relevant results chapters.

2.2.5 Antibodies and reagents

Antibody or reagent	**Concentration**	**Catalogue number or antibody clone**
Fixable Viability Dye eFluor 780	1:1000	65-0865-18
CD16/CD32 Monoclonal Antibody (Fc R block)	1:200	14-0161-86
DAPI	10 pg/ml	62248
FITC-EpCAM	1:200	G8.8
PE-Cy7-Podoplanin	1:200	8.1.1
APC-Pdgfra	1:200	APA5
BV605-CD31	1:200	390
BV711-CD45	1:200	30-F11

2.3 Gene expression analysis

2.3.1 RNA extraction from whole tissue

RNA was extracted from samples using Quiagen RNeasy kits as per the manufacturer's instructions.

2.3.2 RNA extraction from sorted cells

Cells were directly sorted into Eppendorf tubes containing 300 µl RNA lysis buffer and RNA was isolated using Zymo Quick RNA 96 kits as per the manufacturer's instructions.

2.3.3 qRT-PCR protocol

2.9 µl of cDNA of the relevant sample was added to a 384 well plate. 0.6 µl of appropriate forward and reverse TaqMan primers and 3 µl PrecisionPLUS qPCR Mastermix was added to each well and the samples were run on ViiA 7 Real-Time PCR System. Data were analysed using GraphPad Prism 10.

2.3.4 Bulk RNA sequencing library preparation

Libraries were prepared using NEBNext ultra-low input RNA library prep with 1 ng of RNA per sample and sequenced on a NovaSeq6000 (150 paired-end) by the Oxford Genomics Centre.

2.3.5 Single cell RNA sequencing library preparation

Libraries were prepared using Chromium Next GEM Single Cell 3' Reagents with Feature Barcode technology by the single-cell facility at the Kennedy Institute of Rheumatolgy (Moustafa Attar).

2.4 Imaging

2.4.1 2D immunohistochemistry

Formalin-fixed paraffin-embedded (FFPE) slides of interest were dewaxed with a Tissue-Tek DRS 2000 through gradients (Xylene, Ethanol, Water) prior to immersing in 1X Target Retrieval Solution (Dako) and incubated for 15 minutes in a microwave at full temperature. Washing buffer was prepared (PBS 1X with 0.05% Tween) and the samples were then cooled to room temperature on ice and blocked with Avidin/Biotin block as per the manufacturer's instructions (Vector Laboratories). The slides were then blocked with 5% bovine serum albumin + 5% goat serum (serum of species in which secondary antibody has been raised) for one hour at room temperature. Primary antibodies of the listed concentrations were applied to the slides in the same blocking buffer as the previous step and incubated at 4°C overnight with damp filter paper to create a humidified environment. The following day the slides were washed three times with washing buffer and the secondary antibody (biotinylated-goat anti-rat antibody) at 1:500 dilution was added in washing buffer for two hours at room temperature. After washing three times with washing buffer, Avidin/HRP was added to the samples for 30 minutes at room temperature. After washing again three times, DAB (Vector Laboratories) was added to each section and incubated for 15 minutes. Finally, the slides were counterstained in filtered Mayer's Haematoxylin (Sigma) for two minutes and then left under running tap water for a few minutes. The slides were dehydrated through alcohol to Xylene using Tissue-Tek DRS 2000 and automatically mounted with DPX mountant.

2.4.2 Tissue clearing and 3D histology

After euthanising the mouse, it was perfused with 10 ml PBS then perfusion-fixed with 10 ml 4% PFA/30% sucrose. Following this, the tissue of interest was resected and fixed in 4% PFA shaking overnight at 4°C. The following day, the sample was washed three times for five minutes in PBS then permeabilised using 10% CHAPS/25% NMDEA shaking overnight at 4°C. The following day the samples were again washed three times for five minutes in PBS then the tissue was blocked using 5% PBS/BSA + 5% donkey serum + 1% Triton-X 100 (solutions were mixed and filtered prior to use) shaking overnight at room temperature. The next day the tissue was rinsed in PBS + 0.2% Tween-20 then primary antibody was added at the desired concentration in PBS/0.2% BSA + 0.3% Triton-100 and left shaking for seven days at room temperature. Shorter durations were possible, but this needed to be tested with the specific antibody and tissue. After the primary antibody staining the tissue was washed three times for one hour each in PBS + 0.2% Tween-20 then secondary antibody was added at 2 μg/ml (i.e., 1:500 of 1mg/ml) in PBS/0.2% BSA + 0.3% Triton-100 shaking overnight at room temperature. The secondary antibody was filtered to avoid non-specific aggregates. The samples were then washed three times in PBS + 0.2% Tween-20 for one hour. At this stage they were transferred into aqueous clearing solution and left until the tissue appeared transparent (approximately 30 minutes). Prior to the optimisation of the aqueous clearing solution, the tissue was dehydrated in increasing concentrations of ethanol: 50%, 70%, 90%, 100% and a second 100% for at least one hour in each solution. The dehydrated tissue was cleared by adding ethyl cinnamate (ECi) until transparent (usually less than 30 minutes if properly dehydrated). The tissue was then ready to image in a custom-made chamber containing the clearing solution that was used. The majority of the imaging in the thesis was acquired using confocal microscopy with a Leica SP8.

2.4.3 Antibodies and reagents

Antibody	Concentration	Antibody clone
Lyve1	2 µg/ml	ALY7
CD31	2 µg/ml	SZ31
Podoplanin	2 µg/ml	8.1.1
Pdgfra	2 µg/ml	APA5

2.4.4 Imaging analysis

Imaging analysis was done using QuPath v 0.4.4 for 2D images and IMARIS 10.0 for 3D images.

2.5 Interstitial tracer experiments

2.5.1 Intravital fluorescent tracer/antibody injection and imaging

Mice were first anaesthetised using inhalational anaesthesia (isoflurane) with appropriate induction and maintenance. The abdomen was shaved and Nair hair removal cream was applied to the abdomen and wiped off with warmed water to ensure as much hair was removed as possible. This was very important to optimise the imaging conditions as hair is seen as a very clear artifact. The mouse was given 1 ml warmed 0.9% sodium chloride solution subcutaneously to ensure adequate hydration during the procedure. Following this, the animal was placed on a warmed pad under the stereomicroscope with eye ointment applied and the abdomen was opened using surgical instruments. The skin layer was opened followed by careful dissection of the peritoneum along the midline to minimise blood loss and ensure that no organs were damaged during intra-abdominal access. Any small bleeding was managed using VETSPON, which is an absorbable haemostatic sponge that can be applied to areas to stop blood loss. Initially the caecum was located as an anatomical landmark and using cotton buds it was carefully exposed to the operator's right side, with care not to excessively stretch or damage the mesenteric vessels. The mesenteric sheet connecting to the caecum was then pinned into a Sylgard plate to maintain a good view. At this point the mouse was rotated to lie laterally and then taped into position with a steady drip of PBS solution onto the exposed abdominal contents. Further pins were applied into the mesentery along from the caecum down to the proximal colon, which is the most accessible part of the mouse colon. This region was exposed and then placed under the stereomicroscope in order to get the best quality image. Once this had been set up, the mouse was moved so that the exposed proximal colon could be accessed for injection. The injection was performed using a Hamilton syringe which was able to inject 1 μl volumes.

The injection site was found by approaching the mouse colon using a very shallow angle to prevent luminal puncture. The needle was slowly advanced through the outer mesenteric layer and through the external muscle layer. Once it was confirmed to be in the correct location the injection was done slowly by hand. Importantly, these injections were not into the colonic lumen, but rather into the submucosa. We found that this was the only potential space that it was possible to inject into. Later, we managed to perform a similar injection using an externally connected microinjector to go down to a rate of 5 nl/second. Photographs were taken before and after injection. Time series photographs were taken every second to capture the real-time spread of the tracer as it travelled through the colonic lymphatic system and out of the tissue. This was followed to the mesenteric lymphatic vessels as well as the mesenteric lymph nodes. These injections were initially utilised to visualise the outflow of tracers that were administered; however, we adapted this method to inject conjugated antibodies or fluorescent ovalbumin that then labelled the outflow track as they pass through this route.

2.5.2 Luminal tracer administration

Anaesthesia and preparation of the animal was done in a similar fashion to that described in the previous section. When the animal was prepared and the proximal colon was exposed and pinned, a small hole was made into the distal portion of the caecum in order to pass a plastic gavage tube through this hole. Sutures were placed around this gavage needle and then the tracer of interest was injected directly into the colonic lumen, with no backflow into the caecum. This approach was necessary to localise administration to only the proximal colon without first passing through the small intestine as would be the case if the animals had been gavaged in the conventional way.

2.5.3 Plasma sampling

During the procedures above, baseline blood and blood at certain timepoints after tracer administration was drawn from the tail of the animal under anaesthesia. This was gently massaged into a capillary tube containing heparin to prevent coagulation. This was spun down at 2000 x *g* for 10 minutes to remove the red cells and the remaining plasma was analysed using a spectrophotometer for the relevant fluorescent signal of the tracer that was administered.

2.5.4 Wet/dry weight ratio

Wet weight of the colon was calculated by weighing the colon after removal and dabbing dry following stool removal. Dry weight was calculated by using a lyophiliser to dehydrate the same tissue piece for at least 24 hours and taking a repeat measurement of the weight. The ratio was calculated by dividing one by the other, and this was done separately for the proximal and distal colon. The water proportion of the tissue was calculated by subtracting the dry weight from the wet weight then dividing that result by the wet weight.

3 Characterisation of lymphatic endothelial cells over time in a murine colitis model

3.1 Introduction

Tissue inflammation results in interstitial fluid accumulation (oedema) and increased immune cell infiltration. The lymphatic system plays a key role in both the drainage of excess interstitial fluid and the egress of immune cells from the tissue. Therefore, it would be expected that the lymphatic system changes in the context of inflammation to meet this increase in demand for fluid and cellular clearance. The thesis introduction highlighted numerous studies that discuss the idea of lymphangiogenesis in the context of intestinal inflammation. However, the precise definition of this term is unclear, as is its measurement. Many studies quantify lymphangiogenesis by calculating the area of staining of lymphatic vessels from 2D sections of inflamed tissue. This is limited by the fact that these vessels are not evenly distributed throughout the tissue and the plane of the section makes a significant difference to what is quantified.

Our starting point in understanding the colonic lymphatic vasculature was to characterise the number of lymphatic endothelial cells (LECs) using flow cytometry from the colon of mice at steady state, and over multiple time-points of a well-established murine colitis model using dextran sulphate sodium (DSS) (129). Our hypothesis was that LEC number would increase in the context of inflammation and remain increased in the resolution phase to assist with the clearance of inflammatory cells and interstitial fluid.

To generate this data, we first had to develop and optimise a method to isolate live LECs from the murine colon to analyse with flow cytometry. Flow cytometry is a robust method to quantify traditional immune cell populations in the colon; however, using this technique to study rarer cell types such as endothelial cells quantitatively has not been done in an analogous way. We therefore sought to adapt these methods of analysis to endothelial cell populations.

Quantification of LEC number across time results in only partial understanding of changes in LECs in inflammation and resolution. In addition to the LECs themselves, we also wanted to understand more about how these cells are regulated. To do this, we turned to understanding how the transcriptional profiles of LECs, as well as the cells that are hypothesised to interact with these cells, vary over time. In addition to quantifying the number of LECs, flow cytometry also serves as a precursor to cell sorting, which is required for extracting RNA from the cells to further characterise them in this way.

Transcriptional analysis was shifted with the introduction of bulk RNA sequencing, which has provided numerous insights into the pathogenesis of IBD. As this technology has evolved, it has become possible to perform this on fewer and fewer cells, to the point where it can be assessed at a single cell level, which has revolutionised research in IBD (130–135). Our initial approach was to pool together the LECs that we were able to isolate, as well as other cell types we hypothesised would be interacting with the LECs, and perform bulk sequencing on these small, sorted populations over the same time course of DSS colitis outlined in this chapter. We then progressed to single-cell RNA sequencing of LECs from the colon in health and inflammation. This was done to identify whether changes found at a bulk level were occurring across all LECs or whether there were specific subsets that changed in inflammation.

We conclude the chapter by discussing methods used to validate the data generated from the sequencing analysis as well as the hypotheses these datasets generated that will be further explored in the remainder of the thesis.

3.1.1 Chapter aims

- To optimise the isolation of lymphatic endothelial cells from the murine colon and validate this using a lymphatic reporter mouse strain
- To quantify the change in lymphatic endothelial cell number over a time course of a murine colitis model
- To transcriptionally profile sorted lymphatic endothelial cells at the bulk and single cell RNA level in a murine colitis model

3.2 Optimisation of isolation of lymphatic endothelial cells

3.2.1 Enzyme optimisation

In contrast to lymphocytes, which are cells generally accustomed to travelling in isolation through the circulation, LECs form three-dimensional structures in the tissue by their inter-cellular junctions that connect them to neighbouring LECs and create lymphatic vessels (47). This proved to be a challenge when attempting to purify this population for flow cytometric analysis of individual LECs. We first trialled Collagenase VIII and DNAse to isolate LECs from the murine colon, adapting a protocol used in our laboratory to isolate lymphocytes from the murine colon. Our initial experiments resulted in very few live LECs recovered from the digestion despite good leukocyte recovery (data not shown), which we suspected was due to the nature of the enzyme and required us to reassess of our methods.

On the advice of others in the field and from reading the literature we trialled several other enzymes to digest the tissue, including Collagenase/Dispase, Collagenase IV and Liberase TL. Our conclusion was that Liberase TL was the most efficient at isolated live LECs (data not shown). However, we also noted that this enzyme took longer to digest the tissue in comparison to Collagenase VIII. Therefore, we undertook multiple rounds of digestion with the enzyme to fully digest the tissue. To confirm whether this was worthwhile, we undertook an experiment where we separated out the individual fractions that were digested (Figure 3.1). As highlighted, numerous lymphatic endothelial cells were isolated in each round of the digestion, and we suspected again that this was due to their structurally embedding within the tissue, requiring a longer duration of digestion to dissociate from neighbouring cells in the tissue. We therefore decided to proceed with three rounds of digestion going forwards for the remainder of the experiments in the thesis. Since these experiments were conducted, newer methods of cell dissociation that have emerged in the field (136).

a

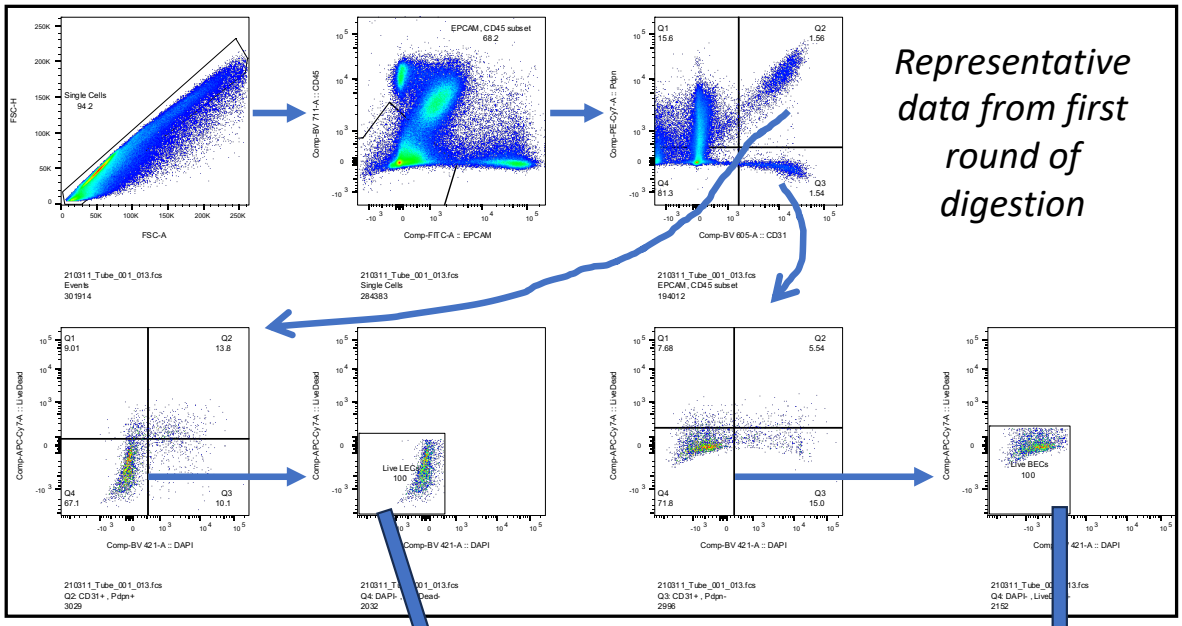

b

Digest round	Live LECs	Live BECs
1	2032	2152
2	4058	2572
3	2451	1579
4	940	503
5	329	165

Figure 3.1: **Multiple rounds of digestion are required to optimise the release of lymphatic endothelial cells from the tissue.** Flow cytometry data from the first digestion round is shown (a), followed by a table of the numbers of cells that were released for a total of five rounds of digestion (b).

3.2.2 Validation of Prox1-CreER^{T2} mouse model

From the literature, we knew that endothelial cells could be identified based on CD31 (PECAM1) (137) expression, as well as being negative for CD45 (expressed by haematopoietic cells) and EpCAM (expressed by epithelial cells) . LECs can be further discriminated from blood endothelial cells (BECs) based on their expression of the cell-surface marker podoplanin (138). To be confident of these markers to identify LECs, we used a reporter mouse widely utilised in the lymphatic field, the Prox1-CreER^{T2} mouse (128), which results in Cre-mediated recombination and deletion of floxed sequences under the induction of tamoxifen, specifically in Prox1-expressing cells. Prox1 is a master transcription factor that specifies LEC fate (139, 140). Therefore, we crossed this mouse to a reporter strain that has Cre-mediated deletion of a STOP cassette preventing the expression of tdTomato. This results in tdTomato expression in cells that express Cre recombinase. Both strains are viable and fertile in the homozygous state, and so were bred to homozygosity for convenience of genotyping. This mouse crossing helps to confirm that the markers from flow cytometry are truly identifying the cells of interest by triangulating with a reporter strain for LECs (Figure 3.2).

We established that after gating out CD45 and EpCAM expressing cells, CD31 and podoplanin expression was a valid way to detect LECs (Figure 3.2). This gave us confidence in our strategy of marking LECs by flow cytometry, as well as establishing a tool that we could use to selectively manipulate gene expression in LECs going forwards in the project. A limitation of this approach is that there is no gold-standard to know the total number of LECs in the colon, and so the yield is impossible to calculate. Furthermore, we assumed that all LECs are positive for podoplanin, which would have missed any podoplanin negative LECs.

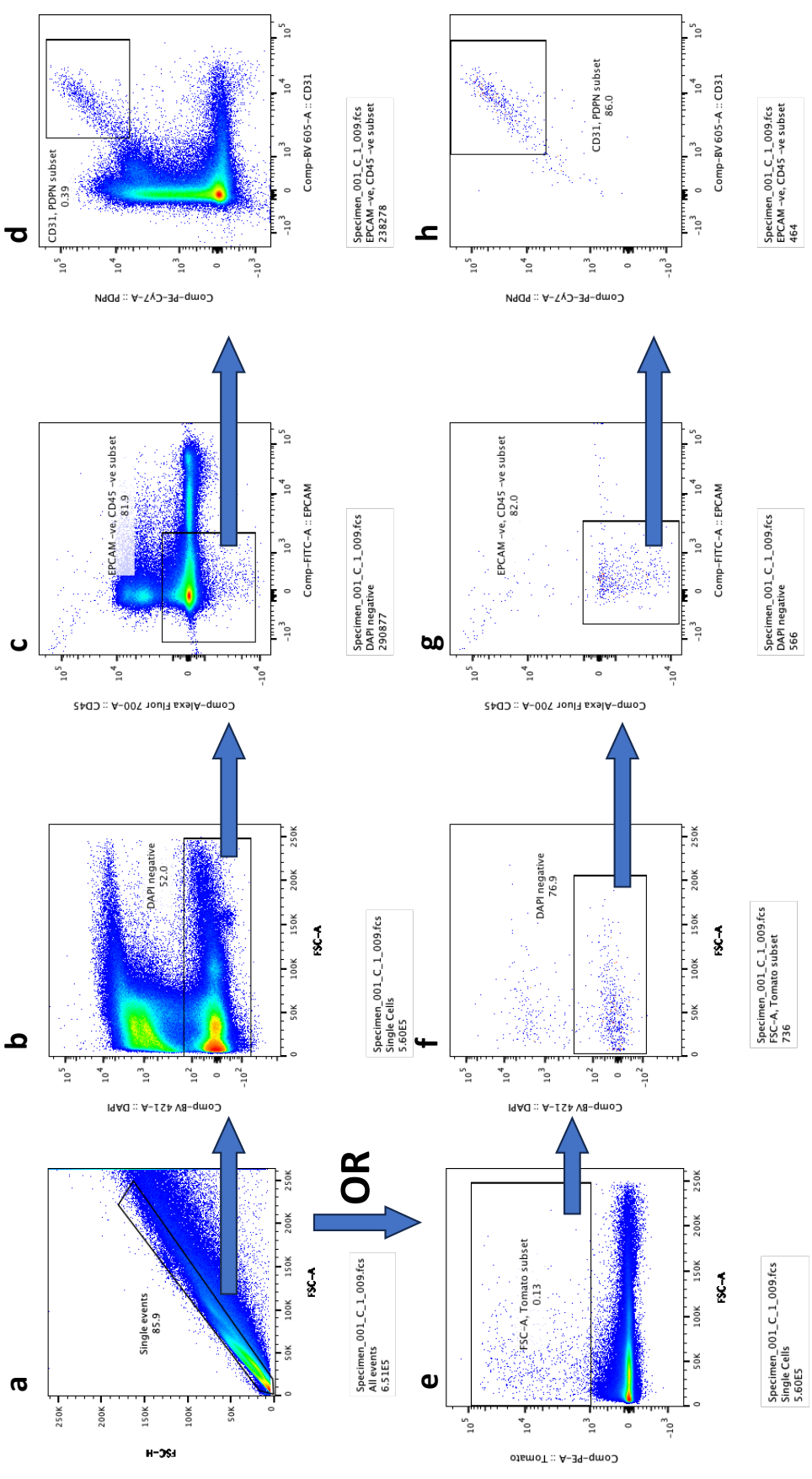

Figure 3.2: **Prox1-CreER^{T2}-tdTomato mice confirm appropriate gating strategy for isolating colonic lymphatic endothelial cells.** The gating strategy in (a-d) highlights all single events (a) which are DAPI negative (b) and CD45 and EpCAM negative (c). Within this, the CD31 and podoplanin positive events are shown (d). The same gating is used on only the tdTomato positive events (e) and the vast majority of reporter-positive cells are in the region we are gating in (d), (h), which confirms that this gating strategy is appropriate for colonic lymphatic endothelial cells when using reporter-negative wildtype mice.

3.3 A disease model enables the study of inflammation and resolution of colitis

3.3.1 Establishment of a time course model of murine colitis

We used DSS as a model of murine colitis because it was an established model in the field (129), as well as because it enables the study of various phases of inflammation (141). It is a model that is commonly used to study the peak of inflammation, but when the DSS is replaced with normal drinking water, it can be used to model the resolution phase of inflammation as the mice eventually recover. This is an aspect that we were particularly interested in with regards to the lymphatic vasculature as we had hypothesised that the lymphatic drainage of the tissue may contribute to the resolution of inflammation. Furthermore, as these experiments were initiated during the Covid-19 pandemic, it was challenging to use other models because this would have required additional people to be present in the lab simultaneously, which was not permitted at the time.

We ran a time-course experiment where animals were given six days of 2.5% DSS in the drinking water followed by a return to drinking plain water. This allowed the study of the different phases of colitis taken out to a time point near full resolution. This experiment was run twice with a summary of both experiments presented in the data. The first time we ran the experiment we proceeded to day 14, but as the mice still have evidence of inflammation, we took this out further to day 22 in the second experiment.

Having established a method to quantify LECs in the colon, we were able to correlate this data with known immune markers of colitis to address the question of how LECs change in number in the context of inflammation, as well as the resolution of inflammation, in a novel way.

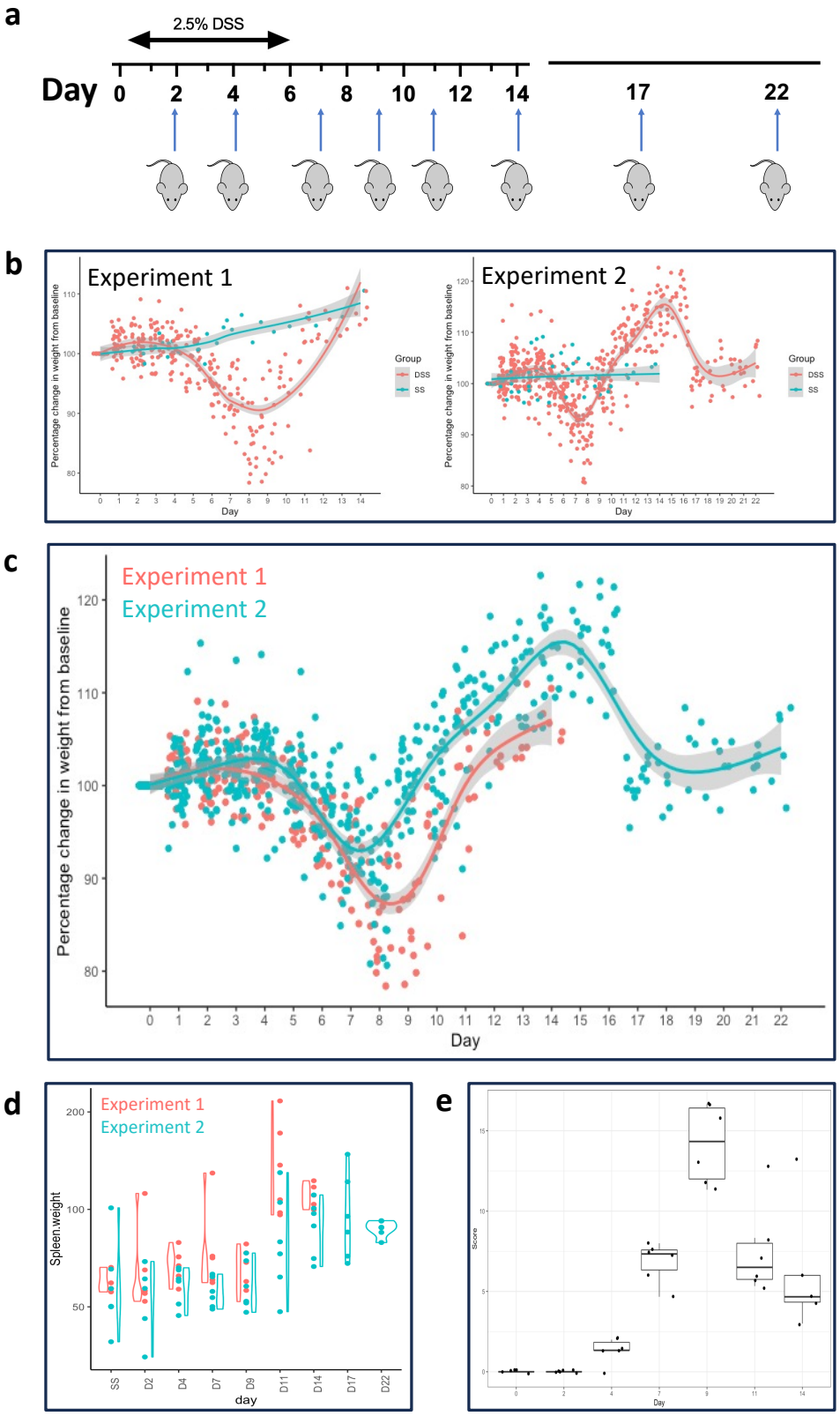

Figure 3.3: **Two independent DSS colitis time course experiments demonstrate kinetics of this model and summarise**. The figure shows the timepoints that were selected for the experiment (a) as well as weights over time (b) and (c), spleen weights (d) and histology score (e). Each dot represents an individual animal (n = 6 mice per timepoint for each experiment).

3.3.2 Flow cytometry gating and quantification of lymphatic endothelial cell number and ratio

Firstly, we confirmed that the animals used in these experiments were inflamed by using multiple readouts (Figure 3.3). Weight, spleen weight, total leukocyte number, neutrophil number and histology scores all triangulate to demonstrate that these animals indeed developed acute illness then began to recover (Figure 3.3). Weight loss peaked at day eight following the induction of colitis (Figure 3.3b and 3.3c). Our flow cytometry gating strategy is illustrated (Figure 3.4). Total leukocyte number (CD45-expressing cells) peaked at day nine (Figure 3.5a). When breaking the analysis down by immune cell, we found that all myeloid cells follow a similar trend peaking between day seven and day nine (Figure 3.5a), although there were some differences between myeloid cell types, for instance neutrophils peaking at day seven and eosinophils peaking at day nine (Figure 3.5a).

Having confirmed the presence of robust inflammation in our model, we next wanted to characterise the number of LECs. Our results showed that LECs, as well as BECs and fibroblasts, did not change significantly in number over time in this model (Figure 3.5b). This was true over two independent experiments, with the second experiment taken out to later timepoints to see whether further time was required for lymphangiogenesis. There may have been a trend towards increased LEC number at day 17 and day 22 in the second experiment but there was also large variation in the data, limiting interpretation beyond inspecting trends (Figure 3.5b).

We next calculated the ratio of LECs, BECs and fibroblasts as a proportion of the total number of stromal cells (LECs + BECs + fibroblasts) (Figure 3.5c). We found that the ratio of LECs as a proportion of stromal cells peaked at day seven and BECs peaked at day nine. This suggests LECs may expand earlier than BECs, but again with the large variation in the data on small numbers of cells it is hard to draw firm conclusions from this approach.

a

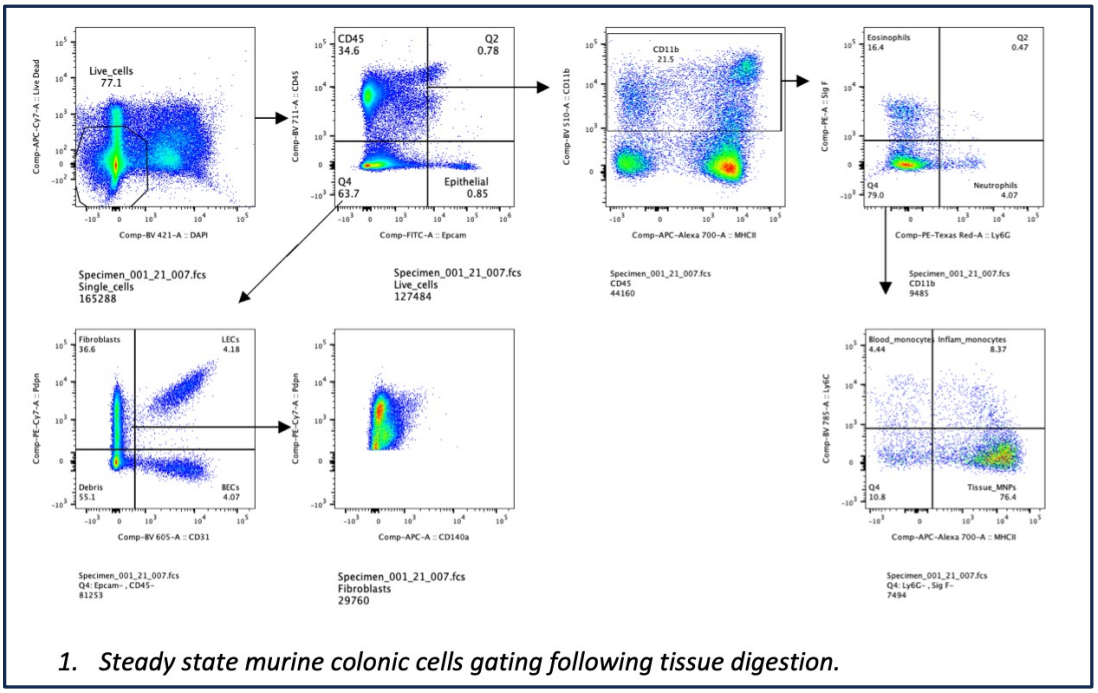

1. *Steady state murine colonic cells gating following tissue digestion.*

b

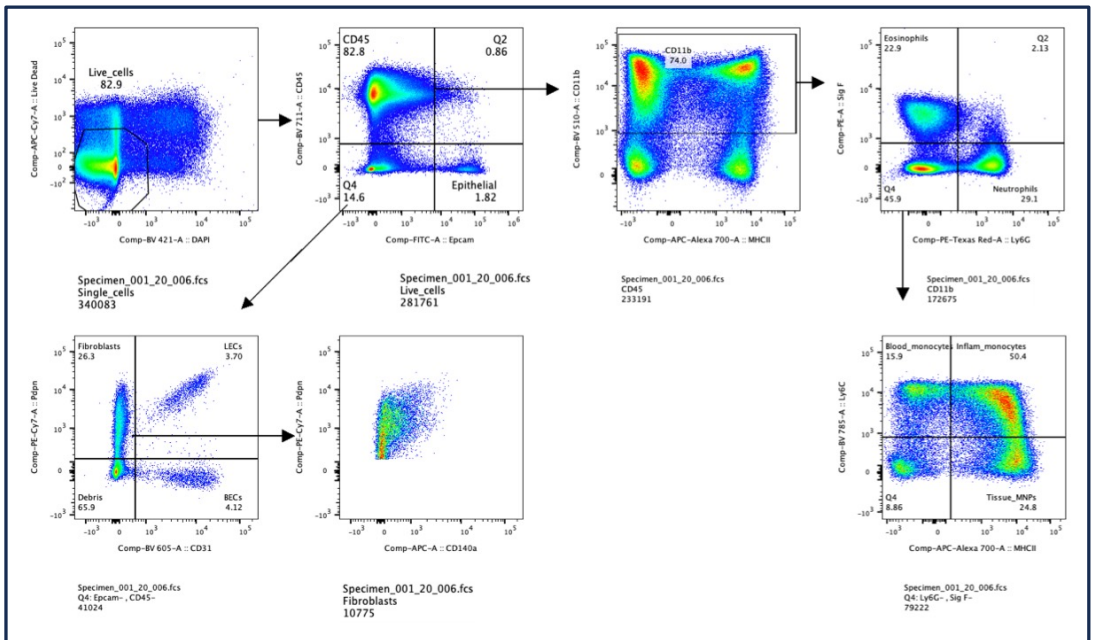

2. *Inflamed murine colonic cells gating following tissue digestion.*

Figure 3.4: **Gating strategy for flow cytometry data generated from the time course experiment**. The steady state (a) and inflamed (b) conditions are shown.

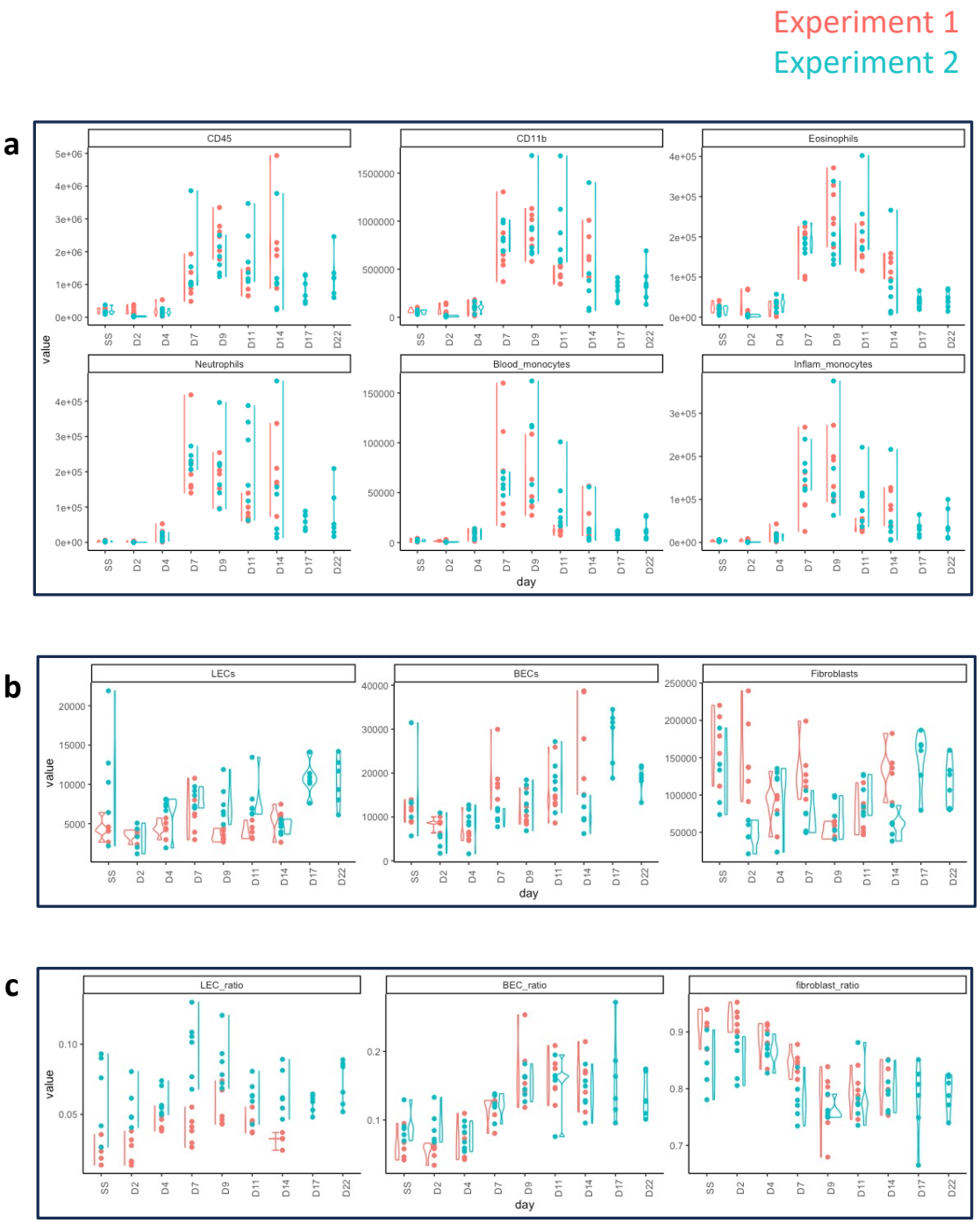

Figure 3.5: **Flow cytometry data demonstrates robust increase in leukocyte number but no significant change in lymphatic endothelial cell number**. The haematopoietic cells show robust increase in inflammation (a) but stromal cells (b) do not. Ratios of stromal cells also do not change significantly in inflammation (c). Two independent experiments have been combined with the first in red and second in blue. Each dot represents an individual animal (n = 6 mice per timepoint for each experiment).

3.3.3 Distinguishing immune responses occurring in distinct lymph nodes

As we were interested in the lymphatic drainage of immune cells from the tissue to the lymph node, we conducted a parallel analysis of the lymph node immune cell populations over time in the second DSS time course experiment that we performed. It has been shown that distinct lymph nodes drain the murine small intestine and colon (41, 42) and so we were interested in separating these lymph nodes to evaluate what is specific to the colon versus the small intestine-draining lymph nodes, as we know that DSS causes a colitis and not inflammation of the small intestine.

Lymph nodes predominantly contain lymphoid cells and we found that B lymphocytes proportionately rose in the colon-draining lymph nodes (Figure 3.6a) compared to the small intestine-draining lymph nodes at day nine, which is close to the peak of inflammation. Correspondingly, both $CD4^+$ and $CD8^+$ T lymphocytes fell as a proportion of lymphocytes at day nine (Figure 3.6b-c). This ties in with increasing evidence implicating a dysfunctional B lymphocyte response in ulcerative colitis, with an increase in the IgG:IgA ratio of plasma cells observed from intestinal biopsies of patients with active ulcerative colitis (142), which would have been stained in this experiment if repeated. B cell priming in the mesenteric lymph nodes is likely responsible for this, but the relevance compared to local immune responses within colon-associated lymphoid tissue remains an unresolved question.

Interestingly, within $CD4^+$ lymphocytes, $Foxp3^+$-expressing cells had similar proportions of cells between the colon and small intestine-draining lymph nodes at all time points; however, $Rorgt^+$-expressing $CD4^+$ lymphocytes peaked at day 11 and were increased in the colon-draining lymph node compared to the small intestine-draining lymph node at this time point (Figure 3.6d-e). Again, an open question in the field is what proportion of colonic immune responses occur in the draining lymph node versus the local lymphoid structures in the colon.

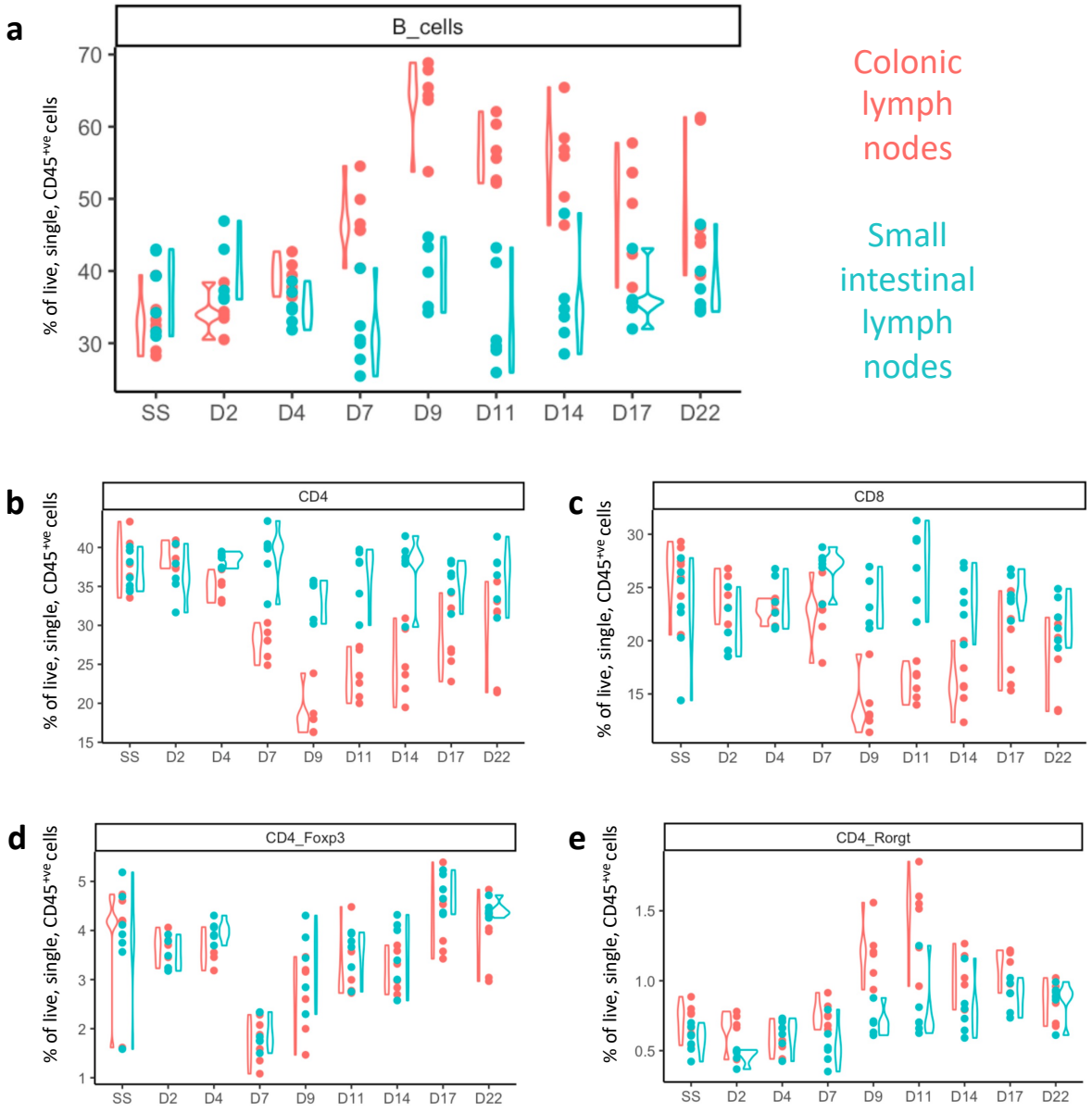

Figure 3.6: **Different lymphoid immune responses in small intestinal versus colonic lymph nodes in DSS colitis.** The B (a) and T lymphocytes (b-e) are shown here. Each dot represents an individual animal (n = 6 mice per timepoint for each experiment).

When considering the myeloid cells in a similar manner, we found most cells showed an increase in proportion in the colon-draining lymph node at day nine (Figure 3.7), but interestingly the neutrophil was an exception, which started increasing in proportion from day 11 in the colon-draining lymph node all the way to the end of the experiment at day 22 (Figure 3.7a). This contrasts with the neutrophil number within the colonic tissue itself, which has already been shown to peak at day seven (Figure 3.7b).

It is unclear whether these neutrophils are arriving at the lymph node via high endothelial venules directly from the blood circulation, or whether they can migrate via the colon-draining lymphatic vessels to the lymph nodes. The former route is thought to be the case, as neutrophils are considered to be short-lived cells, but some evidence exists that they can traffic via the lymphatic vessels in addition to direct recruitment from the blood circulation (143). There is also a concept in the field that inflammatory chemokines originating from inflamed tissue can drain via the lymph and act on high endothelial venules within the draining lymph node to augment cellular recruitment of monocytes from the blood circulation into the lymph node prior to antigen arrival (144). Such a system could be imaged to have evolved to prepare the lymph node for antigen and cellular arrival from tissues that may occur at a later stage. In this case it may be that colonic factors produced in the resolution of inflammation may act directly in the colon-draining lymph node to induce the expression of neutrophil-specific chemoattractants to aid with clearing debris in the process of tissue repair. This avenue is something to explore further in the context of obstructing lymphatic drainage, for example by surgical ligation, to see how tissue repair is affected if signals from the tissue cannot drain via the lymphatic vasculature. If resources permitted it would have also been interesting to compare this to systemic lymph nodes to understand regional versus systemic effects of intestinal inflammation. This was not possible as colonic digestion of fresh tissue was being undertaken concurrently.

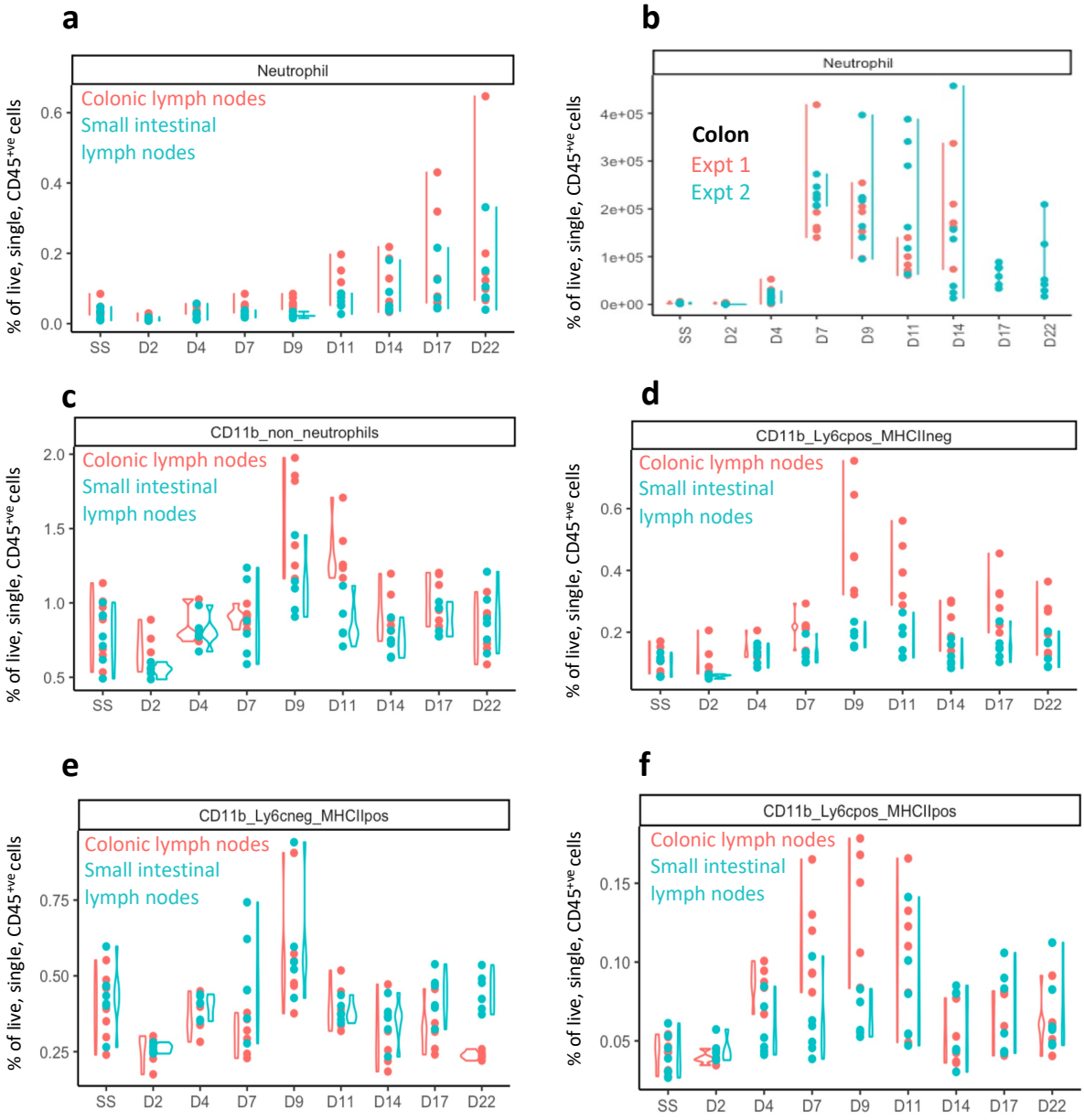

Figure 3.7: **Different myeloid immune responses in small intestinal versus colonic lymph nodes in DSS colitis.** The myeloid cells are shown here with all data from lymph node analysis except (b) from the colonic tissue to compare neutrophils to those in the lymph node (a). Each dot represents an individual animal (n = 6 mice per timepoint for each experiment).

3.4 Longitudinal bulk transcriptional profiling of lymphatic endothelial cells in a murine colitis model

From the time course data presented so far, we concluded that quantifying LEC number by flow cytometry is not an effective way to characterise changes in lymphatics in this colitis model. We therefore turned our focus to applying the method of cell isolation we developed to transcriptionally profiling LECs over the time course. The data presented here are from the first time course experiment outlined previously (Figure 3.3). In this experiment we concurrently flow sorted the LECs for transcriptional analysis. In addition to LECs we flow sorted the cells that we hypothesised to interact with the LECs from the literature including BECs, fibroblasts and mononuclear phagocytes as outlined in the introduction on the regulation of lymphangiogenesis. Prior to progressing with bulk sequencing of these sorted cell populations, we ran qPCR on the cDNA generated from the cell sorting to verify that there were changes seen across cell types and time points, which will be outlined.

3.4.1 Cell sorting strategy for lymphatic endothelial cells and interacting cells in DSS colitis

As outlined, the first stage in this experimental strategy was to isolate live lymphatic endothelial cells, and the cells that we hypothesised were most likely to interact with these cells, by cell sorting using flow cytometry. We have outlined the sorting strategy for the four cell types mentioned (Figure 3.8), and sorted 1000 cells from each population as endothelial cells were infrequent and we wanted to ensure comparable numbers between samples to enable a fair analysis.

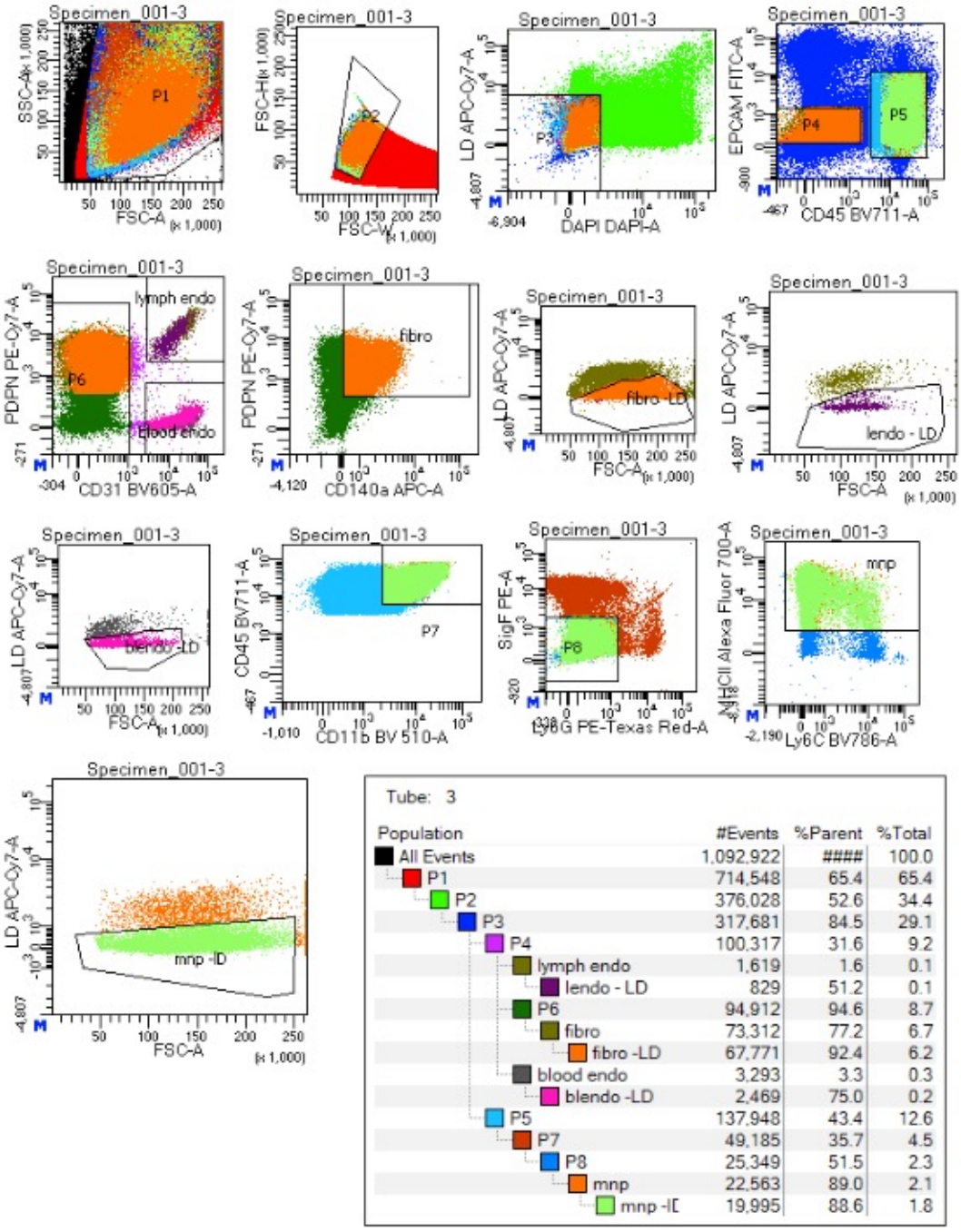

Figure 3.8: **Sorting strategy for mouse colon for RNA sequencing**. This demonstrates the sorting strategy used for this experiment. The approach was to take 1000 of each lymphatic endothelial cells (LEC), blood endothelial cells (BEC), mononuclear phagocytes (MNP) and fibroblasts (Fib). The live/dead threshold was set for each individual population as it differed between stromal cell type. *Thanks to Jon Webber for assistance with cell sorting.*

3.4.2 Transcriptional assessment of inflammation from whole tissue

Inflammation was confirmed in this time course earlier in this chapter (Figure 3.3 and Figure 3.5). To augment this data, we conducted qPCR from pieces of the whole colon over the time course experiment. We specifically took pieces of mid and distal colon as the DSS model is known to predominantly cause colitis in the distal colon (145). Therefore, we reasoned that including the proximal colon in this analysis would dilute the inflammatory signal that we would expect. We saw an increase in the pro-inflammatory cytokines TNF, IFN-g, CXCL1, CXCL5, IL1b, and IL6, all peaking at day seven to day nine of the DSS model (Figure 3.9a-f). We also concurrently assessed for the angiogenic and lymphangiogenic factors VEGF-A, VEGF-B, VEGF-C and VEGF-D (Figure 3.9g-j). These all did not appear to change much in inflammation at the whole tissue level (Figure 3.9j).

Since we did not find clear changes in the angiogenic and lymphangiogenic factors in DSS colitis at the whole tissue level despite confirmation of inflammation using the same modality of assessment, this gave us further reason to pursue for gene expression signatures from the rarer cell types that we had sorted for, to focus in on these that would otherwise be drowned out by the magnitude of change contributed to by other more abundant inflammatory cell types.

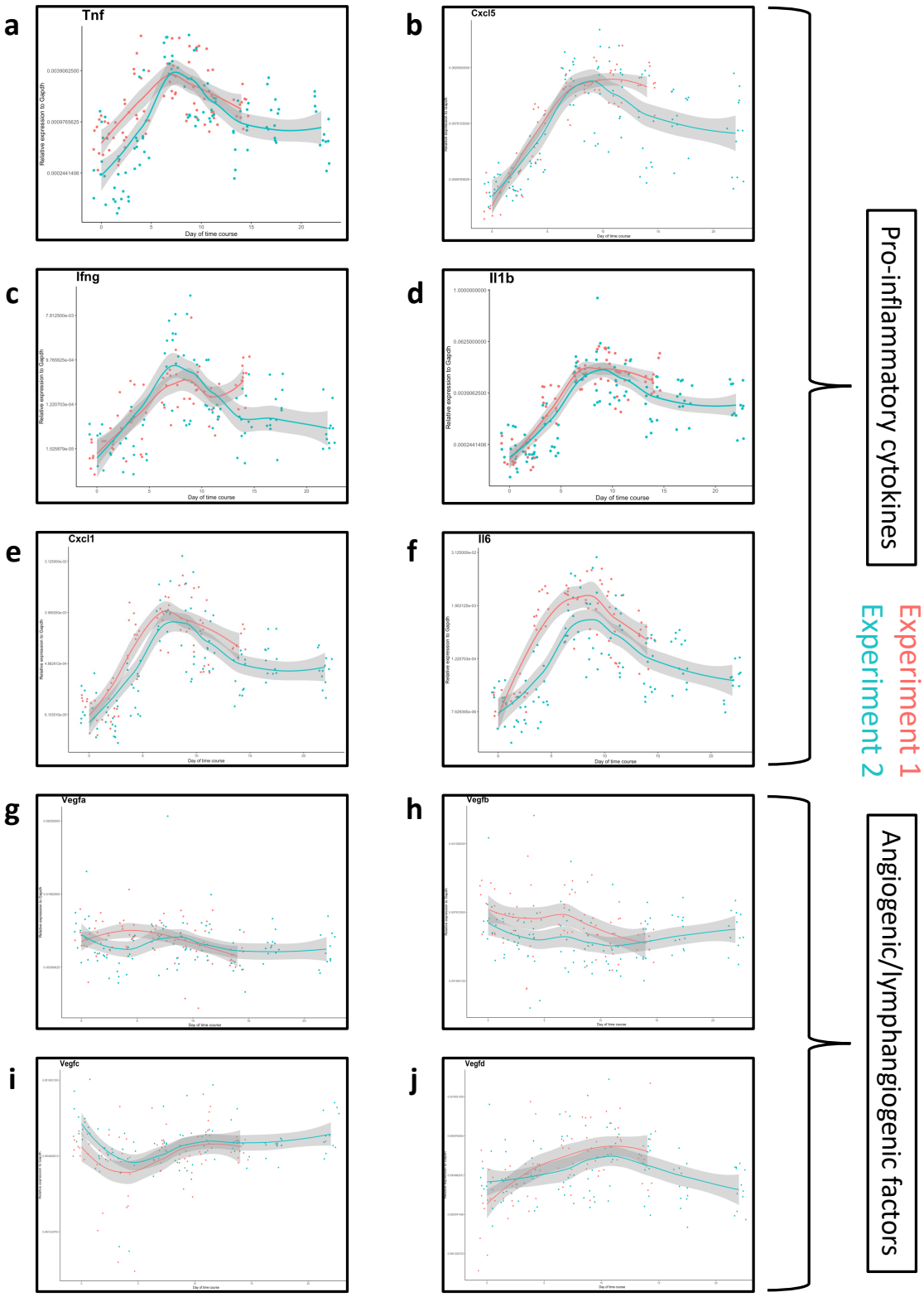

Figure 3.9: **Whole tissue colonic transcriptional signatures confirm induction of inflammation, but not a similar change in angiogenic and lymphangiogenic factors.** RNA from pieces of mid and distal colon were used for this experiment as they were thought to reflect the most inflamed region of tissue. Panels (a-f) highlight inflammatory genes and (g-j) highlight those associated with angiogenesis and lymphangiogenesis that were assessed. Each dot represents an individual animal (n = 6 mice per timepoint for each experiment).

3.4.3 qPCR from sorted cells confirms appropriate cell sorting and highlights possible regulators of lymphangiogenesis

Prior to progressing with bulk RNA sequencing, we wanted to confirm that the cells we had sorted were pure populations of interest, as well to further probe whether any known regulators of lymphangiogenesis were present and, if so, change over the time course. We were able to confirm cell identities using canonical genes (Figure 3.10 and Figure 3.11). Ptprc (CD45) expression was found only in the mononuclear phagocytes, and not in the LECs, BECs or fibroblasts (Figure 3.10a), confirming that there was no significant haematopoietic cell contamination of the stromal cells. Prox1, Lyve1, Pdpn (podoplanin), Pecam1 (CD31), Flt4 (VEGFR3) and Kdr (VEGFR2) expression all confirmed LEC identity (Figure 3.10 and 3.11). Pecam1 (CD31), and Kdr (VEGFR2) along with the absence of Pdpn (podoplanin), Flt4 (VEGFR3) and Ptprc (CD45) confirmed BEC identity (Figure 3.10 and 3.11). Pdpn, Pdgfra, Fap and the absence of Pecam1 and Ptprc confirmed fibroblast identity (Figure 3.10 and 3.11).

Returning to factors that may support angiogenesis and lymphangiogenesis, VEGF-C is the main known lymphangiogenic growth factor, and we assessed its expression amongst the cells that we sorted, which highlighted that it was expressed in blood endothelial cells and fibroblasts but not lymphatic endothelial cells or mononuclear phagocytes (Figure 3.12).

We were intrigued to see changes in Vegfd in fibroblasts particularly in inflammation (Figure 3.12d). These data gave interesting insights into the cells that may support the lymphatics and provided us with the confidence to progress with unbiased transcriptomic analysis of the sorted cell populations.

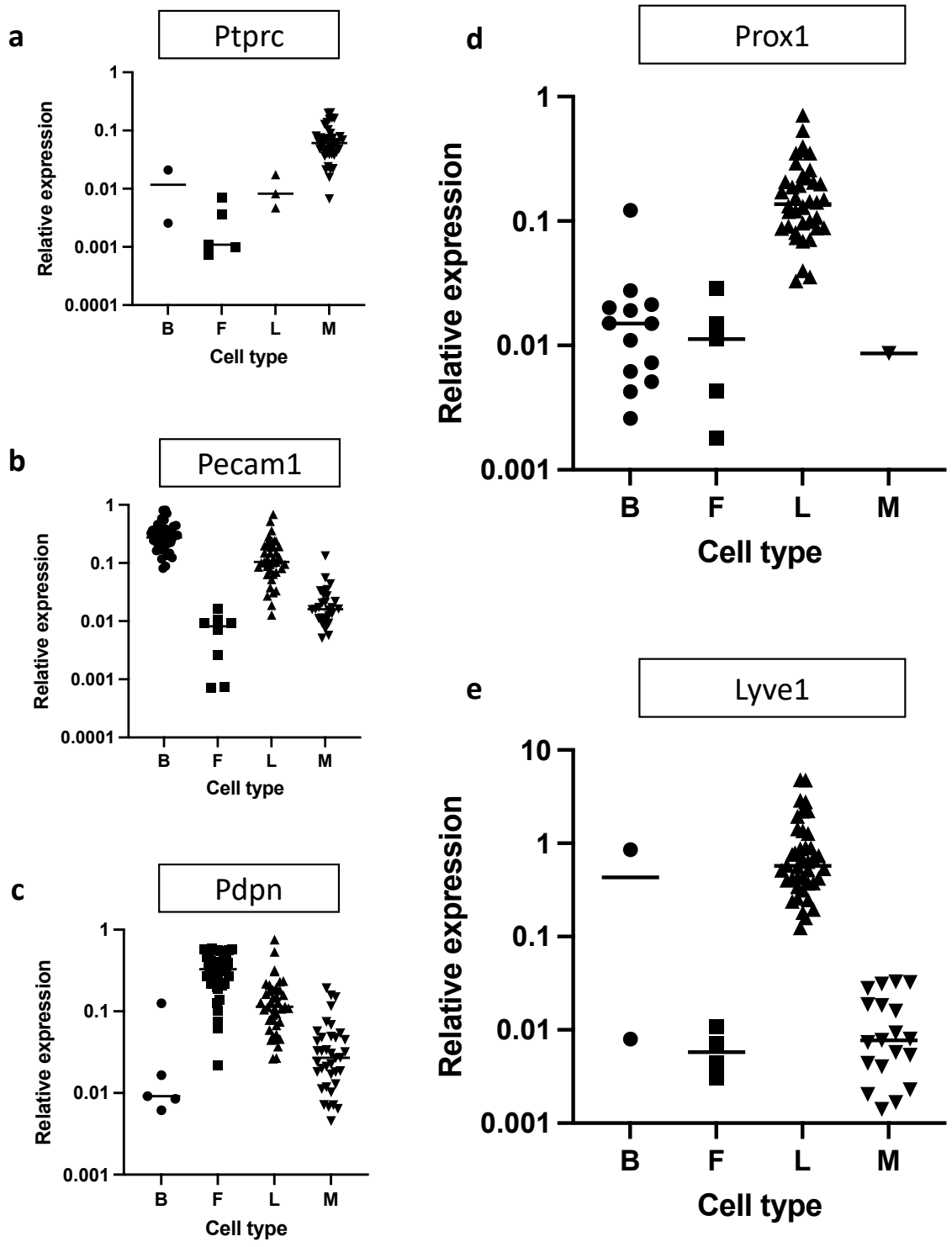

Figure 3.10: **Confirmation of the cellular identity of sorting colonic stromal and myeloid populations in the DSS time course experiment**. B – blood endothelial cells, F – fibroblasts, L – lymphatic endothelial cells, M – mononuclear phagocytes. Each dot represents an individual animal (n = 96 mice).

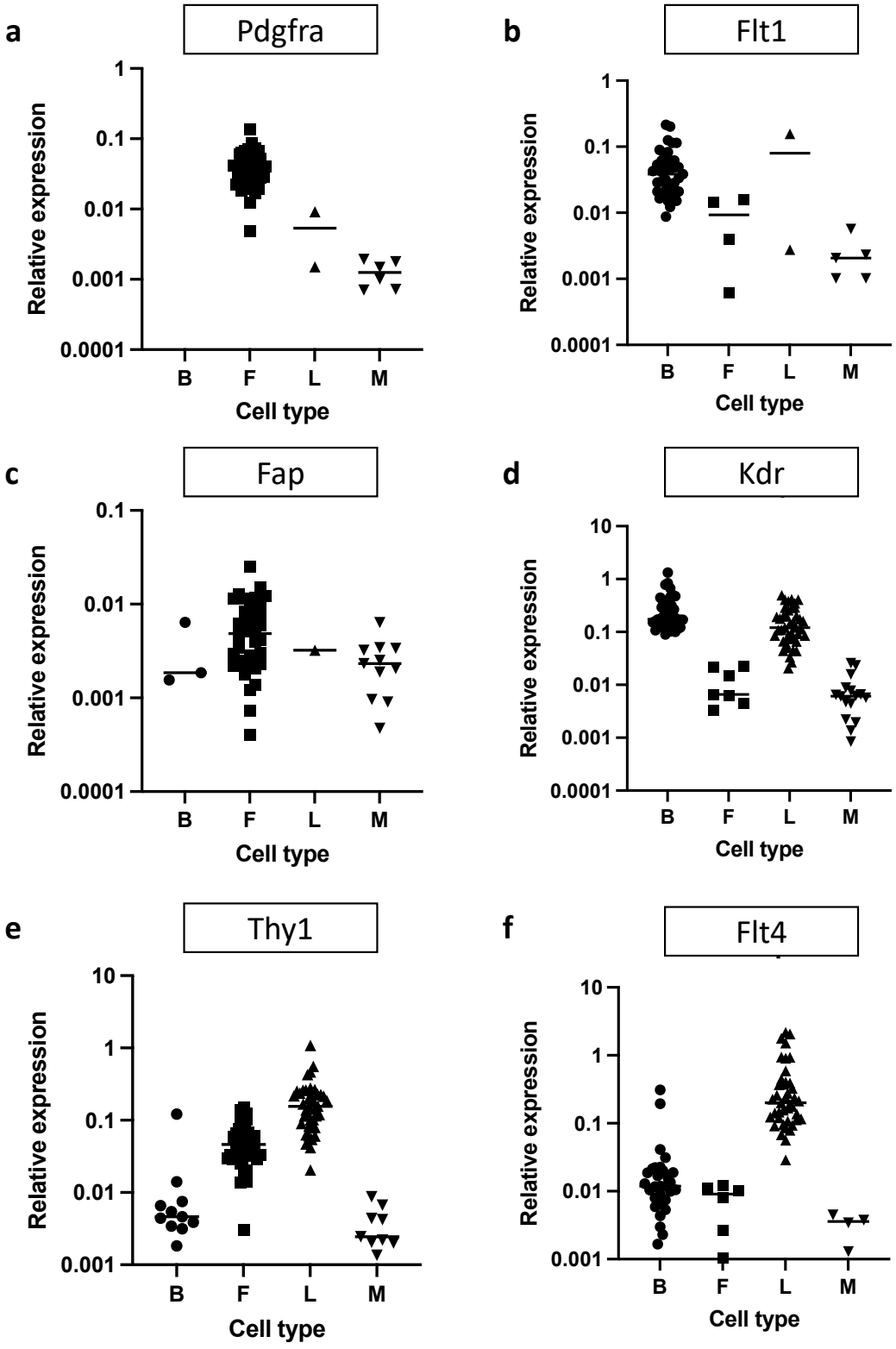

Figure 3.11: **Confirmation of the cellular identity of sorting colonic stromal and myeloid populations in the DSS time course experiment (cont'd)**. B – blood endothelial cells, F – fibroblasts, L – lymphatic endothelial cells, M – mononuclear phagocytes. Each dot represents an individual animal (n = 96 mice).

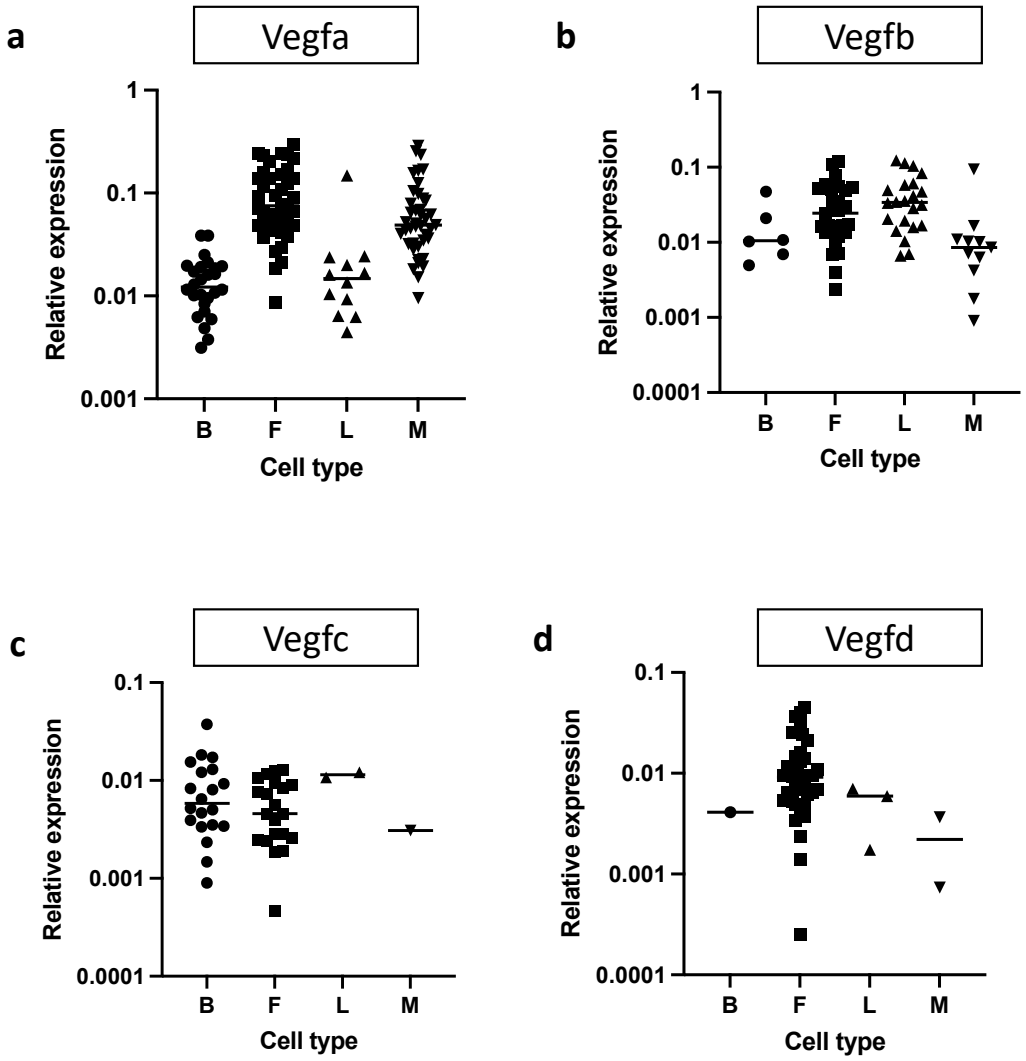

Figure 3.12: **Assessment of angiogenic and lymphangiogenic factors from sorted colonic stromal and myeloid populations in the DSS time course experiment.** B – blood endothelial cells, F – fibroblasts, L – lymphatic endothelial cells, M – mononuclear phagocytes. Each dot represents an individual animal (n = 96 mice).

3.4.4 Quality control and initial analysis of bulk RNA sequencing dataset

We sorted 1000 cells from each of: LECs, BECs, fibroblasts, mononuclear phagocytes. As we had low RNA, we sequenced the sorted cell populations using an Ultra Low RNA protocol and outlined some of the basic quality control metrics. The first assessment was to verify that the libraries were adequate to proceed with further analysis. We began by plotting the individual library size per sample (Figure 3.13a). We found that there was some variation, but this was evenly distributed amongst the different groups and conditions, as we would have expected with biological variation, and one group was not systematically underrepresented compared to any other (Figure 3.13a). Following this we plotted how many unique genes were expressed in each individual sample (Figure 3.13b). Again, we were reassured by the spread across the cell types and timepoints from the time course experiment.

Plotting these analyses against one another, we observed that there is a relatively even distribution of the library sizes and number of genes in a sample (Figure 3.14a). This indicated that we have not introduced any obvious bias with regards to technical factors such as the sequencing depth being vastly different across samples, or confounders based on cell type.

The next key analysis to perform and plot was a principal component analysis (PCA) to identify the major sources of variation within the samples. Reassuringly, we found that the major factor differentiating the samples was the cell type itself (Figure 3.14b), which is what we had expected. There was one exception where a BEC and LEC sample clustered with the other cell type and these two samples were excluded from the analysis on the grounds of being significant outliers in the dataset.

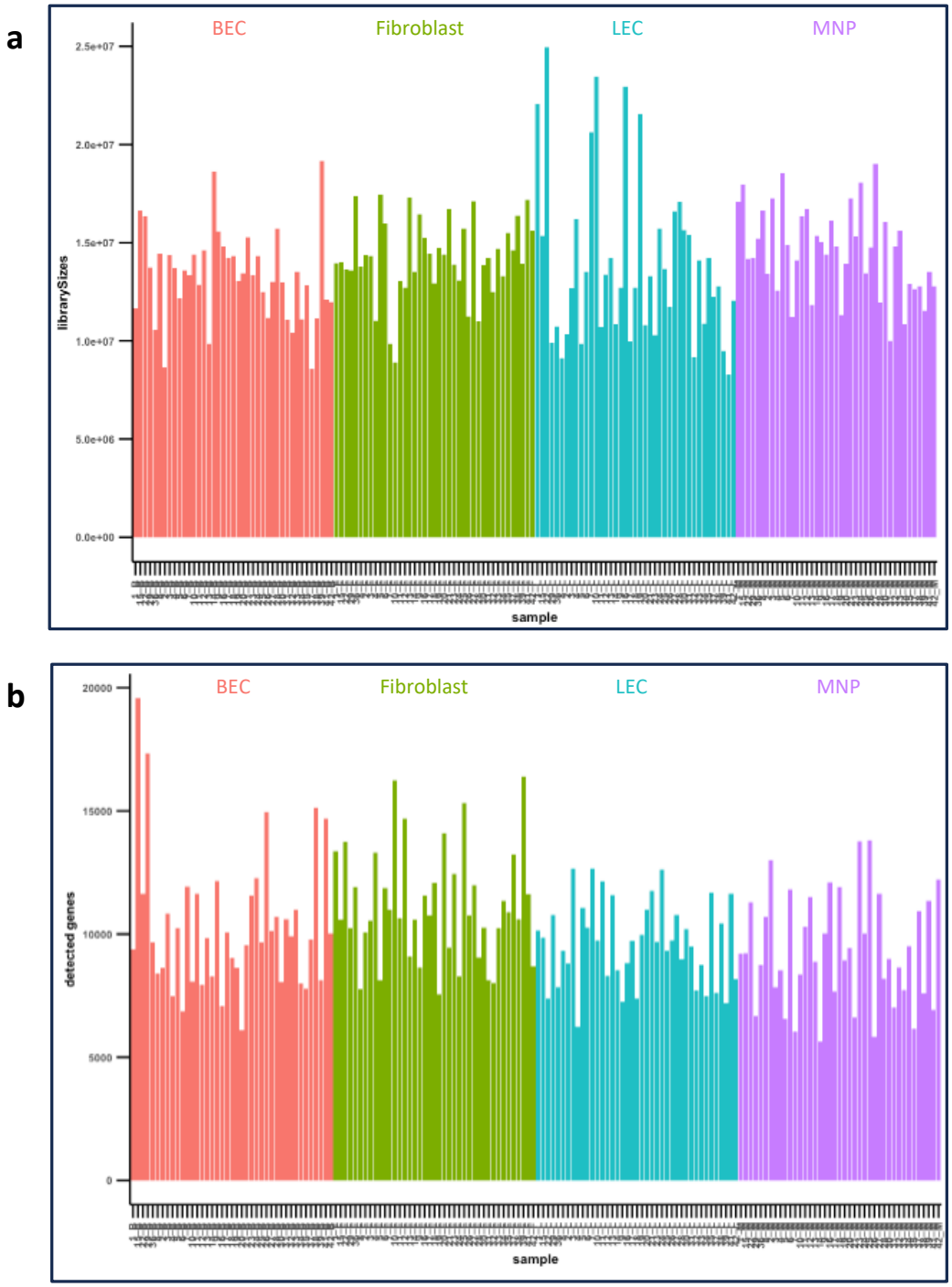

Figure 3.13: **Bulk RNA sequencing quality control.** Confirmation of library size (a) and number of detected genes (b) across individual samples. BEC – blood endothelial cells, LEC – lymphatic endothelial cells, MNP – mononuclear phagocytes. (n = 42 mice).

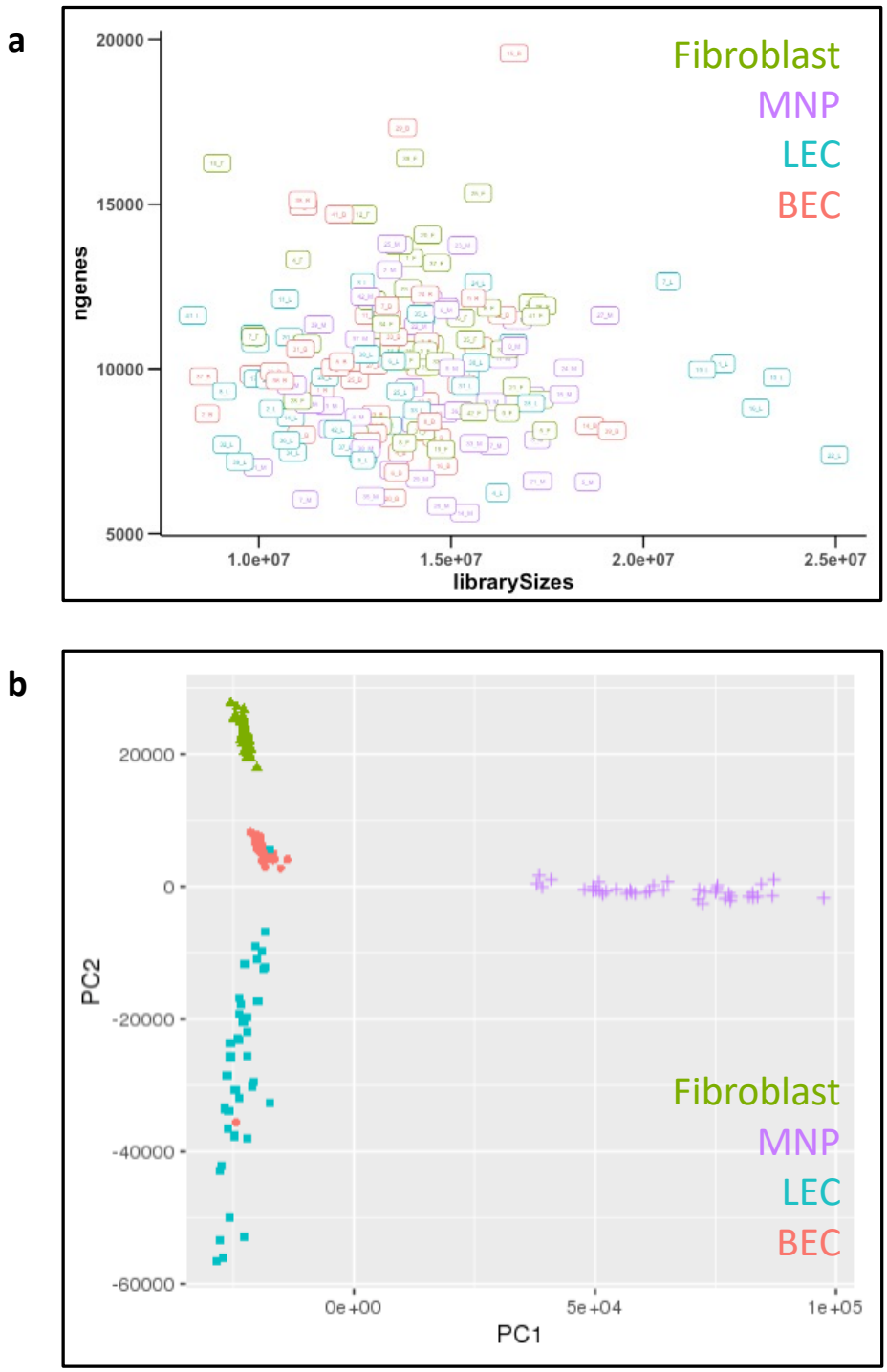

Figure 3.14: **Bulk RNA sequencing quality control and principal component analysis.** Confirmation of library size against number of detected genes (a) and plot of PC1 vs PC2 from principal compenent analysis of all samples (b) (n = 42 mice).

3.4.5 Focused analysis of lymphatic endothelial cell gene expression

The initial data analysis approach was to plot known genes expressed in LECs similar to what we had analysed by qPCR (Figure 3.15a-b). This highlighted that Lyve1 was expressed by the majority of LEC samples, and lower levels of Lyve1 was expressed by mononuclear phagocytes prior to inflammation, as we would expect. However, Prox1 expression was quite variable in the LEC dataset signifying that despite being appropriately sorted, there was concern that more lowly expressed genes (such as Prox1) may have dropout even though it is recognised as a canonical lymphatic-specific marker gene, which we realised may limit the interpretation of this dataset.

Our next analysis was to subset the LECs and group them as non-inflamed, early inflamed (day two and day four combined), inflamed (day seven and day nine combined) and resolving (day 11 and 14 combined). This was to increase the power to detect differences between the groups considering the variation that we had noted from plotting genes known to be expressed by LECs. We performed a PCA similar to the initial analysis between cell types (Figure 3.15c). In this plot, in contrast to the clear separation seen between cell types in the previous figure (Figure 3.14b), the separation of the samples was not as clear (Figure 3.15b).

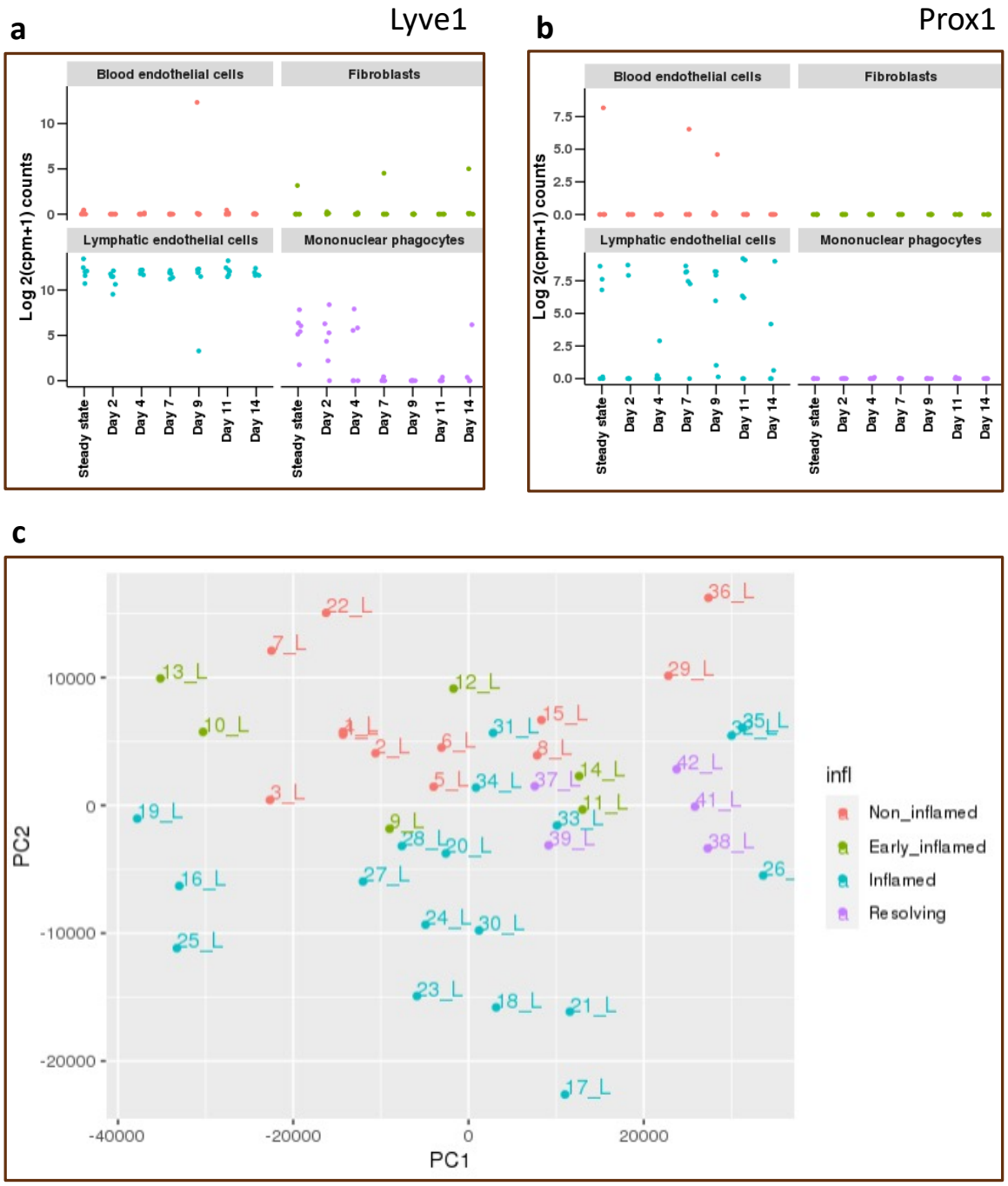

Figure 3.15: **Focused bulk RNA sequencing analysis of lymphatic endothelial cells. control.** Confirmation of Lyve1 (a), Prox1 (b) and plot of PC1 vs PC2 from principal compenent analysis of all lymphatic endothelial cell samples (c) (n = 42 mice). Each dot represents an individual animal (n = 6 mice per timepoint).

3.4.6 Differential gene expression analysis within lymphatic endothelial cells

To identify significantly varying genes between steady state and inflammation, we performed differential gene expression within LECs between steady state samples and those at the peak of inflammation at day seven using DESeq2 (146). A volcano plot with the most differentially up and downregulated genes from this analysis is displayed (Figure 3.16a). When we plotted the highest upregulated and downregulated genes back over the time course data (Figure 3.16b-c), we noticed that there was also significant expression from the other cell types in our dataset in addition to the LECs.

Furthermore, we saw significant noise in the data between the biological replicates in our dataset. This was particularly the case for the most highly downregulated gene, Deptor, which was entirely driven by large variation within the steady state gene expression rather than truly being downregulated at the peak of inflammation (Figure 3.16b).

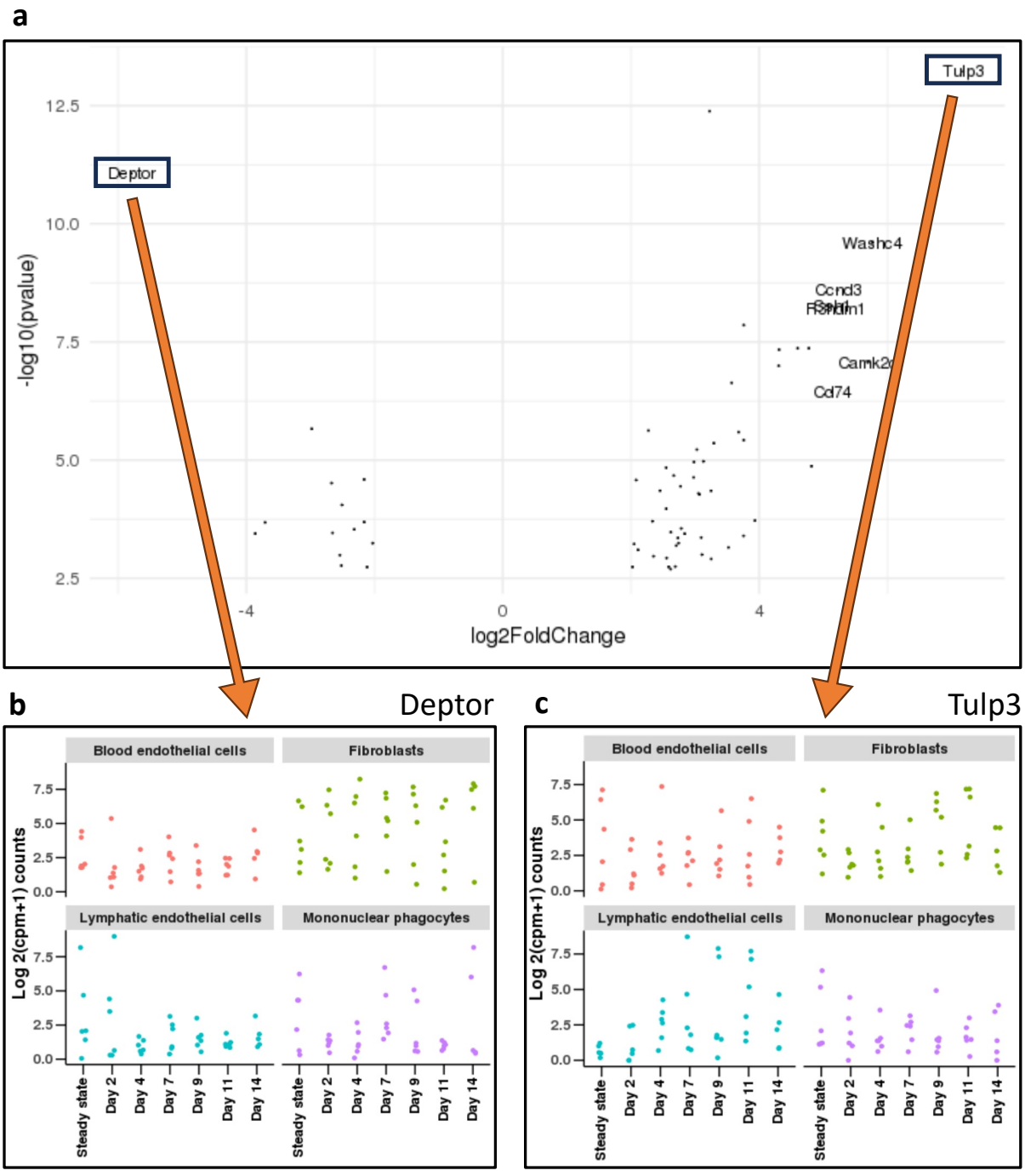

Figure 3.16: **Bulk RNA differential gene expression within lymphatic endothelial cells.** Volcano plot of all differentially expressed genes (a) with most downregulated gene (b) and most upregulated gene (c) plotted over the time course. Each dot represents an individual animal (n = 6 mice per timepoint).

3.4.7 Identification of specific genes varying in lymphatic endothelial cells over time

Since the differential gene expression analysis did not seem to be a promising approach, we filtered the dataset manually to include only genes that were expressed in LECs, whilst simultaneously also not highly expressed by the other cell types in the dataset. We then looked through the literature and identified genes associated with inflammation within LECs (130). We manually plotted these to see which ones varied over time in the dataset (Figure 3.17). This included Ackr2 (D6) (Figure 3.17a), which is a chemokine decoy receptor expressed by both leukocytes and LECs, but LEC-specific expression was found to control intestinal inflammation (147). Another gene of interest, Sema3a (Figure 3.17b), has been investigated in LECs previously and LEC expression of Sema3a was shown to be required for dendritic cell transmigration via the lymphatic vessels (148). It is interesting to see the pattern of these genes rising in inflammation and falling towards the resolution phase of inflammation confirming validity of the dataset for genes with adequate expression levels. These genes likely did not come out as significant in the DESeq analysis because of high variability in the steady state gene expression levels (Figure 3.17).

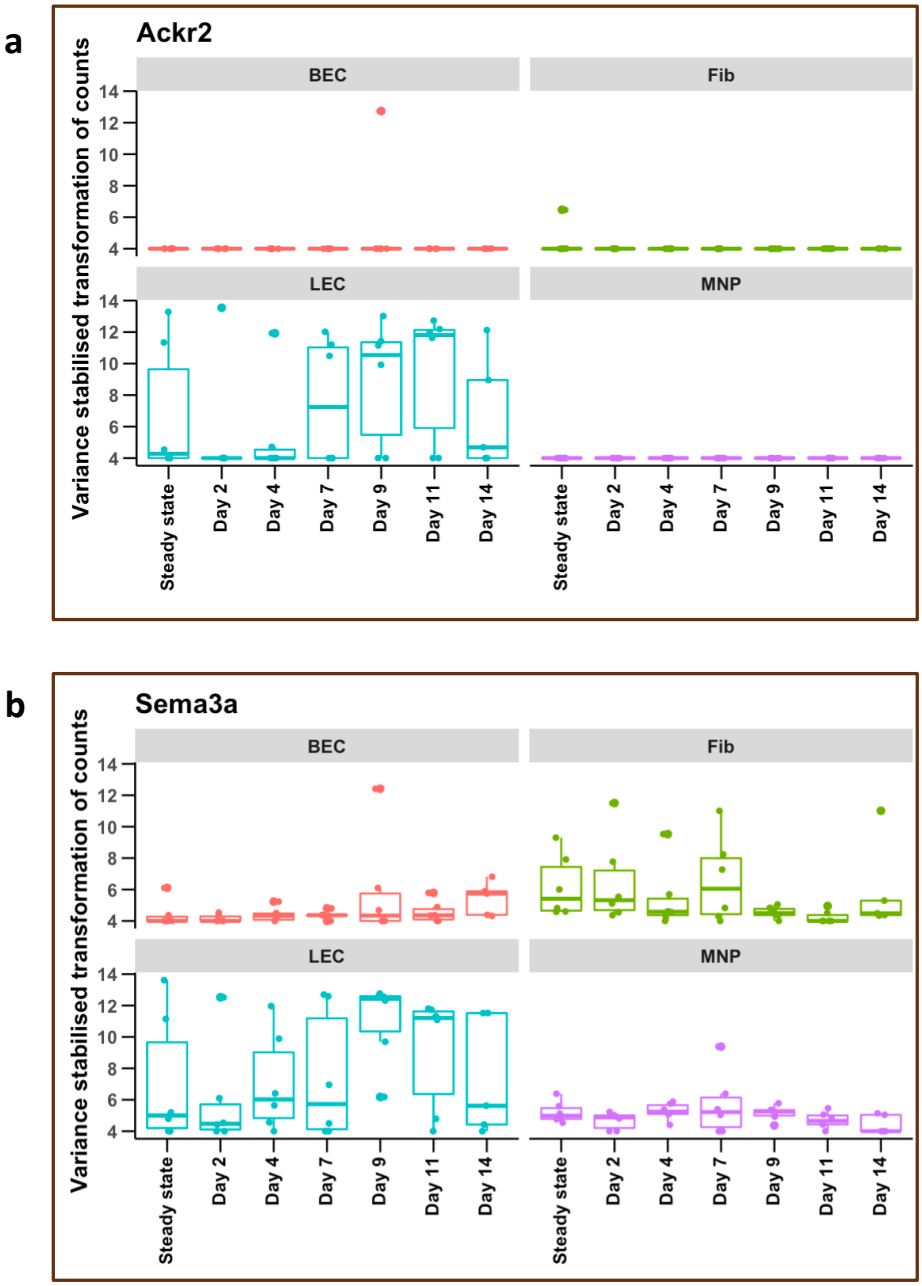

Figure 3.17: **Lymphatic-specific gene expression changing over the time course confirms validity of the dataset.** Gene expression was summed and filtered for what was high in lymphatics and low in other cells, then overlaid with genes hypothesised to rise in LECs in colitis to select genes of interest from this intersection. Ackr2 (a) and Sema3a (b) gene expression visualised across the all cell types in the time course. Each dot represents an individual animal (n = 6 mice per timepoint).

3.4.8 Conclusions from analysis of bulk RNA sequencing data

The sorted bulk sequencing approach from LECs provided an interesting starting point from which to assess changes in LECs over time in a murine colitis model. It was reassuring to see that the samples separated according to cell type and that canonical marker genes of LECs were expressed. However, the noise in the dataset and dropout of lowly expressed transcripts limited the ability to make significant conclusions. Other approaches to analysing this data include linear modelling over the timepoints or omitting the baseline data, but the core limitations of the dataset remain a barrier to further interpretation. Therefore, further formal analyses of the data have not been presented, but this bulk RNA dataset forms a useful means to cross-reference genes of interest from other sources.

A more general limitation of bulk RNA sequencing is the inability to discriminate between cellular subsets responsible for driving transcriptional differences found in the data. To address this limitation, we undertook single cell sequencing of LECs and other stromal and myeloid cells, which will form the next subchapter of the thesis.

3.5 Single-cell transcriptional profiling of lymphatic endothelial cells in health and inflammation

From the sorted bulk data in the previous subchapter, we concluded that LECs change transcriptionally in inflammation, but the specific nature of the change was challenging to pick out due to the stated limitations. Furthermore, we were unable to make any conclusions on LEC subsets from the sorted bulk sequencing approach. As it remained unclear whether changes occurred in specific subsets of LECs, we turned to single cell RNA sequencing to gain further cellular resolution on this question. We chose to focus in on just the peak of inflammation for this dataset as this is where we saw the greatest difference in gene expression from qPCR and the sorted bulk dataset.

3.5.1 Hashing antibody optimisation with MHC I

To gain meaningful information from the single cell sequencing experiment, biological replicates are a necessity, which were often omitted from early studies using single cell sequencing approaches. To obtain this data, individual biological samples can be loaded in separate sequencing lanes. However, this can introduce a batch effect between lanes, where the sequencing result is confounded by the fact that the lane was different between samples. This also becomes prohibitively expensive as the number of samples increases. A relatively recent solution to this is a technology termed 'cell-hashing' (149). This uses a unique oligonucleotide barcode that is conjugated to MHC I (expressed on all cells) and CD45 (on haematopoietic cells) that is used to bind to the cells. Following this binding the cells can be mixed and sequenced in the same lane, avoiding batch effect, then computationally deconvoluted based on the unique barcode that is sequenced together with the rest of the cell's mRNA. We purchased 10 unique antibody-barcode conjugates, meaning we could theoretically run 10 unique biological samples in the same lane. Prior to using this, we ran a pilot experiment using only FITC-conjugated MHC I antibody (Figure 3.18a) of the same clone as the hashing antibodies and compared this to isotype (Figure 3.18b) and FMO (Figure 3.18c) controls to confirm that the cell types we were interested in bound at the concentration we would use for the hashing antibody in the main single cell sorting experiment. We observed clear separation between the MHC I stained cells across all cell types compared to the isotype and FMO control. We therefore proceeded to using the hashing antibody in the experiment where cells were isolated for single cell RNA sequencing. This enabled us to sort cells from 10 steady state mice and 10 inflamed mice in one experiment and have single cell data from individual mice.

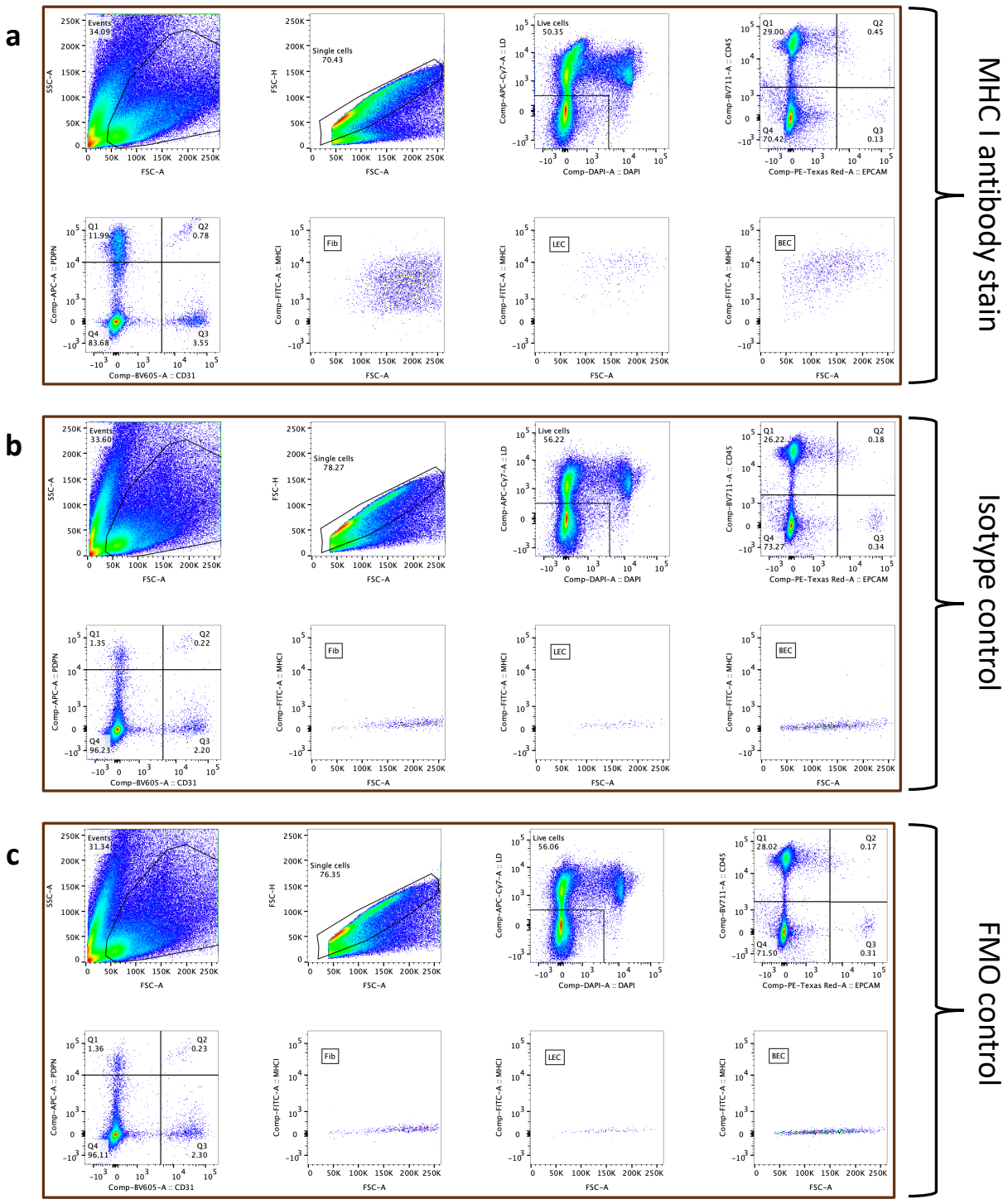

Figure 3.18: **MHC I antibody staining confirmed that hashing antibodies would appropriately label cells in single cell sequencing experiment.** Appropriate isotype control (b) and FMO control (c) confirm the binding of MHC I to all stromal cells of interest (a).

3.5.2 Summary of flow cytometry data from cell sorting

Similar to the bulk RNA sequencing, the sorting strategy for the single cell sequencing experiment is outlined (Figure 3.19).

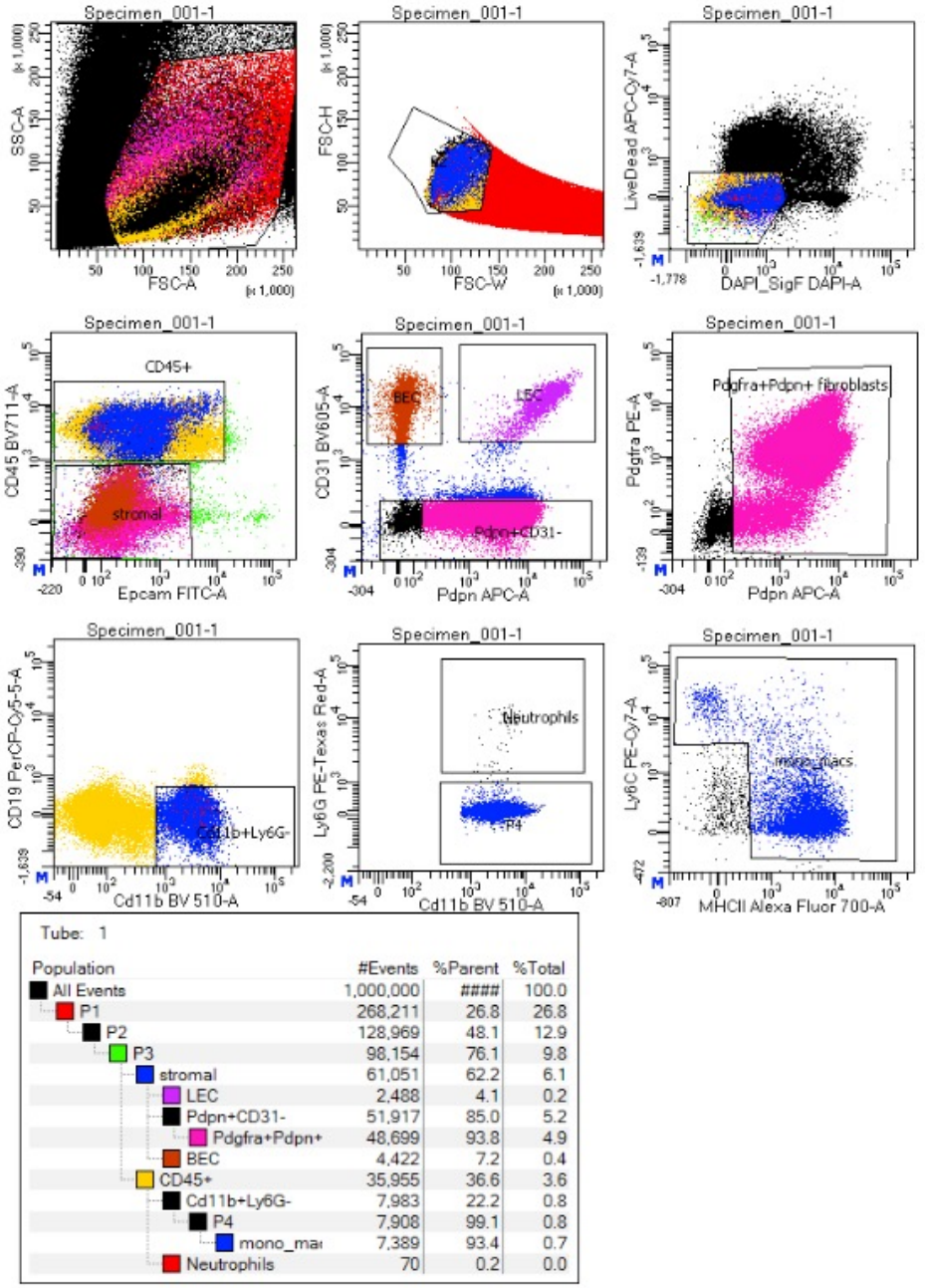

Figure 3.19: **Sorting strategy for mouse colon for single cell RNA sequencing**. The approach was to take as many lymphatic endothelial cells as possible per mouse colon in addition to 1000 of each blood endothelial cells, mononuclear phagocytes and fibroblasts for single cell sequencing. *Thanks to Jon Webber for assistance with cell sorting.*

3.5.3 Initial analysis and quality control of single cell data

We obtained 2610 LECs from 10 steady state mice colons and 3466 LECs from 10 inflamed mice colons (Figure 3.20a). The RNA molecules detected within each cell (Figure 3.20b), the number of genes detected in each cell (Figure 3.20c), and the percentage of mitochondrial reads (Figure 3.20d) were broadly similar between groups. After normalisation, highly variable gene detection, data scaling and dimensionality reduction, cells were clustered using the Louvain algorithm and plotted on a umap (Figure 3.20e) using Seurat integration between the steady state and inflamed samples (150). Plotting Lyve1 gene expression highlighted a clearly separate cluster of the LECs, which was reassuring.

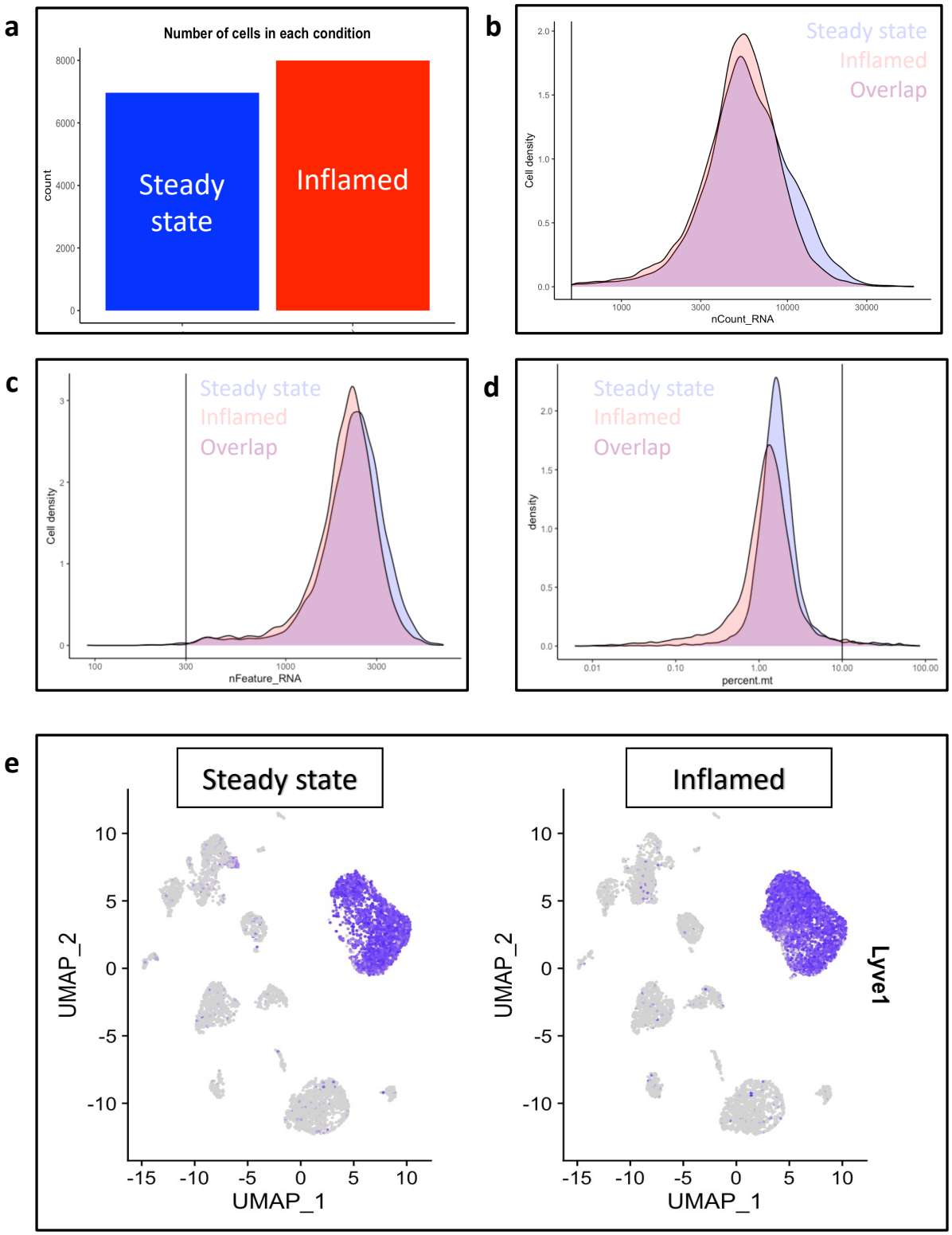

Figure 3.20: **Single cell quality control and confirmation of lymphatic endothelial cells**. The numbers of lymphatic endothelial cells (a) as well as RNA counts (b), unique genes (c) and mitochondrial reads (d) are displayed. Lyve1 gene expression was plotted on the UMAP in both steady state and inflamed conditions (e). (n = 10 mice steady state; n = 10 mice inflamed).

3.5.4 Summary of single cells isolated in health and inflammation

Further data analysis was performed to cluster the cells into 18 clusters (0-17) (Figure 3.21a) and find marker genes to identify their cell type using canonical marker genes. (Figure 3.21b) The visual appearance of these populations shifted in inflammation (Figure 3.22a-b), particularly noticeable amongst the LEC clusters (0, 2, 5 and 10).

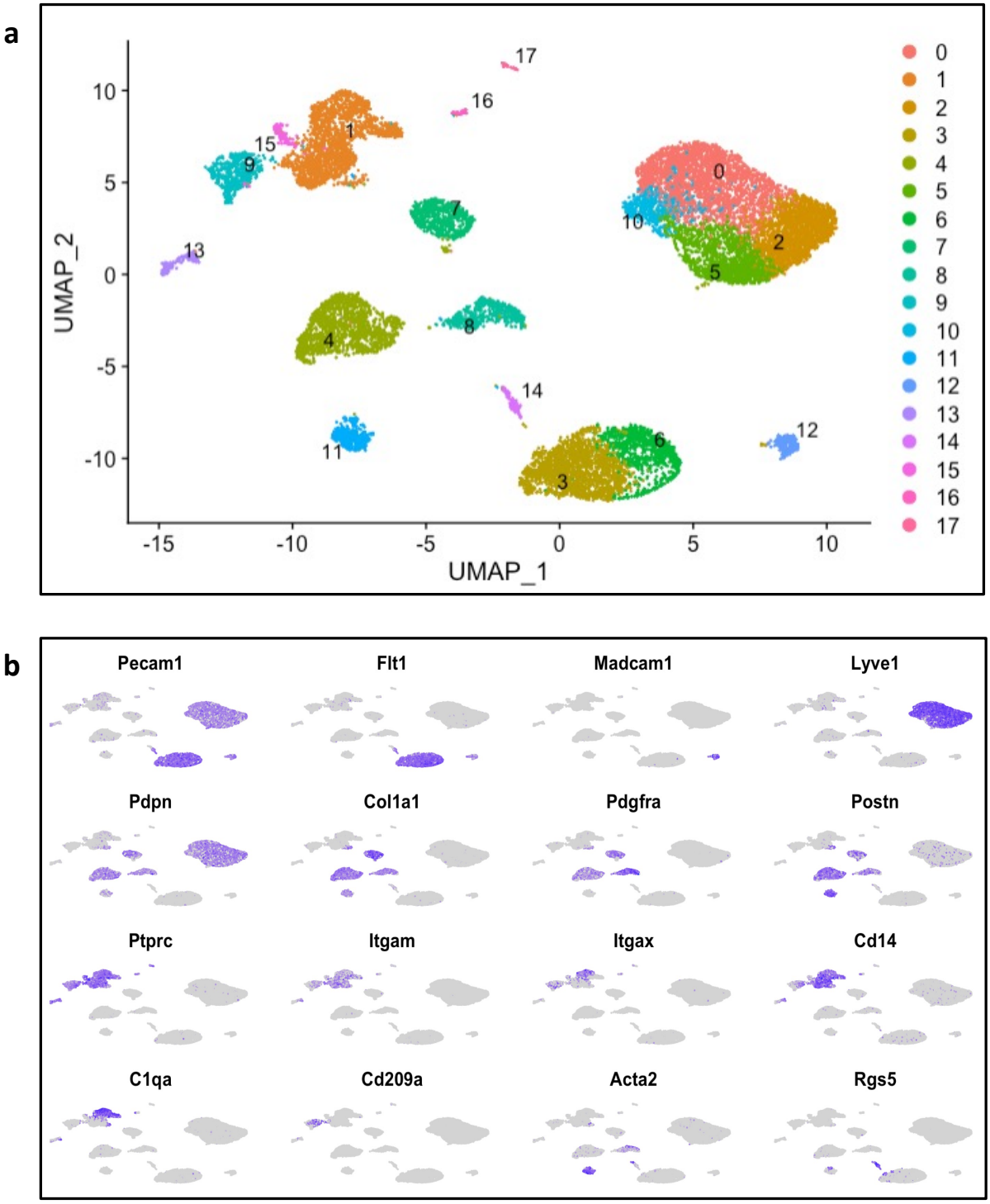

Figure 3.21: **Single cell RNA sequencing identifies cell types expected in dataset.** The lymphatic clusters (0, 2, 5, 10) are recognisable (a) with Lyve1, Pecam1 and Pdpn expression (b) (n = 10 mice steady state; n = 10 mice inflamed).

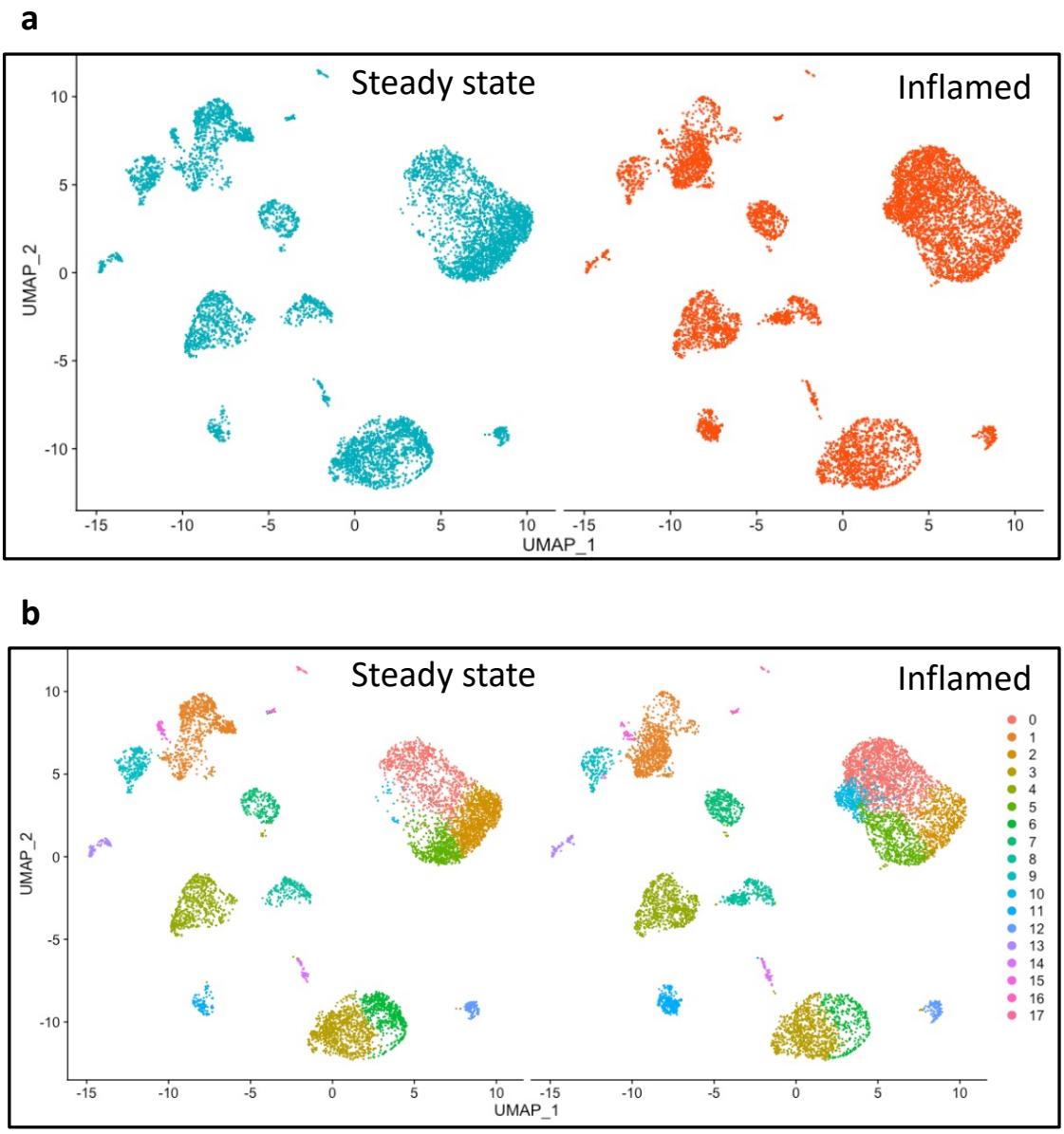

Figure 3.22: **Separating cells by condition after integration of dataset demonstrates shifts in cell populations in inflammation.** UMAP plots of all cells coloured by condition (a) or cell cluster (b), separated by condition (n = 10 mice steady state; n = 10 mice inflamed).

3.5.5 Subsets of lymphatic endothelial cells

We subset the LECs for further analysis of cellular heterogeneity (Figure 3.23). We had 2610 LECs from 10 steady state mice (Figure 3.23a and 3.23c), and 3466 LECs from 10 inflamed mice at the peak of DSS colitis at day seven (Figure 3.23b and 3.23d).

The first analysis was to cluster the cells independent of inflammatory condition to assess the marker genes making up each cluster for any clear patterns. The smallest and most easily distinguishable cluster in both steady state and inflamed samples expressed Foxp2, which is known to be a flow-induced regulator of collecting lymphatic vessels (151). Moreover, the cited study looked at dermal collecting lymphatic vessels in contrast to capillaries by the absence or presence of Lyve1 expression respectively which was confirmed by imaging to reflect collecting vessels or capillaries. From their dataset, five out of six of the remaining marker genes from this cassette (Clca3a1, Ugcg, Cfh, Nsg1, Foxp2) are also upregulated in collecting vessels compared to capillaries, enabling us to be confident in the assignment of this small cluster of cells as lymphatic collector cells (Figure 3.23c-d).

Cluster number two in the inflamed LECs expressed genes downstream of interferon signalling including Stat1, and MHC II (Figure 3.23b and 3.23d). To gain further clarity on this, data analysis was repeated following integration of the steady state and inflamed datasets in the next section.

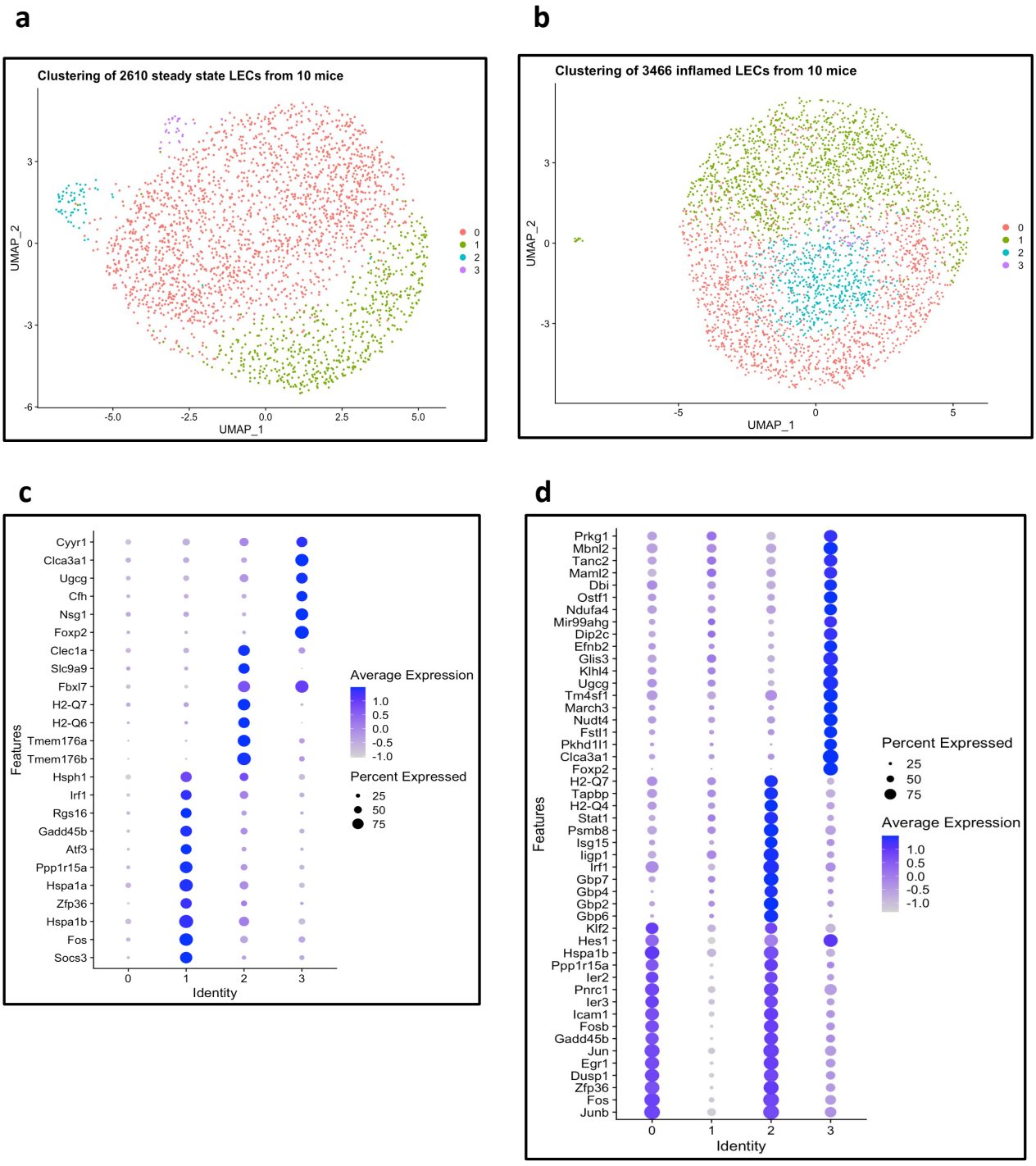

Figure 3.23: **Single cell data of lymphatic endothelial cells in SS vs DSS reveal heterogeneity in this cell type.** UMAP plots of lymphatic endothelial cells in steady state (a) and inflammation (b). Dot plots of lymphatic endothelial cells in steady state (c) and inflammation (d) (n = 10 mice steady state; n = 10 mice inflamed).

3.5.6 Differential lymphatic gene expression in inflammation

To establish the differences between LECs in steady state and inflammation, Seurat integration was performed (152). This enables corresponding cells to be combined between the steady state and inflamed conditions and provides the ability to contrast the cellular clusters between the conditions (Figure 3.24a). The striking finding was that of a cellular cluster appearing in the inflamed state, which is cluster number four (Figure 3.24b). The genes that were upregulated in this cluster included Stat1, H2-Ab1, Cd274 (Pdl1), Cd74, Gbps and Irf1 (Figure 3.27a, Figure 3.25b). MHC II (153) and PDL1 (154) have been described to be downstream of interferon-gamma signalling and Stat1 phosphorylation is required for signal transduction of interferon-gamma signalling (155). Gbps and Irf1 are also downstream of interferon signalling, so this cluster would appear to be a subset of LECs that are interferon responsive. This is also in keeping with the known requirement for the cytokine interferon-gamma to cause pathology in DSS colitis (156). Furthermore, endothelial-specific knockout of interferon-gamma signalling was shown to be protective in DSS colitis (157). This study targeted endothelial cells using Tie2-Cre and Cdh5-Cre mice crossed to Ifngr2-flox. However, these Cre-promoters also target lymphatic endothelial cells and so perhaps some of the protective effect may have been from interferon-gamma signalling into LECs, which may have been overlooked. As a result, we had the idea to cross Prox1-CreER^{T2} with Ifngr1-flox animals to see to what degree the protective effect was down to LECs as opposed to BECs.

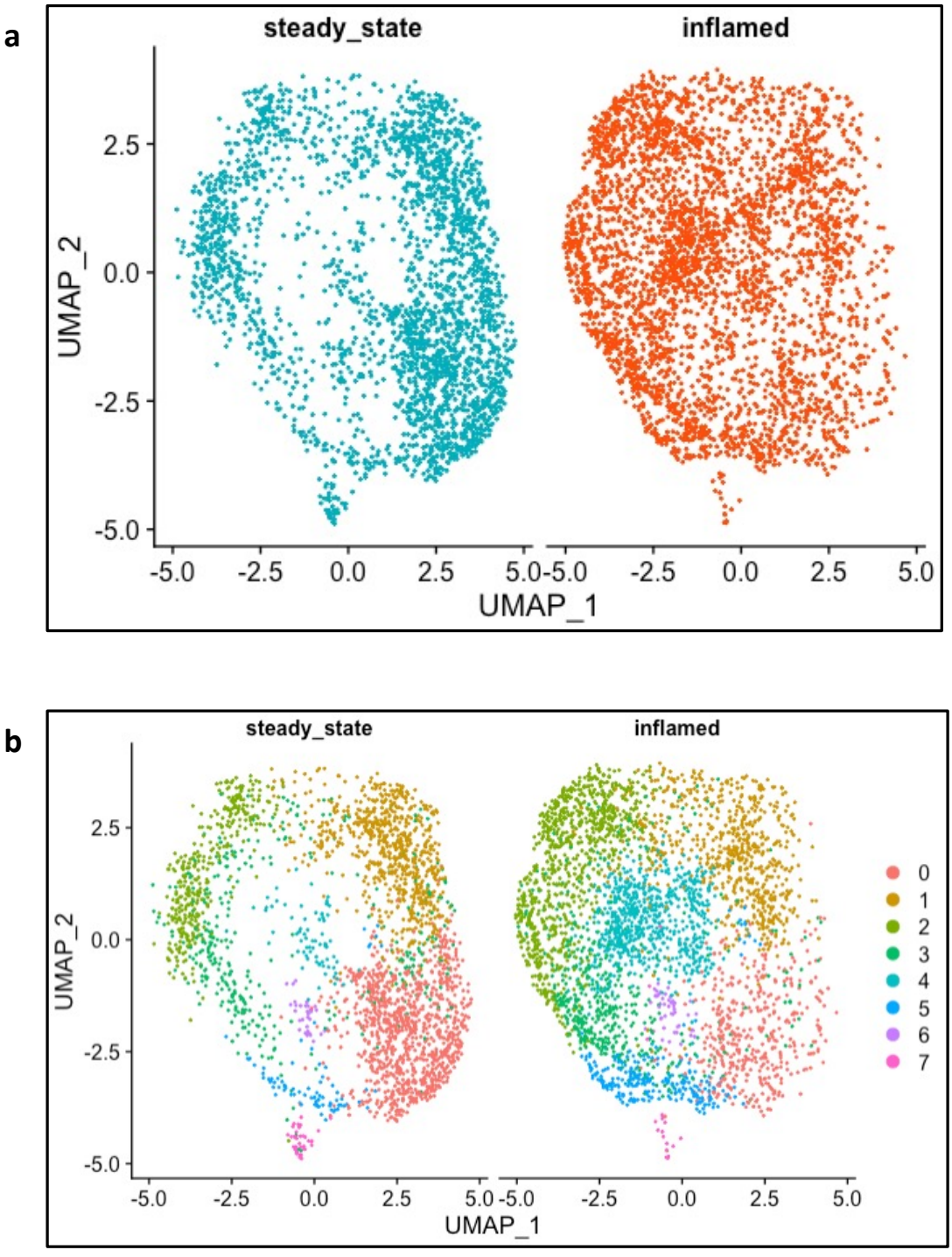

Figure 3.24: **Integrated single cell data of lymphatic endothelial cells reveal heterogeneity in this cell type.** UMAP plots of all integrated lymphatic endothelial cells coloured by condition (a) or cell cluster (b), separated by condition (n = 10 mice steady state; n = 10 mice inflamed).

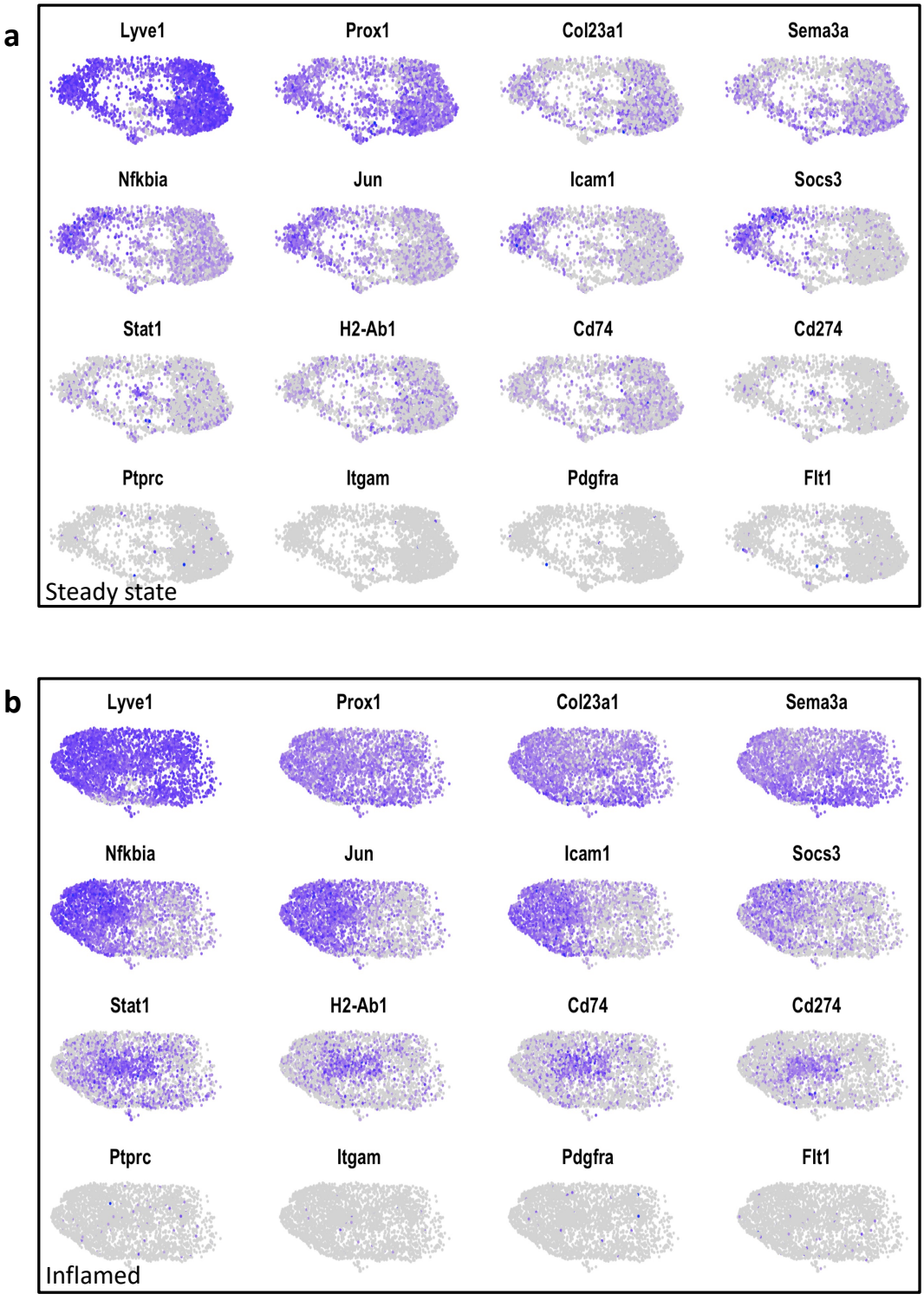

Figure 3.25: **Integrated single cell data of lymphatic endothelial cells reveal heterogeneity in this cell type (cont'd).** UMAP plots of genes of interest in integrated lymphatic endothelial cells in steady state (a) inflamed (b) (n = 10 mice steady state; n = 10 mice inflamed).

3.5.7 Different flavours of inflammatory lymphatic endothelial cell exist in DSS colitis

When we plotted some of the key genes upregulated in the inflamed LECs, we saw the appearance of the interferon-stimulated genes in the central cluster, but also a distinct subset of cells (cluster number two) expressing Icam1, Jun, Socs3 and Nfkbia (Figure 3.27a).

Icam1 is a cell surface glycoprotein best known for regulating leukocyte recruitment from the blood into tissues via the blood endothelial cells; however, Icam1 expression on LECs has also been shown to have a role in the extravasation of T leukocytes from the tissue into the draining lymphatic vessels in a model of skin inflammation (158). Icam1 has also been found on a wide variety of cells and has an outside-in signalling mechanism enabling it to function as a biosensor (159). It was intriguing to us to note the presence of these two distinct flavours of inflammatory LEC, and we were curious as to the location of these in the tissue.

When we plotted the proportion of LECs within each cluster per mouse as either a stacked bar plot (Figure 3.26a) or a dot plot (Figure 3.26c), we found that cluster number two and four described were increased in the inflamed mice compared to the steady state. We also plotted the absolute number of cells originating from each mouse (Figure 3.26b), highlighting that each biological replicate contributed towards the data.

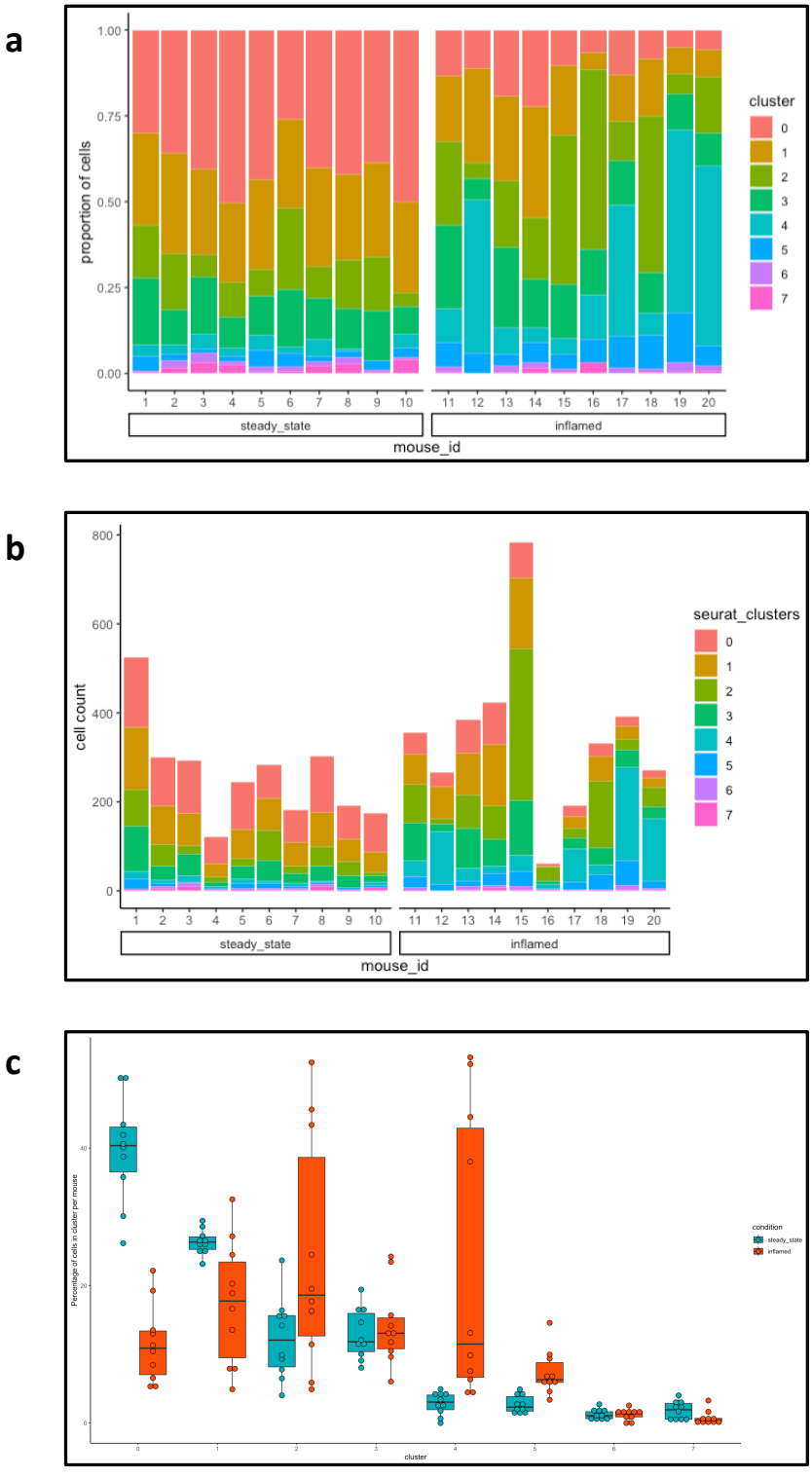

Figure 3.26: **Integrated single cell data of lymphatic endothelial cells reveal heterogeneity in this cell type (cont'd).** Stacked bar plot of proportion (a) or absolute number (b) of lymphatic endothelial cells contributing to each cluster per mouse. Dot plot of proportion of cells contributing to each cluster split by condition (c) (n = 10 mice steady state; n = 10 mice inflamed).

a

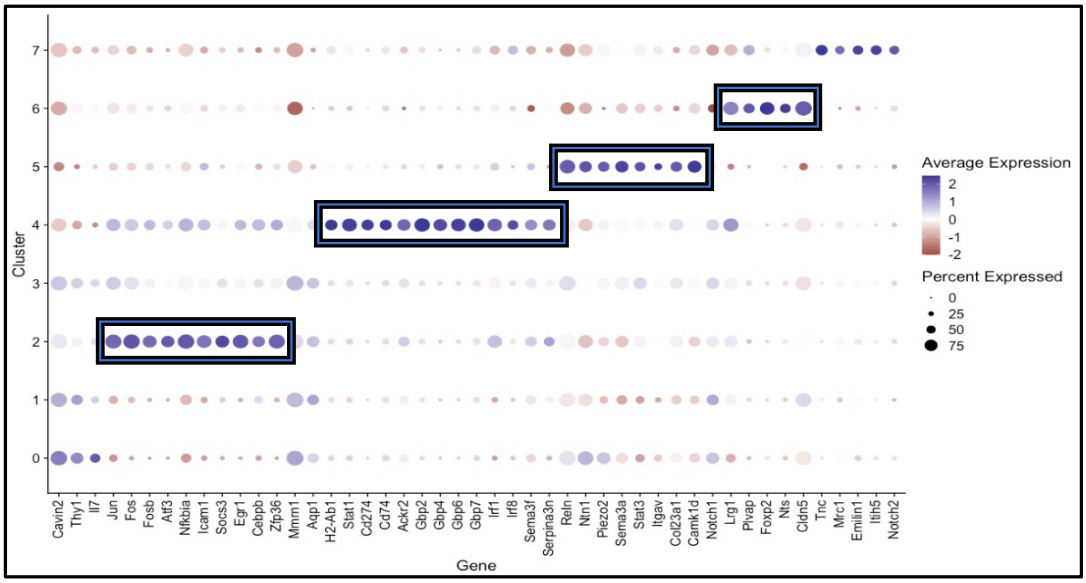

b

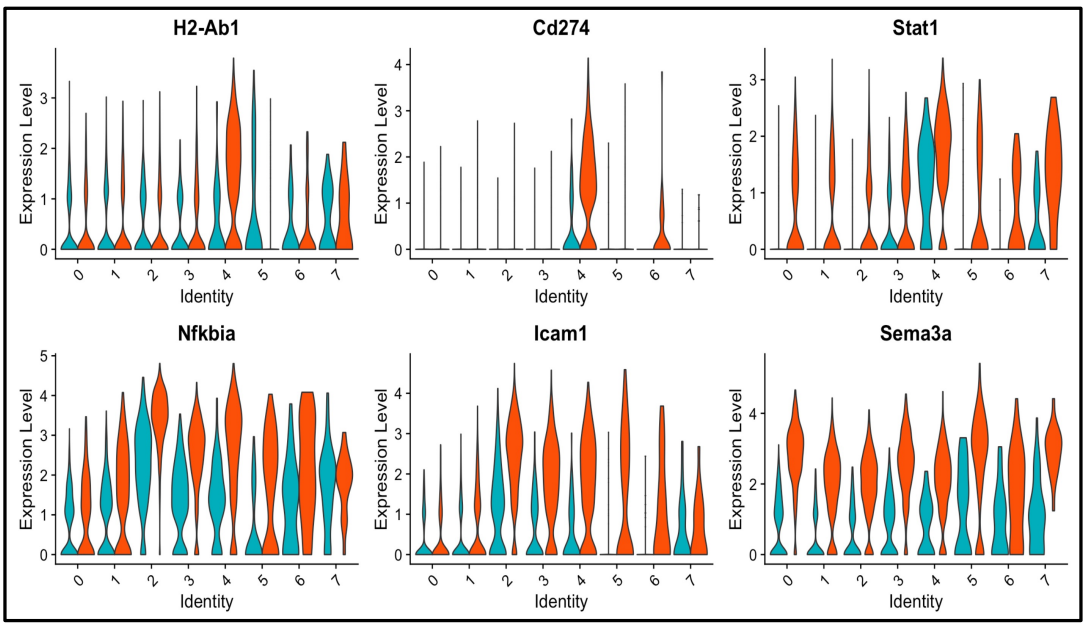

Figure 3.27: **Integrated single cell data of lymphatic endothelial cells reveal heterogeneity in this cell type (cont'd).** Dot plot of genes of interest per cluster (a). Violin plot of genes of interest split by condition (b) (n = 10 mice steady state; n = 10 mice inflamed).

3.5.8 Conclusion from analysis of single cell sequencing data

We identified the presence of distinct LEC subsets within the healthy murine colon, as well as changes in DSS colitis. We were particularly interested that inflammation resulted in multiple subsets of inflammatory LEC, which is only possible to have identified via single cell sequencing analysis.

3.6 Discussion

We established a novel approach to isolating LECs from the murine colon and using this method with flow cytometry concluded that there is no change in LEC number over time in a murine colitis model, despite a robust inflammatory response. This addresses a question that is inconclusive in the field in a novel way and it was reassuring to use the Prox1-Cre-ER^{T2} mouse model to confirm that we were isolating LECs from the murine colon. Despite these results, there are several limitations to this methodology that requires further discussion. Even though we were able to isolate live LECs, there were still a high number of dead cells. We are assuming that the ratio of live to dead cells remains constant between different conditions, however a clear limitation is if inflammation itself promotes more cell death compared to steady state. Furthermore, as we are only isolating small numbers of cells, the noise is significantly greater compared to quantifying lymphocyte numbers. Another limitation is the significant baseline variability in LEC number. This was because a single steady state mouse was taken on each day of the time course experiment, highlighting the variability of enzymatic digestion of the tissue between different days. If this could be repeated, I would have ensured that the baseline variability was minimised before proceeding with the inflammatory model.

We were limited in profiling the expression patterns of growth factor receptors or chemokine receptors on LECs by the number of antibodies that we had available for flow cytometry. We wanted to concurrently profile immune cell populations and were unable to split the sample due to the low number of LECs that were obtained from each mouse. Since the time of these experiments, we have adopted spectral flow cytometry and if starting this again now I would profile these cells with this new platform. Furthermore, we made the assumption that all lymphatic endothelial cells expressed podoplanin, which we could confirm by assessing the co-expression of other lymphatic markers.

We established some preliminary findings from the analysis of the bulk transcriptomic data from sorted cell populations over time in a DSS time course experiment. We observed subsets of lymphatic endothelial cells change in inflammation from single cell RNA sequencing data and wanted to validate this using different methodologies.

The single cell sequencing data highlighted that there are LECs sensing interferon signalling in the tissue and we thought to deplete the interferon gamma receptor on lymphatic endothelial cells utilising the Prox1-Cre-ER^{T2} mouse that was introduced at the start of this chapter. However, this unfortunately did not work in depleting the interferon gamma receptor as verified by flow cytometry and we also had issues with this Cre driver being unable to delete podoplanin expression from LECs in a complementary experiment, but which was able to be deleted using a different Cre driver. This highlighted that the Prox1-Cre-ER^{T2} mouse was adequate as a lymphatic reporter but inefficient at deleting targets of interest. On further discussion with the lymphatic community, it came to our knowledge that this mouse model is poor compared to an alternative Prox1-Cre from the laboratory of Professor Tajia Makinen, but due to time limitations it was not possible to obtain this alternate mouse and repeat this crossing.

We have created a cellular atlas of lymphatic endothelial cells at steady state and inflammation from the murine colon, which has highlighted that interferon signalling occurs in a subset of lymphatic endothelial cells in inflammation, and moreover, this is occurring in a subset of the cells rather than all of them. This led us to consider where in the tissue these changes may be occurring. As alluded to several times so far, the lymphatic vasculature is fundamentally a 3D structure and so we decided to pursue a 3D understanding of this using novel imaging methods and tracer studies, which we will turn to in the next chapter.

4 3D imaging and physiological tracer studies illustrate colonic lymphatic vascular anatomy and the pathway of colonic tissue drainage

4.1 Introduction

Having characterised lymphatic endothelial cells in the colon by flow cytometry, and transcriptomic analysis, it became apparent that the method to best understand the orientation and architecture of the lymphatic vasculature would be to visualise the lymphatic vascular network in 3D. This is because these vessels are long and tortuous and inevitably a 2D section only reveals the cross-section of a vessel, which cannot be consistently orientated, adding to the challenge of understanding. We also developed a method to understand interstitial outflow from the colon to map out the pathway of colonic tissue drainage draining into the lymphatic vessels.

4.1.1 3D imaging of colonic tissue

Significant progress has been made on 3D imaging methods to study tissue architecture in the past few years. This is both due to improved methods of optically clearing tissue as well as improved capabilities in imaging acquisition and computing power to handle large datasets (160). The lymphatic vessels have been imaged in 3D in the mouse, but this has mainly focused on the small intestine (41, 88) with the colon being relatively neglected. Of course, in medicine, 3D imaging is regularly used clinically in the form of CT and MRI scans that have transformed clinical care by enabling the cross-sectional visualisation of structures that were previously only visible stacked in one plane with conventional x-rays. This field-change is now being paralleled in the research setting. New insights can be gleaned by understanding the three-dimensional structure of tissue at the macroscopic scale where gross pathology is often visualised, but then also be able to zoom in on the same image to visualise cellular resolution in areas of interest. We move between these macro- and microscopic scales in the imaging data presented in the remainder of this thesis.

4.1.2 Microinjections to visualise interstitial outflow from the colon

We wanted to couple the visualisation of the tissue in 3D with an understanding of how interstitial fluid drains out of the colon and its path to the draining lymph node. To do this we were inspired by the work of Czepielewski et al. who demonstrated the lymphatic drainage of the small intestine by injecting fluorescent tracers into Peyer's patches and visualising the exit using a fluorescent stereomicroscope in a living mouse (102). Working together, we developed an analogous injection method in the colon, the results of which will be presented in the latter half of this chapter.

4.1.3 Chapter aims

- Create a 3D map of the colonic lymphatic vasculature
- Chart the outflow of interstitial fluid from the colonic tissue to the draining lymph node

4.2 3D imaging reveals novel insights into the anatomical orientation of the colonic lymphatic vasculature

4.2.1 Two lymphatic networks exist in the murine colon and contrast significantly from the lymphatic network of the small intestine

Our initial 2D imaging of the colon using the marker Lyve1, which is specific for lymphatic vessels (161), revealed a hint of staining in two regions – beneath the epithelium and in the muscle layer (Figure 4.1). However, as we had expected with 2D imaging, it was difficult to visualise the nature of these vessels and where they originated and ended. We were able to gain clarity on the lymphatic orientation and structure as we developed the use of 3D imaging techniques.

After several months of optimisation, we developed the ability to use tissue clearing methods and 3D confocal imaging with Prox1-GFP mice and observed the presence of two networks of lymphatic vessels in the colon. One tracked beneath the epithelium and the other was embedded in the muscle layer of the colon, which we will describe further. The figure illustrates movement through the colon from the outside muscle layer in towards the lumen, and the full orientation of the colonic lymphatic vasculature can be appreciated (Figure 4.2).

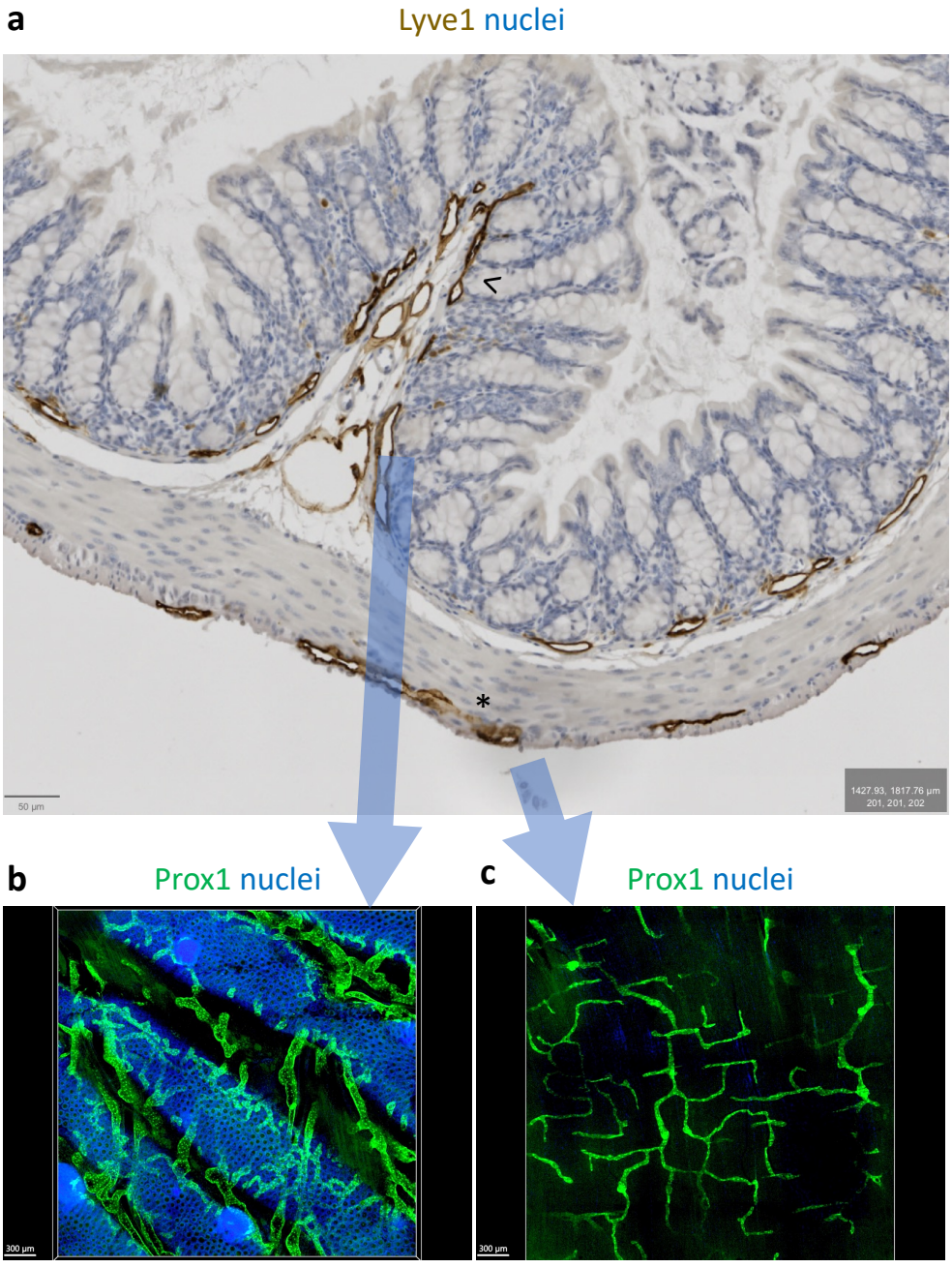

Figure 4.1: Colonic lymphatic vessels are located beneath the epithelium and between the circular and longitudinal muscle layers of the colon. Lyve1 antibody staining in the cross-section of the murine colon suggests that there are lymphatic vessels that line the base of the crypts (<) as well as being found within the external muscle layer (*) (a). The architecture of the vessels that line the crypts are fully appreciated using 3D imaging, with the subepithelial lymphatics (b) demonstrating quite a different morphology to those found in the muscle layer (c). *Images are representative of at least five independent experiments.*

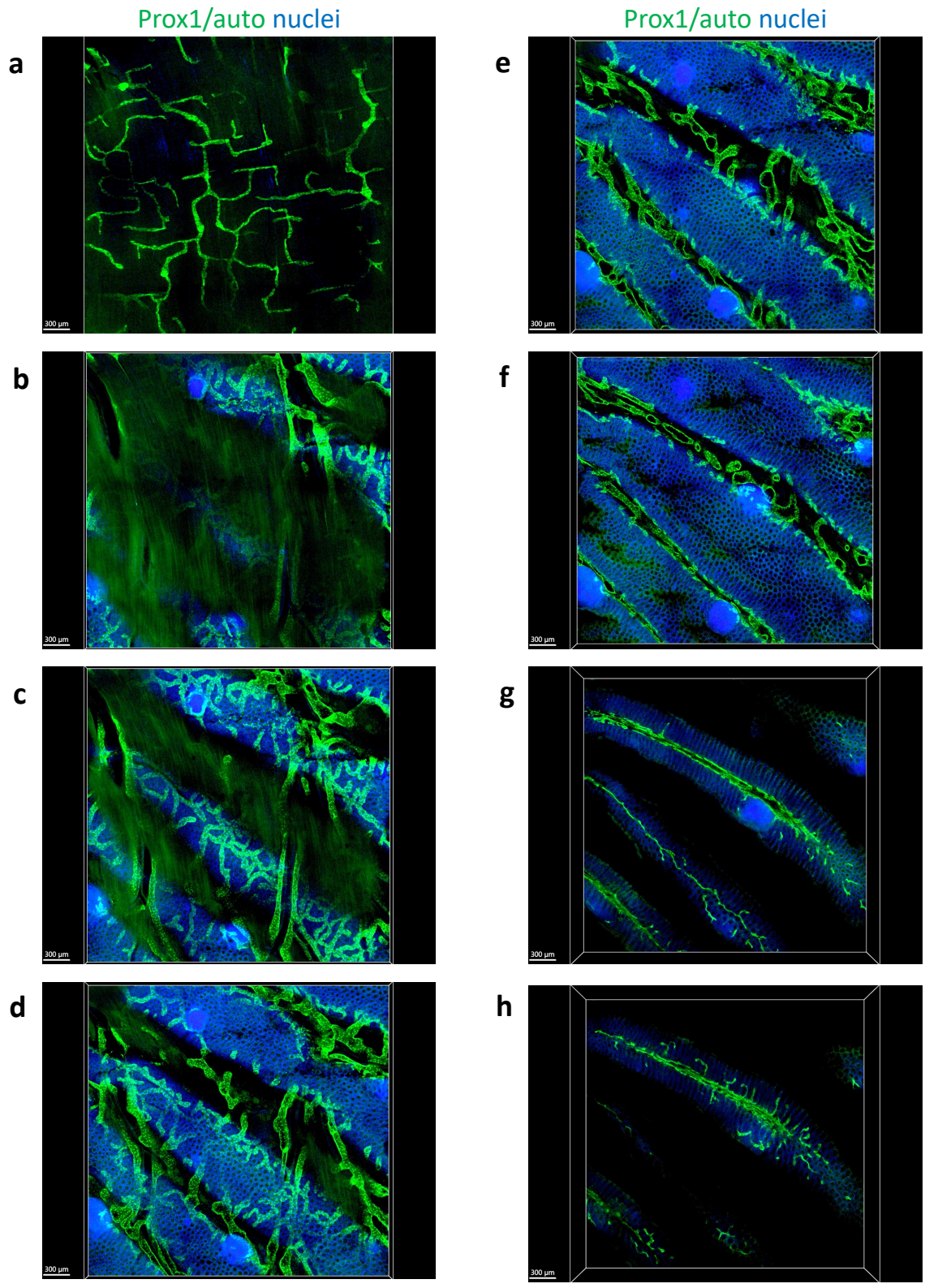

Figure 4.2: Colonic lymphatic vessels are located beneath the epithelium and between the circular and longitudinal muscle layers of the colon. Prox1-GFP mouse with DAPI going from the muscle layer (outside) of the colon towards the lumen. *Images are representative of at least five independent experiments.*

4.2.1.1 Sub-epithelial colonic lymphatics feature finger-like projections in distinct regions

We observed that the colonic lymphatics that lie beneath the epithelium formed a dense network that ran in parallel with the blood capillaries (Figure 4.3a-b). We were curious to see the relationship of this network with the muscularis mucosae was that there were vessels found both above (Figure 4.4a, arrowhead) and below this muscle layer (Figure 4.4a, double arrowhead). We also noted that the lymphatic vessels in this layer were associated with lymphoid follicles found in the tissue (Figure 4.2d), which we will focus on in more depth later.

When inspecting the images of the colonic lymphatic vessels acquired with a lower magnification objective, we realised that they lined colonic tissue folds, and specifically in these regions we noted the presence of finger-like projections that branched from the vessels towards the lumen (Figure 4.3a, arrowhead). We were curious that these morphologically distinct finger-like projections were particularly concentrated in certain anatomical regions of the colon. When looking at the 3D cross section of the image (Figure 4.3a) we can appreciate these lymphatic projections only because we visualised 100 micron-thick digital section that we reconstructed from the raw confocal data. This is in contrast to the traditional 5 micron sections that are cut for 2D histology, where this feature of the vascular architecture would not be visible and would be overlooked.

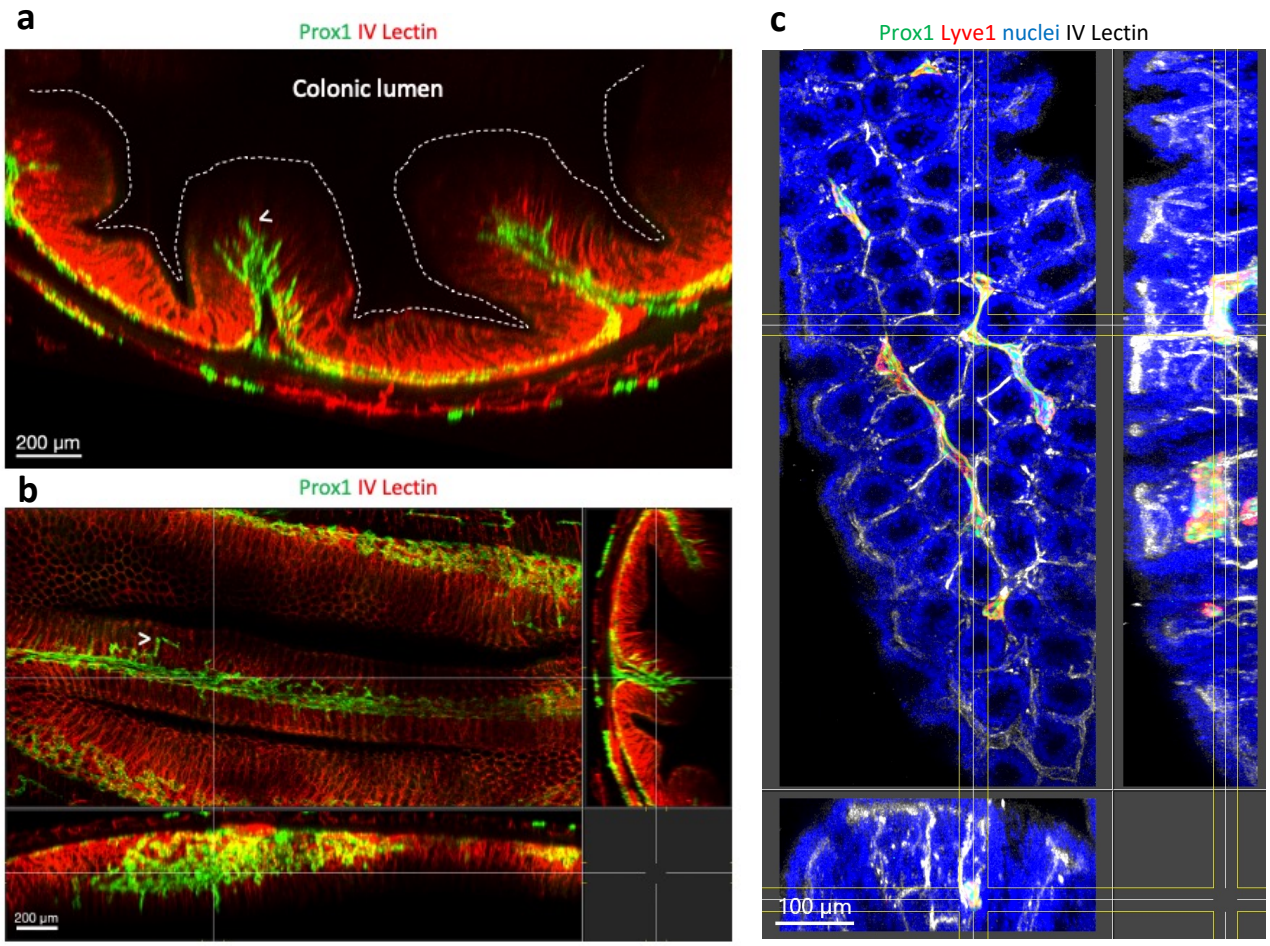

Figure 4.3: Lymphatic projections are intermittently found in the lymphatic vessels that line the epithelial crypts specifically in regions of tissue folds. Dotted white line represents the border of the colonic tissue with the lumen (labelled) (a). The colonic cross-section highlights that lymphatic vessels are running in the tissue folds (arrowheads in a and b). Further imaging focusing on one colonic fold highlights that these projections are Lyve1 and Prox1 positive lymphatic vessels (c). *Images are representative of at least five independent experiments.*

4.2.1.2 Muscle layer colonic lymphatics sit between circular and longitudinal muscle

The muscle layer lymphatic vessels formed a much sparser network compared to the sub-epithelial lymphatic network (Figure 4.1c, Figure 4.2a). At higher magnification, we realised that the muscle layer lymphatic vessels were located in between the circular and longitudinal layer of muscle (Figure 4.4a-b). Furthermore, we realised that there was a close relationship between this network of lymphatic vessels and what was morphologically consistent with nerves of the myenteric plexus (Figure 4.4b, asterisk) as well as morphologically consistent with glial cells that lie in this region (Figure 4.4c, asterisk) as evidenced by podoplanin staining, which we had initially utilised to visualise the lymphatic vessels. We hypothesised that this second layer of lymphatic vessels exists in the colon to prevent excess interstitial fluid from leaking out from the tissue into the peritoneal cavity, which may lead to a peritonitis if left unchecked.

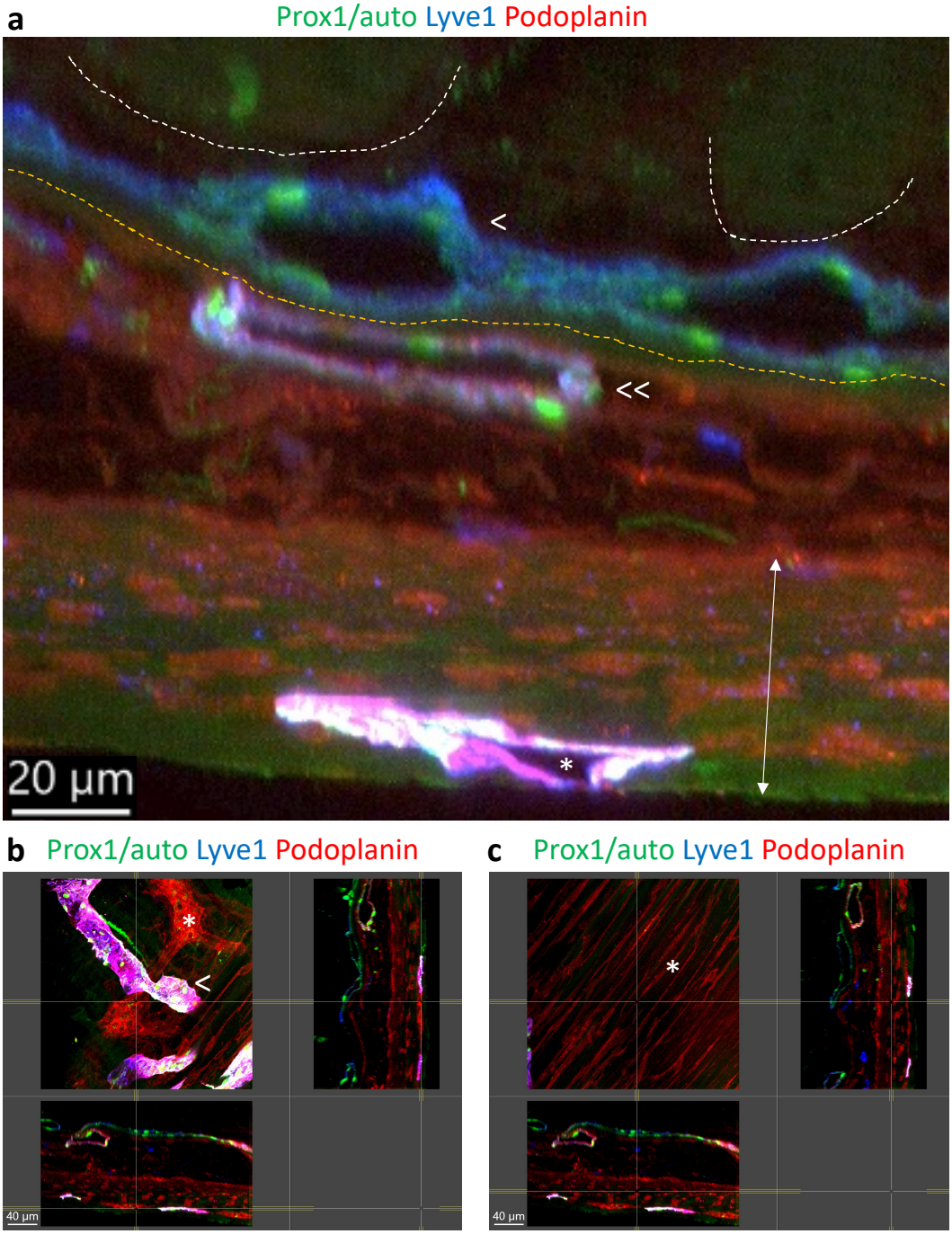

Figure 4.4: Lymphatic vessels are found above and beneath the muscularis mucosa, as well as between the circular and longitudinal muscle in association with the enteric nervous system and glial cells. The lymphatic vessels run beneath the epithelial crypts (highlighted by the white dotted line) (a). They are found on either side of the muscularis mucosa (highlighted by the orange dotted line) The lymphatic vessel above the muscularis mucosa is single arrowhead and beneath is double arrowhead in (a). Furthermore, the external muscle is demonstrated by a double arrowhead, with the lumen of a lymphatic vessel beneath the two layers highlighted by an asterisk in (a). The close association of the lymphatics (arrowhead) in the external muscle layer to the glial cells of the enteric nervous system (asterisk) is depicted in (b) Immediately above this, numerous glial cells are found in the external muscle highlighted by an asterisk in (c). *Images are representative of at least three independent experiments.*

4.2.2 Small intestinal lymphatic orientation stands in significant contrast to the colon

The arrangement of the small intestinal lymphatic vasculature is relatively well-understood in the literature. It is known that each villus in the small intestine has a central lymphatic vessel called a lacteal, which is responsible for lipid absorption from the diet (162). As a comparison to the colon, we imaged a portion of the murine small intestine (Figure 4.5). The 3D projection starts from the outside muscle (Figure 4.5a) and rotates (Figure 4.5b-c) to finish looking at the sample from the luminal side (Figure 4.5d). The second half of the panel (Figure 4.5e-h) highlights the cross-section of of the small intestinal lymphatic vasculature starting from the muscle layer which is generally devoid of lymphatics compared to the colon (Figure 4.5e), followed by the crypt base where the lacteals drain (Figure 4.5f-g) and finally towards the luminal side of the small intestinal where individual lacteals can be seen in the centre of each villus (Figure 4.5h). As the colon is rich in bacteria compared to the small intestine, we speculated that this could be why it may be unnecessary to have such a developed layer of lymphatics in the muscle layer, as there may be a lower likelihood of bacterial translocation to the peritoneal cavity compared to the colon.

From the small intestinal cross-section, we also noted that the tissue was not arranged in a similar folding pattern to that seen in the colon, but rather was a flat network with the only luminal projections being the intestinal villi themselves (Figure 4.5c). These data highlighted that the colonic lymphatic architecture was completely distinct to that seen in the small intestine.

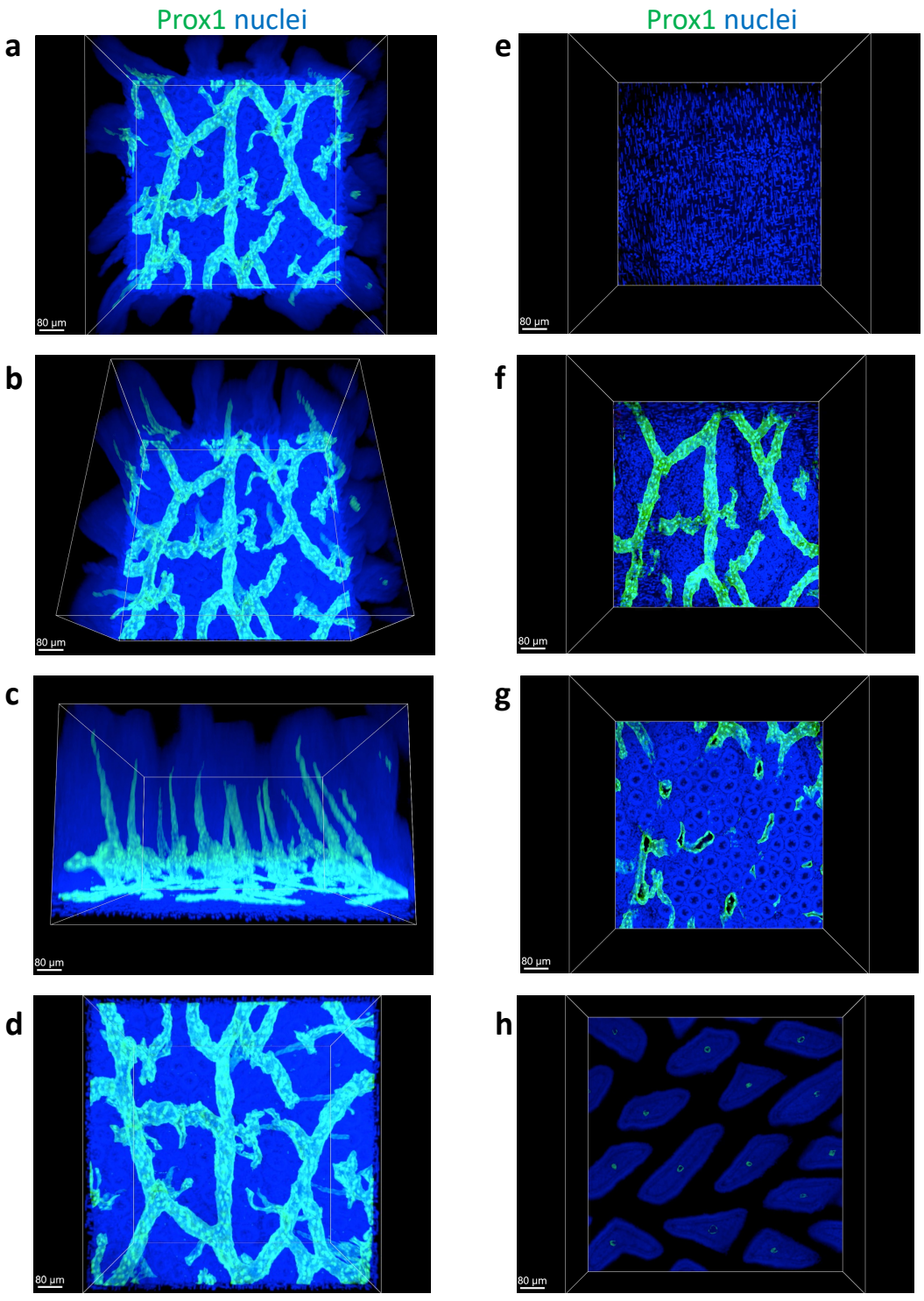

Figure 4.5: Small intestinal lymphatic vessels form lacteals draining into one network without a significant muscle layer as seen in the colon. The 3D reconstruction of a region of the small intestine is displayed in (a-d). The cross-section flying through from the lumen towards the muscle layer is visualised in (e-h). *Images are representative of at least three independent experiments.*

4.2.3 Lymphatic straps connecting colonic folds to the draining lymphatics

When returning to visualise the colonic lymphatic network from the outside with an even larger field of view, we noticed the lymphatic network of folds, as well as pairs of what appeared to be lymphatic 'straps' that were found perpendicular to the colonic luminal direction of flow (Figure 4.6, arrowhead). We hypothesised that these lymphatic 'straps' formed regular units within the colon and were the common endpoints of where interstitial fluid accumulated prior to exiting the colon.

4.2.4 Valves are found within lymphatic straps and muscle layer lymphatics

When we focused in more on these 'straps', as well as the muscle layer lymphatics, we noted that they appeared to contain valves by the presence of more intense Prox1-GFP signal, highlighting the increased number of lymphatic endothelial cells found at valves (Figure 4.7, double arrowheads in all images). Lymphatic valves are typically described in the larger collecting lymphatic vessels, for example in the legs, and have two leaflets and prevent the backflow of lymph, analogous to venous valves (49). Fluid shear stress is important in valve development (49). To our knowledge, this is the first description of lymphatic valves being found within the colonic tissue itself, which we also did not see when we examined the small intestinal lymphatic vessels. This also ties in with the few lymphatic valve cells that we identified from our single cell sequencing data of the murine colon presented in the previous chapter (Figure 3.23).

This data suggested to us that unidirectional flow is important in the drainage of colonic lymph, and we will return to this idea later when considering the interstitial drainage pattern identified from tracer studies.

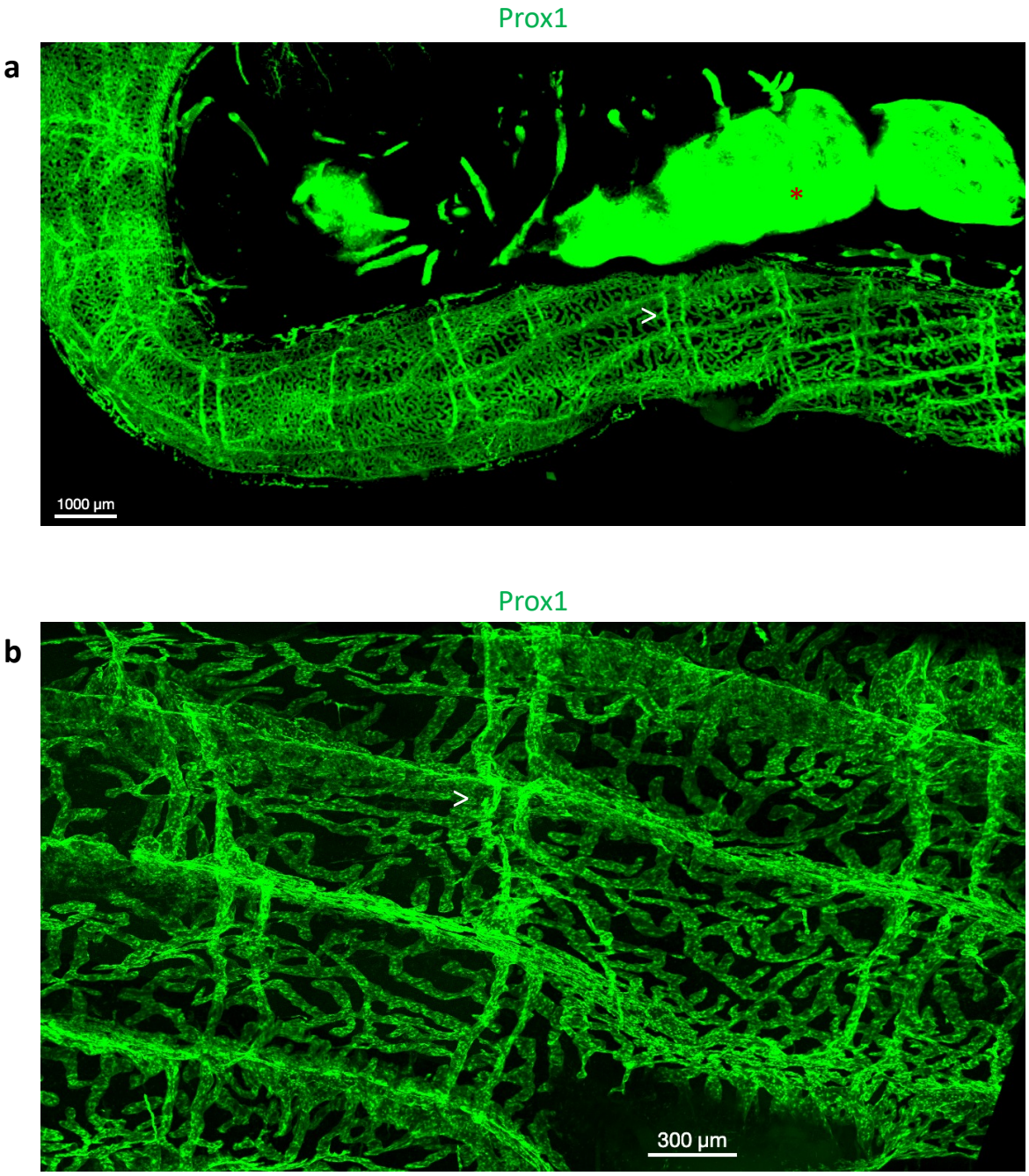

Figure 4.6: Colonic lymphatic straps are found throughout the length of the colon at regular intervals and drain the colonic folds. The colon is visualised with Prox1 signal (a) with the lymph nodes very bright for Prox1 (red asterisk in (a)) and a colonic lymphatic strap marked with an arrowhead in (a). The entry point of the fold lymphatics into the colonic strap is marked by an arrowhead in (b). *Images are representative of at least three independent experiments.*

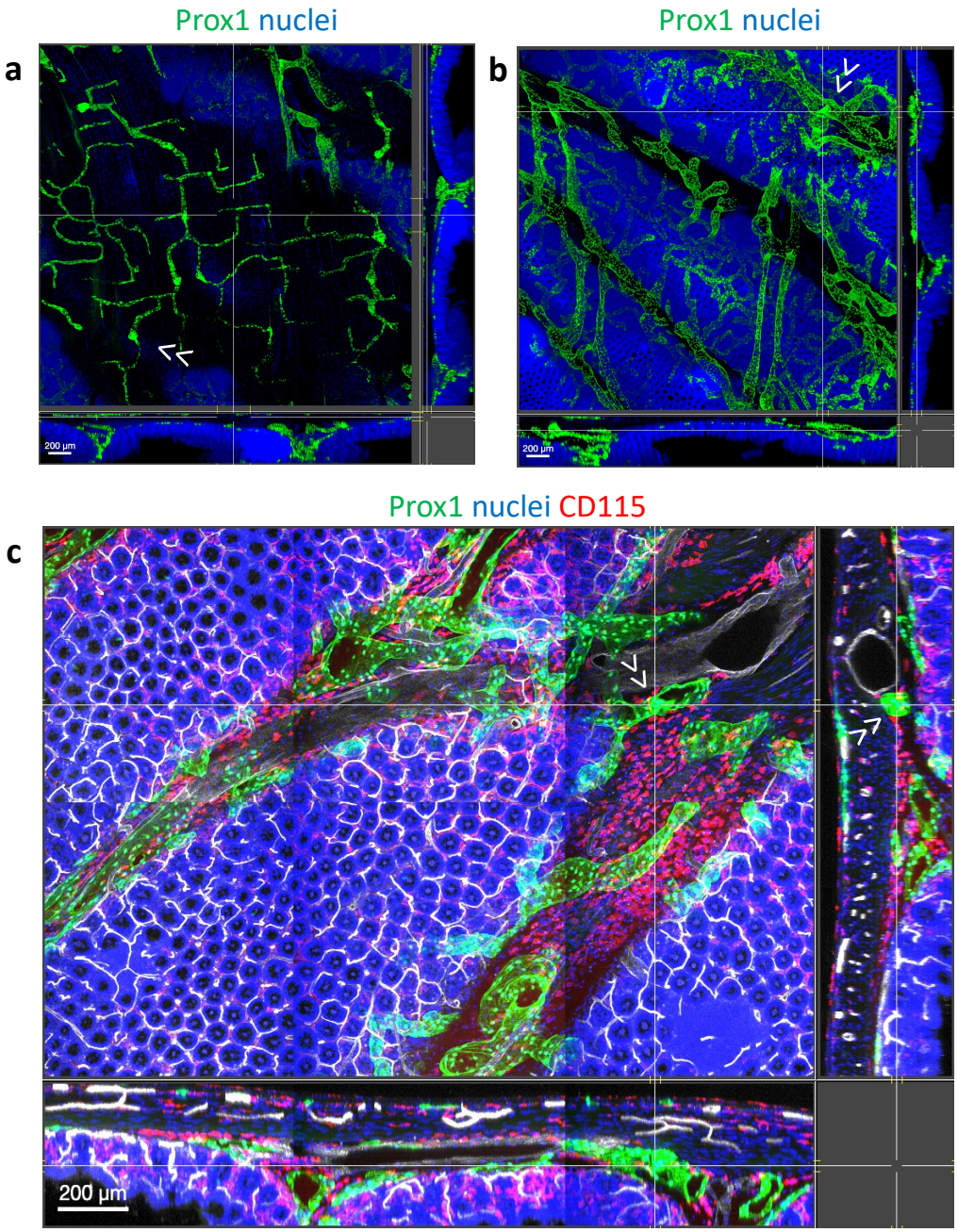

Figure 4.7: Colonic lymphatic vessels appear to have valves within the layer of lymphatics that drains the folds as well as the muscle layer. The muscle layer lymphatics (a) and fold-draining lymphatics (b) and (c) all show examples of intense Prox1 staining which represent valves (double arrowheads in all images). *Images are representative of at least three independent experiments.*

4.2.5 Lymphatic quantification must be cautioned in 2D sections

The quantification of the lymphatic vasculature from 2D sections has long been a challenge. Visual inspection can often reveal changes between conditions, but it is difficult to know what aspect to measure, as well as the inherent challenge with sectioning in that the anatomical orientation is not consistent throughout the tissue. Therefore, chance plays a significant role in the identified region.

To demonstrate this, we projected the view of a 5-micron section from one of our 3D images, which was specifically orientated to demonstrate a cross-section of the epithelial crypts and crypt-base associated sub-epithelial lymphatics that we had described earlier (Figure 4.8). Moving the section by just a few microns (Figure 4.8a-b, double arrowhead), which could easily be the difference between adjacent sections of tissue, shows what a difference this makes to the visible lymphatics. However, the mononuclear phagocytes (stained with CD115) and the epithelial crypts maintain a similar orientation and signal as these colonic cells are more regularly arranged across the tissue. This highlights the importance of careful appraisal of any quantification of lymphatic surface area from 2D sections, especially if there is no consideration as to which colonic region this is from and the orientation is not consistent between samples.

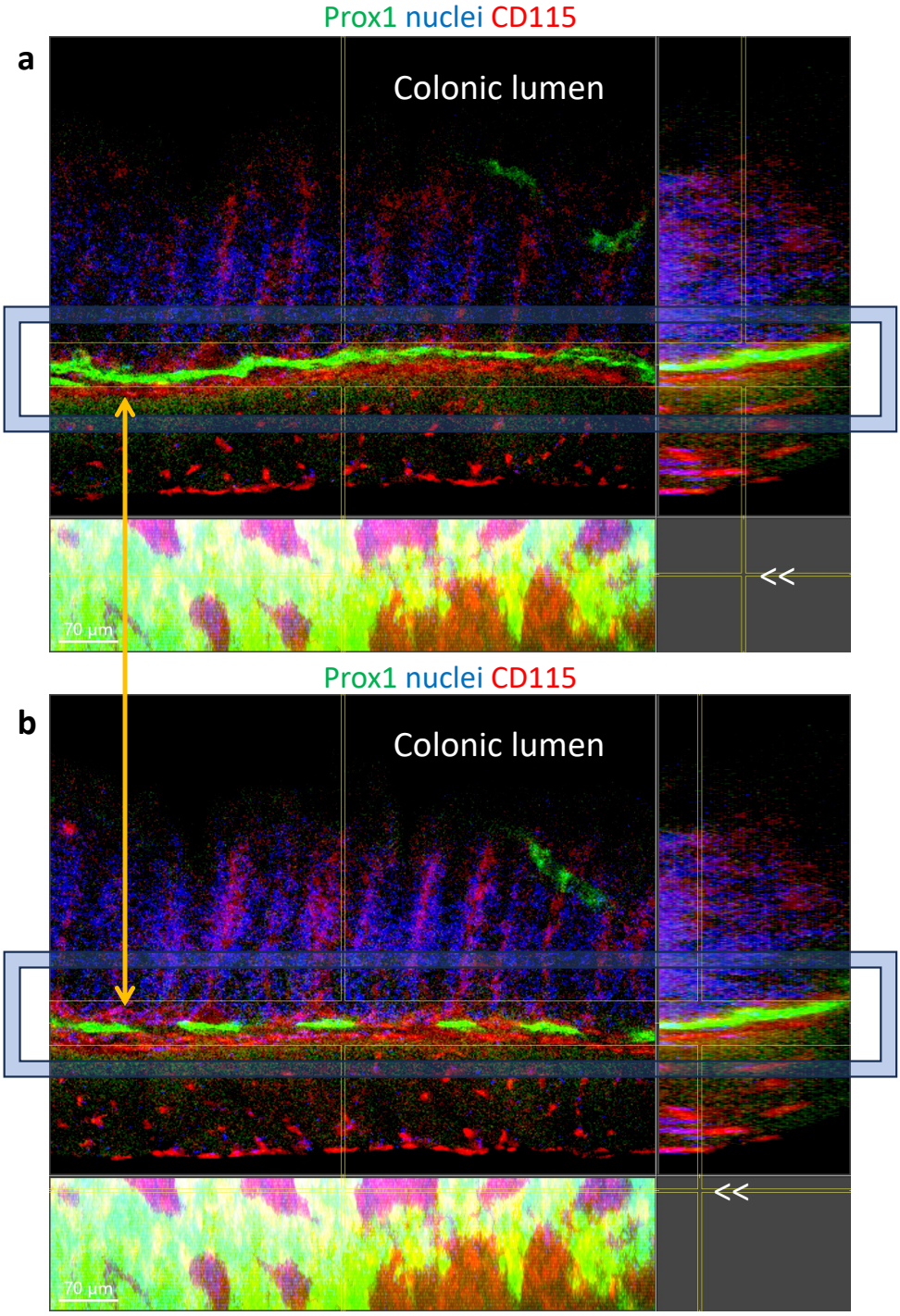

Figure 4.8: Cross-sectional views of 3D imaging of lymphatics reveals significant limitations in quantification of 2D histology. The difference between (a) and (b) is a few microns, which could easily be the difference between adjacent sections when cut manually (double arrowhead highlights the region from which the digital section has been imaged). When comparing the sub-epithelial lymphatic vessels (within transparent blue boxes and compared with orange double-headed arrow) between (a) and (b), quantifying this by percentage surface area of stain or number of lymphatic vessels would lead to huge variability in the quantification. *Images are representative of at least three independent experiments.*

4.3 Imaging human colonic lymphatic vessels in 3D shows similarity in arrangement to mouse

We were interested to compare the imaging data that we had acquired from the mouse colon to what is seen in human. To do this, we obtained a healthy piece of human colon from a resection specimen and stained for LYVE1, podoplanin, smooth muscle actin and DAPI to visualise nuclei. Once this was completed, we imaged the tissue in 3D after tissue clearing (Figure 4.9). The data is of a large piece that starts from looking from the luminal surface (Figure 4.9a, d, g) and progressively goes deeper into the tissue to the submucosa (Figure 4.9c, f, i). This highlights the lymphatic network beneath the muscularis mucosa, as seen in the mouse. Furthermore, the lymphatic vessels were associated with lymphoid follicles in a similar manner. We were also surprised to see holes that the lymphoid follicles made in the muscularis mucosa, with muscle fibres running at the base of the lymphoid tissue, suggesting that the whole follicle may undergo squeezing by contraction of these fibres (Figure 4.9d).

Finally, we noted that LYVE1 stained not only for lymphatic vessels but also macrophages that were found specifically in the submucosa of the human colon (Figure 4.9i, Figure 4.10f, Figure 4.11), which is also in keeping with LYVE1 macrophages being in the submucosa from published work in the human colon (163)

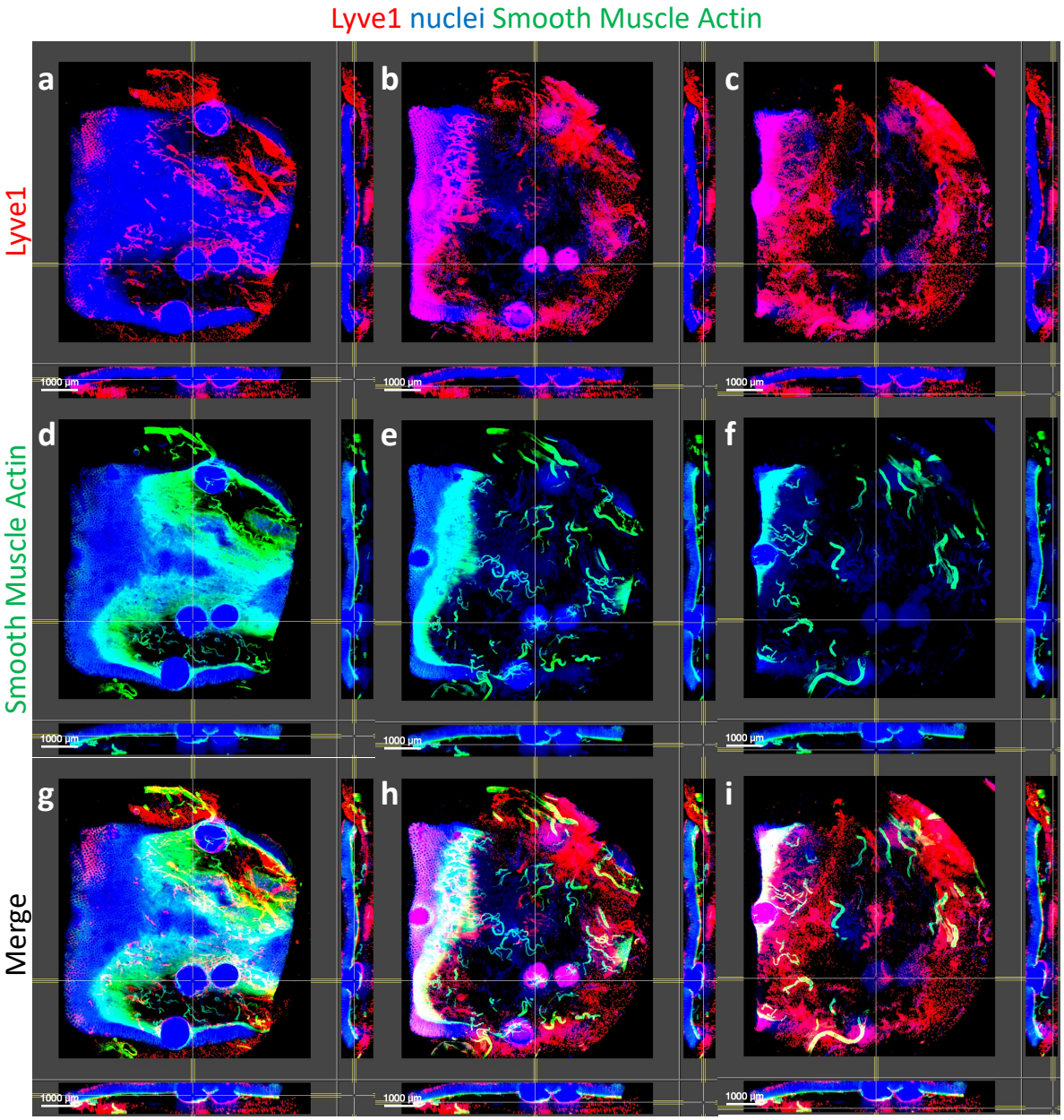

Figure 4.9: Human colon imaging reveals lymphatic drainage of lymphoid aggregates that cross the muscularis mucosa. The human colon was imagined using whole-mount microscopy techniques and representative images are displayed from the lumen on the left towards the deeper structures on the right. *Images are representative of a single experiment.*

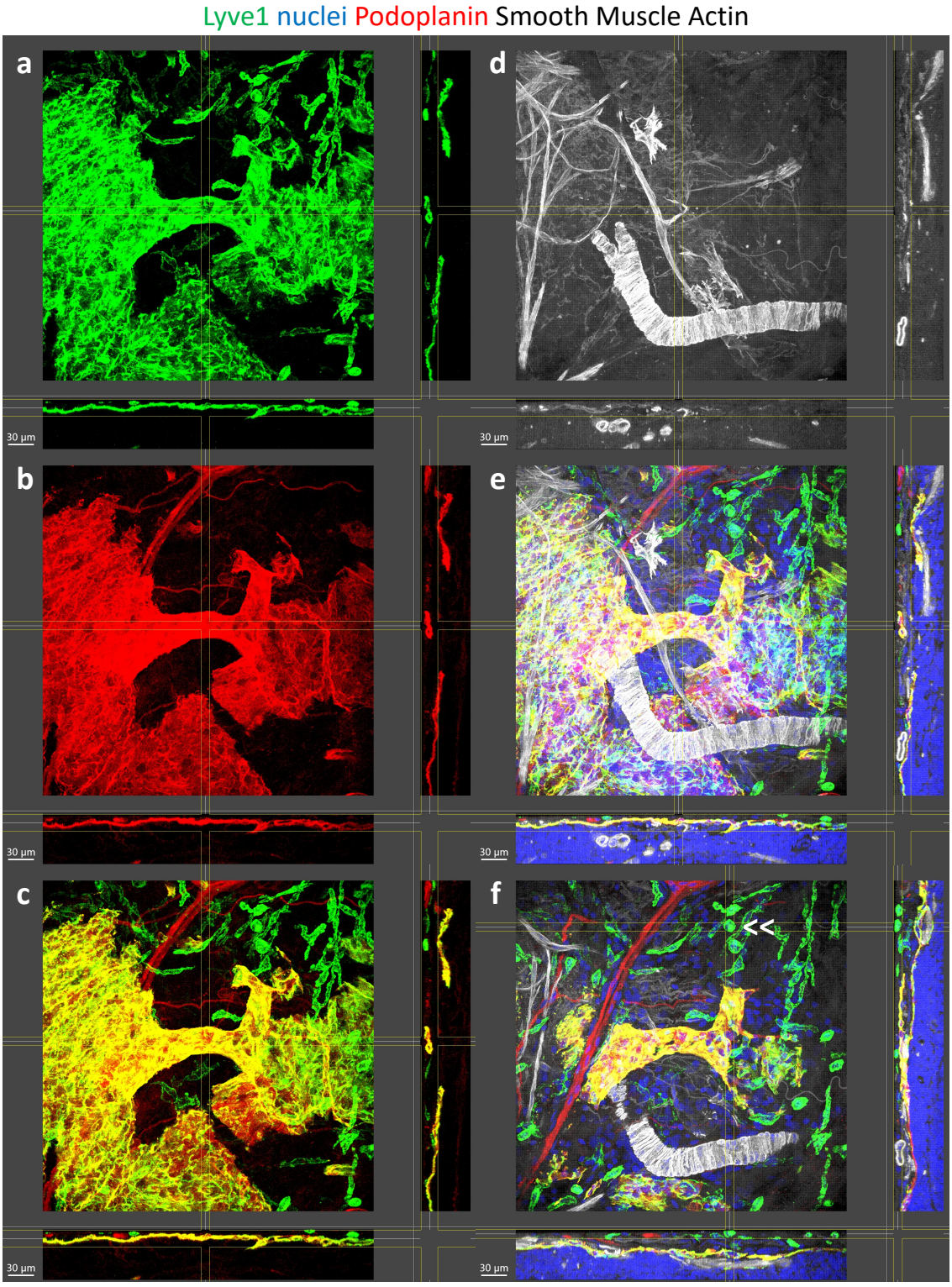

Figure 4.10: Human colon lymphatic imaging reveals similar orientation to mouse. The human colon was imagined using whole-mount microscopy techniques like the mouse (a-f). Lymphatic vessels were in a similar location adjacent to the epithelium. Lyve1 macrophages were present in the submucosa (double arrowhead in f). *Images are representative of a single experiment.*

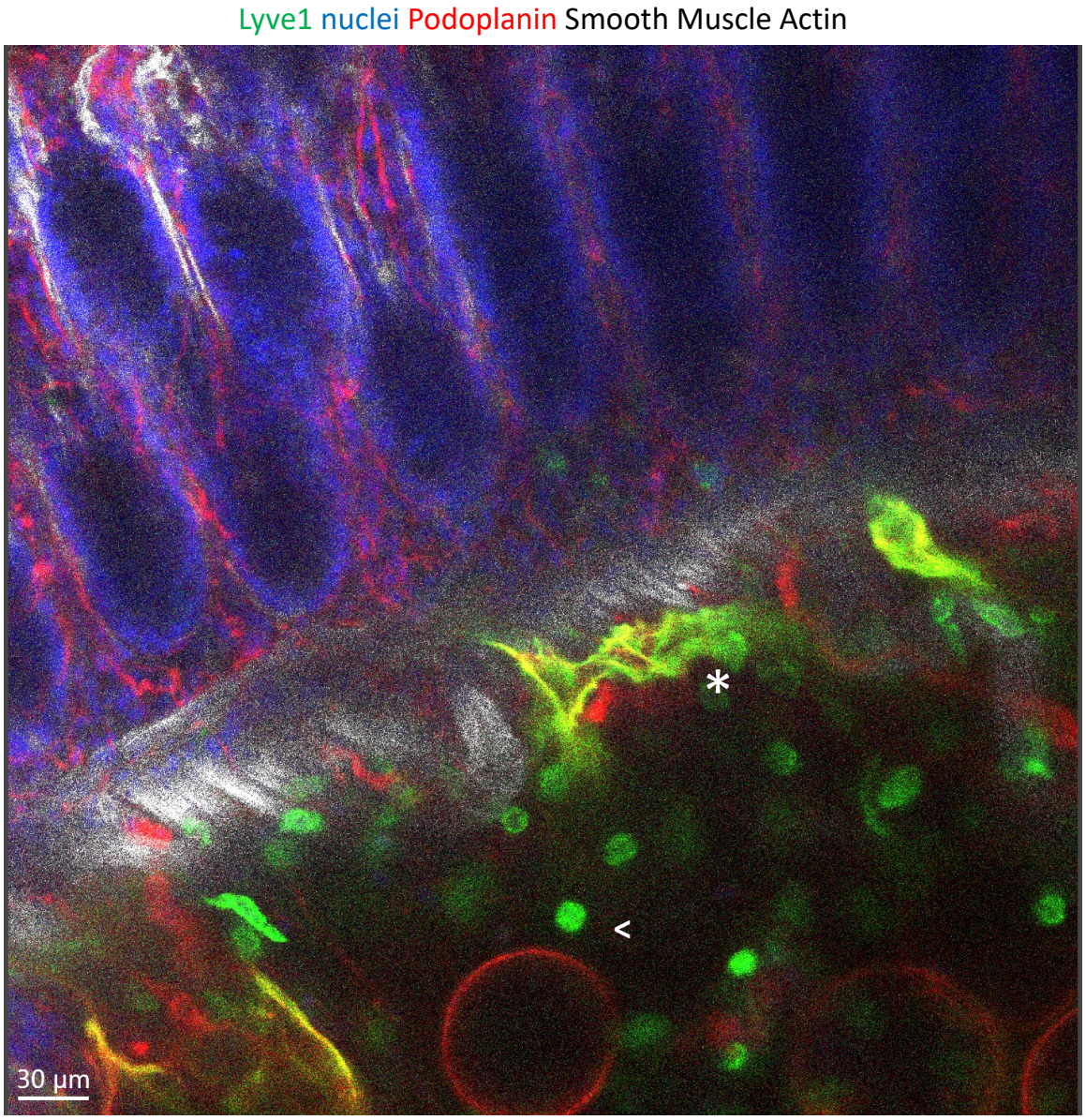

Figure 4.11: Human colon lymphatic imaging reveals Lyve1 macrophages in the submucosa. The human colon was imagined using whole-mount microscopy techniques like the mouse. Lyve1 macrophages are numerous in the submucosa (arrowhead) and lymphatic vessels can be seen beneath the crypts (asterisk). *Images are representative of a single experiment.*

4.4 Tracking interstitial fluid trafficking using microinjection and intravital microscopy reveals pathway of lymphatic outflow from the colon

Visualising the lymphatic system in 3D prompted us to delve into understanding outflow from the colon to bridge the anatomical discoveries that we had made with the physiological understanding of how interstitial fluid exits the colon via these vessels. To do this, we devised a novel method of intra-colonic tissue injection and data from these experiments will be presented in this sub-chapter of the thesis.

4.4.1 Injection of tracer and visualisation of colonic outflow

As outlined earlier, the work of Czepielewski et al. had utilised an injection method, both with a glass micropipette directly into the small intestinal tissue in collaboration with Professor Michael Davis, as well as using a Hamilton syringe to inject into Peyer's patches of the small intestine (102). Working together with Dr Rafael Czepielewski in the lab of Prof Gwen Randolph formed a unique opportunity to collaborate and develop new methods to adapt this technique to the study of colonic outflow.

To begin, we injected the tissue with 2000 kDa FITC-Dextran, which is an inert, fluorescent molecule with a large molecular weight, which we could be confident would only exit the tissue via the lymphatic vasculature. The colon has no Peyer's patches and externally there is little in the way of lymphoid landmarks that could be easily injected like the small intestine. Therefore, using a Hamilton syringe, we elected to inject 1-2 microlitres directly into the colon of an anaesthetised mouse and used a fluorescent stereomicroscope to visualise the drainage of the tracer (Figure 4.12a-b). Due to the technical factors involved in exposing the murine colon, the proximal colon was by far the most accessible portion and so this is where we focused our work. It is important to specify that this

injection was not into the lumen of the colon, but rather it was injected as shallowly as possible into the colonic tissue itself as described in the methods. Over time we noted that the FITC-Dextran made its way to the mesenteric lymphatic vessels and then the mesenteric lymph node itself. The FITC-Dextran reliably drained to the same lymph node at the end of the mesenteric lymph node chain (Figure 4.12b), as it is known that regional lymph node drainage patterns exist in the mouse (41, 42).

We were excited to have created, to our knowledge, the first model system where lymphatic drainage could be visualised from the murine colon. What stood out to us was the pattern of the FITC-Dextran that remained in the colonic tissue itself. We noted the accumulation of the tracer in the wall of the colon distributed unevenly in a grid-like pattern (Figure 4.12a-b). There were regions of tracer that formed parallel lines in the tissue, which then drained alongside the major blood vascular branches that wrap around the colon from the mesentery. By contrast, previous tracer injections in the small intestine did not show accumulation in this fashion (102).

4.4.2 Fixing and imaging tissue following microinjection reveals that tracer is in fold spaces lined by lymphatic vessels

Following the tracer injections described above, we fixed the tissue and imaged using the 3D imaging methods outlined at the start of the chapter. This mode of imaging highlighted that the tracer injection was within the colonic tissue folds and not within the lymphatic vessels lining them (Figure 4.12c). This made us think that the colonic tissue fold was a specialised region of tissue that acts as a reservoir of interstitial fluid that is destined for exit from the colonic tissue via the lymphatic vessels.

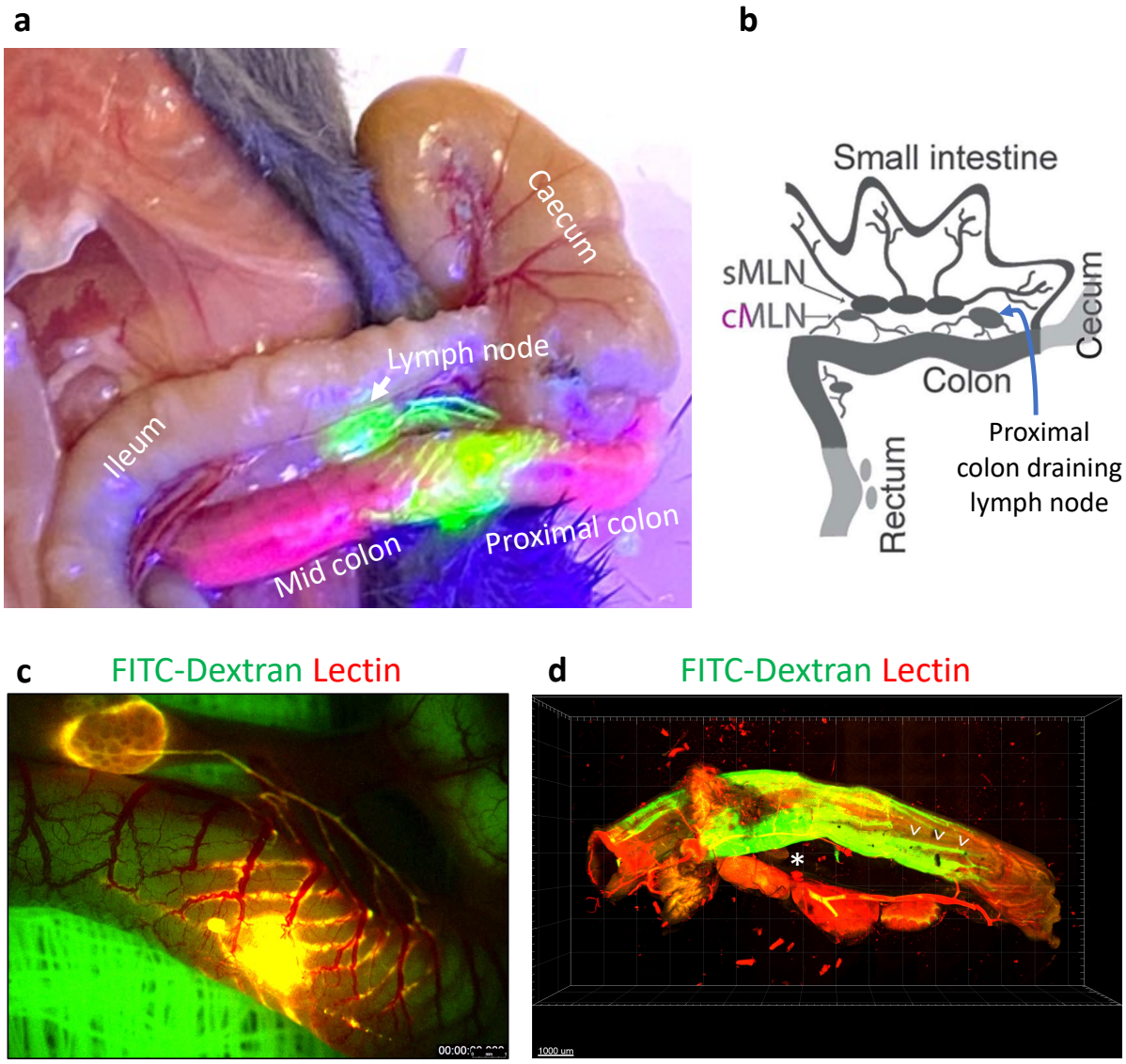

Figure 4.12: Colonic tracers accumulate in the tissue folds. Following intra-colonic injection, the pattern of the tissue folds can be seen at a macroscopic level (a) draining to the proximal colon draining lymph node, highlighted on a diagram from Houston *et al*. (42) (b). The tissue folds can also be seen under the stereomicroscope (c). Imaging of a large region of colon shows that tracer can travel several millimeters within the tissue (d). *Images are representative of at least five independent experiments.*

4.4.3 Microinjector confirms that bolus method is valid to mark the drainage pattern of the colon

A criticism of bolus injection, even of 1-2 microlitres, is that the sudden pressure upon injecting this into tissue is supra-physiological and may disrupt the tissue itself. To address this, we used a microinjector to inject tracer at a rate of 6.6 nanolitres/second (two microlitres over five minutes) (Figure 4.13a-f). The images in the figure are taken from a video of this injection and demonstrates the same pattern of colonic folds and peri-vascular lymphatics being highlighted, confirming that the bolus injection method is valid to highlight the drainage pattern from the colon.

4.4.4 Tracer only flows downstream of injection towards the distal colon

Each time we performed the injection into the colonic tissue, we noted that the tracer always drained within a fold in both directions, or moved to more distal folds. We never observed proximal extension in the colon (Figure 4.13f), and this is even though the injection needle was always pointing towards the proximal direction. This is likely due to peristalsis of the intestine working from proximal to distal, but is intriguing for reasons that we will return to in the next chapter regarding the spread of colonic inflammation.

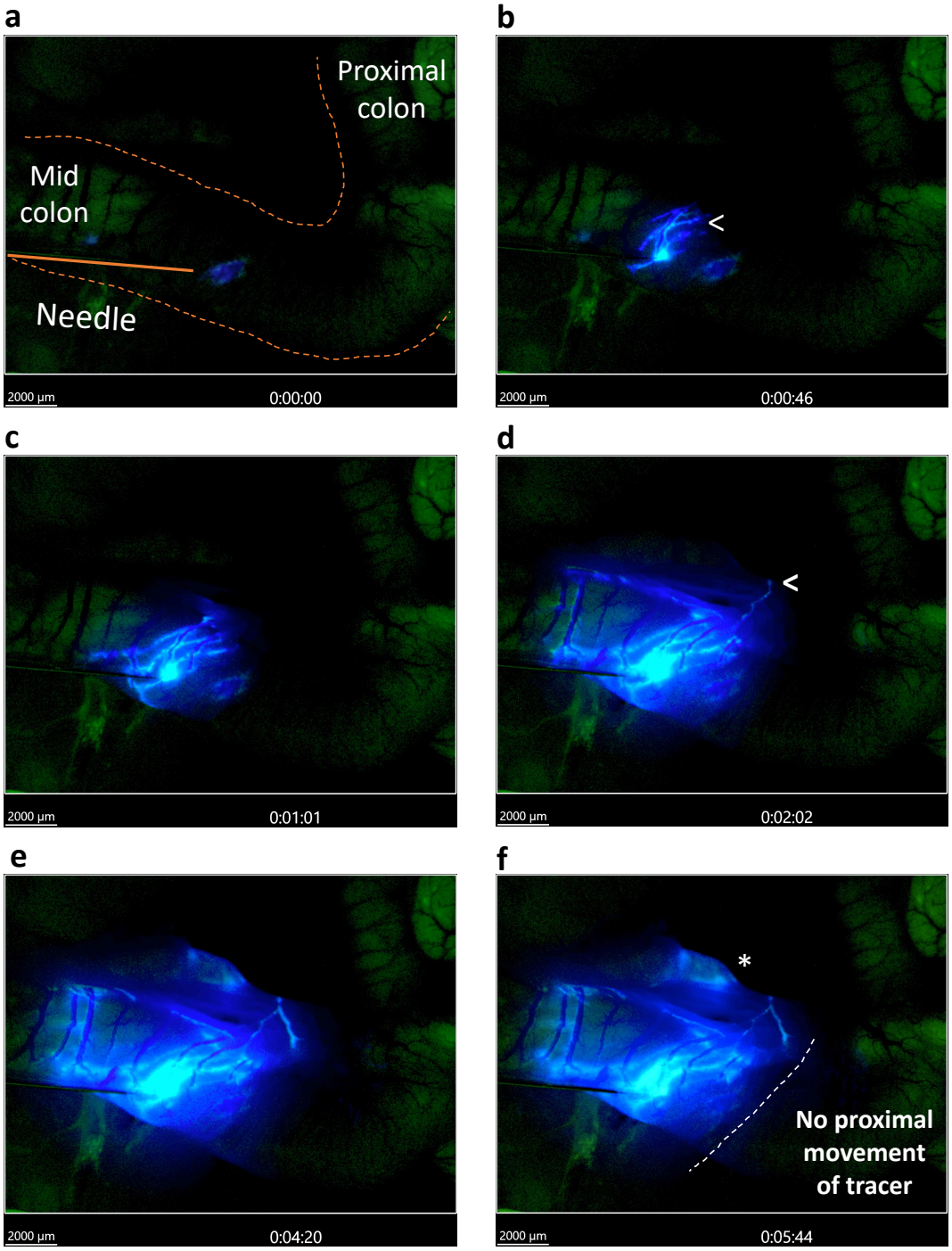

Figure 4.13: Microinjection of interstitial tracer into the proximal colon reveals the drainage pattern from the tissue to lymph node. This figure (a-f) highlights the timelapse video over six minutes of a tracer being injected into the colon at a rate of 5 nanolitres per second using a microinjection needle. It is possible to see tracer filling the colon (arrowhead in b) and then the mesenteric lymphatic vessel draining from the colon (arrowhead in d). Finally, the tracer arrives at the draining lymph node (asterisk in f). *Images are representative of a single experiment.*

4.4.5 Inhibiting colonic lymphatic outflow demonstrates continuity with colonic folds

One innovative aspect of the injection studies that we undertook was injecting a combination of two tracers into the colon simultaneously. The fluorescent properties of the tracers were used to discriminate between them by using appropriate LED sources and fluorescent filters with the stereomicroscope. It was also possible to set the microscope to automatically alternate and capture images between different fluorophores (Figure 4.14). We used this ability to capture the drainage of two different tracers simultaneously in order to track both small (Hydrazide-AF647) and large molecular weight (LPS-FITC) cargo into the draining lymph nodes via the lymphatic vessels (Figure 4.14).

To establish the dependence on the lymphatic vasculature for systemic absorption, and to prove that the colonic tissue folds were directly connected to the outflow lymphatic vasculature, we sutured and cut the mesenteric lymphatic vessels that drain into the proximal colon-draining lymph node (Figure 4.14d, Figure 4.15a-b). Repeating the colonic tracer studies following this ligation in a living mouse, combined with serial systemic blood draws following injection, highlighted that large molecular weight substances could not enter the systemic circulation in the absence of lymphatic drainage (Figure 4.15c). However, small molecular weight compounds could alternatively enter the circulation via the blood vasculature when the lymphatics are blocked (Figure 4.15d).

These data highlight that the injected tracers are in continuity with lymphatic outflow from the colon. Moreover, the images from the concurrent video recording the outflow of the tracers highlights the small molecular weight Hydrazide exiting the colon via a different route to the lymphatic vessels, presumably the venous outflow from the colon (Figure 4.14f).

There was only sufficient time and resource to attempt this technically challenging experiment once together with Dr Rafael Czepielewski. Therefore, it provides supporting data rather than firm evidence, but is in agreement with the many tracer studies we performed without lymphatic vessel ligation that showed tracer entering the lymphatic vessels that were ligated in this experiment.

This suggests that small and large molecular weight substances can both drain via the lymphatic vessels, but if this is obstructed then small molecular weight substances can alternatively enter the systemic circulation via the blood vessels. It is interesting to consider the possibility that therefore large molecular weight substances such as LPS may in fact concentrate in the tissue if there is any obstruction to lymphatic outflow. This accumulation within the tissue would be specifically within the fold regions, and so this is a possible explanation for the lymphatic finger-like projections that are seen specifically in these anatomical areas. The precise factors that lead to the formation of the lymphatic finger-like projections are unknown, and is the focus of ongoing work.

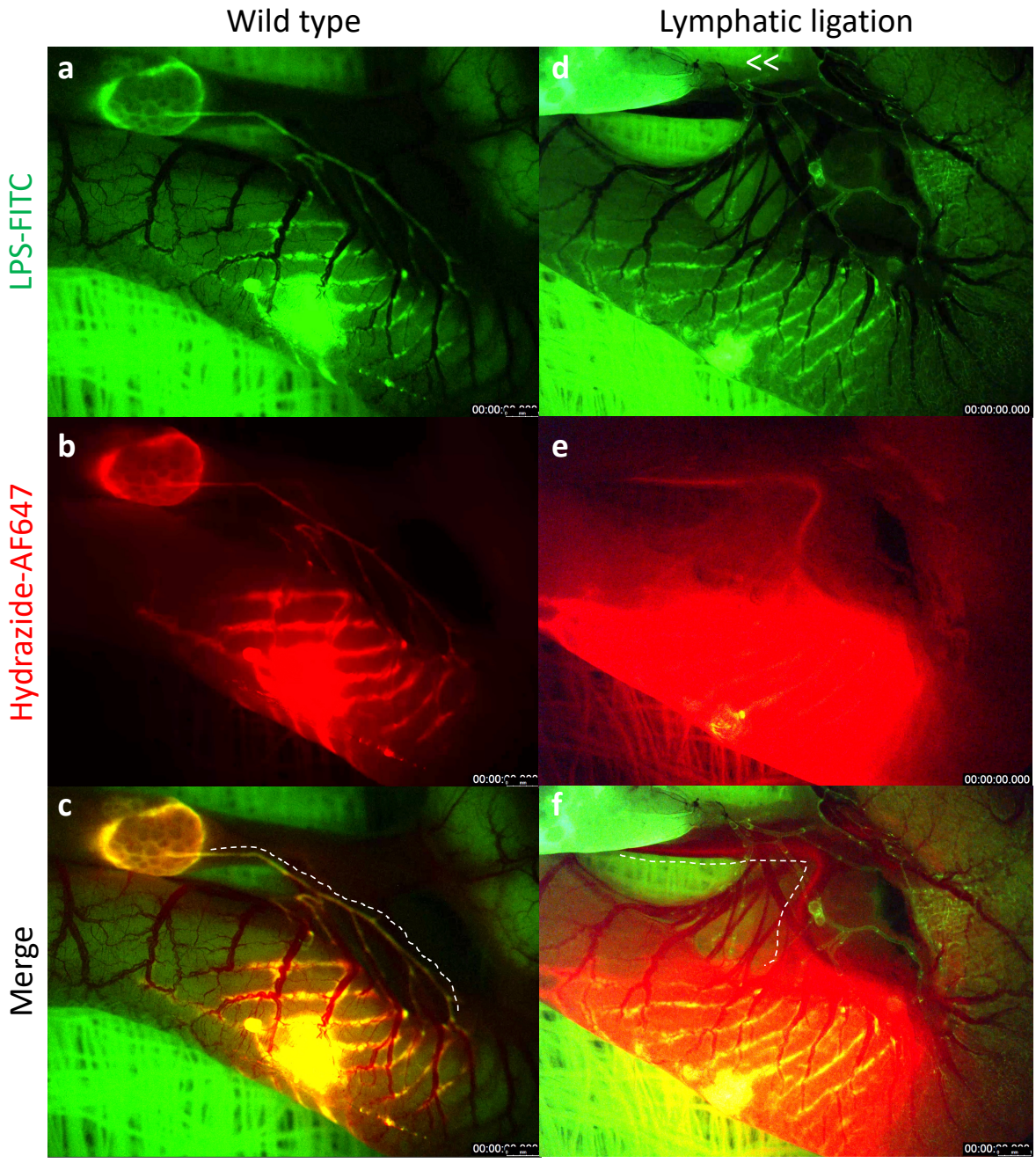

Figure 4.14: Lymphatic ligation confirms that drainage of large molecular weight substances occurs via the lymphatic vessels. A combination of LPS-FITC (large molecular weight) and Hydrazide-AF647 (small molecular weight) was injected into wild type mouse colon (a-c) or into the colon of a mouse that had its colonic draining lymphatics sutured (d-f). In the wild type injection both tracers drain via the lymphatics (dotted line in c). In the lymphatic ligation only the Hydrazide exits the colon and this is not via lymphatic vessels (dotted line in f). *Images are representative of a single experiment.*

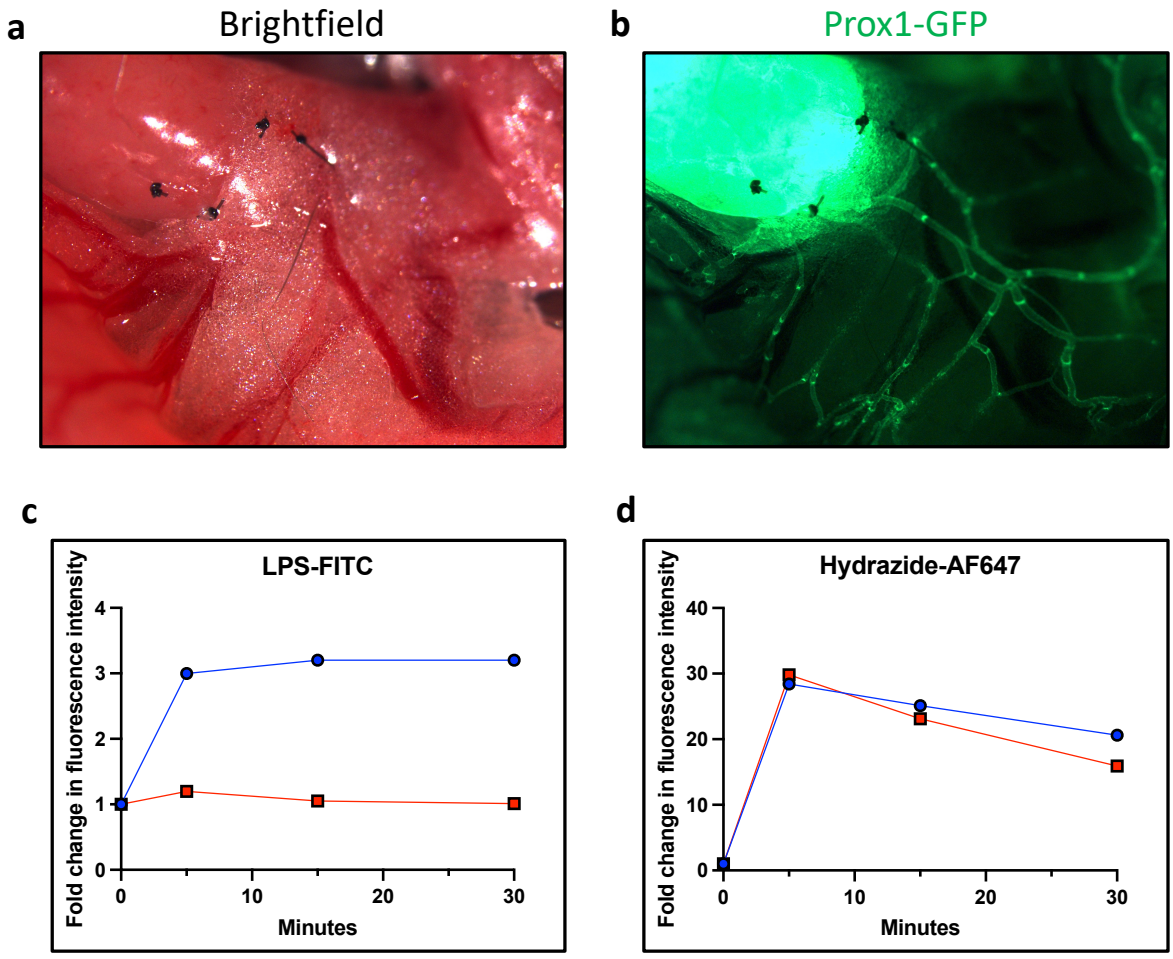

Figure 4.15: Lymphatic ligation confirms that drainage of large molecular weight substances occurs via the lymphatic vessels (cont'd). Lymphatic ligation brightfield image (a) and GFP (b) following procedure. The large molecular weight LPS is unable to access the systemic circulation when the lymphatic vessels have been sutured (c); however, there is no difference in the ability of the small molecular weight hydrazide to enter the circulation whether or not the lymphatic vessels have been ligated. *Images are representative of a single experiment.*

4.4.6 Injection of anti-lymphatic antibody to map physiological drainage route at a cellular level

As the FITC-Dextran tracer we used did not have any specific binding properties, we had the idea to inject antibody that would bind to lymphatic vessels and mark the drainage pattern *in vivo* as it travels through the colonic tissue. Lyve1 is a commonly used lymphatic capillary marker and so we injected this in a similar manner to the FITC-Dextran injections that we had done previously. Moreover, we did this experiment injecting Lyve1 antibody into a Prox1-GFP mouse, that has all lymphatic vessels highlighted with a GFP reporter (Figure 4.16). This enabled us to specifically see out of all the lymphatic vessels which ones are marked by the draining antibody.

Following tissue clearing and imaging of the sample we had a roadmap of how the antibody had travelled through the tissue (Figure 4.16a). The Lyve1 signal overlapped with the GFP signal in the submucosal lymphatics and specifically in those at the base of the tissue folds rather than the finger-like projections towards the lumen (Figure 4.16b, double arrowhead). The muscle layer lymphatics, in contrast, did not stain with the Lyve1 antibody (Figure 4.16b, asterisk). This experiment provides further evidence that the lymphatics lining the tissue folds are the vessels responsible for colonic outflow, as well as suggesting that the finger-like projections sample contents that travel one way down into the tissue folds rather than moving from the tissue fold towards the finger-like projections.

Ideally, we would have repeated this experiment using a Lyve1 antibody to stain the whole tissue to confirm that the muscle layer lymphatics also stain positively. We did this in Figure 4.4 but for clarity it would have helped to be in the same experiment. Furthermore, an injection of isotype control would help confirm that the Lyve1 antibody is not simply binding non-specifically.

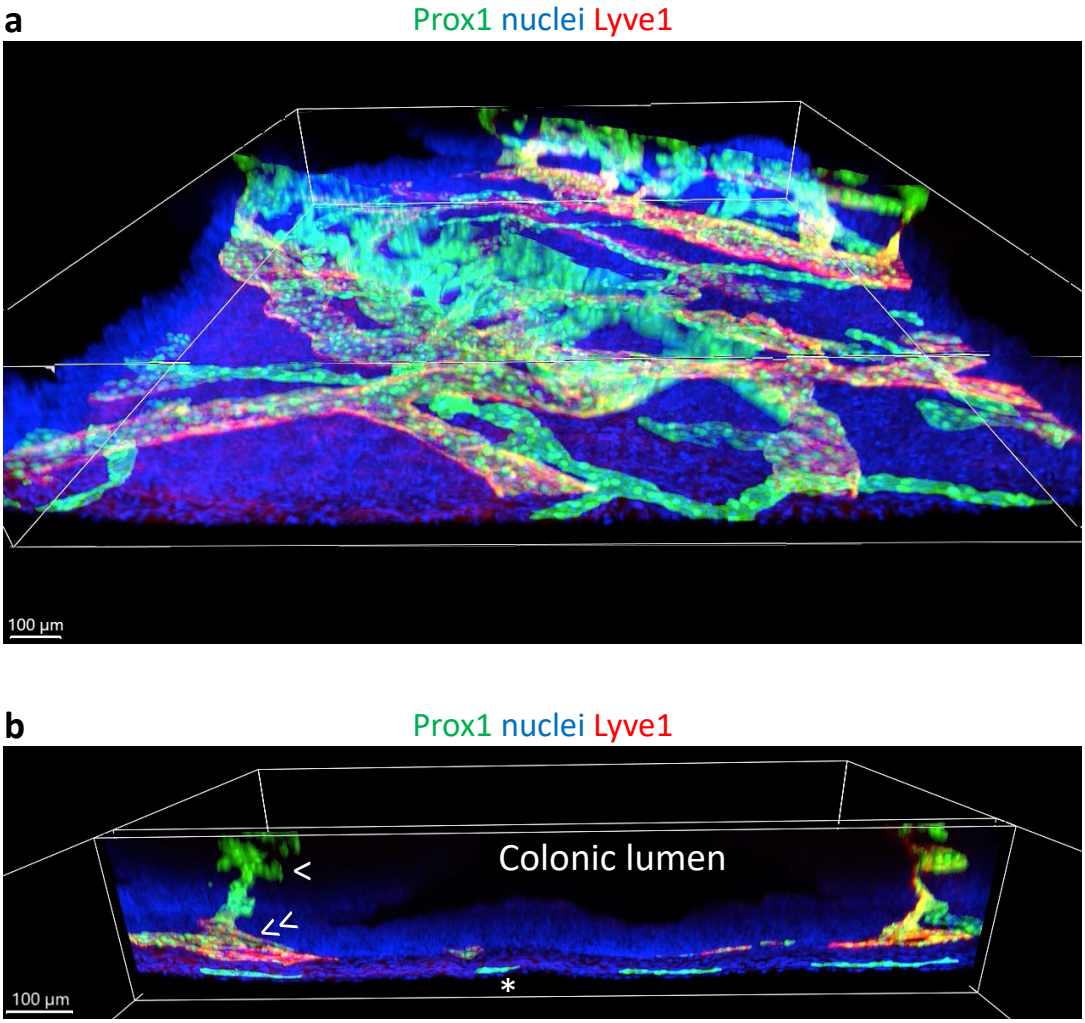

Figure 4.16: Colonic injection of anti-lymphatic antibody into a lymphatic reporter mouse highlights the specific lymphatic vessels involved in colonic interstitial drainage. When Lyve1 antibody is injected into the colon in a similar manner to the fluorescent tracers outlined previously, it outlines the lymphatic drainage of the tissue as it binds to only the lymphatic vessels it encounters as it traffics out of the colon (a). The lymphatic vessels (b) found in the fold (arrowhead) are less stained than at the base of the fold (double arrowhead) and the lymphatics in the external muscle layer do not see the Lyve1 antibody (asterisk in b)). *Images are representative of at least two independent experiments.*

4.5 Discussion

Using a combination of 3D imaging modalities and microinjection techniques, we established the three-dimensional orientation and architecture of the colonic lymphatic vessels, and we coupled this understanding with our newfound visualisation of interstitial outflow from the colon for the first time to our knowledge. We concluded that tissue folds wee regions of the colonic tissue lined by lymphatic vessels and appeared to be involved in interstitial outflow from the colon. Furthermore, they appeared to form reservoirs for interstitial fluid that seemed to sit in the folds prior to draining out via the adjacent lymphatic vessels. The idea that fluid can accumulate in these spaces is augmented by the experimental data that the lymphatic vessels that are specifically lining the tissue folds have a different morphology with finger-like projections, which is distinct to the neighbouring lymphatic vessels that are not found within folds. We hypothesise that this is because inflammatory factors that derive from the colonic lumen may accumulate in the fold regions that prolong signalling to the adjacent fold-associated lymphatic vessels, more than the neighbouring non-fold lymphatic vessels.

The discovery that the colonic tissue folds orchestrate interstitial outflow from the colon was unexpected. As we searched through the literature, we realised that most descriptions of tissue folds seemed to highlight their role in maximising surface area for absorption (164, 165). While this is likely to be the case, we hypothesised that the tissue folds have an associated but overlooked role in the drainage of interstitial fluid from the tissue in the pinches of submucosa beneath the folds. As these colonic tissue folds have received little attention in the literature, we shifted our focus to characterising these structures in more detail in relation to the lymphatic vessels in both health and inflammation, which we turn to in the next and final results chapter of this thesis.

5 Characterising colonic tissue folds in health and inflammation

5.1 Introduction

As described in the previous chapter we concluded that interstitial fluid exits the colon from the colonic tissue folds and so we wanted to gain a deeper understanding of these structures in the tissue and turn our focus to the folds in this final results chapter of the thesis. We set out to characterise the association with the folds to immune structures in the colon including lymphoid aggregates and mononuclear phagocytes. We also consider the connective tissue that occupies the space within the tissue folds and whether this structure is maintained in distension. We outline in more detail the outflow pathway of the injected tracer from the colonic tissue and find that the tissue folds are also connected to perivascular spaces that resemble those seen in the brain (166, 167). As the tissue folds are involved with exit from the colon, we were also curious as to whether they were involved in entry to the colon, which we consider.

We then consider how these structures are affected in the context of inflammation by revisiting the DSS colitis model that has been presented in the first thesis results chapter. We show that the tissue folds change architecturally in the context of inflammation. As we cover this ground, we also pause to consider the lymphatic architectural changes seen in the context of this model. Previous literature focusses in on lymphangiogenesis in the context of inflammation but makes conclusions based mostly on 2D imaging of the lymphatics in tissue. We demonstrate the superiority of visualising these structures in 3D and the true picture of inflammatory lymphangiogenesis in this context.

We conclude the chapter by relating the tissue folds studied so far in the mouse to human colonic tissue. We demonstrate analogous tissue folds on the inner surface of the human colon and highlight how these are lost in the context of ulcerative colitis. Finally, we focus in on the peculiar feature of disease seen in ulcerative colitis where inflammation begins distally and works progressively

proximally in the colon. We propose that the tissue folds may indeed be restraining inflammation, and a loss of function of these folds may be an explanation of rapid disease extension in ulcerative colitis.

5.1.1 Chapter aims

- Characterise the immune cells and structures associated with the colonic tissue folds
- Understand whether cellular entry to the colon is coupled with exit
- Visualise the change of the colonic tissue folds in colitis

5.2 Characterising the composition of the colonic tissue folds highlights that this is a specialised compartment of colonic tissue

5.2.1 The colonic tissue folds act to extract water from the stool

One aspect of the colonic tissue folds that we not yet touched upon is that of their function when considered from the colonic lumen. The immediately apparent feature of tissue folds is that of increasing surface area. Indeed, the colon is specifically optimised for the extraction of water from the intestinal contents that passes through from the small intestine, as clearly illustrated when one considers the loose stool following surgical removal of the colon (colectomy) or when the ileum is externalised as an ileostomy, bypassing the colon.

Indeed, when we visualise the internal surface of the colon with the stool in situ, we see that the stool is liquid and unformed in the region where the large proximal colonic folds are, whereas they become solid quite soon after passing through the proximal colon (Figure 5.1c). When looking at cross-sectional histology of the mouse colon, the folds project into the lumen predominantly in the proximal colon (Figure 5.1e), but also all the way along to the distal colon (Figure 5.1f). This signifies that the proximal colon, and likely the folds that project into the lumen, has a major role in water absorption.

We believe that the drainage of interstitial fluid via the tissue folds is an overlooked additional feature of the fold structure. Indeed, it would in fact make sense if there was a coupling of the absorption of fluid from the lumen with a means of then allowing this to drain out of the tissue, which we think is optimised in the colonic tissue fold unit.

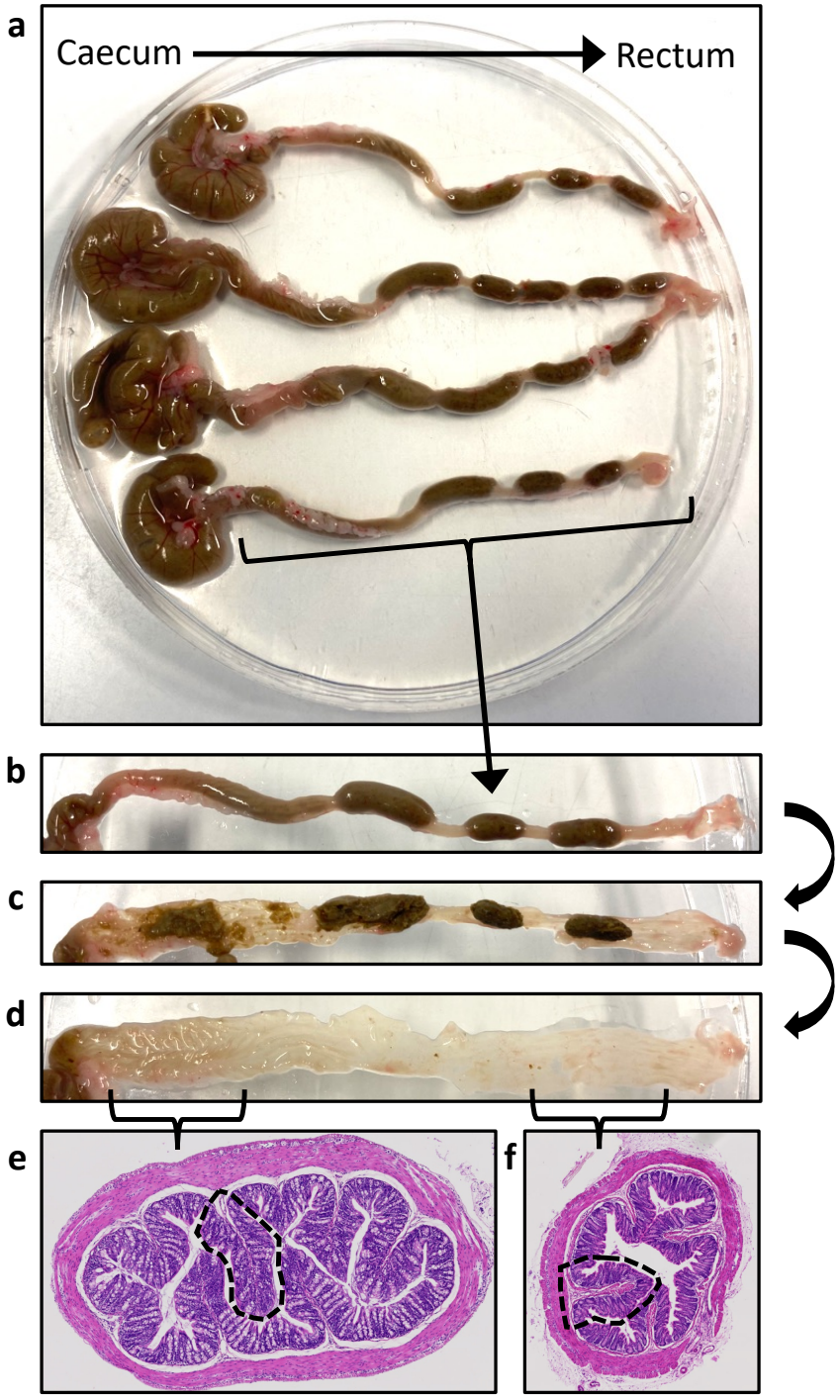

Figure 5.1: The murine colon has prominent folds particularly in the proximal colon associated with water absorption from the stool. Four murine colons have been dissected from wild type mice with caecum on the left and rectum on the right (a). Focusing in on one of these (b), the colon is cut open along the mesenteric border with stool left in situ (c). When the stool is cleaned from this sample, folds can be seen on the luminal surface of the colon, particularly in the proximal colon (d). These are visible histologically in both the proximal (e) and distal colon (f). *Images are representative of at least five independent experiments.*

5.2.2 Lymphoid aggregates are associated with colonic tissue folds

We first wanted to visualise lymphoid structures within the colonic tissue, which are known features but without clear description in relation to the tissue folds (168, 169). Using a CD19-tdTomato reporter mouse and imaging the tissue with a fluorescent stereomicroscope, we confirmed that B cell rich lymphoid aggregates were found throughout the colon but most prominently within the proximal colonic tissue folds (Figure 5.2, double arrowhead).

Turning to confocal imaging, when we utilised DAPI staining for nuclei in conjunction with the Prox1-GFP reporter mouse, we immediately noted the presence of the same cellular aggregates embedded within the tissue folds of the colon (Figure 5.3). These were found throughout the colon but appeared enriched specifically in the proximal colon where the tissue folds were most prominent. Lymphoid structures in the colonic tissue have been described by numerous groups but the terminology is often overlapping and can cause confusion. We noted that these structures are often called 'isolated lymphoid follicles'. However, when we imaged these in conjunction with the lymphatic vessels, we noted that each aggregate had its own network of lymphatic vessels wrapping around it (Figure 5.3b), highlighting that these structures are not at all isolated (which they appear to be with only nuclear staining (Figure 5.3a, asterisk)), but in fact connected by the lymphatic vessels.

We were intrigued that these lymphoid aggregates were so prominent in the proximal colon. We reasoned that perhaps this arrangement existed as this is the region of tissue that has abundant absorption and so it is important to couple this with immunosurveillance of the absorbed content.

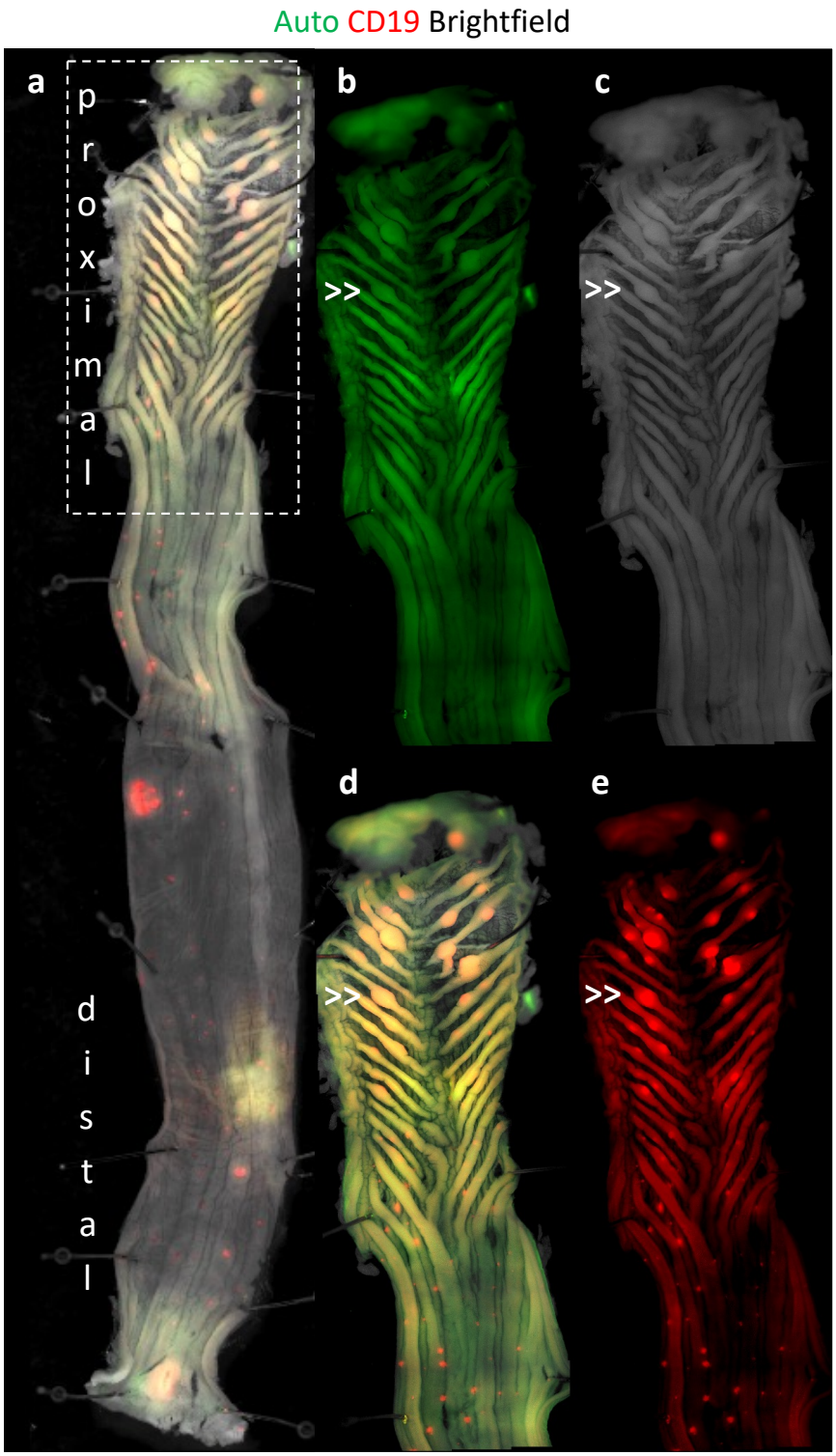

Figure 5.2: The colonic luminal surface has lymphoid tissue that is enriched in the proximal folds. Stereoscopic image of the colon from the luminal surface in a CD19-tdTomato mouse reveals numerous lymphoid aggregates throughout the colon; however, these are enriched in the proximal colon associated with colonic tissue folds (a). Focusing in on the proximal colon, even autofluorescent signal (b) and brightfield imaging (c) show a bulging prominence in the tissue fold (double arrowhead), from which CD19 signal is visible (e), and which can be appreciated on the merged image (d). *Images are representative of at least three independent experiments.*

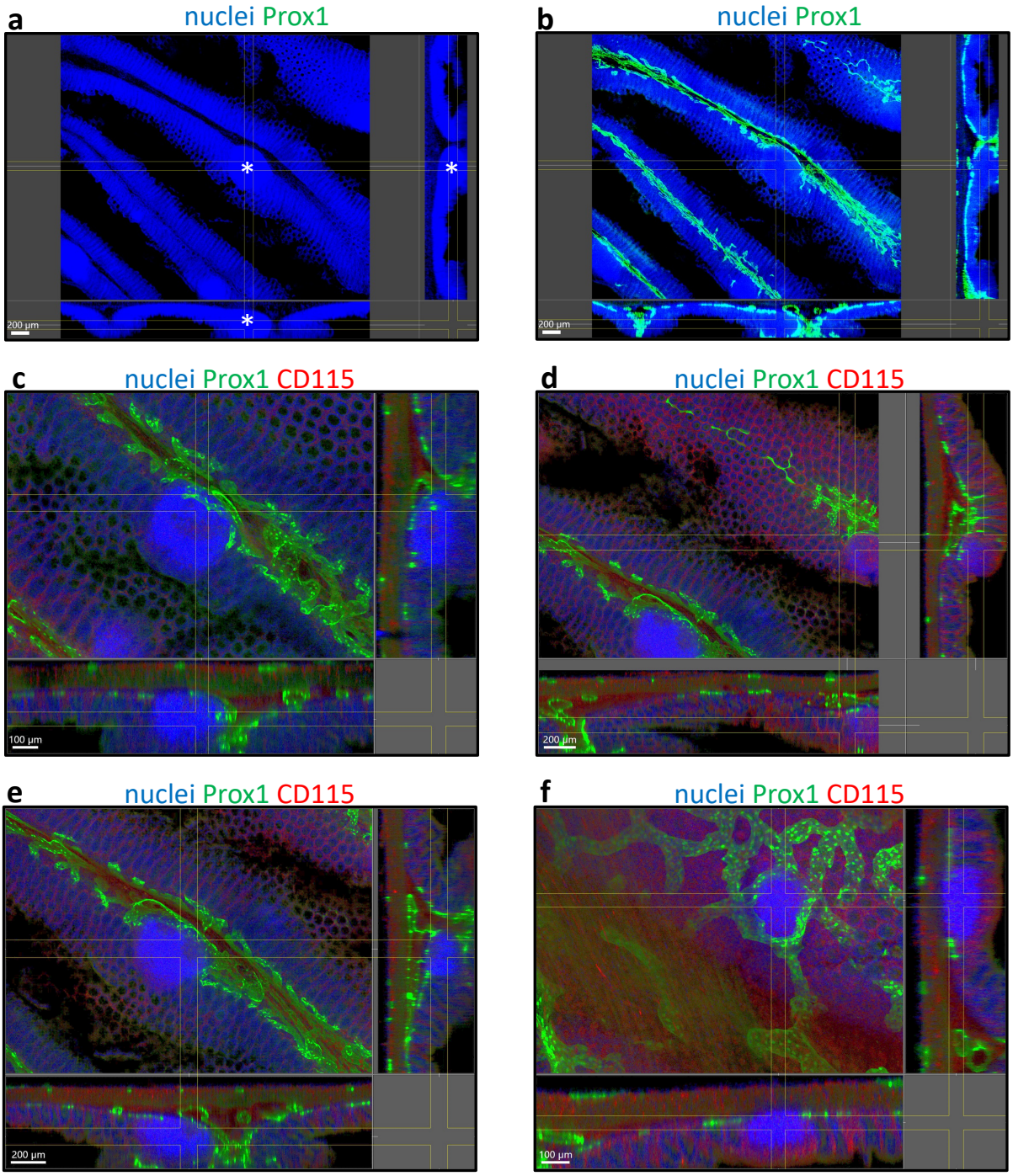

Figure 5.3: Colonic tissue folds are enriched in lymphoid aggregates lined by lymphatic vessels. Confocal imaging of the colonic tissue fold reveals the same lymphoid structures visible macroscopically (* in (a)). When the same image is overlaid with the lymphatic vasculature (b) a close relationship between the lymphoid aggregates and lymphatic vessels can be appreciated. Several examples of this interaction with the lymphoid aggregates and lymphatic vessels are presented in (d-f). *Images are representative of at least five independent experiments.*

5.2.3 Distension does not eliminate the colonic folds

To test the permanence of the colonic folds in relation to colonic distension, we deliberately distended them using 2% agarose and tied either end of the colon using a surgical suture prior to fixing the tissue. When we then removed the agarose, we observed that the tissue had been fixed in a fully distended conformation and when we imaged this we saw the folds were very prominent (Figure 5.4). We realised this would be the same conformation that they would adopt if they were being distended in the context of a faecal pellet moving through the colon. This further established the permanent nature of these structures in the context of homeostasis. We speculated that when these folds were distended this may in fact increase their ability to drain their contents as the squeezing effect may force interstitial fluid to drain via the lymphatics out of the colonic tissue.

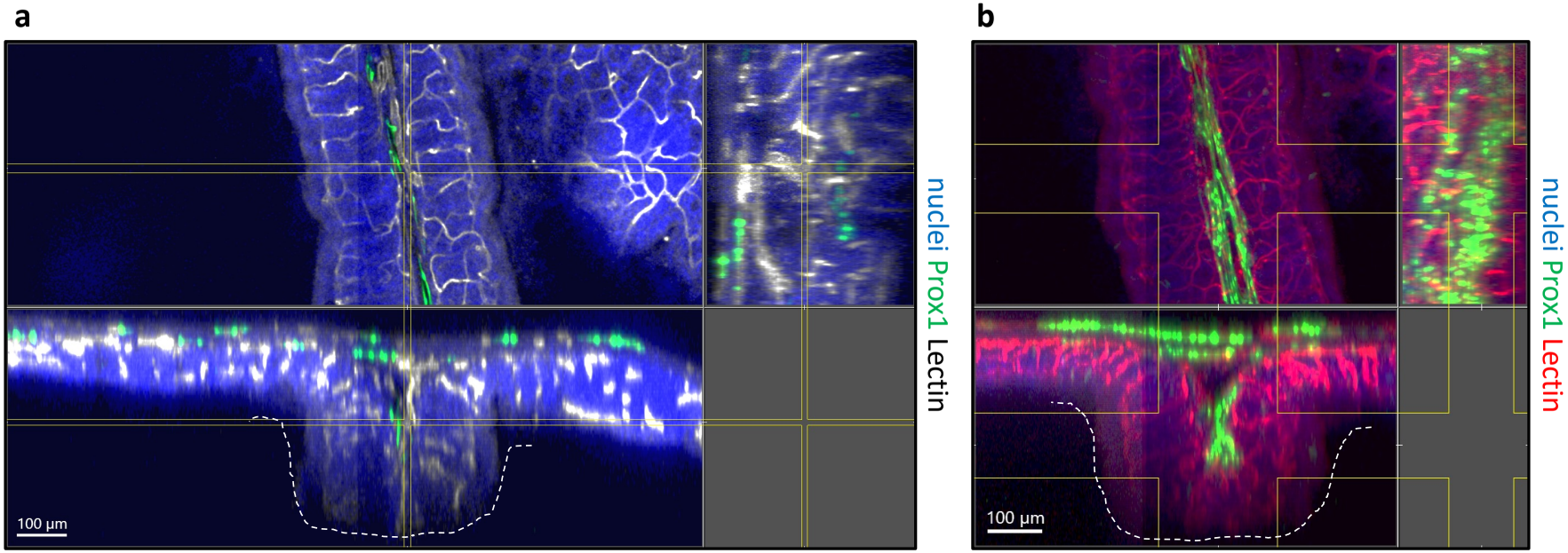

Figure 5.4: Agarose distension of the colon prior to fixation does not result in loss of tissue folds. To determine whether the colonic folds would be lost by distension, animals had their colons infused with agarose and sealed on either end. This solidified prior to fixation, preserving the natural state of the colon when maximally distended. Folds are visible projecting into the lumen as depicted by the dotted lines in (a) and (b). *Images are representative of at least three independent experiments.*

5.2.4 Mononuclear phagocytes are abundant in colonic tissue folds

Returning to the idea of immunosurveillance, we were curious about the location of mononuclear phagocytes in relation to the tissue folds. When we imaged the tissue using our 3D preparation, we noted that mononuclear phagocytes were abundant in the lamina propria and external muscle layers as previously described (Figure 5.5). However, we found a specific mononuclear phagocyte population within the submucosal space. This suggests that the space draining the interstitial fluid of the colon is being surveyed by a subset of mononuclear phagocytes. A specific point to bring out in this is that these mononuclear phagocytes are not in the lamina propria (Figure 5.5a-c). Numerous immunology papers refer to leukocyte isolation from the lamina propria but in reality the entire colon is digested. We highlight that this fold-associated mononuclear phagocyte subset appears to not specifically have been distinguished in the literature to date. On closer inspection, mononuclear phagocytes appeared to wrap around and sit on lymphatic vessels within the tissue folds (Figure 5.6).

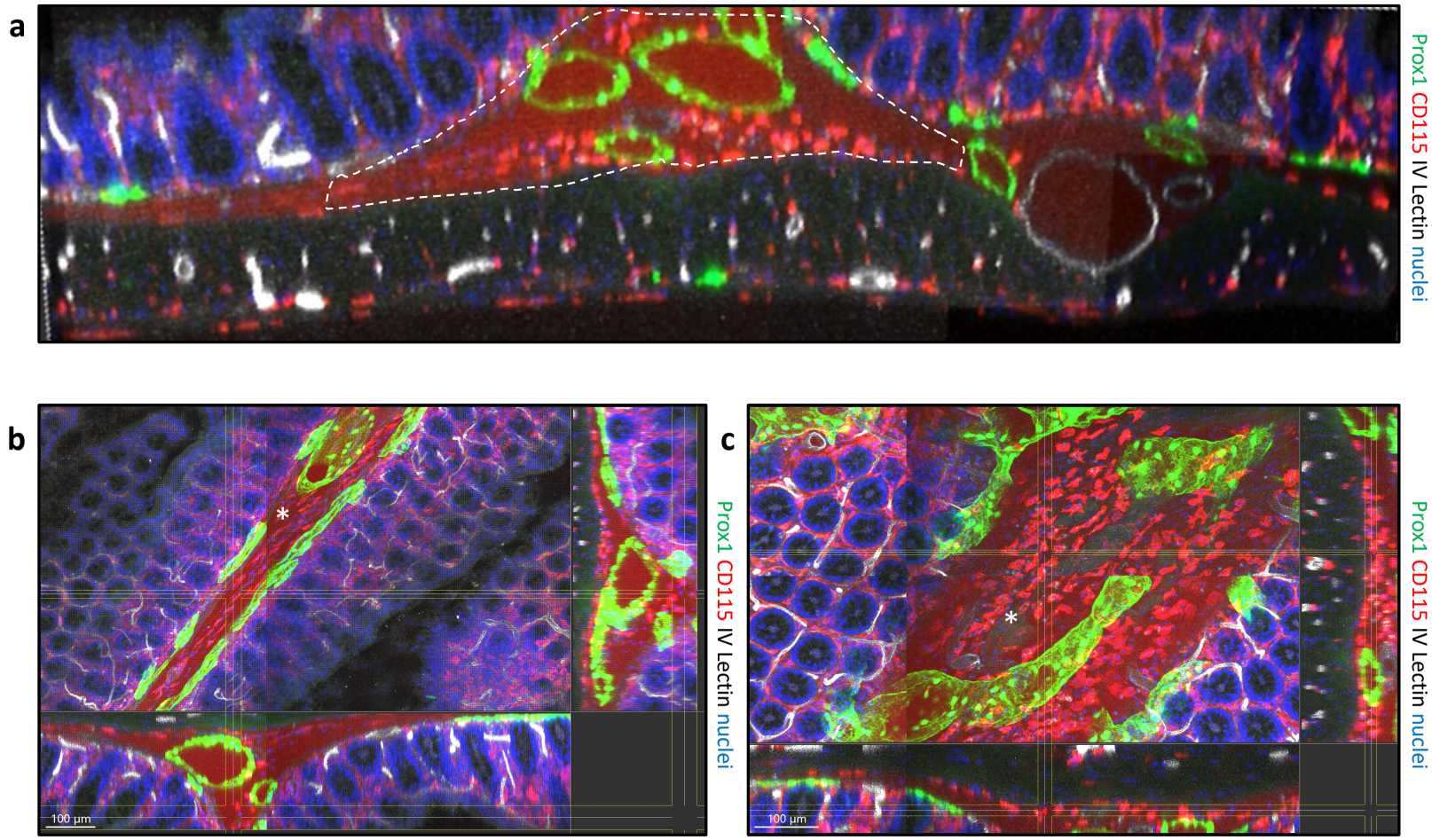

Figure 5.5: The colonic lymphatic network is lined by macrophages. Macrophages are found throughout the colon, but specifically within tissue fold spaces in the submucosa (dotted line in (a)). Further examples are highlighted (asterisk in (b) and (c)). *Images are representative of at least three independent experiments.*

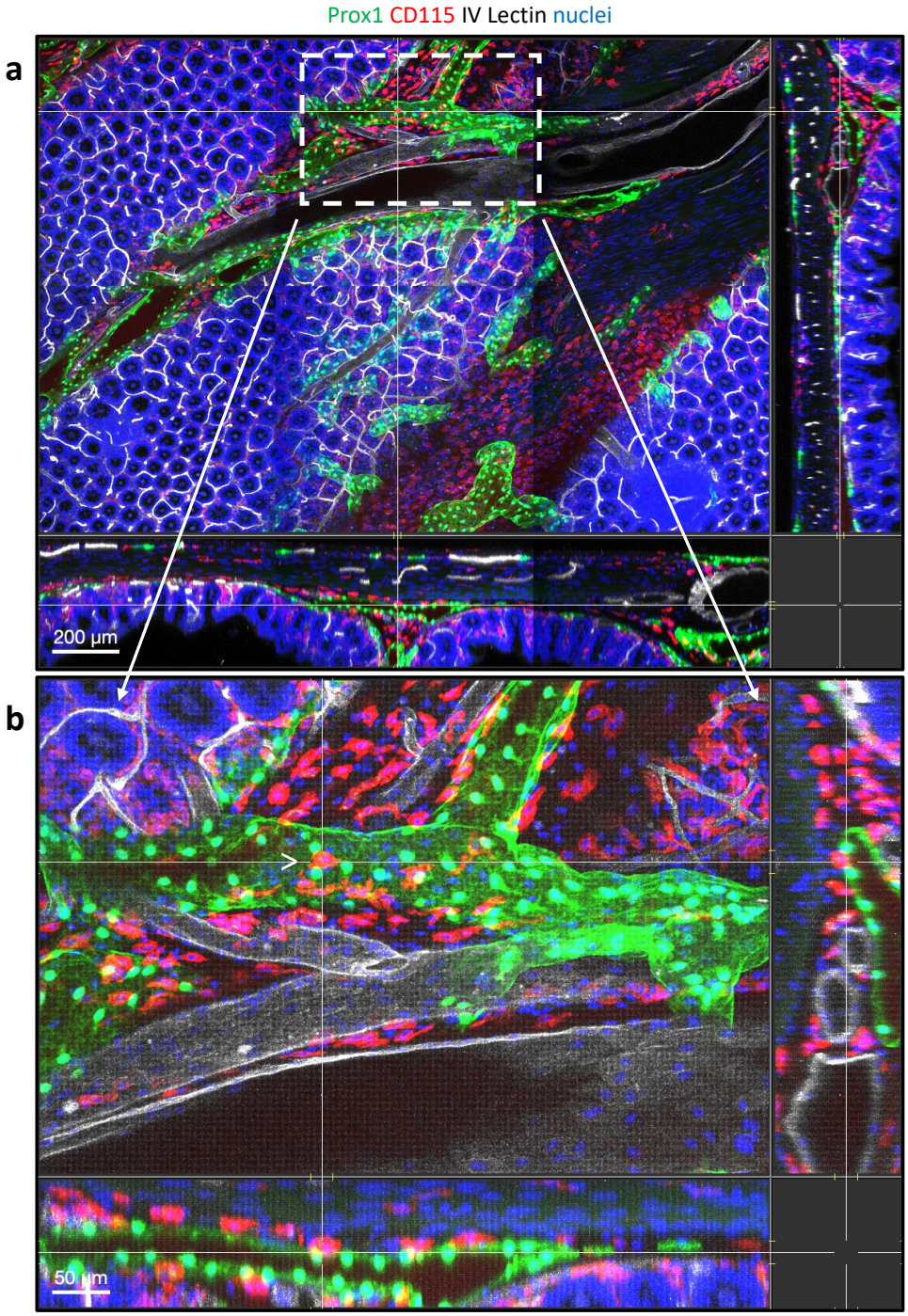

Figure 5.6: Macrophages associate with the lymphatic vessels within colonic tissue folds. Confocal imaging of a colonic tissue fold region highlights macrophages are found close to tissue folds (a). Zooming in on this region (b) reveals numerous macrophages that appear adherent to lymphatic vessels, with an example highlighted (arrowhead). *Images are representative of at least three independent experiments.*

5.2.5 Fold mononuclear phagocytic network surveys vast areas of colonic tissue

To demonstrate the functional role of the submucosal fold-associated mononuclear phagocytes in capturing antigen, we injected fluorescent ovalbumin in a similar manner to the other tracers directly into the wall of the colon. We visualised drainage in the tissue using the fluorescent stereomicroscope and then fixed, cleared, and imaged the tissue. Unlike the previous FITC-Dextran injections where we saw tracer remaining within the fold, ovalbumin did not adopt this pattern but rather was endocytosed by the mononuclear phagocytes we identified predominantly within the folds. We realised the pattern of this endocytosis outlined the shape of the fold (Figure 5.7, Figure 5.9a). This demonstrated that these submucosal spaces were in continuity with this network of fold-associated mononuclear phagocytes and gives further evidence that this space requires active immunosurveillance. Furthermore, when we co-injected the ovalbumin with conjugated Lyve1 antibody, we saw the same network of lymphatics highlighted surrounding the tissue folds that we had previously (Figure 5.9b).

A limitation of this data is that we did not inject an isotype antibody in a similar manner to confirm that the Lyve1 staining was specific, rather than mediated by non-specific Fc receptor binding.

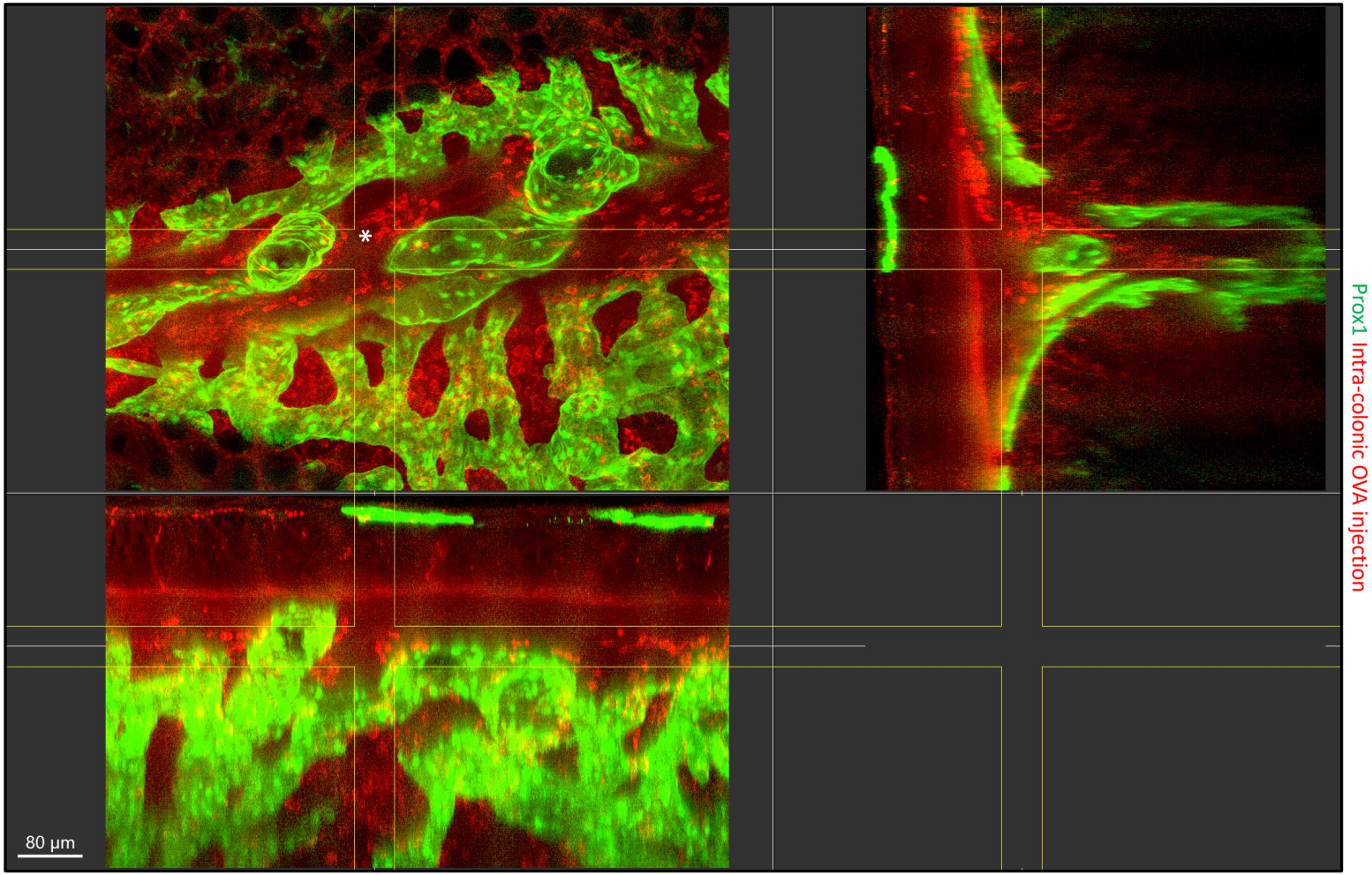

Figure 5.7: The colonic folds contain macrophages capable of endocytosing cargo arriving from distant regions of tissue. Ovalbumin (OVA) was injected into the colonic tissue and a region away from this was imaged with confocal microscopy. A colonic tissue fold lined by lymphatic vessels is visualised with numerous cells that have uptaken ovalbumin enriched within the fold (asterisk). *Images are representative of at least three independent experiments.*

5.2.6 Fold mononuclear phagocytes and MHC II on lymphatics from single cell data

Utilising the in vivo labelling method via colonic injection, we highlighted the MHC II positive cells within the colonic fold tissue. Relating back to the single-cell RNA sequencing, we had the hypothesis that certain subsets of lymphatics are responding to interferon signalling and may switch on MHC II as a result (153). Fitting this together with our injection data, we hypothesised that the interferon-responsive lymphatics would be the ones that line the tissue folds, as these would be the lymphatic vessels that potentially have the longest period in contact with inflammatory mediators such as interferons similar to the fold accumulation of tracers such as FITC-Dextran. In relation to this, injection of antibody against MHC II revealed mononuclear phagocytes in close proximity to lymphatics, but also some lymphatics in the tissue folds stain positively for MHC II (Figure 5.8a-b), further suggesting the idea that the lymphatics lining the folds are receiving prolonged inflammatory signalling compared to the others.

We would have also ideally stained the tissue for the other markers found from the single cell sequencing experiment, however, we found that they were all expressed more abundantly by other cell types compared to the lymphatics. This made it challenging to assess for co-expression of these markers specifically with the lymphatic endothelial cells.

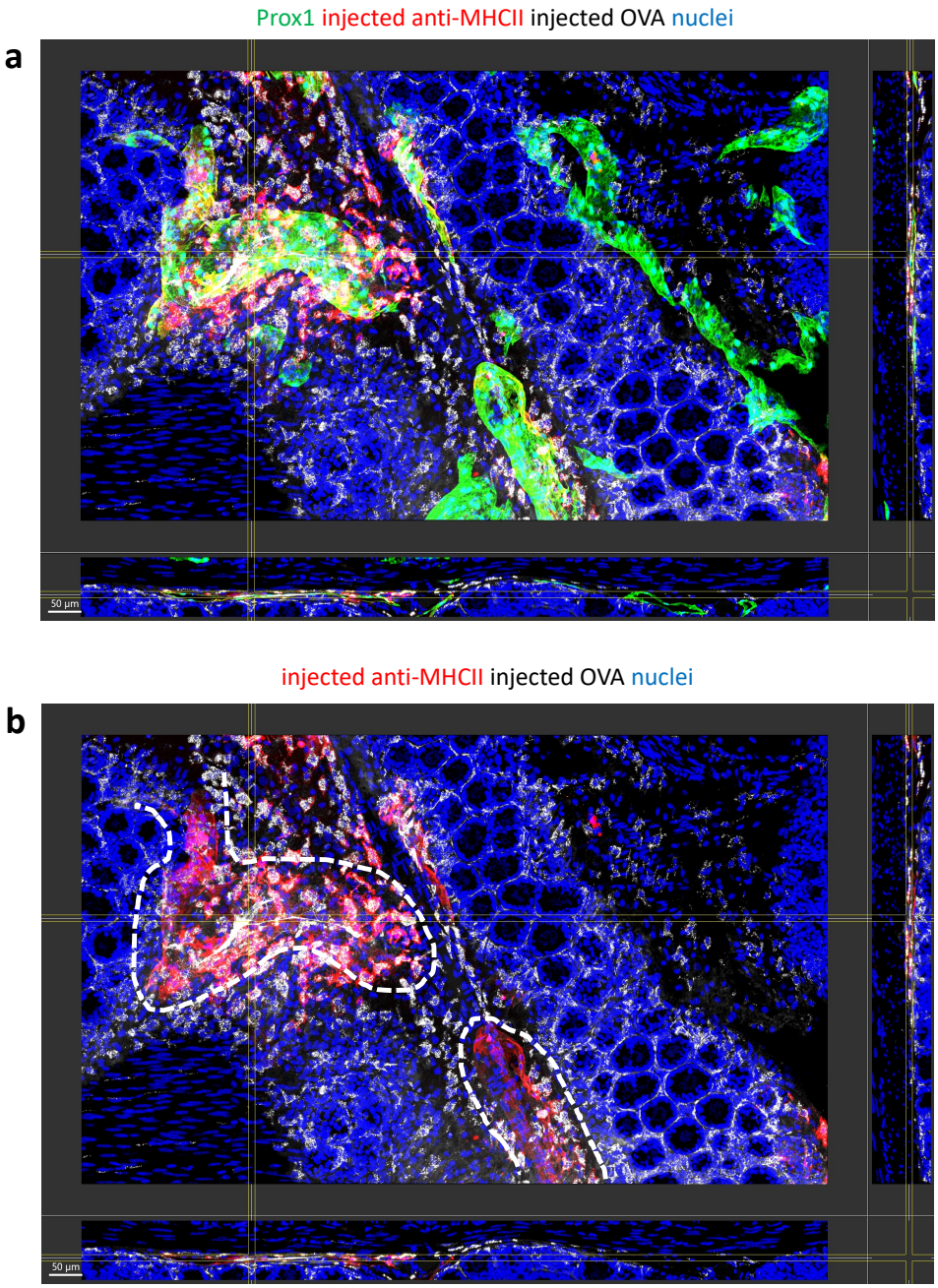

Figure 5.8: The colonic folds contain macrophages lymphatics expressing MHCII. Injecting anti-MHCII into the colon with OVA (g) highlights macrophages around lymphatic vessels phagocytosing OVA. Lymphatics themselves also express MHCII within the tissue folds (thick dashed line in (b)). *Images are representative of at least two independent experiments.*

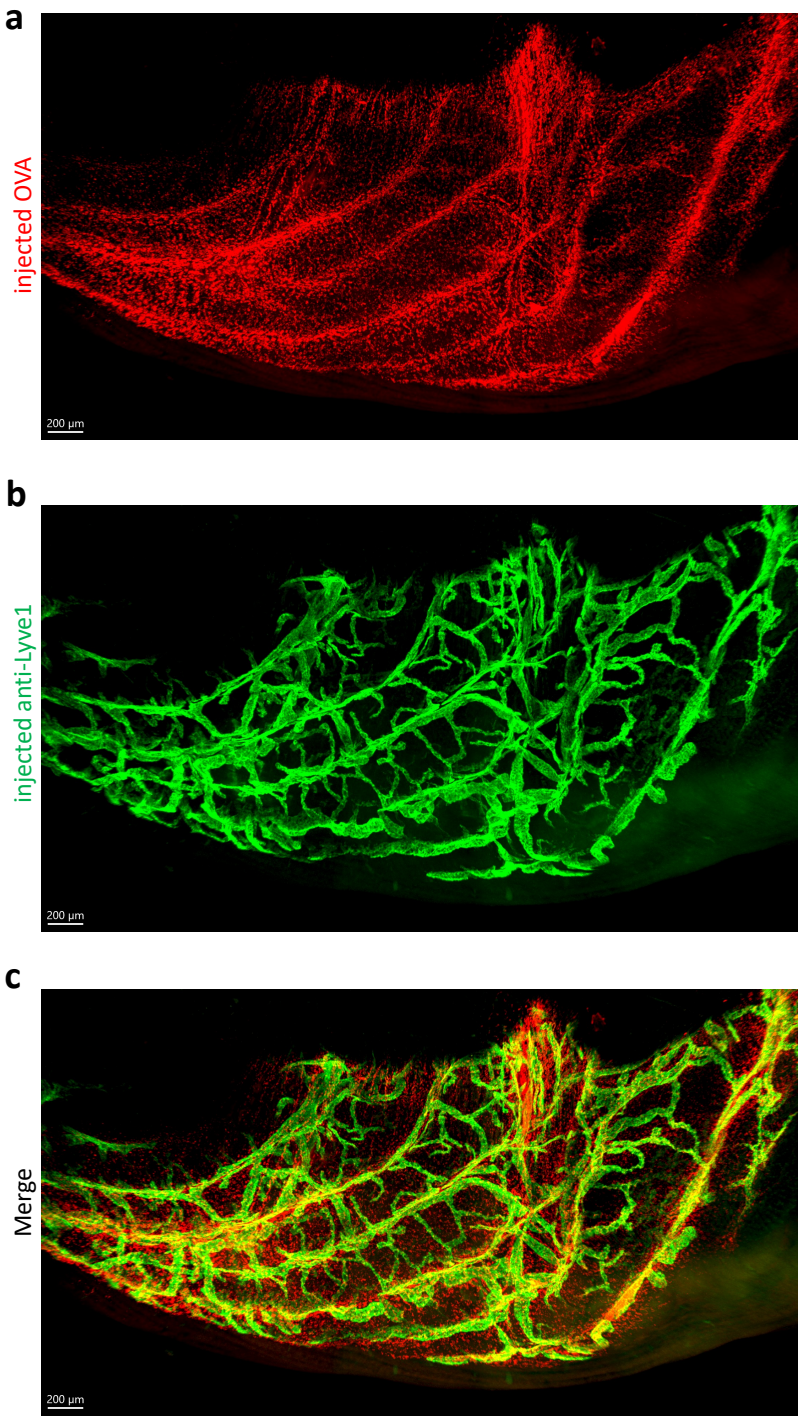

Figure 5.9: Colonic injection of anti-Lyve1 antibody traces the lymphatic route of interstitial drainage concurrently with the macrophages in the tissue folds. An anti-Lyve1 antibody was injected concurrently with ovalbumin (OVA) which highlighted the lymphatic network. The endocytosed OVA signal highlighted the network of colonic fold macrophages (a) and concurrent Lyve1 staining from the injection (b) highlighted the associated lymphatics (c). *Images are representative of at least three independent experiments.*

5.2.7 Lyve1 highlights macrophages specifically in the submucosal space and enriched in the colonic folds

From staining Lyve1 in the colonic tissue to identify the lymphatics, we also noted the presence of macrophages staining positive for Lyve1 (Figure 5.10a-b, d, e). These macrophages were enriched in the submucosa and were orientated in the direction of lymphatic drainage (Figure 5.10a). Lyve1 is a ligand for hyaluronic acid, and this allows binding of water to aid in providing structure to the extracellular matrix. We thought that a niche of Lyve1 macrophages and lymphatics in the tissue folds may be contributing to their structure, but did not formally test this hypothesis.

Ideally we would have also stained a Lyve1 knockout mouse as a control to ensure that the Lyve1 staining was specific, but we did not have this strain.

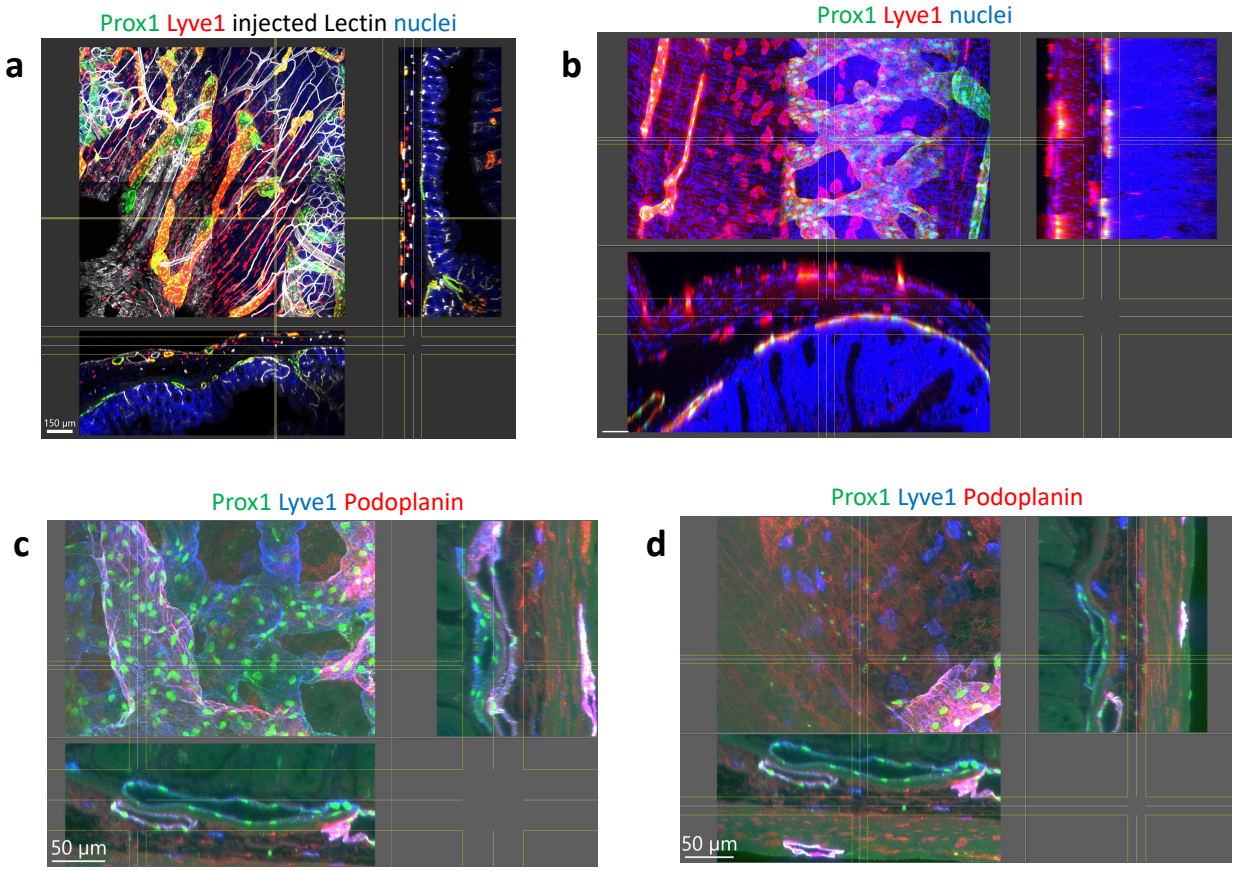

Figure 5.10: **Lyve1 highlights macrophages found in the submucosal space and enriched in colonic tissue folds and perivascular spaces.** Lyve1 macrophages align along lymphatic vessels (a) and lie in the submucosal space (b). Lymphatics beneath the epithelium (c) lie near Lyve1 macrophages in the submucosa (d). *Images are representative of at least three independent experiments.*

5.2.8 Organised connective tissue forms the space where interstitial drainage occurs

As interstitial fluid travelled within the submucosal pinches beneath the tissue folds, we were curious to understand the composition of the connective tissue in these regions. To do this we utilised 2-photon microscopy to evaluate second harmonic signal (170), which revealed the presence of collagen in the tissue. We found that these fold regions had orientated collagen in human colon (Figure 5.11a), and pig colon (Figure 5.11b). Furthermore, we found that elastin fibres ran predominantly in the submucosal space as demonstrated by staining the tissue with hydrazide (171, 172) (Figure 5.11c). These data together suggest that the tissue folds are permanent structures of the colon that support directional flow rather than just a disorganised region of connective tissue.

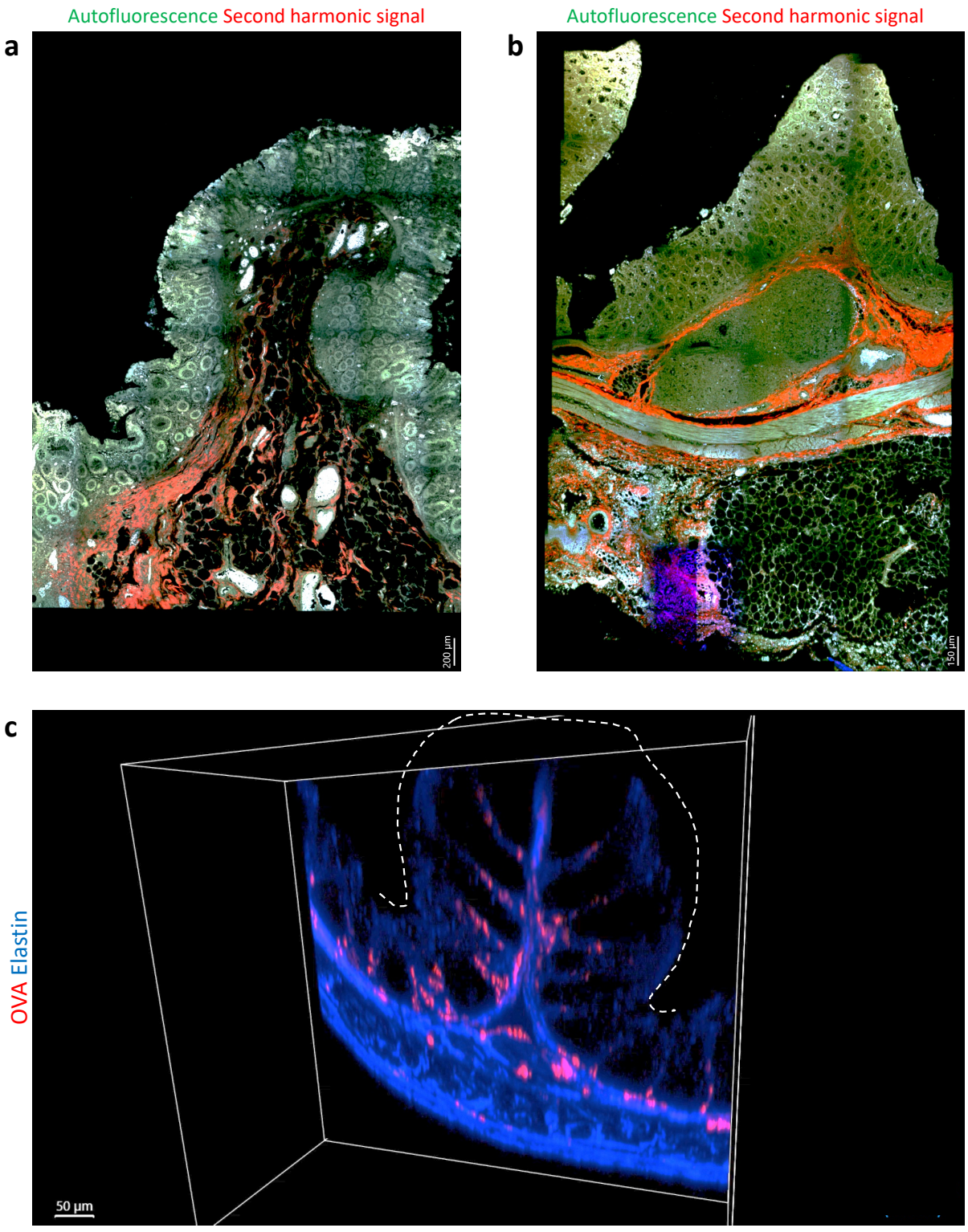

Figure 5.11: Oriented connective tissue runs within the submucosal space in mouse, human and pig colon. Second harmonic imaging of human (a) and pig (b) colon. Fold-cross section of mouse colon (c). *Images are representative of at least two independent experiments.*

5.2.9 Systemic sampling of antigen may occur in the colonic tissue folds

Previous work has demonstrated that intravenous administration of ovalbumin is highlighted within villus macrophages in the small intestine (173), presumably because of the permeability of the small intestinal capillaries, which are fenestrated to maximise absorption (174) which we reproduced (Figure 5.12a). We were curious as to whether equivalent sampling of systemic antigen would take place within the colon. When we imaged the same animal's colon we found that ovalbumin signal appeared to be within the colonic tissue fold (Figure 5.12b). Furthermore, there appeared to be a gradient of ovalbumin signal that was strongest in the fold and diminished proportionately further away from the fold. This experiment was only done once and so is only suggestive and requires repetition. However, if this finding replicates then it suggests that the colonic tissue fold is the first region of the colon where systemic contents are surveyed. If this is the case we hypothesised that post-capillary venules would be present in this region, which we turned to look at next.

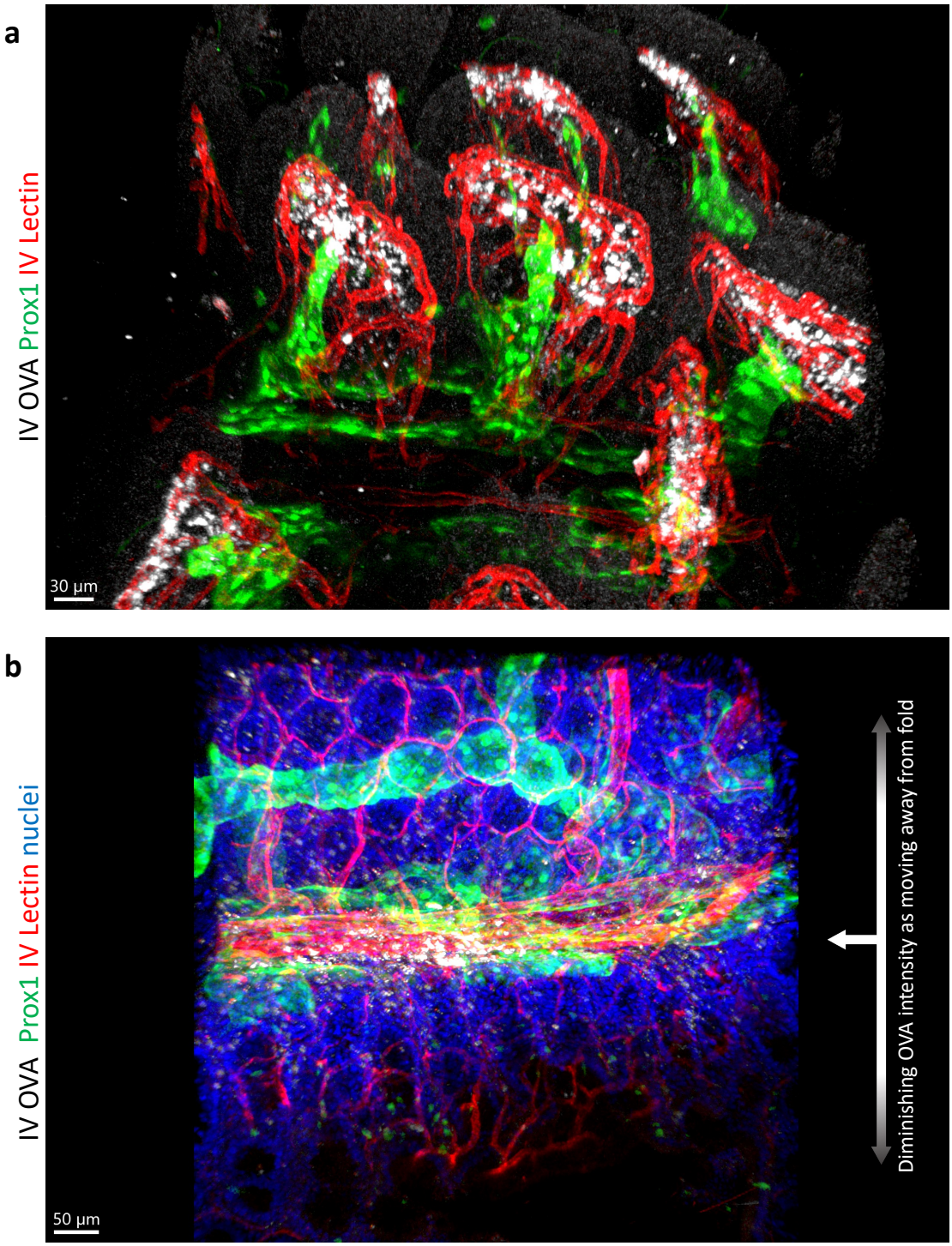

Figure 5.12: Intravenous ovalbumin is sampled by phagocytic cells in the small intestinal villus and this is paralleled in the colonic tissue folds. Administration of intravenous ovalbumin 20 hours prior to sacrificing the mice highlights the villus macrophages of the small intestine (a) where vascular permeability is high. In contrast, the colon from the same animal demonstrates ovalbumin uptake from the systemic circulation within the colonic tissue folds (b). It appears that the intensity of ovalbumin uptake diminishes the further away from the tissue fold. *Images are from a single experiment.*

5.2.10 Post-capillary venules are present in relation to the tissue folds – inflow and outflow

Considering that the lymphatic network orchestrating outflow from the colon lined the tissue folds, we were interested to understand whether inflow into the colon of immune cells was also related to these tissue folds. To investigate this, we stained the tissue for markers of post-capillary venules (PCVs), which have the molecular machinery required to allow cells to extravasate from the blood vasculature and enter the tissue, analogous to high endothelial venules (HEVs) found in secondary lymphoid tissue such as lymph nodes (175). We established that the PCVs were also found in the tissue folds as evidenced by staining for PNAd (Figure 5.13a, arrowheads) and Madcam1 (Figure 5.13b). Madcam1 is particularly relevant to colonic inflammation, as it is the ligand for α4β7 integrin, found on intestinal homing lymphocytes (25), and the target of the medication Vedolizumab, which has transformed the treatment of patients with IBD (176, 177). Madcam1 expression was also seen in association with a colonic tissue fold-associated lymphoid structure, with expression of Madcam1 switching on within the structure itself (Figure 5.13b, double arrowhead), suggesting that this region is where leukocytes are extravasating from the systemic circulation. This characterisation of the tissue folds highlighted to us the coupling of leukocyte inflow and outflow in these regions, which will be of great interest in further targeting these pathways in IBD.

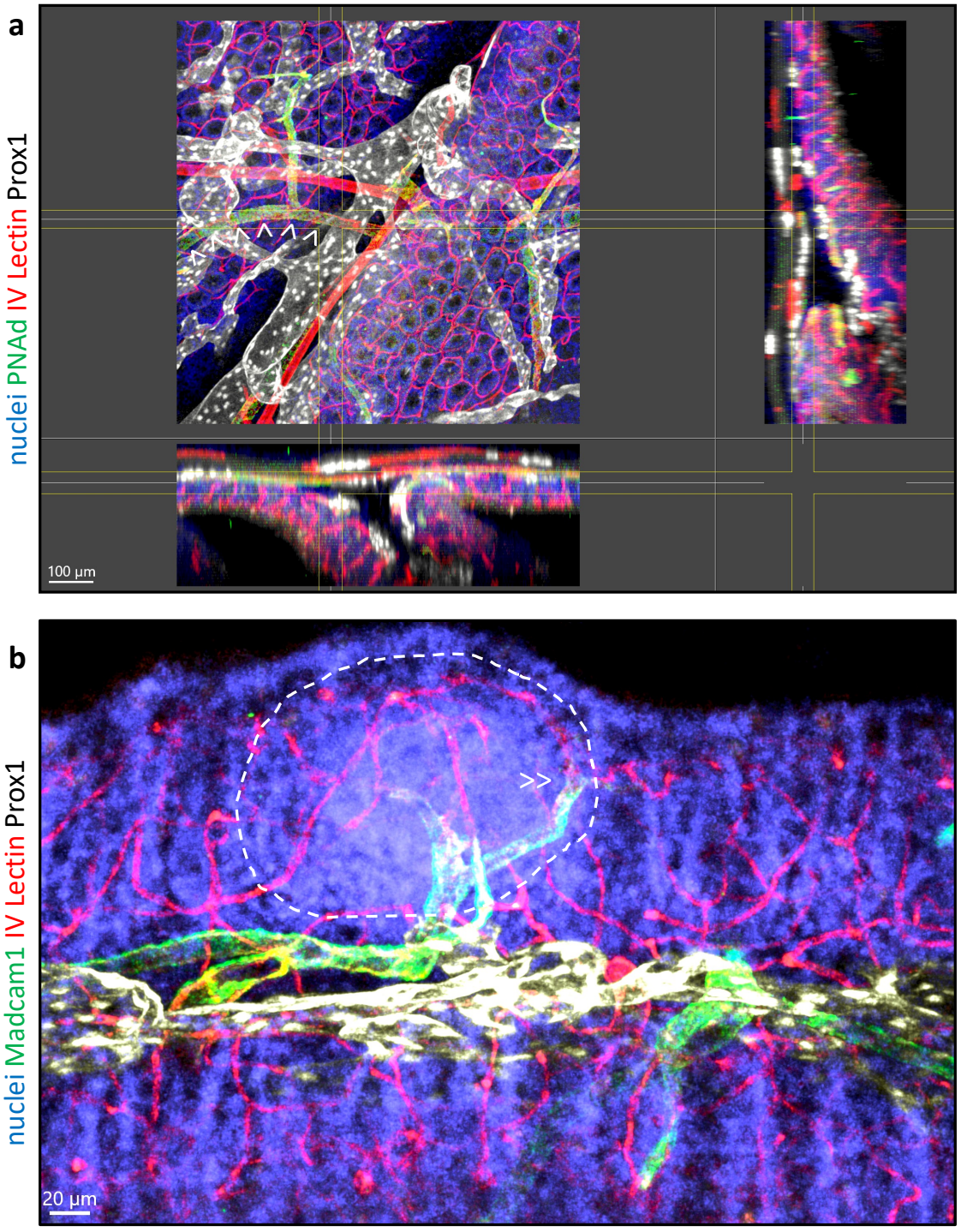

Figure 5.13: The colonic folds as associated with postcapillary venules. PNAd (a) and Madcam1 (b) staining within tissue folds highlight postcapillary venules. In (a) there are arrowheads tracing this vessel, and in (b) the point at which the vessel starts expressing Madcam1 is demonstrated by a double arrowhead. *Images are from a single experiment.*

5.2.11 Colonic photoconversion of endogenous tracer enables visualisation of entry and exit of interstitial fluid

Biological understanding is inevitably restricted when injecting exogenous tracers such as FITC-Dextran into the colon, even if done using a microinjector. Therefore, a longstanding goal was to create a method to track an endogenous substance within the interstitial fluid. High-density lipoprotein (HDL) is made in the liver and is a molecule that travels freely in the interstitium, which has previously been tagged to fluorescent GFP to track interstitial fluid (178). Professor Gwen Randolph has recently made a similar construct using a viral vector to express HDL tagged to Kikume Green-Red (KikGR), which upon laser activation converts from green to red and has previously been used to track cellular trafficking from the ileum (102), but here adapted to track the interstitium with HDL.

The question was whether this tool could track interstitial outflow and if it appears like the previous FITC-Dextran tracer injections. A pre-photoconversion image shows the proximal colon is green with red signal at the bottom reflecting stool autofluorescence (Figure 5.14a). Following photoconversion the green tissue turns red (Figure 5.14b). After 20 minutes imaging a live house it is possible to see the colonic fold stripes form (Figure 5.14e) as well as the lymphatic drainage of the red photoconverted molecule to the draining lymph node (Figure 5.14f, arrowheads).

It must be noted that HDL in the plasma is still green as it has not been photoconverted. On closer inspection, particular foci of green spots are visible which reflect molecules newly entering the colonic tissue (Figure 5.14d, arrowheads). This is where new HDL is entering the tissue and highlights that vascular entry seems to be occurring at ‘hotspots’ along these folds. This experiment has only been done once by Dr Rafael Czepielewski and so remains to be validated further.

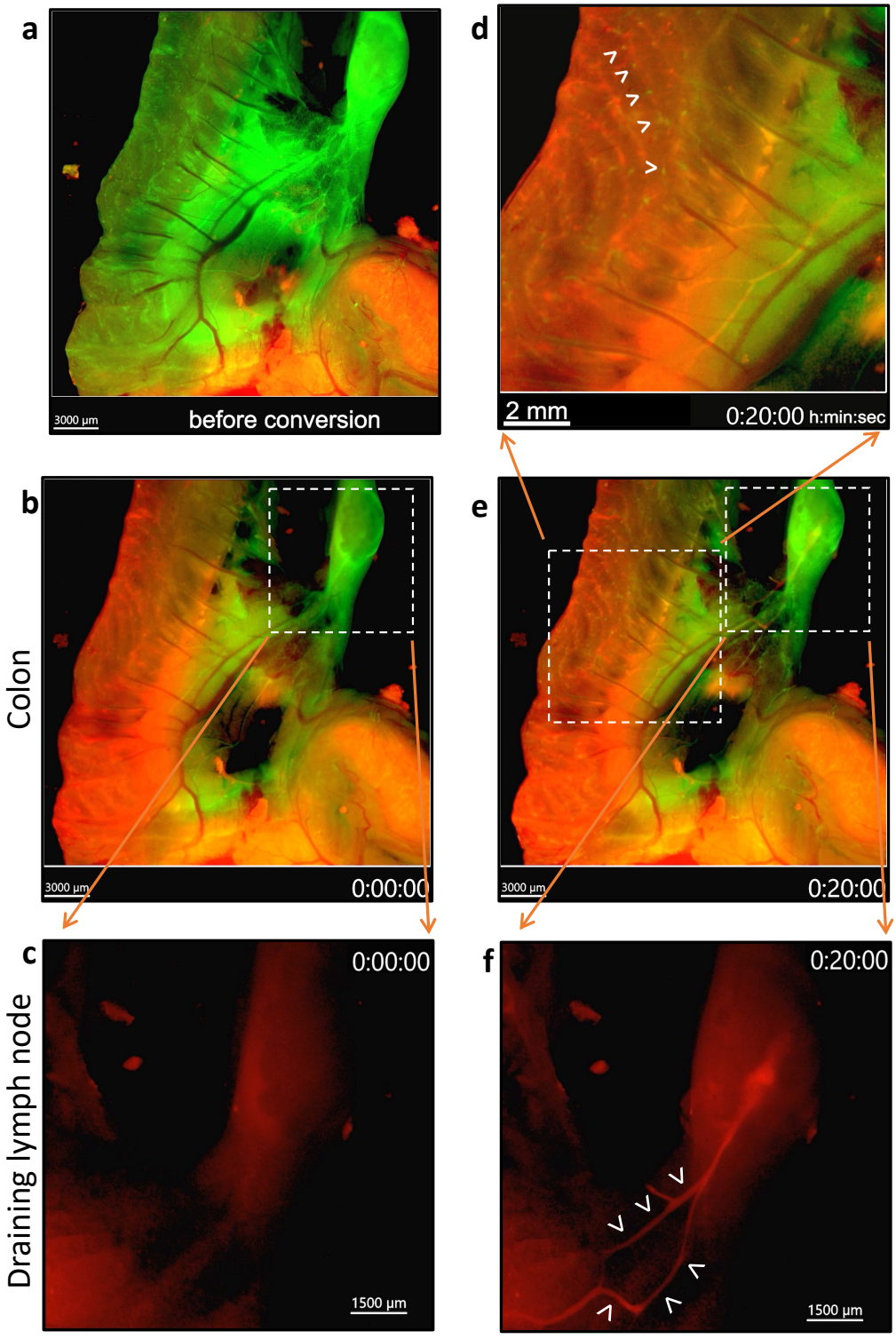

Figure 5.14: Endogenous interstitial tracer demonstrates drainage via folds into the colonic draining lymph node with new contents arriving to the tissue at 'hotspots'. The colon is seen before photoconversion (a), immediately after photoconversion (b-c) and 20 minutes after photoconversion (d-f). I*mages are from a single experiment conducted by Dr Rafael Czepielewski at Washington University in Saint Louis.*

5.2.12 Folds are in continuity with the peri-vascular space

We were curious as to why a specific subset of mononuclear phagocytes are enriched in the fold space and the continuing submucosa. To answer this, we considered the presence of the muscle layer that surrounds the tissue and noted that at the regions where the large vasculature enters the tissue, the muscle was significantly thinner (Figure 5.10e-f cross-sectional images, Figure 5.15b cross-sectional image, Figure 5.16a cross-sectional image). Figure 5.16 follows one of these large vessels along its length and then into a fold, where the perivascular space can be appreciated turning into a colonic tissue fold. This is because all blood supply to the colon enters from the outside in, and so the vasculature must penetrate through the muscle to supply the colon. We have shown that lymphatics drain the contents of the submucosal space and pair up with the large blood vasculature (Figure 5.15). However, we remain unclear as to where exactly in the tissue the contents would enter the lymphatics rather than travel in the perivascular space. As we have seen, the vasculature enters the tissue through these gateways in the muscle and so the space around the vessels could also contain contents from the submucosa that could leak into the peritoneum if not captured by these mononuclear phagocytes. Therefore we hypothesise these fold-associated mononuclear phagocytes that are continue with the perivascular mononuclear phagocytes around large vessels are primarily functioning to prevent leakage of colonic contents that drain via this outflow pathway.

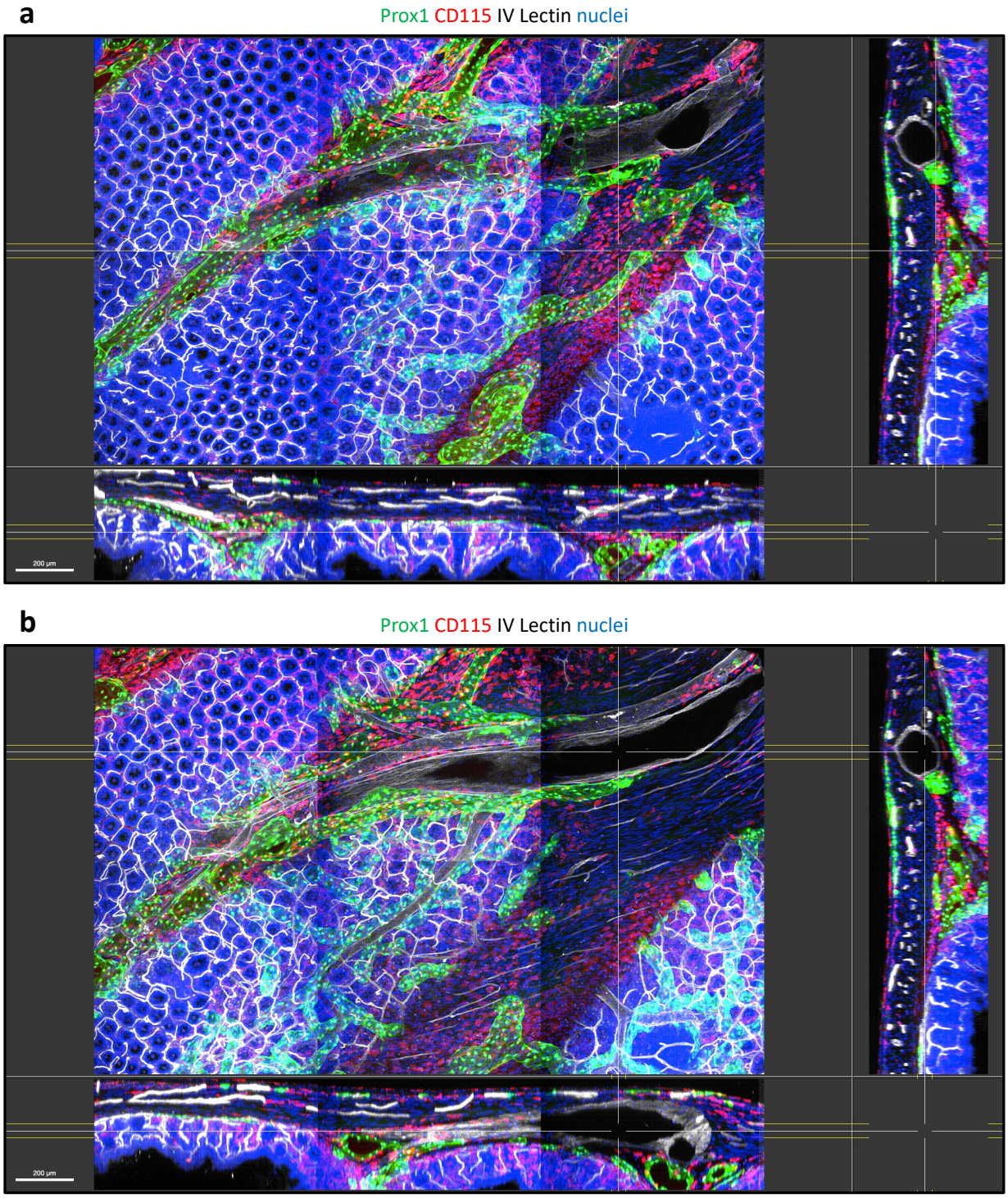

Figure 5.15: The tissue fold spaces are connected to perivascular spaces. The base of a tissue fold is highlighted by crosshairs in (a) and the lumen of a large vessel is highlighted by crosshairs in (b). *Images are representative of at least three independent experiments.*

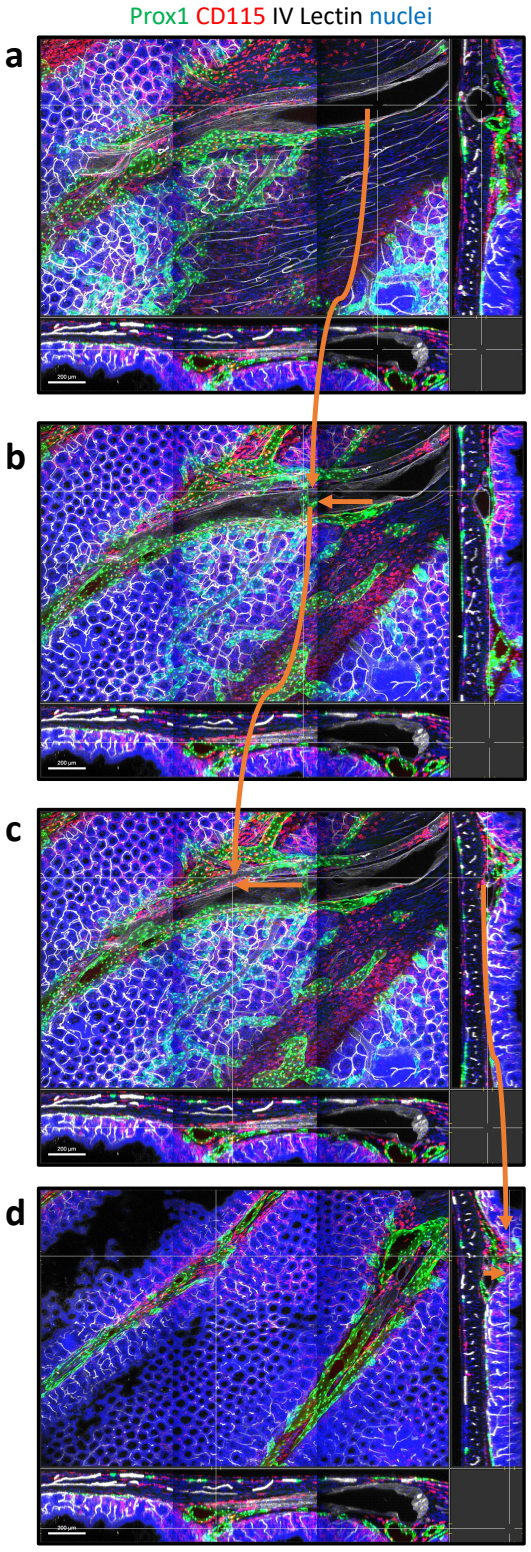

Figure 5.16: The large blood and lymphatic vessels entering the colon must penetrate through the external muscle layer and perivascular spaces are created in continuity with colonic tissue folds. The crosshairs trace the path from a large vessel lumen (a) to where lymphatic straps come near (b) to the edge of a fold (c) to the middle of a fold (d) showing these are all in continuity. *Images are representative of at least three independent experiments.*

5.3 Visualisation of 3D changes in inflamed colon demonstrates loss of tissue folds and true lymphangiogenesis

So far, we have extensively characterised the colonic tissue folds primarily in homeostasis as we realised that this had previously received little attention in the literature. We wanted to turn our attention to inflammation to see how that would affect the tissue folds and this will be the focus of this sub-chapter.

5.3.1 Colonic tissue folds are lost in inflammation

To induce inflammation in the murine colon we used DSS colitis as a model. We observed loss of tissue folds that correlated with the degree of inflammation (Figure 5.17). Early DSS at day two (Figure 5.17a) still has folds that maintain their structure, but by day nine (Figure 5.17b), the fold structure is lost. This was even clearer with 3D imaging from another DSS experiment at day seven where the colonic fold structure has been completely lost (Figure 5.17c and Figure 5.18). As highlighted earlier, fixation of healthy colonic tissue after agarose distension did not get rid of the tissue folds, confirming that inflammation leads to a loss of the fold structure by a mechanism other than increased pressure. We are still unclear on the precise mechanism of how inflammation induces loss of the colonic tissue folds, which forms ongoing research. More recently, I have discussed quantification methods with Dr Adrien Hallou, who is a biophysicist, and aspects such as the periodicity and amplitude of the colonic folds can be quantified and then formally compared with statistical analysis (e.g. t-test between baseline and peak of inflammation) to confirm our initial observations. This forms the immediate next steps in the project.

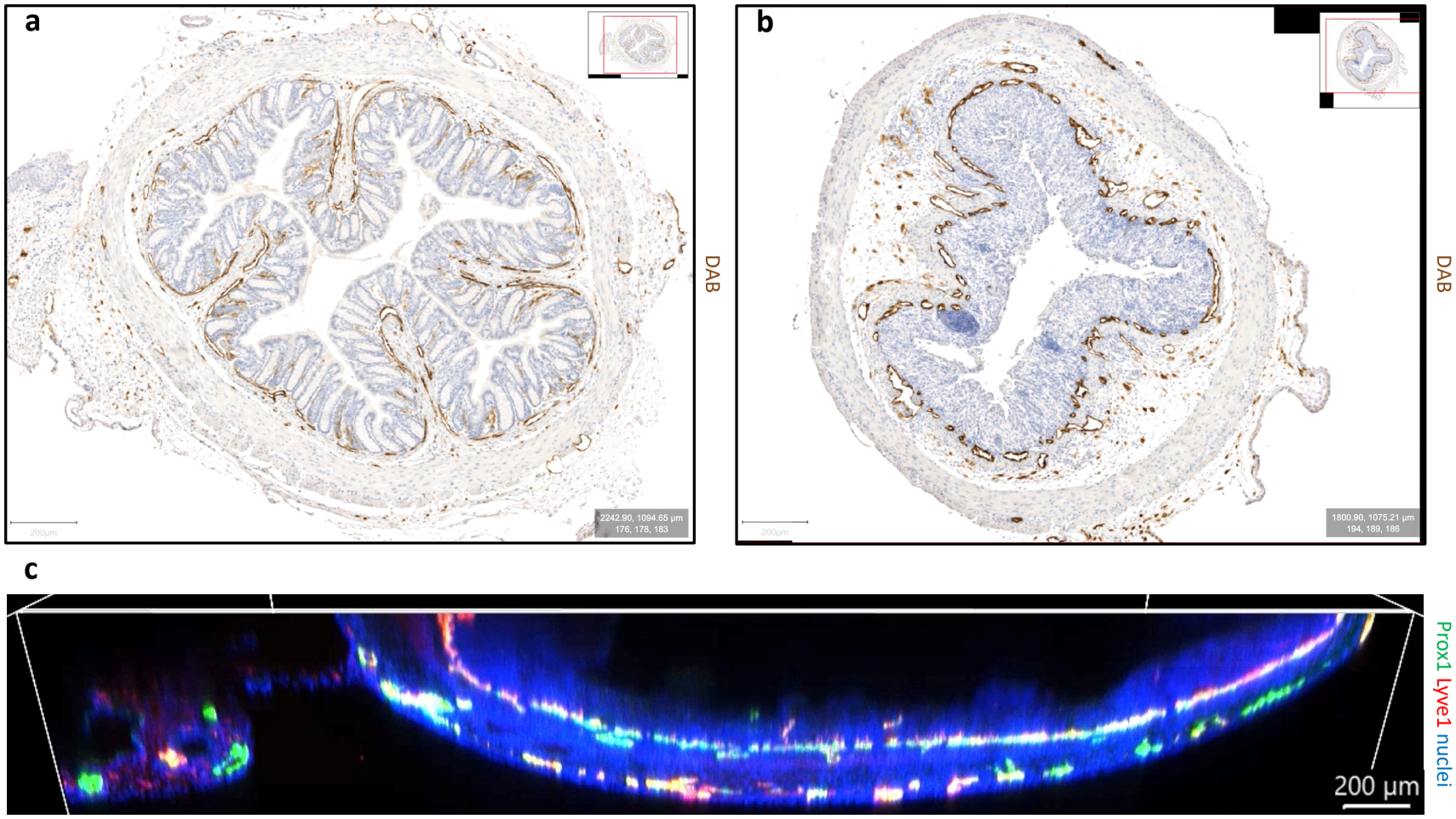

Figure 5.17: Colitis results in loss of tissue folds. The cross-section of a colon after two days of DSS colitis (a), and nine days of DSS colitis (b). 3D imaging of a mouse colon after seven days of DSS colitis (c). *Images are representative of at least three independent experiments.*

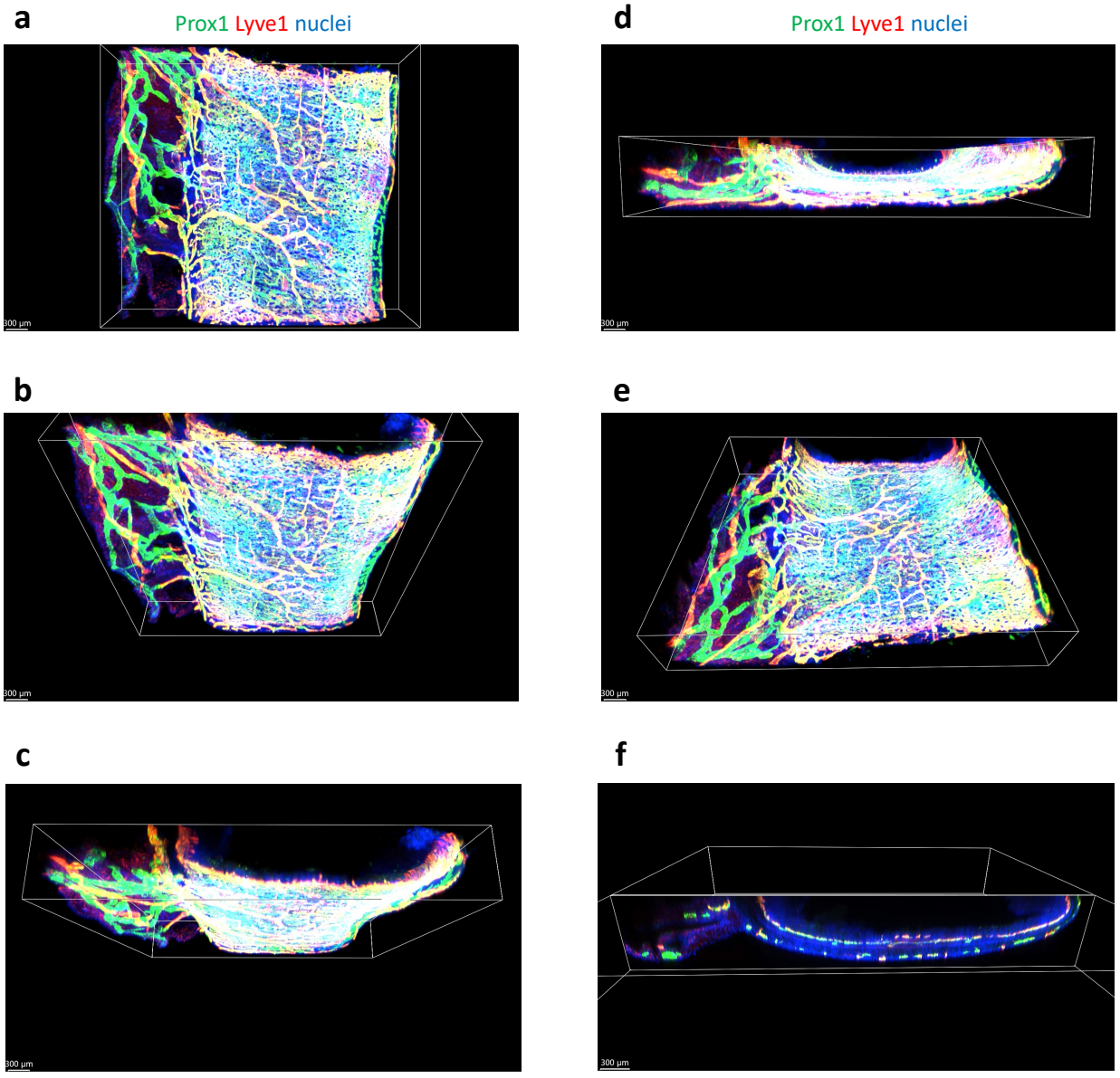

Figure 5.18: Colitis results in loss of tissue folds visualised with 3D imaging. Imaging from the muscle layer (a) rotating through to the luminal side (e) with a cross-section of the colon in (f) showing loss of the tissue folds at day seven of DSS colitis. *Images are representative of at least three independent experiments.*

5.3.2 Colonic lymphangiogenesis is only truly appreciated in 3D imaging

As outlined, many studies on lymphatic vasculature in the context of inflammation state the presence of lymphangiogenesis in inflammation. However, these studies are often making conclusions based on 2D imaging. Here we show the true effect of inflammatory lymphangiogenesis in the context of DSS colitis (Figure 5.19). The muscle layer lymphatics (Figure 5.19a) and sub-epithelial layer lymphatics (Figure 5.19b) are visualised and projections from the main vessels are seen (Figure 5.19a-b, arrowheads). The striking feature of finger-like projections in both the sub-epithelial and muscle layer of lymphatics resembles the finger-like projections that were enriched in the fold regions in the steady state colon (Figure 5.19c, arrowhead). The cellular mechanisms and tissue signals for lymphangiogenesis specific to the colon remain unknown and will form the basis of future work.

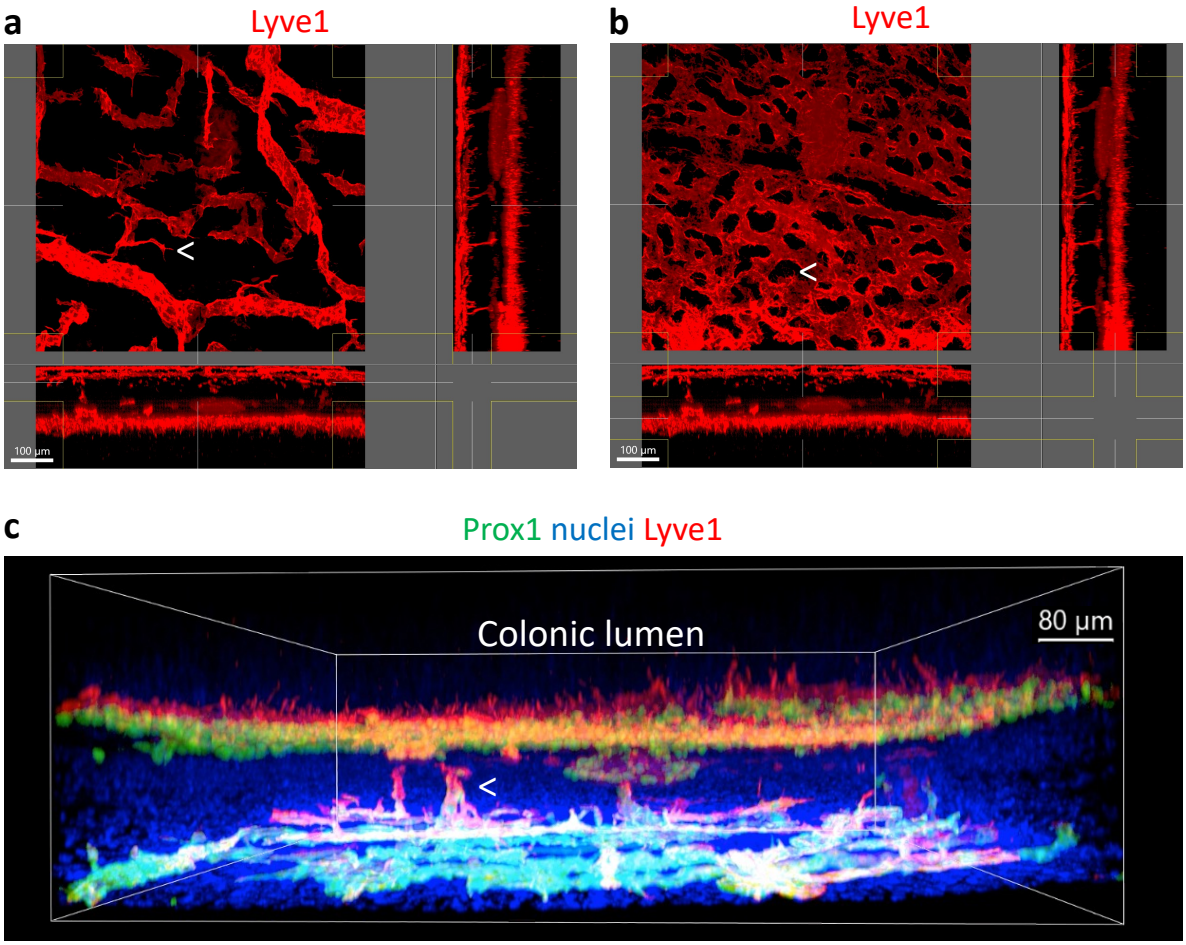

Figure 5.19: Colitis induces lymphatic vessel sprouting in both layers of colonic lymphatics. Dextran sulfate sodium (DSS) was used to induce colitis in mice and the colons were imaged at the peak of colitis at day seven. The muscle layer (a) and subepithelial layer (b) of lymphatics demonstrated architectural changes with small sprouts that appeared from the main lymphatic vessels (arrowheads). When the cross-section of the colon is visualised in colitis (c), the branches of the muscle layer lymphatics towards the lumen can be appreciated (arrowhead). *Images are representative of at least two independent experiments.*

5.4 Human colonic imaging reveals tissue folds which are also lost in inflammation

Having extensively characterised the murine colonic lymphatic vasculature and tissue folds, we wanted to turn our attention to the human colon to understand what similarities there may be. We start by revisiting a gross specimen of freshly resected human colon from a healthy young male patient who was an organ donor following a road traffic accident. Following this examination, we looked at the histology of human colon sections to understand the arrangement of the tissue folds and finally consider the folds in human ulcerative colitis, which was all collaborative work with contributors identified in the text.

5.4.1 Gross human colon specimen reveals tissue folds orientated perpendicular to the lumen

With the help of a surgical colleague, Dr Mark Hoofnagle, we identified the arterial vasculature to the colon and perfused the tissue with 100ml 4% PFA. The tissue had already been perfused with solution prior to transplantation so the majority of the red blood cells had been washed away. We then opened a portion of the proximal colon and after clearing out the stool we inspected the inner (Figure 5.20a) and outer (Figure 5.20b) surface of the tissue after opening it along the mesenteric border. We immediately noticed the presence of numerous tissue folds, similar in appearance to the mouse proximal colon, but in a strictly perpendicular alignment to luminal flow (Figure 5.20a). It is important to specify that these internal folds are not the same as the haustral folds that are observed radiologically but are far more numerous than the haustral folds. We then observed that the tissue folds did not traverse the entire circumference of the colon, but rather formed three discrete sets. This contrasts to the mouse colon where there are two sets of folds in the proximal colon (Figure 5.1d and 5.2).

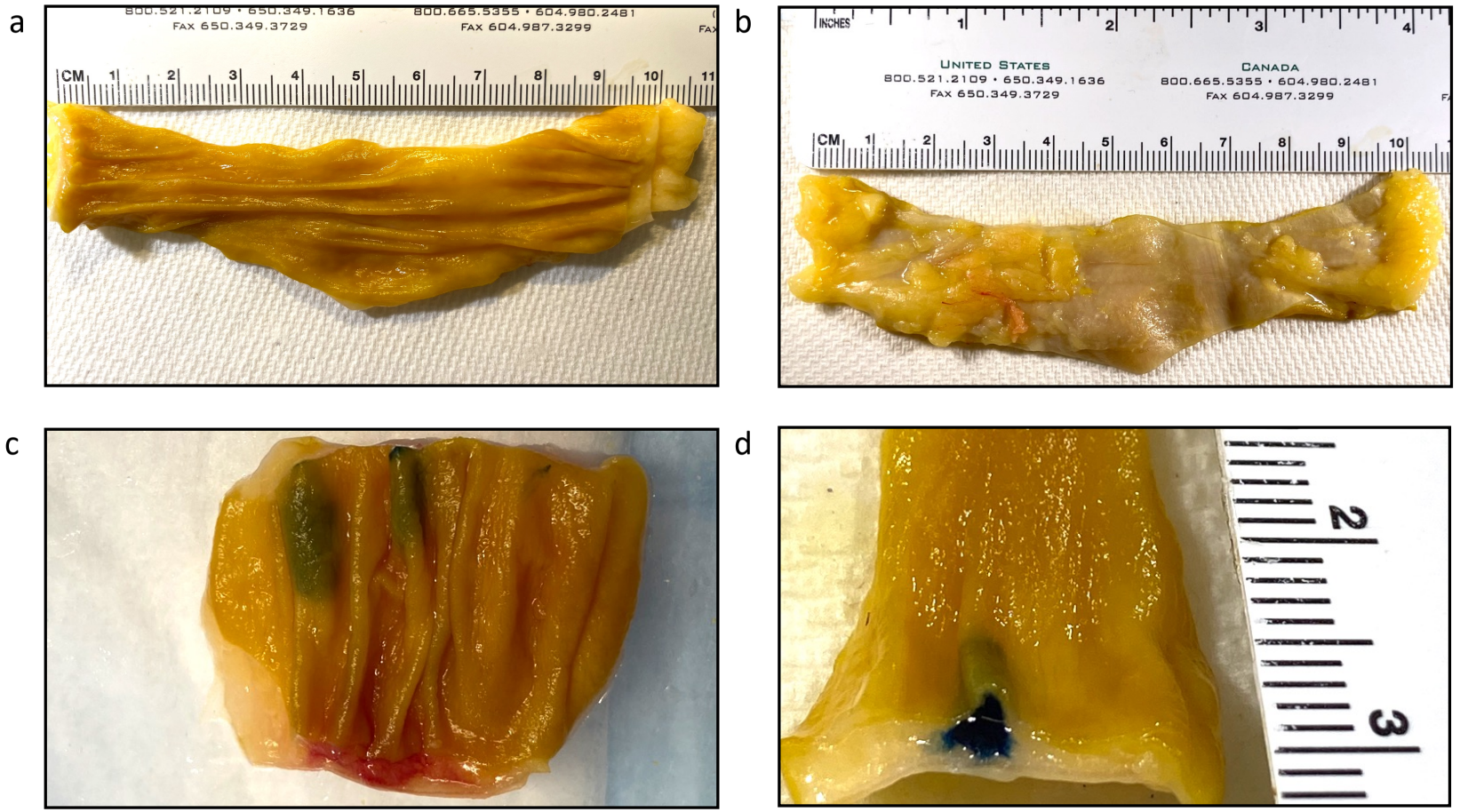

Figure 5.20: Gross anatomical examination of human colon reveals folds that are analogous to mouse that are more frequent than haustrations. Luminal (a) and external (b) surfaces of colon cut along mesenteric border. Injection within two folds (c) and one fold (d) of colon. *Images are from a single experiment.*

We then injected Evans blue dye into one of these colonic tissue folds and observed that it remained within one fold and did not spread laterally to other folds (Figure 5.20c). We injected another specimen with blue dye in two folds separated by a fold in the middle and found that they remained within their folds and did not migrate (Figure 5.20d). Of course, this is an imperfect experiment as the sample was fixed ex vivo and may not reflect true migration pattern and was only done in one patient sample. Nonetheless, it provides evidence that tissue folds in human colon can contain the spread of injected tracers equivalent to the mouse but requires further clarification with injection into fresh tissue.

5.4.2 Histological assessment of human colon confirms colonic folds containing mucosa and submucosa

With the help of an academic pathology colleague, Dr Cathy Ma, we were able to clearly confirm that their histological assessment matched ours in identifying colonic tissue folds (Figure 5.21b-c). In human tissue, unlike the mouse, small intestine has a similar appearance of fold structures projecting into the lumen (Figure 5.21a, Figure 5.21c). Furthermore, histological sections of the colonic tissue demonstrate lymphoid aggregates positioned within folds (Figure 5.21d-e), analogous to those seen in the mouse.

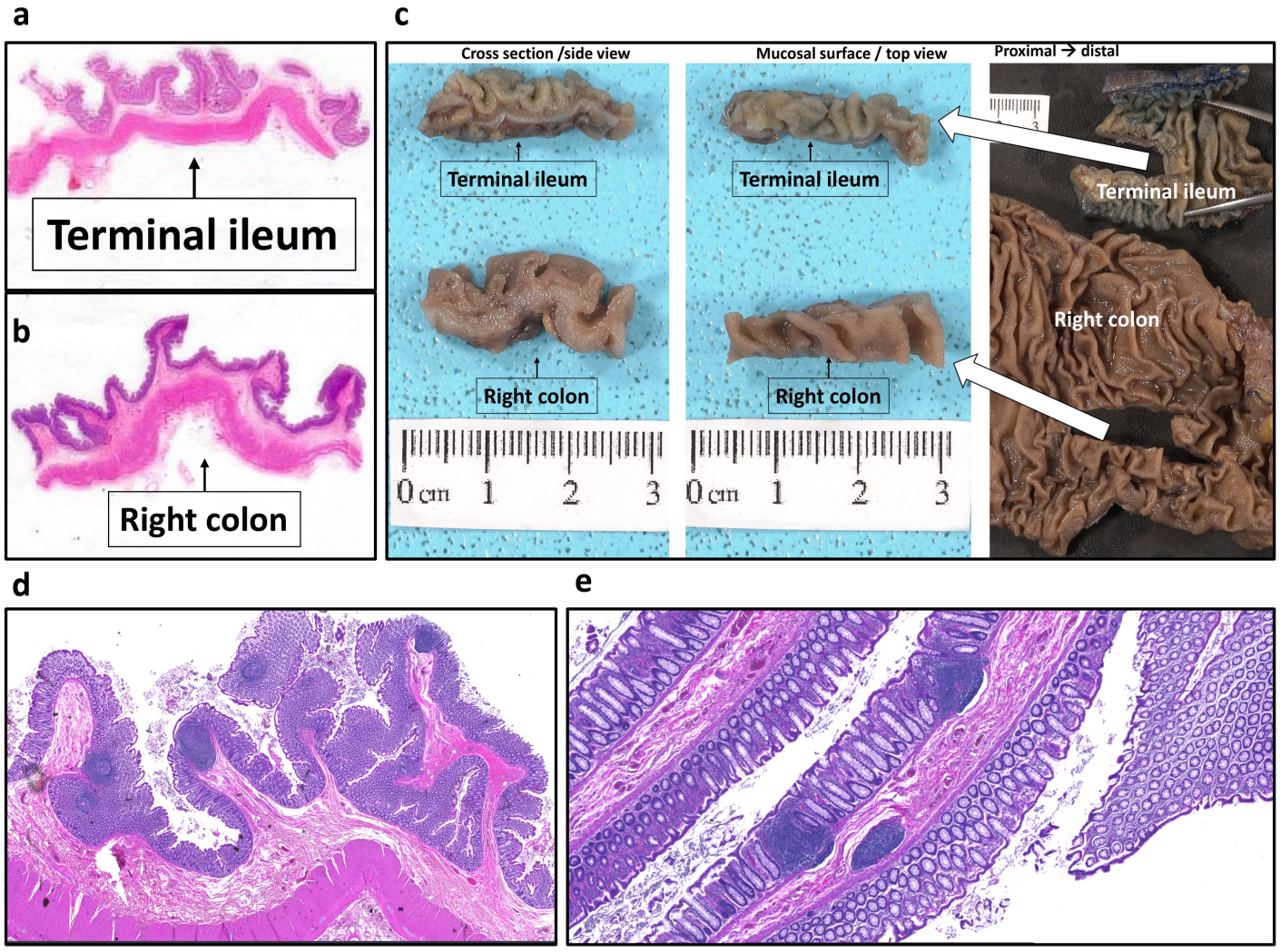

Figure 5.21: Human colonic tissue has a similar arrangement of folds as seen in the mouse. Terminal ileum (a) and colon (b) cross-sections with gross histology in (c) and lymphoid structures within human colonic tissue folds visible in (d-e). *Images (a-c) are from a single experiment by Dr Cathy Ma. Images (d-e) are representative of at least three samples from Professor Gwen Randolph.*

5.4.3 Colonic tissue folds and disease extension in ulcerative colitis

The final section of this chapter turns our attention to inflammation in the human colon in the context of ulcerative colitis. Ulcerative colitis has a peculiar feature where inflammation typically starts in the distal colon and disease extension happens in a distal to proximal manner (179). We consider what contribution the colonic tissue folds may be playing specifically in the case of proximal extension of the disease, which can happen within the space of mere hours, and currently has no plausible explanation in the field.

A sharp demarcation line of often seen between healthy and inflamed tissue (Figure 5.22a, arrow showing disease margin). What is striking to us is the loss of tissue folds in the inflamed regions, but the presence of normal tissue folds in the regions that are uninflamed. When considering the sharp demarcation seen in ulcerative colitis, we can rule out several factors that are very unlikely to explain it. This includes the gut microbiome, which has numerous links to inflammatory bowel disease, but is unlikely to migrate upwards against luminal flow, nor the blood vasculature, which can result in ischaemic colitis affecting discrete regions of the colon.

Professor Gwen Randolph had archived histological sections specifically across the disease margin and shared these slides with us (Figure 5.22b-d). What is clear is the presence and absence of tissue folds across the margin which correlates with the gross histology. What is further made apparent is the presence of inflammatory cells in the submucosa in the regions where the folds are absent (Figure 5.22d, asterisk). This stands in contrast to previous dogma that ulcerative colitis is a superficial disease of the colonic mucosa, and in fact suggests that the route of spread of this inflammation more proximally is via the submucosal space.

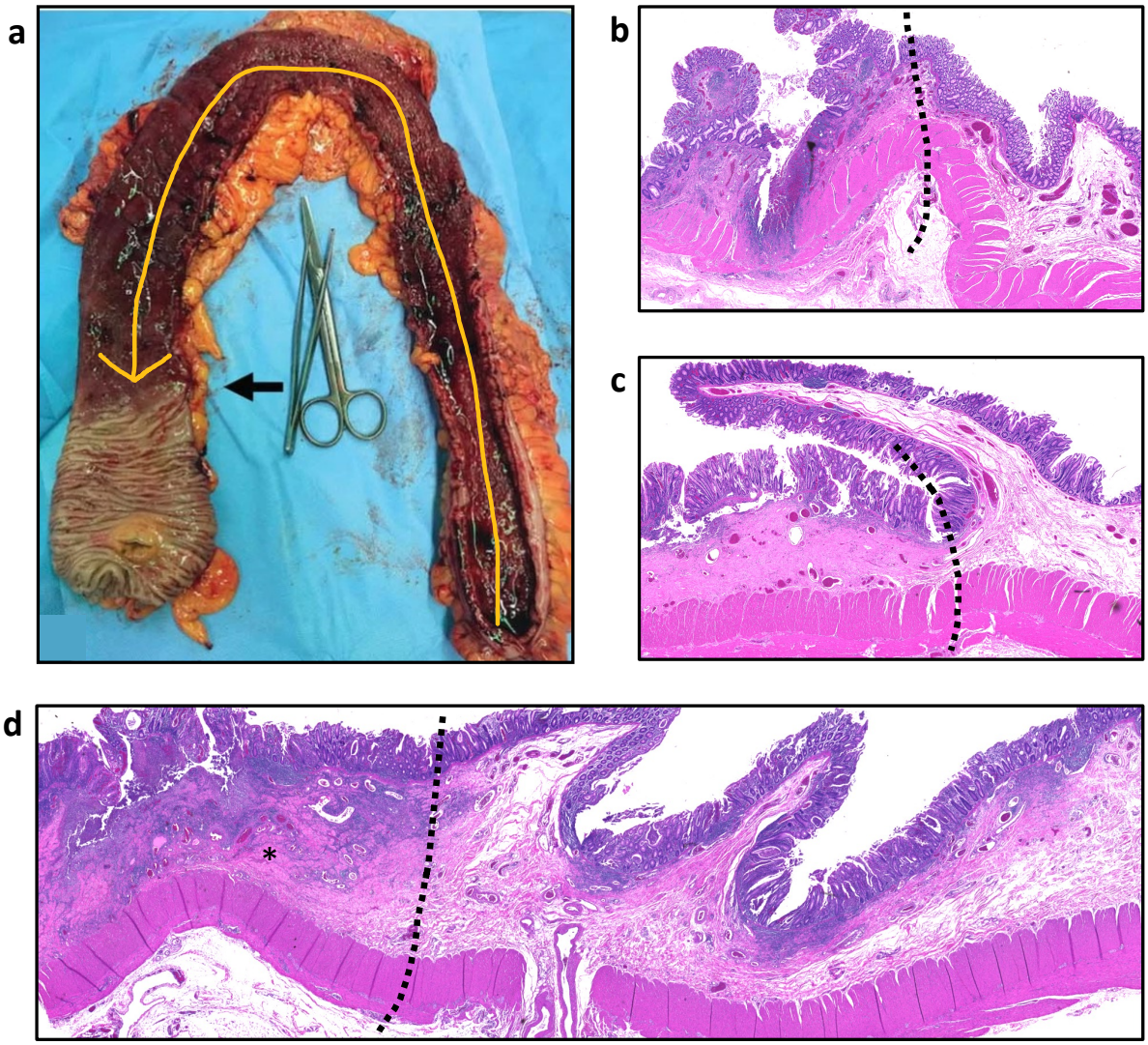

Figure 5.22: Human ulcerative colitis often has a sharp demarcation line between inflamed and healthy tissue with associated loss of tissue folds in inflammation. Inflammatory margin in ulcerative colitis (a) – image adapted from Uzzan et al. Nature Medicine (2022). Border of inflammation between healthy and inflamed samples from Professor Gwen Randolph (b-d) with border highlighted by black dotted line. Example of inflammation in the submucosal space highlighted with an asterisk in (d).

When we turn back to consider the tissue injections of the murine colon, we observed that these did not move proximally, but only within the fold or further distally (Figure 4.13). This gave us the idea that the colonic tissue folds may play a role normally allowing fluid to migrate out of the colon, or more distally, but the proximal extension seen in ulcerative colitis is a rare event where the tissue folds fail to restrain the spread of inflammation in a more proximal manner.

5.5 Discussion

In this chapter we have identified the colonic tissue folds as anatomical units, which are not eliminated by distension, and are associated with immune cells including lymphoid aggregates and a network of fold-associated mononuclear phagocytes capable of endocytosing cargo travelling within the fold such as ovalbumin. The fold units also appeared to be responsible for the uptake of contents from the systemic circulation, which appeared to be at 'hotspots' along the fold itself. In the context of inflammation in both human colitis and mouse models of colitis, the tissue folds were lost, and we speculate that this may lead to progression of disease by enabling inflammatory fluid contents to continue migrating up within the submucosal space rather than being contained by a tissue fold prior to exit from the colon.

This raises the question what happens to tissue folds in the resolution of inflammation. Anecdotally, following endoscopic healing in ulcerative colitis, patients have a return of their colonic folds, but a subset of patients develop a 'tubular' colon, which is characterised by an absence of tissue folds. It is interesting to consider at what point this goes from a reversible to an irreversible process, and to search for the factors that lead to the re-forming of folds, which is an idea for future study.

The fold structure is reminiscent of the small intestinal villus, albeit on a much larger scale. We had the idea that perhaps entire fold units could be shed off into the stool, similar to how villi may be lost. It is an attractive idea biologically as there would only be a short distance required for tissue repair if the tissue broke at the base of the fold. We searched in the stool contents of the mouse after washing the stool through a filter to see whether we could identify any intact fold structures but did not find any.

The limitations of the further study of tissue folds include the absence of mouse models of colitis that cause a distal to proximal progression of inflammation like human ulcerative colitis. It is also understandably challenging to access human inflamed colonic tissue to be able to track interstitial outflow in the way we did for the mouse. However, an interesting approach may be to inject a submucosal tattoo into the disease margin (which is already something that is done endoscopically to mark sites in the colon) just proximal to the colitis margin along with local steroid and/or anti-TNFα medication, to see whether this may prevent further spread of inflammation by the drug staying within the tissue fold itself, as well as being able to assess the disease margin identifiable by the tattoo at future colonoscopy or at the time of resection should this be what the patient requires.

A further limitation to this imaging data is quantification methods. Established tools such as ImageJ (180), QuPath (181) and histoCAT (182) exist to quantify imaging, but this is more challenging with the three-dimensional approaches that we have used. An ongoing aim of this research is to develop ways to quantify the changes that we have observed to be able to compare more systematically between groups.

Finally, we were curious as to whether the colonic tissue folds could mediate local adaptive immune responses, as they have the machinery to allow cellular entry and exit as well being in prime position to sample mucosal antigens. This is something that we were unable to explore within the timeframe of the research, but certainly something to follow up on in the future. A fascinating experiment to conduct would be to tie off the murine colonic draining lymphatics and allow the mouse to recover followed by inducing colitis and inspecting the immune responses that happen when leukocytes cannot leave the tissue, which could form future work in this field.

6 Discussion

6.1 Summary of findings

This thesis sought to characterise the lymphatic vasculature in the colon in both health and inflammation. We did this using several methodologies including flow cytometry, transcriptomic-based approaches, and novel imaging techniques with interstitial tracer studies to look across the tissue in 3D. This is the first time that this has been done to characterise the colonic lymphatic vasculature.

Initially, flow cytometry was undertaken with the intention of mirroring the analyses that is often used to establish the numbers and phenotypes of immune cells in the colon in the context of inflammation. However, despite significant optimisation, we concluded that this method was not particularly well-suited to study the vasculature by assessing changes in the number of endothelial cells in different contexts. This is because the signal-to-noise ratio is far greater with haematopoietic cells in the context of inflammation, which change by an order of magnitude, compared to endothelial cells. This makes intuitive sense as haematopoietic cells can be mobilised from the bone marrow and circulation and are ready to respond rapidly in number in the context of inflammation, whereas the turnover of endothelial cells within vessels is far slower and cannot be increased by recruitment of circulating cells from the blood.

The use of flow cytometry did, however, enable us to optimise the digestion of the tissue for endothelial cells and so then give us the ability to sort these cells for sequencing. This is something that has little precedent in the literature as lymphatic endothelial cells are far more fragile and infrequent compared to most haematopoietic cells. The ability to sequence these cells offered new insights into the transcriptome of lymphatic endothelial cells both in homeostasis and inflammation. We found that a subset of lymphatic endothelial cells changed significantly in the context of

inflammation and demonstrated an interferon-responsive signature. Furthermore, we found that a different subset of lymphatic endothelial cells expressed Icam1 in inflammation. This suggested that these subsets of cells were present in distinct locations, and the localisation of these is the focus of ongoing work.

In the second results chapter, we changed focus to visualising the 3D anatomy of the colonic lymphatic vasculature. We found the orientation and structure of the lymphatic drainage of the colon was markedly different to the small intestine. The lacteal structure that was seen in every villus of the small intestine was absent in the colon, and rather there is a network of lymphatic vessels at the base of the colonic crypts that can be appreciated when visualising a colonic cross-section. What we had also noticed is that when these vessels are then displayed in 3D, there is an even greater superstructure which varies at the colonic tissue folds. Furthermore, these folds contained numerous lymphoid aggregates, which we reasoned were located strategically to gain priority access to absorbed antigen. These findings were only appreciated when we imaged at the scale we were able to and with the methods that we had developed in this project.

This anatomical understanding prompted us to uncover the drainage pattern of interstitial fluid from the colon in the second half of the second results chapter. Our data revealed that the tissue folds in the colon were units that orchestrated interstitial outflow and drainage to the draining lymph node. Again, this was unique to the colon compared to the small intestine and had not previously been described.

In the final results chapter, we further characterised these tissue folds and found that they had a specific network of macrophages within them that were able to phagocytose cargo that was injected a significant distance away. This highlighted that the tissue folds are in continuity over large distances

and form a route within the tissue that permits trafficking of contents that is distinct to the lumen. The tissue fold contents eventually end up in the outgoing colonic lymph, which reaches the colon-draining lymph node in the mesentery.

We found that the colonic tissue folds changed significantly in the context of inflammation, with remodelling and loss of structure observed. We were curious as to whether this was simply a consequence of physical distention and confirmed that this was not the case by infusing the health colon with agarose and seeing that the folds were still present projecting into the lumen.

Our overall findings outline the drainage pathway of the colonic tissue for the first time to our knowledge. We have identified a function for an overlooked aspect of colonic anatomy, which are the tissue folds. We will next turn to understanding how we can place this in the context of the wider research literature.

6.2 Placing these findings in the wider context and future directions from our work

6.2.1 Pathogenesis of inflammatory bowel disease

The pathogenesis of IBD is multifactorial, involving aspects of host genetics, tissue immunity, and environmental factors, and remains incompletely understood (29). Our findings fit into the wider context of towards further understanding the pathogenesis by shedding light on a neglected aspect of colonic anatomy and outflow from the colonic tissue. Some evidence for continuity of the interstitial space has been described by injection of tattoo into the human colon endoscopically and identifying the tattoo pigment within macrophages and free within the submucosa, muscularis propria and mesenteric fascia, as well as in the draining lymph node at the time of colonic resection (183, 184). We build on this by finding that the predominant flow within the tissue appears to be within the fold region.

Indeed, submucosal injection is a technique used during colonoscopy to help raise lesions to prevent perforation during endoscopic resection. This demonstrates that the submucosal space is one that has the potential to expand and accommodate fluid. Whether injections of therapy can be placed directly into this space is an open question and may be something to explore in the future if this can then spread via the submucosal space to the rest of the colon. A study in mice has shown that injection via colonoscopy of a compound can spread via the submucosal space, which demonstrates proof of principle of this approach (185). Furthermore, the use of submucosal injection in colonoscopy is commonly performed in the context of endoscopic mucosal resection and endoscopic submucosal dissection, so it may be possible to adapt this to administering therapeutics. It would make sense to start initially with therapies that are known to work in IBD such as anti-TNFα to see if

direction injection would be of benefit. It may also be the case that this can be injected just above the inflamed margin of disease in ulcerative colitis to prevent further extension.

We believe the tissue-fold niche is significant in the context of ulcerative colitis. As mentioned in the thesis, ulcerative colitis typically starts in the distal colon and progresses proximally (186). We hypothesise that the tissue fold niche that we have described may be functioning to restrain the spread of inflammation within the submucosa. As spread of inflammation and extension of disease is a relatively rare event, it may be the case that the folds normally function to restrain spread of inflammation, but when these get overwhelmed or fail, then the only remaining direction for inflammation to travel is more proximally up the colon. Interestingly, meta-analysis of clinical data highlights that approximately a quarter of patients with limited ulcerative colitis extend over time, but that this largely limited to happening within the first 10 years of diagnosis (187). This raises the possibility that some patients may have a predetermined ability to adequately promote tissue outflow linked to the tissue folds.

Furthermore, most studies in IBD are based on human tissue from biopsy samples. Very few utilise full thickness resections, and indeed even when this is done, they are by definition therapy-refractory so it is a different cohort to those who would respond to medication. The findings from our work highlight that the immune cells of the mucosa and lamina propria is just the tip of the iceberg when it comes to understanding the pathogenesis of IBD. An example of this idea is a study that identified the contribution of enteric glia in the muscle layer of the murine intestine to sense and respond to enteric helminth infection (188). Moreover, even when looking at the mucosa, histology specimens from biopsies are often orientated in various ways, and so only general patterns of inflammation can be commented on rather than the larger anatomical structures that we have identified through our work. Our future direction from this is to use well-orientated sections of colonic tissue from health

and inflammation and pursue spatial transcriptomics to identify whether inflammatory signatures follow the pathway of tissue drainage that we have identified.

The increased utilisation of cross-sectional imaging may go some way in improving our understanding of IBD. It is increasingly appreciated that the mesentery is involved in the pathogenesis of Crohn's disease (189), and bowel wall oedema is a feature of severe ulcerative colitis (190). Mesenteric lymph nodes may be enlarged and correlates of these radiological features at a histological and cellular level are lacking for understandable reasons. Animal models of colitis can prove helpful in this context in identifying the mechanisms of what may be occurring in the deeper regions of tissue such as the submucosa, muscle layer and mesentery. Correlating these findings with human cross-sectional imaging may help us progress our understanding of the disease processes in IBD.

Another aspect of the tissue fold relevant to immunity is that it enables inflammatory contents time to be dealt with prior to draining. In the context of loss of folds in IBD this may set up a vicious cycle of inflammation where the loss of a fold impacts on the next one in a sequential way. Another anecdotally relevant clinically feature is that patients with loss of folds in inflammation tend to have the folds return when inflammation resolves. However, there is a small group of patients who end up with resolved inflammation but a featureless, tubular colon. This may reflect the idea that longstanding inflammation permanently remodels the tissue folds and results in fibrosis of the tissue which becomes irreversible. A future direction related to this will be to perform further histological assessment of the colon from animal models of colitis in the resolution of inflammation and evaluate whether the folds return or not. Alongside this, in the resolving phase, it would be interesting to profile the tissue to try to identify factors that may contribute to the re-forming of the tissue folds, and this is a question that we would also assess whilst evaluating spatial transcriptomic data.

6.2.2 Intestinal immune responses

6.2.2.1 Lymphoid structures and leukocyte trafficking

We identified numerous lymphoid structures within the colonic tissue folds in mice and human. Work has been done to isolate the lymphoid structures in the human colon to characterise immune responses in this specific locations (191, 192). An ongoing field of active research in intestinal immunity is the understanding of immune responses that occur in the tissue compared to the draining lymph node. If lymphatic drainage is disrupted then we can imagine that leukocytes that would typically exit to the draining lymph node would get sequestered in the tissue folds for a longer duration, and then may get primed in the regional lymphoid structures. Moreover, it may be possible for the leukocytes to travel via the tissue fold spaces to other regions of the intestine and mount immune responses at the nearest lymphoid structure that is associated with the folds that we have identified anatomically.

A way to experimentally test this would be to perform lymphatic ligation surgery on mice and then compare the fold contents to control animals in both health and inflammation. The forced accumulation of leukocytes that are destined for exit to the colonic lymph nodes may result in differential immune responses in the tissue. Furthermore, they may be able to traffic within the tissue along the tissue folds to adjacent lymphoid structures to mount immune responses in these regions. In addition to impairment in cellular trafficking, the interstitial contents and cytokines would also accumulate in the fold regions, similar to the tracers that we injected in our studies. Small molecular weight substances could leave via the blood vasculature, but in the presence of lymphatic impairment, as has been described in IBD (102, 193–195), it is possible to imagine large molecular weight substances such as LPS accumulating in the tissue fold spaces, much like a sieve allowing

smaller particles through but not larger ones. This concentrating effect of potentially inflammatory mediators may well be responsible for the differential lymphatic finger-like projections that are seen in the tissue in the fold regions, and this is something that we plan to characterise further in other cell types using spatial transcriptomic technology. Of course, a ligation model would make it hard to tease apart the effects of impaired cellular trafficking compared to inhibiting interstitial fluid outflow.

Within the scope of the research, further questions arise as to what the consequence of altered leukocyte trafficking is on the immune response. Another aspect of leukocyte trafficking of relevance to IBD is that of egress from lymph nodes to then recirculate to the intestinal tissue. It is known that modulation of S1P by medications such as ozanimod (196) is effective in the induction and maintenance of remission in ulcerative colitis. S1P modulation is generally thought to work by preventing egress of leukocytes from the lymph nodes and therefore returning to the inflamed tissue (34, 197, 198). However, S1P modulation also effects leukocyte egress from the tissue to the lymph nodes (Sci Rep 2024 ref). It would be of interest to understand the similarities and differences of leukocyte egress from the tissue compared to the lymph nodes.

Further questions related to the localisation of immune responses arise from our work. The lymphatic vasculature is typically the route of cellular drainage from the intestine, but the venous drainage is via the hepatic portal vein to the liver. A study characterised that in intestinal inflammation, bacteria can enter the portal vein and the liver is able to prevent systemic spread; however, in the context of liver dysfunction, systemic immune responses were detected to commensal organisms (199). It is intriguing to further consider the location of immune responses from our work. In particular, whether the rerouting of bacteria in intestinal inflammation to the liver affects the immune response. A relevant clinical observation to this is that there is often a discrepancy between intestinal and systemic inflammation in the context of IBD, where patients can have severe intestinal inflammation

but relatively normal systemic inflammatory markers or vice versa. It would be of interest to correlate this with the route of drainage of intestinal contents.

6.2.2.2 Intestinal mononuclear phagocytes

We have identified a subset of mononuclear phagocytes that are predominantly found in the fold region. These stand in contrast to the lamina propria macrophages often studied from intestinal biopsies, as well as the more recently characterised muscle layer associated macrophages associated with neurons and are self-maintaining (200–202).

An obvious next step would be to deplete them to test the hypothesis that this subset of mononuclear phagocytes plays a specific role in prevent systemic spread of colonic contents. This would be interesting to compare to depleting all mononuclear phagocytes and mononuclear phagocytes from other locations in the colon to see whether this phenocopies the result of depleting the specific subset that is located within the tissue folds. Different strategies exist to deplete mononuclear phagocytes. Colony-stimulating factor 1 (CSF1) or CSF1 receptor (CSF1R) is crucial for the differentiation of macrophage populations and deficiency of these factors lead to macrophage deficiency (203). Furthermore, CSF1 signalling is also required for the maintenance of macrophages in adult mice, and administering a blocking anti-CSF1R antibody depletes macrophages in a similar manner (204). We had the idea to administer the anti-CSF1R antibody by injection directly into the colonic fold to leverage the drainage pattern of the antibody to anatomically target the mononuclear phagocytes in the folds. However, we realised that the injection would only be able to target the folds that are visible to us and in the proximal colon during the intravital injection, and this would not be sufficient to target the entire population of fold-associated mononuclear phagocytes.

We identified Lyve1 as a marker on the submucosal fold-associated macrophages in both mouse and human, in keeping with other studies (163). Lyve1 is also expressed on lymphatic capillaries, and we hypothesised that there may be some synergy in Lyve1 expression on macrophages and lymphatics as a ligand for hyaluronic acid (205). Further experiments to test this could be done in Lyve1 deficient animals, which survive and have functioning lymphatic vessels (206). Alternatively, Lyve1 itself may not be required for the protective effect of these macrophages and just serve as a marker for their anatomical location in the submucosa. In this case, using a Lyve1-Cre animal would be a way to target both the lymphatics and macrophages, but to selectively deplete the Lyve1-expressing macrophages, this strain could be crossed to a Csf1r-flox animal so that only the macrophages expressing Lyve1 are depleted without affecting the lymphatics.

6.2.3 Intestinal endothelial cell biology

Often, the main consideration of endothelial cell biology in the context of immunity is their permeability and ability to recruit immune cells from the circulation. Indeed, targeting this is the presumed mechanism of action of vedolizumab, which blocks α4β7 integrin on leukocytes, which is normally used to enter intestinal tissue via binding Madcam1 on intestinal endothelial cells, and is a successful therapy in IBD (18). However, it is increasingly being appreciated that endothelial cells have further biological roles in addition to permeability and leukocyte recruitment. Endothelial cells have been shown to be environmental sensors and secretors of niche factors. For example, dietary metabolites such as aryl hydrocarbon receptor (AHR) ligands have recently been shown to be sensed by intestinal endothelial cells (207). Furthermore, single-cell sequencing of endothelial cells across organs has revealed significant endothelial diversity (208). However, the specific role of the lymphatic endothelial cell-specific factors has received relatively less focus to blood endothelial cells.

In the context of inflammation, a paper highlighted the importance of endothelial cell-specific sensing of interferon-gamma in contributing to intestinal inflammation, as when the interferon-gamma receptor signalling was deleted specifically in endothelial cells, this ameliorated experimental DSS colitis (157). As the Cre drivers used in these studies target both blood and lymphatic endothelial cells, it is important to consider whether some of the effect was mediated by changes in interferon-gamma sensing in lymphatic endothelial cells, which wasn't directly addressed by the authors.

We showed that the lymphatic endothelial cells of the colon resided in distinct locations, and one specific area was beneath the epithelial stem cell niche. Recent interest has been drawn to these cells as studies have highlighted that intestinal lymphatic endothelial cells that lie near the crypt base are able to secrete factors, termed 'lymphangiocrine factors' that can support the stem cell niche (53, 55, 209). From our work, we aim to continue understanding the lymphatic-specific factors that are generated and especially if this has any link to the tissue fold structure that is observed to be lined by lymphatic endothelial cells.

6.2.4 Tissue niches

The intestine is comprised of repeating crypt units in the colon, and crypt-villus units in the small intestine (210, 211). The intestine stem cell niche is well-described with more differentiated epithelial cells towards the top of the crypts and a stromal cell layer supporting the niche immediately beneath. We believe that we have described a novel niche in the intestine, which is the tissue fold. This niche has a dedicated subset of mononuclear phagocytes for immunosurveillance and a distinct bed of lymphatic vessels. Furthermore, there are numerous lymphoid aggregates that are specifically associated with the fold units.

When intestinal tissue is examined histologically, it is made up of repeating crypt units. We believe that we have uncovered another repeating unit of the colon, which is the tissue fold. This can only be appreciated on larger-scale imaging and so this is why it may have been overlooked until now. When studying intestinal immunity histologically it is possible to get significant findings by repeating experiments and averaging the results over many samples, but we believe that if we can target histological analysis to comparable units of the intestine, it may be possible to have more homologous groups and thus make it more straightforward to identify differences between groups.

The closest previous description to the fold-niche is from a microbial perspective from the luminal side of the colon. Using laser-capture microdissection techniques it has been understood that the microbial populations that are associated with the folds are quite distinct to that found in the main lumen of the colon (212).

6.2.5 Tissue outflow across organs

The idea of tissue drainage is important as if there is a choice of outflow pathways this could impact on the immune response depending on where cells and antigens drain to. The meningeal lymphatics and glymphatics are an example, where it was thought for a long time that there was no lymphatic drainage of these structures. When this discovery was made there was a paradigm shift in the understanding of neuroimmunology (213). More recently, it has been hypothesised that Alzheimer's disease, where there is a build-up of amyloid beta peptides (214) can be alleviated by stimulating the lymphatic clearance of these proteins.

We believe that the tissue outflow from the colon has been similarly overlooked and that by taking this step to uncover this pathway, we will be able to further examine questions related to immune

function. In the colon, there may be build-up of analogous inflammatory substances that may have pro-inflammatory effects from the submucosa. Indeed, as evidenced in histological sections of ulcerative colitis, it appears that disease spread is from the submucosal space, and so it would be of great relevance to profile what is in these spaces in health and inflammation, and to understand whether lymphatic clearance would assist in reducing inflammation.

Targeting specific substances for lymphatic clearance is an unmet challenge, as of course simply increasing the lymphatic vessel number by stimulating with pro-lymphangiogenic factors would not necessarily result in any differentiation of what is drained from the tissue. Furthermore, one detrimental consequence of lymphatic drainage is in fact the priming of immune responses against the antigens that drain from the colon. What dictates whether pro-inflammatory or regulatory adaptive immune responses occur in the draining lymph node is still not fully established, and it would be important to consider whether other substances could be administered alongside stimulating lymphatic drainage to ensure that a tolerogenic response would occur.

Another contrasting example of tissue drainage is that from the liver. The liver has a rich blood supply but how this is parsed and the degree to which it drains out of the liver via the blood vessels versus the liver lymphatic vessels is understudied (215–217). It would be very interesting to characterise the contents that drains to the blood versus lymphatics and understand whether this changes in disease states such as cirrhosis. The research findings from our work will serve as an interesting comparator to tissue drainage in other sites such as the brain and the liver as outlined here.

6.3 Overall conclusion of the thesis

This thesis has highlighted the lymphatic anatomy and outflow pathway of interstitial fluid from the colon for the first time. The regional drainage patterns are distinct to the colon and this understanding can be built upon to further study tissue immunity. The techniques developed during this thesis will be undoubtedly helpful to further study the colonic tissue in 3D as well as to appreciate the role of the deeper structures of the colon in the context of IBD pathogenesis, which cannot be readily studied with the use of colonic biopsy. We will continue to progress with the study of the colonic tissue in health and disease and deciphering the lymphatic outflow has stimulated new ideas for clearance of inflammatory components that may speed up the resolution of inflammation in IBD and help those patients who do not respond to the therapeutics that are currently available.

7 Bibliography

1. Ng SC, Shi HY, Hamidi N, Underwood FE, Tang W, et al. 2017. Worldwide incidence and prevalence of inflammatory bowel disease in the 21st century: a systematic review of population-based studies. *Lancet*. 390(10114):2769–78

2. Luo Y, De Lange KM, Jostins L, Moutsianas L, Randall J, et al. 2017. Exploring the genetic architecture of inflammatory bowel disease by whole-genome sequencing identifies association at ADCY7. *Nat. Genet.* 49(2):186–92

3. Huang H, Fang M, Jostins L, Umićević Mirkov M, Boucher G, et al. 2017. Fine-mapping inflammatory bowel disease loci to single-variant resolution. *Nature*. 547(7662):173–78

4. Ni J, Wu GD, Albenberg L, Tomov VT. 2017. Gut microbiota and IBD: causation or correlation? *Nat. Rev. Gastroenterol. Hepatol.* 14(10):573–84

5. Fitzpatrick JA, Melton SL, Yao CK, Gibson PR, Halmos EP. 2022. Dietary management of adults with IBD — the emerging role of dietary therapy. *Nat. Rev. Gastroenterol. Hepatol.* 19(10):652–69

6. Piovani D, Danese S, Peyrin-Biroulet L, Nikolopoulos GK, Lytras T, Bonovas S. 2019. Environmental Risk Factors for Inflammatory Bowel Diseases: An Umbrella Review of Meta-analyses. *Gastroenterology*. 157(3):647-659.e4

7. Friedrich M, Pohin M, Powrie F. 2019. Cytokine Networks in the Pathophysiology of Inflammatory Bowel Disease. *Immunity*. 50(4):992–1006

8. Truelove SC, Witts LJ. 1955. Cortisone in Ulcerative Colitis. *BMJ*. 2(4947):1041–48

9. Thomas S, Baumgart DC. 2012. Targeting leukocyte migration and adhesion in Crohn's disease and ulcerative colitis. *Inflammopharmacology*. 20(1):1–18

10. Panés J. 1999. Adhesion molecules in inflammatory bowel disease. *Pathophysiology*. 5(4):271–82

11. Muller WA. 2013. Getting Leukocytes to the Site of Inflammation. *Vet. Pathol.* 50(1):7–22

12. Ma TY, Iwamoto GK, Hoa NT, Akotia V, Pedram A, et al. 2004. TNF-α-induced increase in intestinal epithelial tight junction permeability requires NF-κB activation. *Am. J. Physiol. Liver Physiol.* 286(3):G367–76

13. Nourshargh S, Hordijk PL, Sixt M. 2010. Breaching multiple barriers: leukocyte motility through venular walls and the interstitium. *Nat. Rev. Mol. Cell Biol.* 11(5):366–78

14. Monaco C, Nanchahal J, Taylor P, Feldmann M. 2015. Anti-TNF therapy: past, present and future. *Int. Immunol.* 27(1):55–62

15. Gordon FH, Lai CWY, Hamilton MI, Allison MC, Srivastava ED, et al. 2001. A randomized placebo-controlled trial of a humanized monoclonal antibody to α4 integrin in active crohn's disease. *Gastroenterology*. 121(2):268–74

16. Sandborn WJ, Colombel JF, Enns R, Feagan BG, Hanauer SB, et al. 2005. Natalizumab induction and maintenance therapy for Crohn's disease. *N. Engl. J. Med.* 353(18):1912–25

17. Miller DH, Khan OA, Sheremata WA, Blumhardt LD, Rice GPA, et al. 2003. A Controlled Trial of Natalizumab for Relapsing Multiple Sclerosis. *N. Engl. J. Med.* 348(1):15–23

18. Feagan BG, Rutgeerts P, Sands BE, Hanauer S, Colombel J-F, et al. 2013. Vedolizumab as induction and maintenance therapy for ulcerative colitis. *N. Engl. J. Med.* 369(8):699–710

19. Colombel J-F, Sands BE, Rutgeerts P, Sandborn W, Danese S, et al. 2016. The safety of vedolizumab for ulcerative colitis and Crohn's disease. *Gut*, pp. 1–13

20. Keshav S, Vaňásek T, Niv Y, Petryka R, Howaldt S, et al. 2013. A Randomized Controlled Trial of the Efficacy and Safety of CCX282-B, an Orally-Administered Blocker of Chemokine Receptor CCR9, for Patients with Crohn's Disease. *PLoS One*. 8(3):e60094

21. Feagan BG, Sandborn WJ, D'Haens G, Lee SD, Allez M, et al. 2015. Randomised clinical trial: vercirnon, an oral CCR9 antagonist, vs. placebo as induction therapy in active Crohn's disease. *Aliment. Pharmacol. Ther.* 42(10):1170–81

22. Danese S. 2023. Combining Mechanisms of Action to Treat Patients With Inflammatory Bowel Disease. *Gastroenterol. Hepatol. (N. Y).* 19(1):31–33

23. Habtezion A, Nguyen LP, Hadeiba H, Butcher EC. 2016. Leukocyte Trafficking to the Small Intestine and Colon. *Gastroenterology*. 150(2):340–54

24. Pérez-Jeldres T, Tyler CJ, Boyer JD, Karuppuchamy T, Bamias G, et al. 2019. Cell Trafficking Interference in Inflammatory Bowel Disease: Therapeutic Interventions Based on Basic Pathogenesis Concepts. *Inflamm. Bowel Dis.* 25(2):270–82

25. Briskin M, Winsor-Hines D, Shyjan A, Cochran N, Bloom S, et al. 1997. Human mucosal addressin cell adhesion molecule-1 is preferentially expressed in intestinal tract and associated lymphoid tissue. *Am. J. Pathol.* 151(1):97–110

26. Danese S. 2011. Role of the vascular and lymphatic endothelium in the pathogenesis of inflammatory bowel disease: "brothers in arms." *Gut*. 60(7):998–1008

27. Fraser AG. 2002. The efficacy of azathioprine for the treatment of inflammatory bowel disease: a 30 year review. *Gut*. 50(4):485–89

28. Park JH, Peyrin-Biroulet L, Eisenhut M, Shin J Il. 2017. IBD immunopathogenesis: A comprehensive review of inflammatory molecules. *Autoimmun. Rev.* 16(4):416–26

29. Uhlig HH, Powrie F. 2018. Translating Immunology into Therapeutic Concepts for Inflammatory Bowel Disease. *Annu. Rev. Immunol.* 36(1):755–81

30. Peppelenbosch MP. 2004. T cell apoptosis and inflammatory bowel disease. *Gut*. 53(11):1556–58

31. Mudter J, Neurath MF. 2007. Apoptosis of T cells and the control of inflammatory bowel disease: therapeutic implications. *Gut*. 56(2):293–303

32. Oliver G, Kipnis J, Randolph GJ, Harvey NL. 2020. The Lymphatic Vasculature in the 21st Century: Novel Functional Roles in Homeostasis and Disease. *Cell*. 182(2):270–96

33. Dal Buono A, Gabbiadini R, Alfarone L, Solitano V, Repici A, et al. 2022. Sphingosine 1-Phosphate Modulation in Inflammatory Bowel Diseases: Keeping Lymphocytes Out of the Intestine. *Biomedicines*. 10(7):1735

34. Cyster JG, Schwab SR. 2012. Sphingosine-1-Phosphate and Lymphocyte Egress from Lymphoid Organs. *Annu. Rev. Immunol.* 30(1):69–94

35. Galván-Peña S, Zhu Y, Hanna BS, Mathis D, Benoist C. 2024. A dynamic atlas of immunocyte migration from the gut. *Sci. Immunol.* 9(91):

36. Karkkainen MJ, Haiko P, Sainio K, Partanen J, Taipale J, et al. 2004. Vascular endothelial growth factor C is required for sprouting of the first lymphatic vessels from embryonic veins. *Nat. Immunol.* 5(1):74–80

37. Hartiala P, Suominen S, Suominen E, Kaartinen I, Kiiski J, et al. 2020. Phase 1 Lymfactin® Study: Short-term Safety of Combined Adenoviral VEGF-C and Lymph Node Transfer Treatment for Upper Extremity Lymphedema. *J. Plast. Reconstr. Aesthetic Surg.* 73(9):1612–21

38. Leppäpuska IM, Hartiala P, Suominen S, Suominen E, Kaartinen I, et al. 2022. Phase 1 Lymfactin® Study: 24-month Efficacy and Safety Results of Combined Adenoviral VEGF-C and Lymph Node Transfer Treatment for Upper Extremity Lymphedema. *J. Plast. Reconstr. Aesthetic Surg.* 75(11):3938–45

39. Bernier-Latmani J, Petrova T V. 2017. Intestinal lymphatic vasculature: structure, mechanisms and functions. *Nat. Rev. Gastroenterol. Hepatol.* 14(9):510–26

40. OHTANI O. 1992. Structure of Lymphatics in Rat Cecum with Special Reference to Submucosal Collecting Lymphatics Endowed with Smooth Muscle Cells and Valves. I. A Scanning Electron Microscopic Study. *Arch. Histol. Cytol.* 55(4):429–36

41. Esterházy D, Canesso MCC, Mesin L, Muller PA, de Castro TBR, et al. 2019. Compartmentalized gut lymph node drainage dictates adaptive immune responses. *Nature*. 569(7754):126–30

42. Houston SA, Cerovic V, Thomson C, Brewer J, Mowat AM, Milling S. 2016. The lymph nodes draining the small intestine and colon are anatomically separate and immunologically distinct. *Mucosal Immunol.* 9(2):468–78

43. Redder E, Kirschnick N, Fang S, Kuhlmann M, González-Loyola A, et al. 2023. Specialized mesenteric lymphatic capillaries by-pass the mesenteric lymph node chain to transport peritoneal antigens directly into mediastinal lymph nodes. *BioRxiv*, pp. 1–44

44. Petrova T V., Koh GY. 2018. Organ-specific lymphatic vasculature: From development to

pathophysiology. *J. Exp. Med.* 215(1):35–49

45. Escobedo N, Oliver G. 2016. Lymphangiogenesis: Origin, Specification, and Cell Fate Determination. *Annu. Rev. Cell Dev. Biol.* 32(1):677–91

46. Baluk P, McDonald DM. 2022. Buttons and Zippers: Endothelial Junctions in Lymphatic Vessels. *Cold Spring Harb. Perspect. Med.*, p. a041178

47. Jackson DG. 2019. Leucocyte Trafficking via the Lymphatic Vasculature— Mechanisms and Consequences. *Front. Immunol.* 10(March):1–19

48. Scallan J, Huxley VH, Korthuis RJ. 2010. Capillary Fluid Exchange: Regulation, Functions, and Pathology. *Colloq. Ser. Integr. Syst. Physiol. From Mol. to Funct.* 2(1):1–94

49. Scallan JP, Zawieja SD, Castorena-Gonzalez JA, Davis MJ. 2016. Lymphatic pumping: mechanics, mechanisms and malfunction. *J. Physiol.* 594(20):5749–68

50. Buettner M, Lochner M. 2016. Development and Function of Secondary and Tertiary Lymphoid Organs in the Small Intestine and the Colon. *Front. Immunol.* 7(SEP):1–11

51. Breslin JW, Yang Y, Scallan JP, Sweat RS, Adderley SP, Murfee WL. 2018. Lymphatic Vessel Network Structure and Physiology. In *Comprehensive Physiology*. 9(1):207–99. Wiley

52. Wiig H, Swartz MA. 2012. Interstitial Fluid and Lymph Formation and Transport: Physiological Regulation and Roles in Inflammation and Cancer. *Physiol. Rev.* 92(3):1005–60

53. Palikuqi B, Rispal J, Reyes EA, Vaka D, Boffelli D, Klein O. 2022. Lymphangiocrine signals are required for proper intestinal repair after cytotoxic injury. *Cell Stem Cell*. 29(8):1262-1272.e5

54. Niec R, Chu T, Gur-Cohen S, Schernthanner M, Hidalgo L, et al. 2022. A lymphatic-stem cell interactome regulates intestinal stem cell activity. *bioRxiv*

55. Goto N, Goto S, Imada S, Hosseini S, Deshpande V, Yilmaz ÖH. 2022. Lymphatics and fibroblasts support intestinal stem cells in homeostasis and injury. *Cell Stem Cell*. 29(8):1246-1261.e6

56. GOWANS JL. 1957. The effect of the continuous re-infusion of lymph and lymphocytes on the output of lymphocytes from the thoracic duct of unanaesthetized rats. *Br. J. Exp. Pathol.* 38(1):67–78

57. GOWANS JL, KNIGHT EJ. 1964. The route of re-circulation of lymphocytes in the rat. *Proc. R. Soc. London. Ser. B. Biol. Sci.* 159(975):257–82

58. Vestweber D. 2015. How leukocytes cross the vascular endothelium. *Nat. Rev. Immunol.* 15(11):692–704

59. Nourshargh S, Alon R. 2014. Leukocyte migration into inflamed tissues. *Immunity*. 41(5):694–707

60. Hunter MC, Teijeira A, Halin C. 2016. T Cell Trafficking through Lymphatic Vessels. *Front. Immunol.* 7(DEC):

61. Schineis P, Runge P, Halin C. 2019. Cellular traffic through afferent lymphatic vessels. *Vascul. Pharmacol.* 112(March 2018):31–41

62. Bauer A, Tatliadim H, Halin C. 2022. Leukocyte Trafficking in Lymphatic Vessels. *Cold Spring Harb. Perspect. Med.* 12(10):a041186

63. Teijeira A, Russo E, Halin C. 2014. Taking the lymphatic route: dendritic cell migration to draining lymph nodes. *Semin. Immunopathol.* 36(2):261–74

64. Förster R, Davalos-Misslitz AC, Rot A. 2008. CCR7 and its ligands: balancing immunity and tolerance. *Nat. Rev. Immunol.* 8(5):362–71

65. Randolph GJ, Angeli V, Swartz MA. 2005. Dendritic-cell trafficking to lymph nodes through lymphatic vessels. *Nat. Rev. Immunol.* 5(8):617–28

66. Weber M, Hauschild R, Schwarz J, Moussion C, de Vries I, et al. 2013. Interstitial Dendritic Cell Guidance by Haptotactic Chemokine Gradients. *Science (80-.).* 339(6117):328–32

67. Pugh C, MacPherson G, Steer H. 1983. Characterization of nonlymphoid cells derived from rat peripheral lymph. *J. Exp. Med.* 157(6):1758–79

68. Milling S, Yrlid U, Cerovic V, MacPherson G. 2010. Subsets of migrating intestinal dendritic cells. *Immunol. Rev.* 234(1):259–67

69. Breslin JW, Yang Y, Scallan JP, Sweat RS, Adderley SP, Murfee WL. 2018. Lymphatic Vessel Network Structure and Physiology. In *Comprehensive Physiology*. 9(1):207–99. Wiley

70. Schwager S, Detmar M. 2019. Inflammation and Lymphatic Function. *Front. Immunol.* 10(February):308

71. Johnson LA, Clasper S, Holt AP, Lalor PF, Baban D, Jackson DG. 2006. An inflammation-induced mechanism for leukocyte transmigration across lymphatic vessel endothelium. *J. Exp. Med.* 203(12):2763–77

72. Arasa J, Collado-Diaz V, Kritikos I, Medina-Sanchez JD, Friess MC, et al. 2021. Upregulation of VCAM-1 in lymphatic collectors supports dendritic cell entry and rapid migration to lymph nodes in inflammation. *J. Exp. Med.* 218(7):

73. Baluk P, Fuxe J, Hashizume H, Romano T, Lashnits E, et al. 2007. Functionally specialized junctions between endothelial cells of lymphatic vessels. *J. Exp. Med.* 204(10):2349–62

74. Yao L-C, Baluk P, Srinivasan RS, Oliver G, McDonald DM. 2012. Plasticity of Button-Like Junctions in the Endothelium of Airway Lymphatics in Development and Inflammation. *Am. J. Pathol.* 180(6):2561–75

75. Zhang F, Zarkada G, Han J, Li J, Dubrac A, et al. 2018. Lacteal junction zippering protects against diet-induced obesity. *Science (80-.).* 361(6402):599–603

76. Wee JLK, Greenwood DL V, Han X, Scheerlinck J-PY. 2011. Inflammatory cytokines IL-6 and TNF-α regulate lymphocyte trafficking through the local lymph node. *Vet. Immunol. Immunopathol.* 144(1–2):95–103

77. Geleff S, Schoppmann SF, Oberhuber G. 2003. Increase in podoplanin-expressing intestinal lymphatic vessels in inflammatory bowel disease. *Virchows Arch.* 442(3):231–37

78. Fogt F, Pascha T, Zhang P, Gausas R, Rahemtulla A, Zimmerman R. 2004. Proliferation of D2-40-expressing intestinal lymphatic vessels in the lamina propria in inflammatory bowel disease. *Int. J. Mol. Med.* 13(2):211–14

79. Pedica F, Ligorio C, Tonelli P, Bartolini S, Baccarini P. 2008. Lymphangiogenesis in Crohn's disease: an immunohistochemical study using monoclonal antibody D2-40. *Virchows Arch.* 452(1):57–63

80. Rahier J-F, De Beauce S, Dubuquoy L, Erdual E, Colombel J-F, et al. 2011. Increased lymphatic vessel density and lymphangiogenesis in inflammatory bowel disease. *Aliment. Pharmacol. Ther.* 34(5):533–43

81. Kaiserling E, Krober S, Geleff S. 2003. Lymphatic vessels in the colonic mucosa in ulcerative colitis. *Lymphology*. 36:52–61

82. D'Alessio S, Correale C, Tacconi C, Gandelli A, Pietrogrande G, et al. 2014. VEGF-C–dependent stimulation of lymphatic function ameliorates experimental inflammatory bowel disease. *J. Clin. Invest.* 124(9):3863–78

83. Shen W, Li Y, Cao L, Cai X, Ge Y, Zhu W. 2018. Decreased Expression of Prox1 Is Associated With Postoperative Recurrence in Crohn's Disease. *J. Crohn's Colitis*. 12(10):1210–18

84. Rahier J-F, Dubuquoy L, Colombel J-F, Jouret-Mourin A, Delos M, et al. 2013. Decreased Lymphatic Vessel Density Is Associated With Postoperative Endoscopic Recurrence in Crohn's Disease. *Inflamm. Bowel Dis.* 19(10):2084–90

85. Zundler S, Klingberg A, Schillinger D, Fischer S, Neufert C, et al. 2017. Three-Dimensional Cross-Sectional Light-Sheet Microscopy Imaging of the Inflamed Mouse Gut. *Gastroenterology*. 153(4):898–900

86. Klingberg A, Hasenberg A, Ludwig-Portugall I, Medyukhina A, Männ L, et al. 2017. Fully Automated Evaluation of Total Glomerular Number and Capillary Tuft Size in Nephritic Kidneys Using Lightsheet Microscopy. *J. Am. Soc. Nephrol.* 28(2):452–59

87. Susaki EA, Tainaka K, Perrin D, Yukinaga H, Kuno A, Ueda HR. 2015. Advanced CUBIC protocols for whole-brain and whole-body clearing and imaging. *Nat. Protoc.* 10(11):1709–27

88. Bernier-Latmani J, Petrova T V. 2016. High-resolution 3D analysis of mouse small-intestinal stroma. *Nat. Protoc.* 11(9):1617–29

89. Tacconi C, Schwager S, Cousin N, Bajic D, Sesartic M, et al. 2019. Antibody-Mediated Delivery of VEGFC Ameliorates Experimental Chronic Colitis. *ACS Pharmacol. Transl. Sci.* acsptsci.9b00037

90. Schwager S, Renner S, Hemmerle T, Karaman S, Proulx ST, et al. 2018. Antibody-mediated delivery of VEGF-C potently reduces chronic skin inflammation. *JCI Insight*. 3(23):

91. Zhou Q, Guo R, Wood R, Boyce BF, Liang Q, et al. 2011. Vascular endothelial growth factor C attenuates joint damage in chronic inflammatory arthritis by accelerating local lymphatic drainage in mice. *Arthritis Rheum.* 63(8):2318–28

92. Vieira JM, Norman S, Villa del Campo C, Cahill TJ, Barnette DN, et al. 2018. The cardiac lymphatic system stimulates resolution of inflammation following myocardial infarction. *J. Clin. Invest.* 128(8):3402–12

93. Jurisic G, Sundberg JP, Detmar M. 2013. Blockade of VEGF receptor-3 aggravates inflammatory bowel disease and lymphatic vessel enlargement. *Inflamm. Bowel Dis.* 19(9):1983–89

94. Kataru RP, Jung K, Jang C, Yang H, Schwendener RA, et al. 2009. Critical role of CD11b+ macrophages and VEGF in inflammatory lymphangiogenesis, antigen clearance, and inflammation resolution. *Blood*. 113(22):5650–59

95. Guo R, Zhou Q, Proulx ST, Wood R, Ji R-C, et al. 2009. Inhibition of lymphangiogenesis and lymphatic drainage via vascular endothelial growth factor receptor 3 blockade increases the severity of inflammation in a mouse model of chronic inflammatory arthritis. *Arthritis Rheum.* 60(9):2666–76

96. Brouillard P, Witte MH, Erickson RP, Damstra RJ, Becker C, et al. 2021. Primary lymphoedema. *Nat. Rev. Dis. Prim.* 7(1):77

97. Behr MA. 2010. The path to Crohn's disease: Is mucosal pathology a secondary event. *Inflamm. Bowel Dis.* 16(5):896–902

98. Sura R, Colombel J-F, Van Kruiningen HJ. 2011. Lymphatics, tertiary lymphoid organs and the granulomas of Crohn's disease: an immunohistochemical study. *Aliment. Pharmacol. Ther.* 33(8):930–39

99. Van Kruiningen HJ. 2020. What the early pathologists got wrong, and right, about the pathology of Crohn's disease: a historical perspective. *APMIS*. apm.13081

100. Heatley R V., Bolton PM, Hughes LE, Owen EW. 1980. Mesenteric Lymphatic Obstruction in Crohn's Disease. *Digestion*. 20(5):307–13

101. Randolph GJ, Bala S, Rahier J-F, Johnson MW, Wang PL, et al. 2016. Lymphoid Aggregates Remodel Lymphatic Collecting Vessels that Serve Mesenteric Lymph Nodes in Crohn Disease. *Am. J. Pathol.* 186(12):3066–73

102. Czepielewski RS, Erlich EC, Onufer EJ, Young S, Saunders BT, et al. 2021. Ileitis-associated tertiary lymphoid organs arise at lymphatic valves and impede mesenteric lymph flow in response to tumor necrosis factor. *Immunity*. 54(12):2795-2811.e9

103. Reichert FL, Mathes ME. 1936. EXPERIMENTAL LYMPHEDEMA OF THE INTESTINAL TRACT AND ITS RELATION TO REGIONAL CICATRIZING ENTERITIS. *Ann. Surg.* 104(4):601–16

104. CROHN BB. 1932. REGIONAL ILEITIS. *J. Am. Med. Assoc.* 99(16):1323

105. Kalima T V., Collan Y. 1970. Intestinal Villus in Experimental Lymphatic Obstruction. *Scand. J. Gastroenterol.* 5(6):497–510

106. Becker F, Romero E, Goetzmann J, Hasselschwert DL, Dray B, et al. 2019. Endogenous Specialized Proresolving Mediator Profiles in a Novel Experimental Model of Lymphatic Obstruction and Intestinal Inflammation in African Green Monkeys. *Am. J. Pathol.* 189(10):1953–72

107. Coffey CJ, Kiernan MG, Sahebally SM, Jarrar A, Burke JP, et al. 2018. Inclusion of the Mesentery in Ileocolic Resection for Crohn's Disease is Associated With Reduced Surgical Recurrence. *J. Crohn's Colitis*. 12(10):1139–50

108. Sakurai T, Katsuno T, Saito K, Yoshihama S, Nakagawa T, et al. 2017. Mesenteric findings of CT enterography are well correlated with the endoscopic severity of Crohn's disease. *Eur. J. Radiol.* 89:242–48

109. Rimola J, Alfaro I, Fernández-Clotet A, Castro-Poceiro J, Vas D, et al. 2018. Persistent damage on magnetic resonance enterography in patients with Crohn's disease in endoscopic remission. *Aliment. Pharmacol. Ther.* 48(11–12):1232–41

110. Li Y, Zhu W, Zuo L, Shen B. 2016. The Role of the Mesentery in Crohn's Disease: The Contributions of Nerves, Vessels, Lymphatics, and Fat to the Pathogenesis and Disease Course. *Inflamm. Bowel Dis.* 22(6):1483–95

111. Kuan EL, Ivanov S, Bridenbaugh EA, Victora G, Wang W, et al. 2015. Collecting Lymphatic Vessel Permeability Facilitates Adipose Tissue Inflammation and Distribution of Antigen to Lymph Node–Homing Adipose Tissue Dendritic Cells. *J. Immunol.* 194(11):5200–5210

112. Fonseca DM da, Hand TW, Han S-J, Gerner MY, Zaretsky AG, et al. 2015. Microbiota-Dependent Sequelae of Acute Infection Compromise Tissue-Specific Immunity. *Cell*. 163(2):354–66

113. Ha CWY, Martin A, Sepich-Poore GD, Shi B, Wang Y, et al. 2020. Translocation of Viable Gut Microbiota to Mesenteric Adipose Drives Formation of Creeping Fat in Humans. *Cell*, pp. 1–18

114. Massier L, Chakaroun R, Tabei S, Crane A, Didt KD, et al. 2020. Adipose tissue derived bacteria are associated with inflammation in obesity and type 2 diabetes. *Gut*. 69(10):1796–1806

115. Siggins MK, Lynskey NN, Lamb LE, Johnson LA, Huse KK, et al. 2020. Extracellular bacterial lymphatic metastasis drives Streptococcus pyogenes systemic infection. *Nat. Commun.* 11(1):4697

116. Shen W, Li Y, Zou Y, Cao L, Cai X, et al. 2019. Mesenteric Adipose Tissue Alterations in Crohn's Disease Are Associated With the Lymphatic System. *Inflamm. Bowel Dis.* 25(2):283–93

117. Vetrano S, Borroni EM, Sarukhan A, Savino B, Bonecchi R, et al. 2010. The lymphatic system controls intestinal inflammation and inflammation-associated colon cancer through the chemokine decoy receptor D6. *Gut*. 59(2):197–206

118. Becker F, Potepalov S, Shehzahdi R, Bernas M, Witte M, et al. 2015. Downregulation of FoxC2 Increased Susceptibility to Experimental Colitis. *Inflamm. Bowel Dis.* 21(6):1

119. Sabine A, Bovay E, Demir CS, Kimura W, Jaquet M, et al. 2015. FOXC2 and fluid shear stress stabilize postnatal lymphatic vasculature. *J. Clin. Invest.* 125(10):3861–77

120. von der Weid P-Y, Zawieja DC. 2004. Lymphatic smooth muscle: the motor unit of lymph drainage. *Int. J. Biochem. Cell Biol.* 36(7):1147–53

121. Fullerton JN, Gilroy DW. 2016. Resolution of inflammation: a new therapeutic frontier. *Nat. Rev. Drug Discov.* 15(8):551–67

122. Serhan CN, Savill J. 2005. Resolution of inflammation: the beginning programs the end. *Nat. Immunol.* 6(12):1191–97

123. Karpanen T, Alitalo K. 2008. Molecular Biology and Pathology of Lymphangiogenesis. *Annu. Rev. Pathol. Mech. Dis.* 3(1):367–97

124. Becker F, Kurmaeva E, Gavins FNE, Stevenson E V., Navratil AR, et al. 2016. A Critical Role for Monocytes/Macrophages During Intestinal Inflammation-associated Lymphangiogenesis. *Inflamm. Bowel Dis.* 22(6):1326–45

125. Nurmi H, Saharinen P, Zarkada G, Zheng W, Robciuc MR, Alitalo K. 2015. VEGF-C is required for intestinal lymphatic vessel maintenance and lipid absorption. *EMBO Mol. Med.* 7(11):1418–25

126. Martin JC, Chang C, Boschetti G, Ungaro R, Giri M, et al. 2019. Single-Cell Analysis of Crohn's Disease Lesions Identifies a Pathogenic Cellular Module Associated with Resistance to Anti-TNF Therapy. *Cell*, p. 503102

127. Kinchen J, Chen HH, Parikh K, Antanaviciute A, Jagielowicz M, et al. 2018. Structural Remodeling of the Human Colonic Mesenchyme in Inflammatory Bowel Disease. *Cell*. 175(2):372-386.e17

128. Srinivasan RS, Dillard ME, Lagutin O V., Lin F-J, Tsai S, et al. 2007. Lineage tracing demonstrates the venous origin of the mammalian lymphatic vasculature. *Genes Dev.* 21(19):2422–32

129. Chassaing B, Aitken JD, Malleshappa M, Vijay-Kumar M. 2014. Dextran Sulfate Sodium (DSS)-Induced Colitis in Mice. In *Current Protocols in Immunology*. 15.25.1-15.25.14. Hoboken, NJ, USA: John Wiley & Sons, Inc.

130. Kinchen J, Chen HH, Parikh K, Antanaviciute A, Jagielowicz M, et al. 2018. Structural Remodeling of the Human Colonic Mesenchyme in Inflammatory Bowel Disease. *Cell*. 175(2):372-386.e17

131. Parikh K, Antanaviciute A, Fawkner-Corbett D, Jagielowicz M, Aulicino A, et al. 2019. Colonic epithelial

cell diversity in health and inflammatory bowel disease. *Nature*, p. 1

132. Smillie CS, Biton M, Ordovas-Montanes J, Sullivan KM, Burgin G, et al. 2019. Intra- and Inter-cellular Rewiring of the Human Colon during Ulcerative Colitis. *Cell*. 178(3):714-730.e22

133. Martin JC, Chang C, Boschetti G, Ungaro R, Giri M, et al. 2019. Single-Cell Analysis of Crohn's Disease Lesions Identifies a Pathogenic Cellular Module Associated with Resistance to Anti-TNF Therapy. *Cell*, p. 503102

134. Fawkner-Corbett D, Antanaviciute A, Parikh K, Jagielowicz M, Gerós AS, et al. 2021. Spatiotemporal analysis of human intestinal development at single-cell resolution. *Cell*. 184(3):810-826.e23

135. Elmentaite R, Kumasaka N, Roberts K, Fleming A, Dann E, et al. 2021. Cells of the human intestinal tract mapped across space and time. *Nature*. 597(7875):250–55

136. Sokol L, Geldhof V, García-Caballero M, Conchinha N V., Dumas SJ, et al. 2021. Protocols for endothelial cell isolation from mouse tissues: small intestine, colon, heart, and liver. *STAR Protoc.* 2(2):100489

137. Ordóñez NG. 2012. Immunohistochemical Endothelial Markers. *Adv. Anat. Pathol.* 19(5):281–95

138. Astarita JL, Acton SE, Turley SJ. 2012. Podoplanin: emerging functions in development, the immune system, and cancer. *Front. Immunol.* 3(SEP):1–11

139. Escobedo N, Oliver G. 2016. Lymphangiogenesis: Origin, Specification, and Cell Fate Determination. *Annu. Rev. Cell Dev. Biol.* 32(1):677–91

140. Francois M, Harvey NL, Hogan BM. 2011. The Transcriptional Control of Lymphatic Vascular Development. *Physiology*. 26(3):146–55

141. Czarnewski P, Parigi SM, Sorini C, Diaz OE, Das S, et al. 2019. Conserved transcriptomic profile between mouse and human colitis allows unsupervised patient stratification. *Nat. Commun.* 10(1):2892

142. Uzzan M, Martin JC, Mesin L, Livanos AE, Castro-Dopico T, et al. 2022. Ulcerative colitis is characterized by a plasmablast-skewed humoral response associated with disease activity. *Nat. Med.* 28(4):766–79

143. Voisin M, Nourshargh S. 2019. Neutrophil trafficking to lymphoid tissues: physiological and pathological implications. *J. Pathol.* 247(5):662–71

144. Palframan RT, Jung S, Cheng G, Weninger W, Luo Y, et al. 2001. Inflammatory Chemokine Transport and Presentation in HEV. *J. Exp. Med.* 194(9):1361–74

145. Ozanne J, Shek B, Stephen LA, Novak A, Milne E, et al. 2022. Tenascin-C is a driver of inflammation in the DSS model of colitis. *Matrix Biol. Plus*. 14:100112

146. Love MI, Huber W, Anders S. 2014. Moderated estimation of fold change and dispersion for RNA-seq data with DESeq2. *Genome Biol.* 15(12):550

147. Vetrano S, Borroni EM, Sarukhan A, Savino B, Bonecchi R, et al. 2010. The lymphatic system controls intestinal inflammation and inflammation-associated colon cancer through the chemokine decoy receptor D6. *Gut*. 59(2):197–206

148. Takamatsu H, Takegahara N, Nakagawa Y, Tomura M, Taniguchi M, et al. 2010. Semaphorins guide the entry of dendritic cells into the lymphatics by activating myosin II. *Nat. Immunol.* 11(7):594–600

149. Stoeckius M, Zheng S, Houck-Loomis B, Hao S, Yeung BZ, et al. 2018. Cell Hashing with barcoded antibodies enables multiplexing and doublet detection for single cell genomics. *Genome Biol.* 19(1):224

150. Stuart T, Butler A, Hoffman P, Hafemeister C, Papalexi E, et al. 2019. Comprehensive Integration of Single-Cell Data. *Cell*. 177(7):1888-1902.e21

151. Hernández Vásquez MN, Ulvmar MH, González-Loyola A, Kritikos I, Sun Y, et al. 2021. Transcription factor FOXP2 is a flow-induced regulator of collecting lymphatic vessels. *EMBO J.* 40(12):1–16

152. Stuart T, Butler A, Hoffman P, Hafemeister C, Papalexi E, et al. 2019. Comprehensive Integration of Single-Cell Data. *Cell*. 177(7):1888-1902.e21

153. Steimle V, Siegrist C-A, Mottet A, Lisowska-Grospierre B, Mach B. 1994. Regulation of MHC Class II Expression by Interferon-γ Mediated by the Transactivator Gene CIITA. *Science (80-.).* 265(5168):106–9

154. Garcia-Diaz A, Shin DS, Moreno BH, Saco J, Escuin-Ordinas H, et al. 2017. Interferon Receptor Signaling Pathways Regulating PD-L1 and PD-L2 Expression. *Cell Rep.* 19(6):1189–1201

155. Hu X, Ivashkiv LB. 2009. Cross-regulation of signaling pathways by interferon-gamma: implications for immune responses and autoimmune diseases. *Immunity*. 31(4):539–50

156. Ito R, Shin-Ya M, Kishida T, Urano A, Takada R, et al. 2006. Interferon-gamma is causatively involved in experimental inflammatory bowel disease in mice. *Clin. Exp. Immunol.* 146(2):330–38

157. Langer V, Vivi E, Regensburger D, Winkler TH, Waldner MJ, et al. 2019. IFN-γ drives inflammatory bowel disease pathogenesis through VE-cadherin–directed vascular barrier disruption. *J. Clin. Invest.* 129(11):4691–4707

158. Teijeira A, Hunter MC, Russo E, Proulx ST, Frei T, et al. 2017. T Cell Migration from Inflamed Skin to Draining Lymph Nodes Requires Intralymphatic Crawling Supported by ICAM-1/LFA-1 Interactions. *Cell Rep.* 18(4):857–65

159. Bui TM, Wiesolek HL, Sumagin R. 2020. ICAM-1: A master regulator of cellular responses in inflammation, injury resolution, and tumorigenesis. *J. Leukoc. Biol.* 108(3):787–99

160. Richardson DS, Guan W, Matsumoto K, Pan C, Chung K, et al. 2021. Tissue clearing. *Nat. Rev. Methods Prim.* 1(1):84

161. Banerji S, Ni J, Wang S-X, Clasper S, Su J, et al. 1999. LYVE-1, a New Homologue of the CD44

Glycoprotein, Is a Lymph-specific Receptor for Hyaluronan. *J. Cell Biol.* 144(4):789–801

162. Cifarelli V, Eichmann A. 2019. The Intestinal Lymphatic System: Functions and Metabolic Implications. *Cell. Mol. Gastroenterol. Hepatol.* 7(3):503–13

163. Domanska D, Majid U, Karlsen VT, Merok MA, Beitnes ACR, et al. 2022. Single-cell transcriptomic analysis of human colonic macrophages reveals niche-specific subsets. *J. Exp. Med.* 219(3):

164. Hawkins CF, Hardy TL. 1950. On the nature of haustration of the colon. *J. Fac. Radiol.* 2(1):95–98

165. Huizinga JD, Pervez M, Nirmalathasan S, Chen J-H. 2021. Characterization of haustral activity in the human colon. *Am. J. Physiol. Liver Physiol.* 320(6):G1067–80

166. Lohela TJ, Lilius TO, Nedergaard M. 2022. The glymphatic system: implications for drugs for central nervous system diseases. *Nat. Rev. Drug Discov.* 21(10):763–79

167. Rasmussen MK, Mestre H, Nedergaard M. 2022. Fluid transport in the brain. *Physiol. Rev.* 102(2):1025–1151

168. Brandtzaeg P, Kiyono H, Pabst R, Russell MW. 2008. Terminology: nomenclature of mucosa-associated lymphoid tissue. *Mucosal Immunol.* 1(1):31–37

169. Mörbe UM, Jørgensen PB, Fenton TM, von Burg N, Riis LB, et al. 2021. Human gut-associated lymphoid tissues (GALT); diversity, structure, and function. *Mucosal Immunol.* 14(4):793–802

170. Scheele CLGJ, Herrmann D, Yamashita E, Lo Celso C, Jenne CN, et al. 2022. Multiphoton intravital microscopy of rodents. *Nat. Rev. Methods Prim.* 2(1):89

171. Shen Z, Lu Z, Chhatbar PY, O'Herron P, Kara P. 2012. An artery-specific fluorescent dye for studying neurovascular coupling. *Nat. Methods*. 9(3):273–76

172. Clifford PS, Ella SR, Stupica AJ, Nourian Z, Li M, et al. 2011. Spatial Distribution and Mechanical Function of Elastin in Resistance Arteries. *Arterioscler. Thromb. Vasc. Biol.* 31(12):2889–96

173. Chang S-Y, Song J-H, Guleng B, Cotoner CA, Arihiro S, et al. 2013. Circulatory Antigen Processing by Mucosal Dendritic Cells Controls CD8+ T Cell Activation. *Immunity*. 38(1):153–65

174. Bernier-Latmani J, González-Loyola A, Petrova T V. 2024. Mechanisms and functions of intestinal vascular specialization. *J. Exp. Med.* 221(1):1–18

175. Girard J-P, Moussion C, Förster R. 2012. HEVs, lymphatics and homeostatic immune cell trafficking in lymph nodes. *Nat. Rev. Immunol.* 12(11):762–73

176. Feagan BG, Rutgeerts P, Sands BE, Hanauer S, Colombel J-F, et al. 2013. Vedolizumab as Induction and Maintenance Therapy for Ulcerative Colitis. *N. Engl. J. Med.* 369(8):699–710

177. Sandborn WJ, Feagan B, Rutgeerts P, Hanauer S, Colombel J-F, et al. 2013. Vedolizumab as induction and maintenance therapy for Crohn's disease. *N. Engl. J. Med.* 369(8):711–21

178. Huang LH, Zinselmeyer BH, Chang CH, Saunders BT, Elvington A, et al. 2019. Interleukin-17 Drives Interstitial Entrapment of Tissue Lipoproteins in Experimental Psoriasis. *Cell Metab.* 29(2):475-487.e7

179. Krugliak Cleveland N, Torres J, Rubin DT. 2022. What Does Disease Progression Look Like in Ulcerative Colitis, and How Might It Be Prevented? *Gastroenterology*. 162(5):1396–1408

180. Schneider CA, Rasband WS, Eliceiri KW. 2012. NIH Image to ImageJ: 25 years of image analysis. *Nat. Methods*. 9(7):671–75

181. Bankhead P, Loughrey MB, Fernández JA, Dombrowski Y, McArt DG, et al. 2017. QuPath: Open source software for digital pathology image analysis. *Sci. Rep.* 7(1):16878

182. Schapiro D, Jackson HW, Raghuraman S, Fischer JR, Zanotelli VRT, et al. 2017. histoCAT: analysis of cell phenotypes and interactions in multiplex image cytometry data. *Nat. Methods*. 14(9):873–76

183. Cenaj O, Allison DHR, Imam R, Zeck B, Drohan LM, et al. 2021. Evidence for continuity of interstitial spaces across tissue and organ boundaries in humans. *Commun. Biol.* 4(1):1–9

184. Benias PC, Wells RG, Sackey-Aboagye B, Klavan H, Reidy J, et al. 2018. Structure and Distribution of an Unrecognized Interstitium in Human Tissues. *Sci. Rep.* 8(1):4947

185. Suzuki K, Arumugam S, Yokoyama J, Kawauchi Y, Honda Y, et al. 2016. Pivotal role of carbohydrate sulfotransferase 15 in fibrosis and mucosal healing in mouse colitis. *PLoS One*. 11(7):1–17

186. Ordás I, Eckmann L, Talamini M, Baumgart DC, Sandborn WJ. 2012. Ulcerative colitis. *Lancet*. 380(9853):1606–19

187. Roda G, Narula N, Pinotti R, Skamnelos A, Katsanos KH, et al. 2017. Systematic review with meta-analysis: proximal disease extension in limited ulcerative colitis. *Aliment. Pharmacol. Ther.* 45(12):1481–92

188. Progatzky F, Shapiro M, Chng SH, Garcia-Cassani B, Classon CH, et al. 2021. Regulation of intestinal immunity and tissue repair by enteric glia. *Nature*. 599(7883):125–30

189. Coffey JC, O'Leary DP. 2016. The mesentery: structure, function, and role in disease. *Lancet Gastroenterol. Hepatol.* 1(3):238–47

190. Macari M, Balthazar EJ. 2001. CT of bowel wall thickening: Significance and pitfalls of interpretation. *Am. J. Roentgenol.* 176(5):1105–16

191. Jørgensen PB, Fenton TM, Mörbe UM, Riis LB, Jakobsen HL, et al. 2021. Identification, isolation and analysis of human gut-associated lymphoid tissues. *Nat. Protoc.* 16(4):2051–67

192. Fenton TM, Jørgensen PB, Niss K, Rubin SJS, Mörbe UM, et al. 2020. Immune Profiling of Human Gut-Associated Lymphoid Tissue Identifies a Role for Isolated Lymphoid Follicles in Priming of Region-Specific Immunity. *Immunity*. 52(3):557-570.e6

193. Rehal S, Stephens M, Roizes S, Liao S, von der Weid P-Y. 2018. Acute small intestinal inflammation results in persistent lymphatic alterations. *Am. J. Physiol. Liver Physiol.* 314(3):G408–17

194. Becker F, Yi P, Al-Kofahi M, Ganta VC, Morris J, Alexander JS. 2014. Lymphatic dysregulation in intestinal inflammation: New insights into inflammatory bowel disease pathomechanisms. *Lymphology*. 47(1):3–27

195. Randolph GJ, Bala S, Rahier J-F, Johnson MW, Wang PL, et al. 2016. Lymphoid Aggregates Remodel Lymphatic Collecting Vessels that Serve Mesenteric Lymph Nodes in Crohn Disease. *Am. J. Pathol.* 186(12):3066–73

196. Sandborn WJ, Feagan BG, D'Haens G, Wolf DC, Jovanovic I, et al. 2021. Ozanimod as Induction and Maintenance Therapy for Ulcerative Colitis. *N. Engl. J. Med.* 385(14):1280–91

197. Danese S, Furfaro F, Vetrano S. 2018. Targeting S1P in Inflammatory Bowel Disease: New Avenues for Modulating Intestinal Leukocyte Migration. *J. Crohn's Colitis*. 12(suppl_2):S678–86

198. Cartier A, Hla T. 2019. Sphingosine 1-phosphate: Lipid signaling in pathology and therapy. *Science (80-.).* 366(6463):eaar5551

199. Balmer ML, Slack E, de Gottardi A, Lawson MAE, Hapfelmeier S, et al. 2014. The Liver May Act as a Firewall Mediating Mutualism Between the Host and Its Gut Commensal Microbiota. *Sci. Transl. Med.* 6(237):1–11

200. De Schepper S, Verheijden S, Aguilera-Lizarraga J, Viola MF, Boesmans W, et al. 2018. Self-Maintaining Gut Macrophages Are Essential for Intestinal Homeostasis. *Cell*. 175(2):400-415.e13

201. Muller PA, Koscsó B, Rajani GM, Stevanovic K, Berres M-L, et al. 2014. Crosstalk between Muscularis Macrophages and Enteric Neurons Regulates Gastrointestinal Motility. *Cell*. 158(2):300–313

202. Gabanyi I, Muller PA, Feighery L, Oliveira TY, Costa-Pinto FA, Mucida D. 2016. Neuro-immune Interactions Drive Tissue Programming in Intestinal Macrophages. *Cell*. 164(3):378–91

203. Dai X-M, Ryan GR, Hapel AJ, Dominguez MG, Russell RG, et al. 2002. Targeted disruption of the mouse colony-stimulating factor 1 receptor gene results in osteopetrosis, mononuclear phagocyte deficiency, increased primitive progenitor cell frequencies, and reproductive defects. *Blood*. 99(1):111–20

204. MacDonald KPA, Palmer JS, Cronau S, Seppanen E, Olver S, et al. 2010. An antibody against the colony-stimulating factor 1 receptor depletes the resident subset of monocytes and tissue- and tumor-associated macrophages but does not inhibit inflammation. *Blood*. 116(19):3955–63

205. Johnson LA, Jackson DG. 2021. Hyaluronan and Its Receptors: Key Mediators of Immune Cell Entry and Trafficking in the Lymphatic System. *Cells*. 10(8):2061

206. Gale NW, Prevo R, Espinosa J, Ferguson DJ, Dominguez MG, et al. 2007. Normal Lymphatic Development and Function in Mice Deficient for the Lymphatic Hyaluronan Receptor LYVE-1. *Mol. Cell. Biol.* 27(2):595–604

207. Wiggins BG, Wang Y-F, Burke A, Grunberg N, Vlachaki Walker JM, et al. 2023. Endothelial sensing of AHR ligands regulates intestinal homeostasis. *Nature*. 621(7980):821–29

208. Kalucka J, de Rooij LPMH, Goveia J, Rohlenova K, Dumas SJ, et al. 2020. Single-Cell Transcriptome Atlas of Murine Endothelial Cells. *Cell*. 180(4):764-779.e20

209. Niec RE, Chu T, Schernthanner M, Gur-Cohen S, Hidalgo L, et al. 2022. Lymphatics act as a signaling hub to regulate intestinal stem cell activity. *Cell Stem Cell*. 29(7):1067-1082.e18

210. Gehart H, Clevers H. 2019. Tales from the crypt: new insights into intestinal stem cells. *Nat. Rev. Gastroenterol. Hepatol.* 16(1):19–34

211. Beumer J, Clevers H. 2021. Cell fate specification and differentiation in the adult mammalian intestine. *Nat. Rev. Mol. Cell Biol.* 22(1):39–53

212. Nava GM, Friedrichsen HJ, Stappenbeck TS. 2011. Spatial organization of intestinal microbiota in the mouse ascending colon. *ISME J.* 5(4):627–38

213. Louveau A, Smirnov I, Keyes TJ, Eccles JD, Rouhani SJ, et al. 2015. Structural and functional features of central nervous system lymphatic vessels. *Nature*. 523(7560):337–41

214. das Neves SP, Delivanoglou N, Da Mesquita S. 2021. CNS-Draining Meningeal Lymphatic Vasculature: Roles, Conundrums and Future Challenges. *Front. Pharmacol.* 12(April):1–17

215. Tanaka M, Iwakiri Y. 2018. Lymphatics in the liver. *Curr. Opin. Immunol.* 53:137–42

216. Jeong J, Tanaka M, Iwakiri Y. 2022. Hepatic lymphatic vascular system in health and disease. *J. Hepatol.* 77(1):206–18

217. Frenkel NC, Poghosyan S, Verheem A, Padera TP, Rinkes IHMB, et al. 2020. Liver lymphatic drainage patterns follow segmental anatomy in a murine model. *Sci. Rep.* 10(1):21808